



© Albert Eshun
University of Cape Coast

UNIVERSITY OF CAPE COAST



SPATIAL AND TEMPORAL ASSESSMENT OF ORGANIC
MICROPOLLUTANTS IN THE PRA RIVER BASIN

BY

ALBERT ESHUN

Thesis submitted to the Department of Chemistry of the School of Physical
Sciences, College of Agriculture and Natural Science, University of Cape
Coast, in partial fulfilment of the requirements for award of Doctor of
Philosophy degree in Chemistry

SEPTEMBER 2023

DECLARATION

Candidate's declaration

I hereby declare that this thesis is the result of my own original research and that no part of it has been presented for another degree in this university or elsewhere.

Candidate's Signature.....Date.....

Name: Albert Eshun

Supervisors' Declaration

We hereby declare that the preparation and presentation of the thesis were supervised in accordance with the guidelines on supervision of thesis laid down by the University of Cape Coast.

Principal Supervisor's Signature..... Date.....

Name: Prof. John Kwesi Bentum

Co-Supervisor's Signature.....Date.....

Name: Prof. David Kofi Essumang

ABSTRACT

The extensive occurrence and potential harmful impacts of per- and polyfluoroalkyl substances (PFAS) and polychlorinated biphenyls (PCBs) have garnered considerable attention. The presence of these organic micropollutants pose threat to river bodies and their sustainability. This study aims to determine the levels and distribution of PFAS and PCBs, in the Pra River basin. A total of 20 sampling points were selected to collect water and sediment samples, covering both upstream and downstream locations along the river. Solid Phase Extraction (SPE) was employed for pre-concentration and pre-cleaning of samples prior to analysis. Liquid chromatography-mass spectrometry (LC-MS) and gas chromatography-mass spectrometry (GC-MS) techniques were employed to analyze water and sediment samples for targeted PFAS and PCBs. The results revealed extensive presence of PFAS and PCBs in the Pra River basin. Multiple PFAS compounds, including perfluorooctanoic acid (PFOA) and perfluorooctane sulphonic acid (PFOS) were detected at varying levels across all the sampling points with a range between 14.5-112.4 ng/L for water samples and 55.9-186.5 ng/g for sediments. Similarly, total PCB level ranged between 0.53 and 5.87 ng/L for water samples and 2.60-139.79 ng/g for the sediment samples. PCBs 138, 149, and 153, were identified as most dominant in the river basin. The human health risks associated with exposure to PFAS and PCBs through surface water and sediment were negligible. Decomposition of perfluorooctanoic acid (PFOA) by water radiolysis led to defluorination efficiency of 98% with solvated electrons and carbon dioxide radical anions being primary reactive species. These findings indicate that the Pra River basin is contaminated with PFAS and PCBs.

KEY WORDS

Gamma irradiation

Perfluoroalkyl substances

Polychlorinated biphenyls

Pra River Basin

Risk assessment

Water radiolysis



ACKNOWLEDGEMENTS

I would like to express my sincere and heartfelt gratitude to all individuals who played significant role in the successful completion of this thesis. Firstly, I am grateful to my supervisors Prof. John Kwesi Bentum and Prof. David Kofi Essumang for their guidance, mentorship, and unwavering support throughout the entire research process. Their expertise, invaluable insights, and constructive feedback have been instrumental in shaping this thesis.

I am indebted to Prof. Mehran Mostafavi and staff of Institut de Chemie Physique, Universite Paris-Saclay, France, whose dedication to academic excellence and resources have provided me with a conducive research environment. The support and facilities extended by Institut de Chemie Physique-CNRS, Universite Paris-Saclay have been immensely helpful in the successful completion of this thesis.

Last but not least, I am filled with profound gratitude towards my family for their unconditional love, encouragement, and belief in my abilities. Their unwavering support and sacrifices throughout my academic journey have been a constant source of inspiration.

DEDICATION

To my sons: Ryan, Caleb and Chris



TABLE OF CONTENTS

	Page
DECLARATION	ii
ABSTRACT	iii
KEY WORDS	iv
ACKNOWLEDGEMENTS	v
DEDICATION	vi
LIST OF TABLES	xvii
LIST OF FIGURES	xx
LIST OF ABBREVIATIONS	xxvii
CHAPTER ONE: INTRODUCTION	
Background to the Study	1
Statement of the Problem	6
Research Objectives	8
Significance of the Study	8
Research Hypothesis (The null hypothesis)	9
Delimitations	10
Limitations	11
Organization of the Study	12
CHAPTER TWO: LITERATURE REVIEW	
Introduction	13
Perfluoroalkyl Substance (PFAS)	14
Introduction	14
Definition and Classification of PFAS	15
Perfluoroalkyl Carboxylic Acids (PFCAs)	16

Perfluoroalkane (or -alkyl) Sulphonic Acids (PFASs)	16
Sources and Pathways of PFAS in the Environment	17
Some Physico-chemical Properties of PFOA and PFOS	19
Pathways of Human Exposure to PFAS	20
Occurrence of PFAS in the Environment	21
Dust	21
Water	22
Levels in Biota and Wildlife	23
Fish and Seafoods	24
Sediment, Sludge and Soil	25
Human Biomonitoring	27
Levels of PFAS in Africa	27
Toxicology of PFAS	28
Cancer	29
PFAS Impact on Reproduction and Development	30
Endocrine Disruption	30
Human Toxicity and Health Risk Assessment	32
PFAS Determination in Aqueous Samples	34
Remediation Technologies for PFAS	36
Polychlorinated Biphenyls (PCBs)	39
Introduction	39
PCB Mixtures and Trade Names	41
Production and Use of PCBs	42
Physico-chemical Properties of PCBs	43
Human Exposure to PCBs	46

Occurrence of Polychlorinated Biphenyls (PCBs) in the Environment	47
Air	47
Water	47
Biota	48
Soil and Sediments	50
Food Crops, Cereals and Vegetables	51
Human Biomonitoring	53
Abiotic Factors	53
Toxicology of PCBs	54
Identified Research Gaps and Measures Implemented to address them	55
Chapter Summary	56
CHAPTER THREE: METHODOLOGY	
Introduction	57
Study Area	57
Sampling	59
Analytical Techniques	60
Chemicals for PFAS Analysis	60
Chemicals for Polychlorinated Biphenyls (PCBs) Analysis	61
Chemicals for Fluoride Determination in Aqueous Samples after Gamma Irradiation	61
Surface Water (Taniyasu <i>et al.</i> (2005))	62
Extraction of PFAS from Sediment	63
Equipment for PFAS Analysis	63
Liquid Chromatography – Mass Spectrometry analysis	64
Liquid Chromatography (LC) Conditions	64

Mass Spectrometer Configuration and Conditions	65
Identification and Quantification of PFAS	68
Extraction of Polychlorinated Biphenyls (PCBs)	70
Gas Chromatography–Mass Spectrometry Analysis of PCBs	70
Identification and Quantification of PCBs	71
Radiolytic Decomposition of PFOA	72
Irradiation Instrumentation	72
Fluoride determination in the irradiated aqueous solutions of PFOA	73
Sample preparation	74
Calibration and electrode conditioning	74
Analysis	75
Quality control	75
Cleaning and storage	75
Human Health Risk Computations	75
Carcinogenic risk	75
Carcinogenic effects for organic micropollutants (PFAS and PCBs) in water	76
Carcinogenic effects of organic micropollutants (PFAS and PCBs) in soils/sediment	76
Non-carcinogenic risks to human health	77
Non-carcinogenic effects for contaminants (PFAS and PCBs)	79
Non-Carcinogenic Effects for Contaminants (PFAS and PCBs)	80
Ecological Risk Analysis	80
Risk Quotient of Single Organic Micropollutants	80
Risk Quotient of Composite Organic Micropollutants	81

Data Analysis	81
Chapter Summary	82
CHAPTER FOUR: RESULTS AND DISCUSSION	
Introduction	83
Perfluoroalkyl Substances (PFAS)	83
Quality Assurance and Control	83
Occurrence and Detection Frequency of PFAS	86
Levels of PFAS in Water and Sediment Samples from the Pra River Basin as compared to Recommended W.H.O and US EPA limits	88
Spatial Distribution of PFAS in the Pra River basin	89
Comparison of PFAS levels in the Pra River Basin with other Studies	95
Multivariate Statistical Analysis of Surface Water and Sediment Data from the Pra River Basin	98
Source Identification (Surface Water)	98
Principal Component Analysis of PFAS in Sediment from the Pra River Basin	102
Carcinogenic and Non-carcinogenic Health Risk Assessment of PFAS in Surface Water and Sediments from the Pra River Basin	106
Surface Water from the Pra River Basin	106
Non-Carcinogenic Analysis of PFAS in Surface Water from Pra River Basin	112
Carcinogenic Risk Analysis of PFAS in Surface Water from Pra River Basin	113
Sediment	114
Non-Carcinogenic Analysis of PFAS in Sediment from Pra River Basin	121

Comparison of Non-Cancer Risk Index of PFAS in the Pra River Basin	122
Carcinogenic Risk Analysis of PFAS in Sediment from Pra River Basin	123
Comparison of Cancer Risk and Exposure through Ingestion and Dermal Contact from Surface Water and Sediment	124
Ecological Risk Assessment	125
Toxicity of PFAS in the Pra River Basin	125
Risk Assessment of Single PFAS Compounds	127
Risk Assessment of PFAS Mixture	128
Decomposition of PFAS using Radiolytic Method: A Case Study of PFOA	130
Role of Solvated Electron ($e(aq)^-$), Carbon Dioxide Radical Ion ($CO_2^{\circ-}$) and Phosphate Buffer in the Decomposition of PFOA	132
Reaction of PFOA with Carbon dioxide Radical ($CO_2^{\circ-}$) in N_2O -saturated Environment	133
Reaction of PFOA with solvated electron ($e(s)^-$) in Argon saturated environment	135
Reaction of PFOA with solvated electron and carbon dioxide radical anion in argon-saturated environment	137
Identification of Optimum Conditions for Higher Yield Polychlorinated Biphenyls (PCBs)	143
Quality Assurance and Quality Control	143
Total PCB Concentration ($\sum PCB$) in the Pra river basin	145
Regression and Correlation of Total PCBs in Water and Sediments	150
Spatial Distribution of PCB Congeners	150
PCB Homologue Profile	153

PCB Congener Profile	155
Congener Profiled Similarity	159
Sampling Points PCB Congener Profile Comparison	161
Seasonal PCB Congener Profile Comparison	161
Hierarchical Cluster Analysis of PCBs	162
Redundancy Analysis of PCBs	164
Human Health Risk Assessment of PCBs	169
Hazard Quotient and Hazard Index of PCBs	171
Chapter Summary	171
CHAPTER FIVE: SUMMARY, CONCLUSION AND RECOMMENDATIONS	
Overview	172
Summary	172
Conclusions	183
Recommendations	188
REFERENCES	190
APPENDICES	238
APPENDIX A: PFAS ANALYSED IN THIS STUDY WITH THEIR ABBREVIATIONS AND NAMES OF SUPPLIERS OF THEIR STANDARDS	238
APPENDIX B: DETECTION FREQUENCY OF PFAS IN THE PRA RIVER BASIN BASED ON THE 8 DETECTED PFAS	239
APPENDIX C: LEVELS OF PFAS DETERMINED IN WATER SAMPLES COLLECTED DURING AUGUST	

AND SEPTEMBER, 2021 FROM THE PRA RIVER BASIN.	240
APPENDIX D: LEVELS OF PFAS DETERMINED IN WATER SAMPLES COLLECTED DURING NOVEMBER AND DECEMBER 2021 FROM THE PRA RIVER BASIN	241
APPENDIX E: LEVELS OF PFAS DETERMINED IN SEDIMENT SAMPLES COLLECTED DURING AUGUST AND SEPTEMBER, 2021 FROM THE PRA RIVER BASIN	242
APPENDIX F: LEVELS OF PFAS DETERMINED IN SEDIMENT SAMPLES COLLECTED DURING NOVEMBER AND DECEMBER, 2021 FROM THE PRA RIVER BASIN	243
APPENDIX G: MEAN LEVELS OF PFAS IN WATER SAMPLES AT THE INDIVIDUAL SAMPLING POINTS FROM AUGUST TO DECEMBER, 2021	244
APPENDIX H: MEAN LEVELS OF PFAS IN SEDIMENT SAMPLES AT THE INDIVIDUAL SAMPLING POINTS FROM AUGUST TO DECEMBER, 2021	245
APPENDIX I: RISK QUOTIENT OF PFAS FOR THE INDIVIDUAL SITES	246
APPENDIX J: LEVELS OF PCBS DETERMINED IN WATER SAMPLES COLLECTED DURING AUGUST AND SEPTEMBER, 2021 FROM THE PRA RIVER BASIN(NG/L)	247

APPENDIX K: LEVELS OF PCBS DETERMINED IN WATER SAMPLES COLLECTED DURING NOVEMBER AND DECEMBER, 2021 FROM THE PRA RIVER BASIN(NG/L)	248
APPENDIX L: LEVELS OF PCBS DETERMINED IN SEDIMENT SAMPLES COLLECTED DURING AUGUST AND SEPTEMBER, 2021 FROM THE PRA RIVER BASIN(NG/G)	249
APPENDIX M: LEVELS OF PCBS DETERMINED IN SEDIMENT SAMPLES COLLECTED DURING NOVEMBER AND DECEMBER, 2021 FROM THE PRA RIVER BASIN(NG/G)	250
APPENDIX N: CORRELATION MATRIX OF SAMPLING POINTS FROM THE PRB (WATER SAMPLES)	251
APPENDIX O: CORRELATION MATRIX OF SAMPLING POINTS FROM THE PRB (SEDIMENT SAMPLES)	252
APPENDIX P: CORRELATION MATRIX OF PCBS IN WATER SAMPLES FROM PRB	253
APPENDIX Q: CORRELATION MATRIX OF PCBS IN SEDIMENT SAMPLES FROM PRB	254
APPENDIX R: CORRELATION MATRIX FOR CONCENTRATION OF PCB CONGENERES IN WATER SAMPLES IN THE DRY SEASON	255

APPENDIX S: CORRELATION MATRIX FOR CONCENTRATION OF PCB CONGENERS IN WATER SAMPLES IN THE WET SEASON	256
APPENDIX T: CORRELATION MATRIX FOR CONCENTRATION OF PCB CONGENERS IN SEDIMENT SAMPLES IN THE WET SEASON	257
APPENDIX U: CORRELATION MATRIX FOR CONCENTRATION OF PCB CONGENERS IN SEDIMENT SAMPLES IN THE DRY SEASON	258
APPENDIX V: HAZARD QUOTIENT AND INDEX FOR NON- CARCINOGENIC HUMAN HEALTH RISKS POSED BY PCBS IN WATER OF STUDY AREA VIA DIFFERENT PATHWAYS	259
APPENDIX W: HAZARD QUOTIENT AND INDEX FOR NON- CARCINOGENIC HUMAN HEALTH RISKS POSED BY PCBS IN SEDIMENT OF STUDY AREA VIA DIFFERENT PATHWAYS	260

LIST OF TABLES

		Page
1	List of Abbreviations and Names of Some PFAS	16
2	Representative Examples of Perfluoroalkyl Sulphonic Acids	17
3	Some Physico-Chemical Properties of PFOA and PFOS	20
4	Dioxin-Like PCB Congeners	40
5	Some Aroclor Mixtures	42
6	Sampling Locations with their Coordinates	58
7	The Gradient Elution Profile of PFAS	64
8	Retention Times for the Various PFAS Analytes	65
9	Mass Spectrometer Configuration and Condition Used	65
10	Mass Spectrometer Parameters of the Targeted Compounds	67
11	Retention Times for the Various PCB Analytes	72
12	An Exemplar Dosimetry of PFOA	73
13	Parameter Definition and Exposure Assumption	77
14	Method Limits, Linearity, Variation and Recovery of the 8 PFAS in Water Samples	84
15	Method Limits, Linearity, Variation and Recovery of the 8 PFAS in Sediment Samples	85
16	Total Mean Levels of PFAS in Surface Water and Sediment in the Pra River Basin	89
17	Comparison of PFAS Concentrations in Water Samples from Pra River Basin with those from Other Countries And Previous Studies	97

18	Comparison of PFAS Concentrations in Sediment Samples from Pra River Basin with those from Other Countries	98
19	Statistics of PFAS Levels(ng/L) in Water Samples Collected from the Pra River Basin During Wet and Dry Seasons	107
20	Chronic Daily Intake (CDI) of PFAS for Cancer Risk through Oral Ingestion and Dermal Contact in Water	108
21	Chronic Daily Intake (CDI) of PFAS for Non-Cancer Risk through Oral Ingestion and Dermal Contact in Surface Water	109
22	Minimum, Maximum and Mean Values of Non-Carcinogenic Human Health Risks Posed by PFAS in Water of Study Area through Oral Ingestion and Dermal Contact	110
23	Cancer Risk Assessment Associated with the Use of Raw Water from the Pra River Basin	111
24	Statistics of PFAS Levels(ng/g) in Sediment Samples Collected from the Pra River Basin during Wet and Dry Seasons	116
25	Chronic Daily Intake (CDI) of PFAS for Cancer Risk through Oral Ingestion and Dermal Contact in Sediment	117
26	Chronic Daily Intake (CDI) of PFAS for Non-Cancer Risk through Oral Ingestion and Dermal Contact in Sediment	118
27	Minimum, Maximum and Mean Values of Non-Carcinogenic Human Health Risks Posed by Pfas in Sediment of Study Area via Different Pathways	119
28	Cancer Risk Assessment Associated with the Exposure of Sediment from Pra River Basin	120

29	NOEC Values of Single PFAS Compounds for Three Selected Aquatic Organisms in the Pra River Basin	127
30	Mean Risk Quotient Of Single Organic PFAS Compounds	128
31	Risk Quotient of Composite PFAS Compounds for an Aquatic System (Pra River Basin)	129
32	Conditions Observed Before Gamma Irradiation of PFOA and Associated Reactive Species	133
33	Percentage of Defluorination and Yield of Fluoride Ions from Reactions Involving PFOA, Solvated Electrons and Carbon Dioxide Radical Anions	143
34	Method Limits, Variation and Recovery of 12 PCBs from Water	144
35	Method Limits, Linearity, Variation and Recovery of the 12 PCBs in Sediment Samples	144
36	Distribution Statistics of PCB Congener Profile of Water Samples from the Pra River Basin	157
37	Distribution Statistics of Pcb Congener Profile of Sediments from the Pra River Basin	158
38	PCB Cancer Risk Values Associated with the Use of Water from Pra River Basin	170
39	Cancer Risk Associated with Exposure to Sediment PCBs from PRB	171

LIST OF FIGURES

	Page
1	Structural Formulae of PFOA and PFOS 19
2	The Electron Density Distribution (Inner Grid) and Electrostatic Potential (Outer Grid) of Three Different PCB Congeners (A) 4,4'-Dichloro-Biphenyl (B) 3,4,4',5-Tetrachloro-Biphenyl And (C) 2,2',4,4',5,5'-Hexachloro-Biphenyl 45
3	A Map of Southern Ghana Showing the Sampling Sites 59
4	Some Calibration Chromatograms of 0.1,5,10 Ppt Pfos (A, B, C) Standards 69
5	An Example of a Calibration Curve of PFOS 70
6	An Electrometer with Flouride Ion Selective Electrode 77
7	Distribution of PFAS in Water Samples Collected from the Pra River Basin during Rainy Season (August-September, 2021). 91
8	Distribution of PFAS in Water Samples Collected from the Pra River Basin during Dry Season (November-December, 2021) 91
9	Boxplot of Total PFAS Levels in Water Samples Collected from the Pra River Basin during Rainy and Dry Seasons (August-December, 2021) 92
10	Distribution of PFAS in Sediment Samples Collected from the Pra River Basin during Rainy Season (August-September, 2021). 93

11	Distribution of PFAS in Sediment Samples Collected from the Pra River Basin during Dry Season (November- December, 2021)	93
12	Boxplot of Total PFAS in Sediment Samples Collected from the Pra River Basin during Rainy And Dry Seasons (August-December, 2021)	94
13	3-Dimensional Plot of PCA Showing Loadings and Score Plots from Three Components in Surface Water across the Sampling Points	99
14	Dendrogram Showing Hierarchical Clustering of PFAS in Surface Water from the Pra River according to Similarity Matrix	99
15	Dendrogram Showing Hierarchical Clustering of Sites Contaminated with PFAS in Surface Water from the Pra River according to Similarity Matrix	100
16	A PCA Biplot Showing Loadings and Score Plots from PC1 And PC2 Components across Sampling Points.	101
17	A Pca Biplot Showing Loadings and Score Plots from PC1 And PC3 Components across the Sampling Points.	102
18	3-Dimensional Plot of PCA Showing Loadings and Score Plots from Three Components in Sediment across the Sampling Points	103
19	A PCA Biplot Showing Loadings and Score Plots from PC 1 And PC2 Components across the Sampling Points	104

20	A PCA Biplot Showing Loadings and Score Plots from PC1 and PC3 Components across The Sampling Points	104
21	Dendrogram Showing Hierarchical Clustering of PFAS in Sediment from the Pra River according to Similarity Matrix	105
22	Dendrogram Showing Hierarchical Clustering of Sites Contaminated with PFAS in Sediment from the Pra River according to Similarity Matrix.	106
23	Non-Cancer Risk Index Of PFAS in the Pra River Basin	122
24	Vertical Bar Chart Illustration of Cancer Risk Summary Results in Surface Water and Sediments	124
25	Toxicity Data of PFAS on Three Trophic Level Organisms (Algae, Crustacea and Fish) in Freshwater Ecosystems	126
26	A Graph Showing the Concentration of Fluoride Ions in $1\mu\text{m}$ PFOA Aqueous Solution at pH 11 Irradiated with Gamma at Defluorination Efficiency of 98%.	131
27	A Graph Comparing the Levels of Fluoride Ions at pH 6 And pH11.	131
28	A Graph Comparing Two pH Values After Absorbed γ -Radiation	132
29	A Graph Comparing the Levels of Fluoride Ions at pH 6 And pH11 in an N_2O -Saturated Environment with Main Species being Carbon Dioxide Radical Anion	134
30	A Graph Comparing the Levels of Fluoride Ions in Buffered Solutions at pH 6 and pH11 in a N_2O -Saturated	

	Environment with Main Species being Carbon Dioxide Radical Anion.	134
31	A Graph Showing pH of PFOA Irradiated Solution Saturated with N ₂ O Gas with Main Reacting Species being Carbon Dioxide Radical Anion.	135
32	A Graph Comparing the Levels of Fluoride Ions at pH 6 and pH11 in an Argon-Saturated Environment with Main Species being Solvated Electron.	136
33	A Graph Comparing the Levels of Fluoride Ions in Buffered Solution at pH 6 and pH11 in an Argon-Saturated Environment with Main Species being Solvated Electron	136
34	A Graph Comparing the Levels of Fluoride Ions at pH 6 and pH11 in an Argon-Saturated Environment with Main Species being Solvated Electron and Carbon Dioxide Radical Anion.	138
35	A Graph Comparing the Levels of Fluoride Ions in Buffered Solution at pH 6 and pH11 in an Argon-Saturated Environment with Main Species being Solvated Electron and Carbon Dioxide Radical Anion.	138
36	A Graph Comparing Two pH Values at 6 and 11 after Absorbed Radiation during PFOA Reaction with Solvated Electrons and Carbon Dioxide Radical Anions	139
37	A Graph Comparing the Levels of Fluoride Ions in Buffered and Non-Buffered Solutions at pH11	

- in an Argon-Saturated Environment with Main Species
being Solvated Electron and Carbon Dioxide Radical Anion. 140
- 38 A Graph Comparing the Levels of Fluoride Ions in Two Buffered
Solutions with Main Reacting Species being (Solvated Electron
and Carbon Dioxide Radical Anion) and (Solvated Electrons
Only) at pH 11 in an Argon-Saturated Environment. 140
- 39 A Graph Comparing the Levels of Fluoride Ions in Buffered
(Solvated Electron and Carbon Dioxide Radical Anion) and
Non-Buffered (Solvated Electrons Only) Solutions at pH 11
in an Argon-Saturated Environment. 141
- 40 A Graph Comparing the Levels of Fluoride Ions in Both
Buffered and Non-Buffered Solutions at pH 11 in an
Argon-Saturated Environment with Main Reacting
Species being $1\mu\text{m}$ PFOA, Solvated Electrons and
Carbon Dioxide Radical Anion. 142
- 41 A Graph Comparing the Levels of Fluoride Ions in
Both Buffered and Non-Buffered Solutions at pH 11
in an Argon-Saturated Environment with Main Reacting
Species being 0.5mm PFOA, Solvated Electrons
and Carbon Dioxide Radical Anion. 142
- 42 Total PCB Concentrations in Water Samples from the
Pra River Basin 145
- 43 Box-Plot of PCB Distribution in Water from the
Pra River Basin 146

44	Total PCB Concentrations in Sediments from the Pra River Basin	147
45	Box-Plot of PCB Distribution in Pra River Basin	147
46	Spatial Dtribution of PCBs in Water Samples in the Wet Season	151
47	Spatial Distribution of PCBs in Water Samples in the Dry Season	151
48	Spatial Distribution of PCBs in Sediments Samples in the Wet Season	152
49	Spatial Distribution of PCBs in Sediments Samples in the dry Season	152
50	Proportions of PCB Cngeners Detected in the Pra River Basin and Soil Sediment	153
51	PCB Homologues in Water and Sediment Samples from the Pra River Basin	154
52	A Graph Showing Correlation between Concentration of PCBs in the Dry and Wet Seasons	160
53	Dendrogram of Water Sampling Sites PCB Profiles	163
54	Dendrogram of Sediment Sampling Sites PCB profiles	163
55	A 3D Principal Components of PCBs Observed in Water Samples Collected from PRB	164
56	Principal Components of PCBs Observed in Water Samples Collected from PRB (2D)	166
57	Principal Components of PCBs Observed in Water Samples Collected from PRB (2D)	167

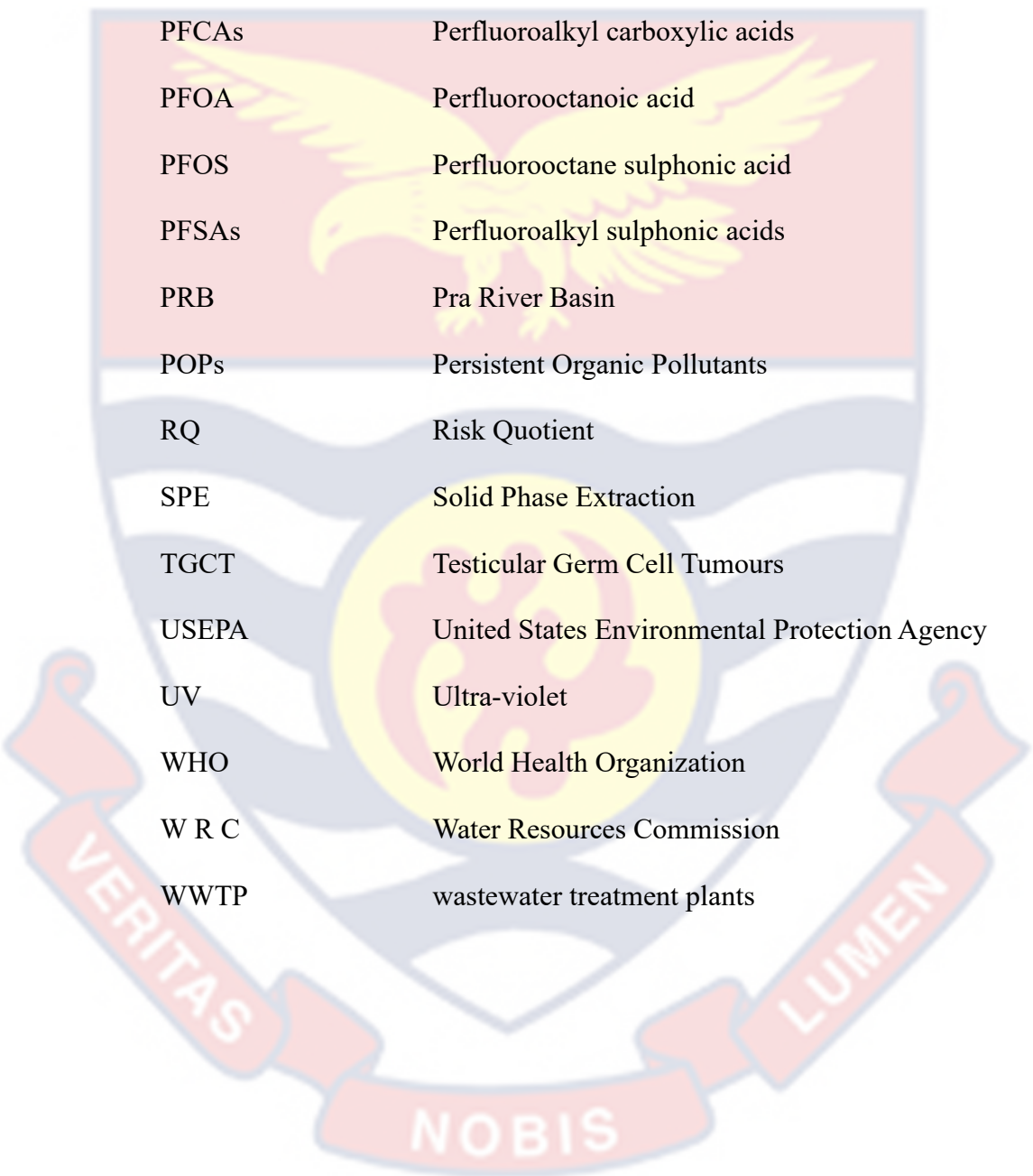
58	Principal Component Analysis of PCBs in Sediments Collected from PRB	168
59	3-D Principal Component Analysis of PCB in Sediments Collected from PRB	169
60	Principal Component Analysis of PCBs in Sediments collected from PRB	169



LIST OF ABBREVIATIONS

The background of the page features a large, semi-transparent watermark of the University of Cape Coast logo. The logo is a shield-shaped crest with a yellow eagle with spread wings in the center. Below the eagle is a yellow circle containing a red figure. The shield is flanked by two red banners with white text: 'VERITAS' on the left and 'LUMEN' on the right. At the bottom of the shield is a red banner with white text: 'NORIS'.

APFO	ammonium perfluorooctanoate
CASRN	Chemical Abstract Service Registry Number
CDI	Chronic Daily Intake
cDNA	Complementary Deoxyribonucleic Acid
CR	Cancer Risk
CYP1A1	Aryl hydrocarbon hydroxylase
EB	Electron Beam
EFSA	European Food Safety Authority
EtFOSE	N-ethyl perfluorooctane sulfonamide
ESI-MS	Electro- Spray Ionization- Mass Spectrometry
EUROSTAT	European Statistical Office
FTOHs	Fluorotelomer alcohols
GWCL	Ghana Water Company Limited
HCA	Hierarchical Cluster Analysis
HI	Hazard Index
HQ	Hazard quotient
IS	Internal Standard
IWRM	Integrated Water Resources Management
LoD	Limit of Detection
LoQ	Limit of Quantification
MEC	Measured Environmental Concentration
NOEC	No Observed Effect Concentration

The background of the page features a large, semi-transparent watermark of the University of Cape Coast crest. The crest is a shield-shaped emblem with a yellow eagle with outstretched wings in the center. The shield is divided into three horizontal sections: a top red section, a middle white section with blue wavy lines, and a bottom blue section. A yellow circular emblem is centered in the white section. Below the shield is a red ribbon banner with the Latin motto 'VERITAS NOBIS LUMEN' written in white capital letters.

OMP	Organic Micropollutant
PCA	Principal Component Analysis
PCBs	polychlorinated biphenyls
PFAS	perfluoroalkyl substance
PFCAs	Perfluoroalkyl carboxylic acids
PFOA	Perfluorooctanoic acid
PFOS	Perfluorooctane sulphonic acid
PFSAs	Perfluoroalkyl sulphonic acids
PRB	Pra River Basin
POPs	Persistent Organic Pollutants
RQ	Risk Quotient
SPE	Solid Phase Extraction
TGCT	Testicular Germ Cell Tumours
USEPA	United States Environmental Protection Agency
UV	Ultra-violet
WHO	World Health Organization
W R C	Water Resources Commission
WWTP	wastewater treatment plants

CHAPTER ONE

INTRODUCTION

Background to the Study

The increased usage and unprecedented release of anthropogenic particles into the environment, made from a plethora of materials and originating from various sources is a specific feature of the fresh water systems. Anthropogenic micropollutants are deliberately or unintentionally released in major amounts into nearly all compartments of the environment (Gavrilescu *et al.*, 2015). Extensive evidence demonstrates a significant surge in the global production of anthropogenic chemicals between the years 1930 and 2000, with an annual output from 1 million to 400 million tons per year (Gavrilescu *et al.*, 2015). Statistics published by EUROSTAT in 2016 revealed that between 2004 and 2013, nearly 50% of the total production of chemicals contained environmentally harmful compounds and approximately 20% of them had significant acute impacts on the environment (Gavrilescu *et al.*, 2015).

The Pra River Basin, located in south western part of Ghana, is a vital freshwater ecosystem that supports numerous socio-economic activities and provides a critical source of water for domestic, agricultural, and industrial purposes (Water Resources Commission, 2012). However, this essential resource is increasingly threatened by the presence of organic micropollutants, such as per- and polyfluoroalkyl substances (PFAS) and polychlorinated biphenyls (PCBs) (Essumang *et al.* 2017; Lapworth *et al.* 2012; Ye *et al.* 2017). These pollutants, originating from various anthropogenic sources, pose significant risks to the ecosystem's health, as well as the well-being of the surrounding communities (Kandie *et al.* 2020).

PFAS and PCB are persistent organic pollutants known for their resistance to degradation, potential toxicity and their ability to accumulate in the environment. PFAS are widely utilized in diverse industrial and consumer applications, including firefighting foams, non-stick coatings, and water-repellent fabrics. PCBs, on the other hand, were widely used in electrical equipment, hydraulic fluids, and as heat transfer agents before their production were banned due to their harmful effects (Adu-Kumi *et al.*, 2015; Asante *et al.*, 2011; Essumang *et al.*, 2013, 2017; Ntow, 2001).

In the environment, organisms, including humans, are not exposed to just individual organic micropollutants such as PFAS and PCBs, but to complex chemical mixtures, the individual components of which might be present at concentrations too low to raise concern (Schwarzenbach, 2016). However, additive or even synergistic effects can render such mixtures dangerously potent. For example, a study has shown that when five estrogenic compounds are mixed in concentrations all below levels at which their individual effects can be detected, their cumulative impact on fish was detrimental (Brian *et al.*, 2005). It was long assumed that only compounds with the same mode of toxic action are concentration-additive in mixtures, but research has shown that even mixtures of compounds with different modes of action may also cause significant adverse effects (Altenburger *et al.*, 2018).

The discharge of organic micropollutants, such as PFAS and PCBs, into the Pra River Basin is a matter of concern due to their detrimental effects on aquatic organisms, wildlife, and human health. Extensive studies have demonstrated that these micropollutants can bioaccumulate in the food chain, leading to prolonged exposure in both humans and wildlife. The potential health

implications include developmental abnormalities, disrupted immune function, and high risk of cancers. Furthermore, these pollutants can disrupt the delicate ecological balance of the river basin, adversely affecting aquatic biodiversity and overall ecosystem functioning. Specifically, PFAS and PCB contamination significantly impacts soil quality. Research has indicated that the presence of these organic micropollutants in soil can reduce microbial activity, thereby influencing nutrient cycling, organic matter decomposition, and soil fertility. Additionally, PFAS and PCBs can alter soil pH and disrupt soil structure, impeding plant growth and nutrient uptake. The impact of PFAS and PCBs on wildlife is also significant. Exposure to these compounds has been linked to reproductive disorders, reduced fertility, developmental abnormalities, and disrupted hormone regulation in various wildlife species. In aquatic environments, studies have demonstrated that both classes of compounds affect fish reproduction, growth, and inhibit the growth and development of aquatic plants and algae. The scientific community has amassed strong evidence associating PFAS and PCB compounds with various cardiovascular risk factors and certain types of cancer in humans and animals (Butenhoff, 2009; Costa et al., 2009; Hamers et al., 2011; Huerta-Fontela et al., 2011; Kennedy et al., 2004; Lau et al., 2004; Liu et al., 1996; Olsen et al., 2003; Robertson & Hansen, 2001; USEPA, 2000; Westerhoff et al., 2005).

It is important to highlight that Ghana has not developed its own specific regulatory standards for POPs and other emerging organic pollutants, but adapts United States Environmental Protection Agency (USEPA) standards (Bruce-Vanderpuije *et al.*, 2021). To strengthen its control on chemicals, Government of Ghana through the act of parliament established the legal framework for the

management of persistent, bioaccumulative and toxic substances including POPs and also implement the content of the Stockholm Convention. The relevant acts of Parliament may include the following but not limited to Environmental Protection Agency Act, 1994 (Act 490), and the Hazardous and Electronic Waste Control and Management Act, 2016 (Act 917) for regulation of pesticides and wastes. Briefly, Act 917 identifies the need for appropriate recycling facilities for the proper disposal and management of POPs e-waste and hazardous wastes. Aside these, the Food and Drugs Law 1992, (PNDCL 305B) was enacted to control the manufacture, import, export, distribution, sale, use and advertisement of food, drugs, cosmetics, household chemicals and medical devices. However, these laws are inadequate and incapable of dealing with the specific requirements of the Stockholm Convention on POPs.

To date, it remains impossible to fully prevent harmful substances from entering an aquatic environment. Some pathways through which pollutants reach surface waters are hardly controllable. These include agricultural runoff and spray operations. The manufacturing and use of chemicals, however, could be controlled more easily. From the regulatory side, Water Resource Commission, Ghana in 2001 established a River Basin Board and its Secretariat as decentralized management body to facilitate the implementation of Integrated Water Resources Management (IWRM) of which Pra River was a fourth priority basin. The Pra Basin Board was given the mandate to regulate the water resource of the basin by administering and monitoring compliance of existing regulations (i.e. water use regulations (LI 1692) and drilling license and groundwater development regulations (LI 1827) as well as any other regulations adopted from time to time; initiating establishment of buffer strips/areas to

protect the quality of open water bodies (rivers and lakes) and enhance community livelihood systems. Another focus of the board was to support programs targeting the management of water resources such as facilitating stakeholder information and networking among partners on IWRM and also complete the IWRM plan for the basin.

Although a supervisory board such as River Basin Board (RBB) has been established to oversee and regulate the activities on the Pra River and other river basins, stakeholders do not adhere to the laws that regulate use of water from the river basin. As a result of non-adherence to the laws and regulations, human activities have led to a heavy pollution of the river basin (Water Resource Commission, 2022). Organic chemicals such as polychlorinated biphenyls and perfluoroalkyl substances have been used in Ghana for several decades, both for agricultural and public health purposes and coolants in transformers, with their residues having been detected in water, sediments, vegetable crops, aquatic organisms and in humans (Adu-Kumi *et al.*, 2010; Asante *et al.*, 2011; Bentum *et al.*, 2012; Essumang *et al.*, 2013, 2017).

Despite the evident risks, limited research has been conducted on the occurrence, distribution, and environmental fate of PFAS and PCBs in the Pra River Basin. It has been observed that the focus of contaminant of concern research on the Pra river basin has been on the nutrients (Akrasi *et al.*, 2008), radioactive nuclides (Adukpo *et al.*, 2015), perfluoroalkyl acids (Essumang *et al.*, 2017), and heavy metals (Duncan *et al.*, 2018). The probable occurrence of a diverse array of OMPs in the Pra River basin, along with the associated risks to human health and the environment, underscores the importance of conducting this research. This research aims to identify the spatio-temporal patterns of these

contaminants, evaluate their levels, assess potential risks, develop remediation strategies, and ensure water safety. Understanding the sources, pathways, and behaviour of these pollutants in the basin is crucial for implementing effective management and mitigation strategies. Furthermore, assessing the potential risks associated with their presence will enable policymakers and stakeholders to make informed decisions and prioritize remediation efforts.

This thesis aims to bridge the existing knowledge gaps by conducting a comprehensive study on distribution, human health and environmental assessment of PFAS and PCBs in the Pra River Basin. The research focused on determining the levels of contamination, identifying potential pollution sources, assessing the risks of these micropollutants, and evaluating their impacts on the environment and human health. The findings of this study will provide a scientific basis for the development of strategies to mitigate the contamination and protect the long-term sustainability of the Pra River Basin.

Statement of the Problem

The water resources of the Pra River Basin are under the threat of pollution from organic micropollutants (OMPs such as PFAS and PCBs) from effluents from industrial, municipalities and urban settlements, agricultural run-offs and fishing, and hazardous chemicals from sprayed operations and mining (Water Resources Commission, 2022). The continuous human activities on the Pra River Basin especially illegal mining had cause massive pollution which had turned the hitherto clean water into brownish colour (Ghana News Agency, 2009). Various scientific reports have also confirmed the pollution of the Pra Basin with heavy metals such as Hg, Pb, Cd, Cr, Ni, Fe, As, Cu, Zn (Ansa – Asare *et al.* 2012; Bessah *et al.* 2021; Duncan *et. al.* 2018; Kortei *et al.*, 2020).

So far scientific literature is one way repleted with the reports on threat of heavy metal pollution as compared to only few published studies on the threat of organic micropollutants (OMPs) pollution including PFAS and PCBs (Essumang *et al.*, 2017) in the Pra basin. This arises from the high cost of procurement of standards and laboratory analyses of OMPs. The presence of organic micropollutants in a river basin such as the Pra reduces the raw water quality and aquatic life. It is reported that water quality tests conducted on samples from Pra River basin indicated a steady deterioration of some raw water quality parameters such as turbidity, colour and pH.(Ministry of Water Resources, Works and Housing, 1998). Another report labelled some reservoirs within the Pra Basin as having poor water quality due to low dissolved oxygen content (Adombire *et al.*, 2013).

Water resources contaminated with PFAS and PCBs have been strongly associated with degenerative health implications for humans and animals, environment and have disrupted traditional cultural uses of river by the resident tribes (Huerta-Fontela *et al.*, 2011; Westerhoff *et al.*, 2005). The existence of OMPs in a river basin can cause detrimental impacts on river water quality and also adversely affect the biota. It has been reported that the presence of PFAS and PCBs in humans is strongly associated with toxic biological effects such as mutagenicity, genotoxicity and estrogenic activities for up to multiple generations (Choi *et al.*, 2013; Patisaul, 2009; Wilkinson *et al.*, 2016a).

To reduce this knowledge gap, this study examines PFAS and PCB contamination across different locations and time periods in surface water and sediments to obtain information on the potential exposure and risk associated with the use of water resources from the Pra River Basin. Based on the outcome,

effective and efficient remediation strategy for OMPs in water resources from the Pra Basin for local use is proposed.

Research Objectives

The main aim of this study was to determine the levels of PFAS and PCB at some sections (Central and Western Regions) of the Pra river basin and decompose PFAS by water radiolysis. The specific objectives were to:

1. determine the types and percentage detection of PFAS and PCBs in surface water and sediment from the Pra River Basin.
2. determine the levels and spatial distribution of PFAS and PCBs in surface water and sediments at the different sampling sites in the Pra River Basin.
3. investigate the temporal distribution of the selected PFAS and PCBs.
4. conduct multivariate analysis of PFAS and PCBs and identify their potential sources.
5. assess the potential human and ecological risks associated with PFAS and PCBs.
6. estimate the risk quotient of composite PFAS based on concentration addition (CA) model at each sampling site.
7. decompose PFAS by water radiolysis using solvated electrons and carbon dioxide radical anion.

Significance of the Study

Upon the recognition of the scope of the potential problems and negative effects of PFAS and PCBs on biota and the environment, this study would among other things help to achieve the following:

1. establish the current levels and extent of pollution of PFAS and PCBs in the Pra Basin.
2. give baseline data to help policymakers in decision making
3. establish the potential of the selected PFAS and PCBs in surface water and sediments to cause harm.
4. develop efficient and effective method of decomposing PFAS such as PFOA in aqueous solution.

By accomplishing these objectives, this study aimed to enhance the understanding of PFAS and PCB contamination in the Pra Basin, facilitate effective management practices, and contribute to the preservation of the basin's ecological integrity and the well-being of its inhabitants.

Research Hypothesis (The null hypothesis)

H₀₁: The percentage detection of PFAS and PCBs in both surface water and sediment is consistent across all sampled locations.

H_{a1}: The percentage detection of PFAS and PCBs in surface water and sediment exhibits variability among the different sampling locations.

H₀₂: The concentrations of PFAS and PCBs in surface water and sediments from the Pra River Basin do not exceed the recommended limits established by both the W.H.O and USEPA.

H_{a2}: The concentration of PFAS and PCBs in surface water and sediments from the Pra River Basin surpass the recommended limits established by either the W.H.O or USEPA.

H₀₃: The spatial and temporal distribution of PFAS and PCBs in surface water and sediments is the same for all sampling locations.

H_{a3}: The spatial and temporal distribution of PFAS and PCBs in surface water and sediment varies across the different sampling locations.

H_{o4}: There is no significant variance in the levels of PFAS and PCBs in the Pra River basin indicating that these contaminants do not have distinct patterns or sources.

H_{a4}: There is a significant variance in the levels of PFAS and PCB in the Pra River basin suggesting distinct patterns and multiple sources of contamination.

H_{o5}: The concentration of PFAS and PCBs in the surface water and sediments from the Pra River Basin do not pose human and ecological risks.

H_{a5}: The concentration of PFAS and PCBs in the surface water and sediments from Pra River Basin pose human and ecological risks.

H_{o6}: The additive concentrations of composite PFAS do not pose risk to each sampling location.

H_{a6}: The additive concentrations of composite PFAS pose risk to each sampling location.

H_{o7}: The radiolytic decomposition of PFOA using ionizing radiation will not result in a significant reduction its concentration.

H_{a7}: The radiolytic decomposition of PFOA using ionizing radiation will result in significant reduction its concentration.

Delimitations

This study focused on examining the spatial and temporal patterns of two categories of Organic Micropollutants (OMPs), namely PCBs (Polychlorinated Biphenyls) and PFAS (Per- and Polyfluoroalkyl Substances), within the Pra River basin. Additionally, it explored the degradation of perfluorooctanoic acid salt through water radiolysis. The study also focused on two environmental

sample matrices of the Pra River Basin. The extent of the study put this into environmental monitoring, as these OMPs (PFAS and PCBs) have not been explicitly investigated. The same situation can be said for the metabolites and transformed products of PFAS and PCBs in the Pra River Basin. The current study only covered the main PFAS and PCBs of interest, even though, as reported by Azzouz & Ballesteros (2016), some transformed products are expected to occur in the aquatic media. Due to the large number of target analytes under consideration, not every single compound will be addressed individually and compared with concentrations presented in the literature. Some compounds which showed prominence in the study were deeply discussed.

Limitations

One of the main constraints of this study was the potential risk of obtaining inaccurate results. When analyzing numerous compounds with diverse physico-chemical properties, an optimal performance of each analyte of interest should not be expected as a single method analysis cannot be universally adapted to accommodate all variations. The extraction of the sediment samples might have introduced some uncertainty in the OMPs content due to the dilution and homogenization as compared to the water samples which were concentrated from 500 mL.

The study made use of cancer slope factors based on animal studies which may not accurately reflect the risk of cancer in humans. Additionally, the study did not consider the potential cumulative effects of exposure to multiple PFAS compounds.

The concentrations of PFAS and PCBs in a river basin can exhibit temporal variability due to factors such as seasonality, rainfall events and changes in

pollution sources. A single sampling campaign may not capture the full range of fluctuations in contaminant levels over time. Also, the scope and duration of study was limited by financial and time constraints, and the availability of materials and equipment.

Organization of the Study

The thesis is divided into five sections. The first chapter discussed the background information on OMPs and the Pra River Basin with its associated use and pollution. The first chapter further gave details of general and specific objectives, as well as the scope, limitations and organization of the study. The literatures on the various selected classes of OMPs, as well as their occurrence in environmental and human samples were all reviewed in Chapter Two. The methods and materials used in the analyses of OMPs together with the quality control measures were detailed in Chapter Three. It also provided information on how the data that originated from analyses were processed. The results, analyses and discussions were presented in Chapter Four. Conclusions and insightful recommendations were made in Chapter Five to inform the direction of future research in this field of study.

CHAPTER TWO

LITERATURE REVIEW

Introduction

The Pra River Basin, the second largest basin in Ghana after the Volta basin, has experienced significant pollution over the past few decades. Among the various types of pollutants, organic micropollutants (OMPs) are widely recognized as significant contaminants of concern. Organic micropollutants (OMPs), a group of lipophilic xenobiotic persistent organic pollutants (POPs), are semivolatile, bioaccumulative, toxic, and have long-range environmental transport ability (Jones & de Voogt 1999). OMPs such as polychlorinated biphenyls (PCBs) and perfluoroalkyl substances (PFASs) represent an important group of such hazardous substances that have caused worldwide concern as toxic environmental contaminants.

In 2001, the Stockholm Convention on POPs acknowledged these as global problems. Although the elevated levels of POPs (Persistent Organic Pollutants) at contaminated hot spots are a significant environmental concern, there has been a growing recognition of the regional and global importance of this issue in recent decades (UNEP/IPCS, 1999). They have been documented to induce a range of effects including immunologic, teratogenic, carcinogenic, reproductive, and neurological problems in organisms (Kodavanti *et al.* 2008) and are of considerable concern to human and environmental health.

This extensive review of literature presents a summary of the existing understanding regarding PFAS and PCBs, encompassing their origins, presence, toxicity, potential risks to human health, and approaches for

remediation. The review synthesizes information from scientific articles, reports and regulatory documents, presenting a comprehensive understanding of the key aspects of PFAS and PCB research. In particular, the review focuses on the identification of PFAS and PCB compounds, their environmental fate, potential health effects, methods of detection and emerging remediation technologies. By critically examining the existing literature, this review contributes to a better understanding of PFAS and PCB, and serves a valuable resource for researchers, policymakers and stakeholders and also facilitates further advancement in research and management in this important field.

Perfluoroalkyl Substance (PFAS)

Introduction

PFAS encompass a range of compounds characterized by the presence of one or more perfluoroalkyl ($-C_nF_{2n-}$) moieties. PFAS are either highly persistent themselves or may transform into highly persistent perfluoroalkyl (ether) acids. Some of them are also bioaccumulative and toxic, and have been detected ubiquitously across the globe. As a result, governments and stakeholders have increasingly acknowledged PFAS as substances that pose emerging global concerns. Many actions are being taken to address PFAS starting from understanding their global presence on the market and in the environment. A new tally has distinguished more than 4,700 individual PFAS species (Buck *et al.*, 2021). PFAS all share the characteristic of being “chains” that contain “links” made of carbon fluorine bonds (C-F). PFAS encompass a big universe of different substances that vary in state from gas to liquid or solid, all with vastly different properties. PFAS have special attributes such as resistance to heat, water, oil and stains that make them helpful in an assortment

of modern applications and famous in shopper merchandise like waterproof outside gear, non-stick cookware and stain-safe upholstery. Numerous PFAS are steady and enduring in the environment, getting the name "forever substances." Industrial utilization of a portion of these compounds has been stopped; notwithstanding, numerous derivatives are as yet in business and more are being worked on. PFAS are currently found in numerous compartments of the environment. Due to their unique performance properties that hold substantial socioeconomic value, commercial products based on PFAS have been widely employed across various industrial and consumer items (Buck et al., 2021). Perfluoroalkyl sulphonates ($C_nF_{2n+1}SO_3^-$), and perfluorocarboxylic acids ($C_nF_{2n+1}COOH$) are the two primary groups of PFAS that have received significant attention. PFOA and PFOS are widely recognized as terminal degradation end-products among the various PFAS compounds. These synthetic substances have been consistently detected in environmental samples and frequently occur at elevated concentrations (Paul et al., 2009; Prevedouros et al., 2006).

Definition and Classification of PFAS

PFAS are aliphatic compounds in which all the hydrogen atoms on at least one carbon atom, as found in their non-fluorinated analogues, have been replaced by fluorine atoms. This substitution leads to the presence of the perfluoroalkyl moiety C_nF_{2n-1} in PFAS (Buck *et al* 2011). They are characterized by the presence of alkyl or polymeric chains and functional groups such as carboxylic acids, sulphonic acids or phosphate esters. Buck et al. (2011) established a comprehensive classification of polyfluorinated alkyl substances,

organizing them into distinct families and proposing a systematic nomenclature and abbreviations for both the families and their constituent members.

Perfluoroalkyl Carboxylic Acids (PFCAs)

Perfluoroalkyl carboxylic acids (PFCAs; listed in Table 1) can be represented by the general chemical formula $C_nF_{2n+1}COOH$. Among the PFCAs, one of the most widely discussed is perfluorooctanoic acid (PFOA) with the chemical formula $C_7F_{15}COOH$. Ammonium perfluorooctanoate (APFO, $NH_4^+C_7F_{15}COO^-$) has been extensively employed as a critical processing aid in the manufacturing of fluoropolymers, specifically polytetrafluoroethylene, through the dispersion (or emulsion) process (Fluoropolymer Manufacturing Group, 2001; Kissa, 1994). To maintain the molecular weight of a polymer, a chemically inert perfluorinated surfactant is employed as the processing aid to prevent any reaction with the growing free-radical polymer chains. APFO and its derivatives have also been developed and marketed as fluorosurfactants (3M Company, 2000a).

Table 1: List of Abbreviations and Names of Some PFAS

Acronym	Name	Structure
PFCA	Perfluorocarboxylic acid	$CF_3(CF)_xCOOH$
TFA	Trifluoroacetic acid	CF_3COOH
PFPrA	Perfluoropropanoic acid	$CF_3(CF)COOH$
PFBA	Perfluorobutanoic acid	$CF_3(CF_2)_2COOH$
PFPeA	Perfluoropentanoic acid	$CF_3(CF_2)_3COOH$
PFHxA	Perfluorohexanoic acid	$CF_3(CF_2)_4COOH$
PFHeA	Perfluoroheptanoic acid	$CF_3(CF_2)_5COOH$
PFOA	Perfluorooctanoic acid	$CF_3(CF_2)_6COOH$
PFNA	Perfluorononanoic acid	$CF_3(CF_2)_7COOH$
PFDA	Perfluorodecanoic acid	$CF_3(CF_2)_8COOH$
PFUnA	Perfluoroundecanoic acid	$CF_3(CF_2)_9COOH$

(Source: Buck et al. 2021)

Perfluoroalkane (or -alkyl) Sulphonic Acids (PFSAs)

PFSAs, listed in Table 2, are a notable group of PFAS compounds characterized by the chemical formula $C_nF_{2n+1}SO_3H$. They are also commonly

referred to as perfluoroalkane sulfonic acids, in accordance with IUPAC recommendations. Among these compounds, perfluorooctane sulfonic acid (PFOS) has gained considerable attention since its global detection in various organisms (Giesy & Kannan, 2001) and humans (Hansen et al., 2001). In 2002, the leading manufacturer discontinued the production of PFOS, as well as other PFAS members and their precursors (3M Company, 2000c). Nonetheless, the production of PFOS and its derivatives persists in China, as evidenced by the manufacturing of over 200 tons of its precursor, perfluorooctane sulfonyl fluoride, in 2006 (Yue, 2008). Through a directive issued by the European Parliament (2006b), the European Union has implemented regulations and limitations on the production and utilization of PFOS and its related compounds. Furthermore, PFOS has been categorized as a persistent, bioaccumulative, and toxic (PBT) substance according to the OECD (2002) guidelines and has been added to Annex B of the Stockholm Convention's roster of POPs, which imposes restrictions on its usage (UNEP, 2009).

Table 2: Representative Examples of Perfluoroalkyl sulphonic acids

Abbreviation	Name	Structure
PFSA	Perfluorosulphonic acid	$\text{CF}_3(\text{CF}_2)_x\text{SO}_3\text{H}$
PFBS	Perfluorobutane sulphonic acid	$\text{CF}_3(\text{CF}_2)_3\text{SO}_3\text{H}$
PFOS	Perfluorooctane sulphonic acid	$\text{CF}_3(\text{CF}_2)_7\text{SO}_3\text{H}$

(Source: Buck *et al.* 2021)

Sources and Pathways of PFAS in the Environment

Polyfluoroalkyl substances (PFASs) enter the environment through multi-media dispersion and significant distance movement during long-term manufacture and utilization of items containing PFASs (Shi *et al.*, 2021).

The occurrence of PFAS, such as PFOA and PFOS, is not natural and can be solely attributed to human activity, according to Lyons (2007). PFOA and PFOS have been employed in various applications, including the production of photographic film, as surfactants in firefighting foams, alkaline cleaners, and floor polishes, ant bait traps, and dirt repellent treatments for textiles. (Kissa, 2001; OECD, 2007; Prevedouros *et al.*, 2006).

Other sources of PFAS which had been widely recognized as secondary points included landfills and waste management sites (Björklund *et al.* 2021). To support this assertion, recent studies have revealed the selective accumulation of PFAS in shallow soil layers, especially in areas affected by firefighting operations, agricultural practices, and atmospheric deposition (Sharifan *et al.*, 2021). PFAS have the ability to adsorb onto soil particles, accumulate at interfaces, undergo volatilization, be taken up by organisms, or leach into the underlying aquifer once they are present in the vadose zone. Furthermore, it is important to note that polyfluorinated precursor compounds have the potential to undergo significant transformation into highly persistent perfluoroalkyl acids, leading to a change in their chemical composition and consequently impacting their transport behavior (Sharifan *et al.*, 2021). Diglasan *et al.* (2006) observed that fluorotelomer alcohols (FTOH) can undergo atmospheric oxidation, as well as metabolic or microbial degradation, leading to the formation of perfluorocarboxylic acids. According to D'eon *et al.* (2007), the atmospheric or microbial degradation of perfluorooctane sulphonamido ethanols is likely to result in the formation of PFOS.

Some Physico-chemical Properties of PFOA and PFOS

Figure 1 illustrates PFOA and PFOS as organic compounds distinguished by a fully fluorinated carbon chain attached to a carboxylic or sulphonate group.

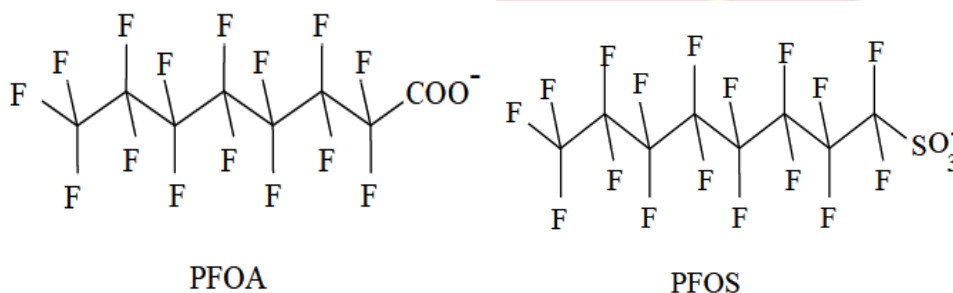


Figure 1: Structural formulae of PFOA and PFOS

PFOA and PFOS are oleophobic, and have polar or hydrophilic properties. They do not exhibit a tendency to accumulate in fatty tissues and occur mostly in anionic form at pH 7 and the anions interact with polar sites in membranes and in sediments (3M, 2000). Due to their non-natural occurrence, they exist in anionic form at pH 7, which can be attributed to their low pKa values (Prevendouros et al., 2006). In the environment, both the free acid and the anionic form of PFOA are present. On the other hand, PFOS predominantly exists in its anionic form, which is the only form present in the environment (Prevendouros *et al.*, 2006).

PFAS possess the property of forming multiple layers when combined with octanol and water due to their simultaneous hydrophobic and lipophobic nature (Prevendouros et al., 2006). Consequently, determining the octanol-water partition coefficient (K_{ow}) values of these substances through conventional methods used for organic chemicals is not feasible (Hanson et al., 2019; Prevendouros et al., 2006). However, according to Ellis et al. (2003),

relying solely on the octanol-water partition coefficient (K_{ow}) does not accurately predict the environmental partitioning behavior of these compounds. For instance, perfluorooctanoate (anion) exhibits a very low Henry's law constant, while the acid form of perfluorooctanoic acid (PFOA) has a relatively high Henry's law constant, as noted by Prevedouros et al. (2006). Consequently, the volatilization of these compounds from water is influenced by pH. At environmental conditions, PFOA and PFOS do not undergo significant volatilization and instead tend to bound with particles in the atmosphere, as reported by OECD (2002) and Prevedouros et al. (2006). Table 3 presents some of the physico-chemical properties of PFAS.

Table 3: Some Physico-chemical Properties of PFOA and PFOS

Compound	PFOS	PFOA
IUPAC name	1,1,2,2,3,3,4,4,5,5,6,6,7,7,8,8,8-heptadecafluorooctane-1-sulfonate	2,2,3,3,4,4,5,5,6,6,7,7,8,8,8-pentadecafluorooctanoic acid
CAS number	1763-23-1 (acidic form)	335-67-1, 90480-55-0 (branched isomers)
Molar mass	500 g/mol (acidic form)	414 g/mol
Melting point	≥ 400 °C	45–50 °C
Boiling point	not calculable	189–192 °C (736 mmHg)
Vapour pressure	3.31×10^{-4} Pa (20 °C)	0.008 Pa (APFO, 20 °C)
Solubility in water	0.57 g/L	3.4 g/L
K_{AW}	$< 2 \times 10^{-6}$	0.001
pK_a	– 3.27(calculated)	2.5 – 3.8

(Source: OECD, 2007).

Pathways of Human Exposure to PFAS

As highlighted by DeLuca et al. (2021), the primary source of human exposure to PFAS is predominantly through consumption of contaminated food and drinking water. PFOS, PFOA, PFNA, and PFHxS are among the PFAS compounds that contribute significantly to human exposure. In 2020, the

European Food Safety Authority (EFSA) published a draft opinion proposing a tolerable intake of 8ng/kg/week for the total concentration of these four substances, which corresponds to an annual dose of 0.42 μ g/kg (Augustsson et al., 2020). The study revealed that dietary consumption played a prominent role as an exposure pathway, with fish and seafood consumption being significantly associated with the intake of PFOS, as highlighted by Augustsson et al. (2020). Aside these sources, other important human PFAS exposure pathways from the indoor media include consumer products, household articles, cleaning products, personal care products, plus indoor air and dust. However, additional PFAS exposure pathways have been raised by a limited number of studies reporting correlations between commercial and industrial products and PFAS levels in human media and biomonitoring (DeLuca *et al.*, 2021).

Occurrence of PFAS in the Environment

Dust

In a comprehensive study conducted by Hall et al. (2020), the levels of PFAS in indoor dust samples from United States and Canada were analyzed. The predominant PFAS compounds detected in both fire station and house dust samples were fluorotelomer alcohols (FTOHs) and di-polyfluoroalkyl phosphoric acid esters (diPAPs), with median concentrations of approximately 100 ng/g dust or higher. Notably, dust from fire stations exhibited significantly higher levels of PFOS, PFOA, PFHxS, PFNA, and 6:2 diPAP compared to dust from homes. Conversely, 8:2 FTOH was found to be significantly higher in homes than in fire stations. Furthermore, the authors observed a decrease in perfluoroalkyl acid levels in residential dust over time, particularly for PFOA and PFOS, when comparing their results to previously published values.

Water

In a study conducted by Essumang et al. (2017), the presence of PFAS contamination in surface water and drinking water from the Pra river basin was investigated. The findings revealed the presence of five prominent PFAS compounds, namely PFOA, PFOS, PFHxA, PFDA, and PFPeA, in both the river water and tap water samples. The mean concentrations of PFAS in the Kakum and Pra Rivers were determined to be 281 ng/L and 398 ng/L. Similarly, the tap water derived from the treatment of water from these rivers exhibited concentrations of 197 ng/L and 200 ng/L for Kakum and Pra Rivers. PFOA and PFOS accounted for approximately 99% of the analyzed PFAS compounds in the study. Risk quotients (RQs) of 1.01 and 1.74 were reported for PFOA and PFOS, associated with the consumption of tap water. The authors expressed specific concerns about the efficacy of local tap water treatment in removing these emerging pollutants, highlighting limitations in the current treatment processes.

Tan et al. (2018) conducted a study focusing on the assessment of PFAS levels originating from tributaries of the Yangtze River. According to Tan *et al.* (2018), the Yangtze River drainage basins are China's most important economic development zones and also the locations of several large-scale fluorine chemical industries. Samples of surface water, groundwater, and tap water samples were collected from the tributary system of the Jiujiang section of the Yangtze River. The surface waters exhibited a wide range of total PFAS concentrations, varying from 7.8 to 586.2 ng/L. High levels of short-chain compounds such as PFBS was observed in surface waters from Nanchang City,

Poyang Lake, and the Yangtze River which were likely of WWTPs' origin according to the authors.

Elevated levels of PFOA and PFOS were likewise detected in the Moehne River, originating from the illegal disposal of wastewater contaminated with these substances (Skutlarek et al., 2006). Similarly, the Tennessee River in the USA exhibited high levels of PFOA and PFOS, which were traced back to a manufacturing plant involved in the production of these compounds (Hansen et al., 2002). Japan, China, and North Carolina also reported elevated levels of PFOA in their respective river waters (Saito et al., 2004; So et al., 2007; Nakayama et al., 2008). However, rivers in Sweden and Poland displayed relatively low levels of PFOA and PFOS contamination (McLachlan et al., 2007).

Levels in Biota and Wildlife

The global contamination and widespread presence of PFOS in wildlife were initially reported in 2001 by Giesy and Kannan. Through the analysis of tissue samples collected from various aquatic species such as seals, otters, sea lions, dolphins, minks, and amphibians during the 1990s, PFOS, PFOSA, PFHxS, and PFOA were examined (Giesy & Kannan, 2001). In the majority of the samples, PFOS was detected at levels exceeding 1 part per billion (ppb) (Giesy & Kannan, 2001).

In Antwerp, Belgium, PFOS levels in biota were established and the levels fell between 36 - 1700 ppb in some rivers near a fluorochemicals factory (Hoff *et al.*, 2003). Levels of PFOS in seals have been found to be higher in Europe than in the USA, whereas PFOS levels in dolphins and seabirds have been found to be higher in the USA than in Europe (Giesy & Kannan., 2001).

In a separate study conducted by Hoff et al. (2004), wild wood mice (*Apodemus sylvaticus*) captured from a forest reserve adjacent to a fluorochemicals factory in Belgium exhibited high levels of PFOS in their livers, ranging from 470 to 17,855 ng/g ww. In comparison, wood mice residing 3 km away from the factory displayed significantly lower average levels, approximately one hundred times lower, at 280 ng/g ww. The study also indicated that PFOS levels were independent of sex, increased with age in mice, and were transferred from mother to offspring. Another investigation focused on the blood serum of two pet rabbits from Tokyo, revealing PFOS levels ranging from 6 to 9 ng/mL (Taniyasu et al., 2003). Guruge et al. (2004) examined the accumulation of 13 different perfluorinated chemicals (PBFS, PFHxS, PFOS, PFPeA, PFHxA, PFHpA, PFOA, PFNA, PFDeA, PFUnA, PFDoA, PFOSA, THPFOS) in cattle from Japan through the analysis of blood plasma. The study found no clear age-dependency, and the levels detected were lower than those observed in fish.

Fish and Seafoods

In their investigation, Valsecchi et al. (2020) analyzed the levels of PFAS in fish specimens obtained from diverse lakes within the European subalpine region. The researchers analyzed different body fractions of eight fish species, including fillets, viscera, liver, and residual carcass. The findings indicated that the sampling season did not significantly impact PFAS levels, and the content of protein could not be used for normalizing tissue concentrations due to the specific protein binding of PFAS. However, the polar lipid content proved useful in reducing the PFAS variability in phospholipid-rich portions such as viscera and carcass. The study also revealed that PFAS contamination

in fish generally correlated with the degree of urbanization in the lake catchment areas.

Sediment, Sludge and Soil

In their investigation, Sammut et al. (2019) conducted a comprehensive examination of perfluoroalkyl substances (PFAS) levels in sediments, soil, and groundwater across the Maltese Islands. The findings revealed the presence of at least one PFAS in all sediment, soil, and groundwater samples. The main PFAS identified in all samples were PFOS, PFOA, and PFDA, with concentrations ranging from below the limit of quantification (LOQ) to 5.91 ng/g for PFOS, LOQ to 0.58 ng/g for PFOA, and LOQ to 1.05 ng/g for PFDA. However, only PFOA was detected in all groundwater samples, with concentrations ranging from below the limit of detection (LOD) to 2.68 ng/L.

Pignotti et al. (2017) examined the presence and seasonal variations of 13 PFAS in the Ebro Delta and its surrounding environs in Spain. Their investigation included analyzing water, sediments, and fish samples. The findings revealed that PFOA was frequently detected in both water and sediments. Sediments, on the other hand, displayed a greater enrichment of PFOS with concentrations ranging from <1.02 to 22.6 ng/g dry weight. The PFAS levels in water remained relatively stable throughout the year, but in sediments, there was a gradual decrease from autumn to summer, suggesting that environmental factors affect PFAS distribution in sediments. PFOS was the most commonly found compound in fish living in seawater, which is consistent with its ability to persist, accumulate, and increase in concentration through the food chain. Interestingly, PFASs were found to be more abundant in fish skin compared to their muscle tissues. River fish exhibited elevated levels of PFASs,

especially perfluoroalkyl carboxylic acids, with concentrations ranging from 63.8 ng/g wet weight to 938 ng/g wet weight. The levels of PFASs in water, sediment, and organisms provided evidence that Isla de Buda, situated at the downstream end of the estuary, had the highest contamination among the sites in the Ebro Delta. This observation aligns with the fact that multiple irrigation channels converge in that particular area.

A number of research studies have examined the concentrations of PFAS in sludge and wastewater effluent released into Lake Victoria, Kenya (Chirikona et al., 2015). The findings revealed that the levels of PFOS and PFOA in sludge samples varied from 98 to 683 pg/g and 117 to 673 pg/g respectively. In wastewater, PFOA concentrations ranged from 1.3 to 28 ng/L, while PFOS concentrations ranged from 0.9 to 9.8 ng/L.

A study conducted by 3M in six urban locations in the USA revealed elevated levels of PFAS in sewage sludge from cities involved in the production or use of PFAS (3M, 2001). Similarly, the levels of PFAS in sewage sludge samples from Norway, Denmark, Sweden, Finland, Iceland, and the Faroe Islands were investigated by Berger et al. (2004) and Kallenborn et al. (2004). PFOS was found to be present at high levels in Denmark, Norway, and Sweden, while the highest levels of PFOA were detected in samples from Iceland and the Faroe Islands. In Sweden, Denmark, and Norway, PFOS concentrations ranged from 1041 to 2644 pg/gram wet weight. Norwegian, Danish, and Finnish sludge samples exhibited lower levels of PFHxA and PFNA. Additionally, sediment samples generally had lower PFAS levels compared to sludge samples.

Human Biomonitoring

In a research study conducted in Sweden by Augustsson et al. (2020), the researchers estimated range of PFOS intake among average Swedish individuals who were categorized as either normal or high consumers of freshwater fish. Based on the assumption that normal consumers ate fish three times a year and high consumers ate fish once a week, the yearly tolerable intake for normal and high consumers was reached when PFOS levels in fish were 59 and 3.4 μg per kg of fish meat, respectively. The average PFOS levels in fish varied from 0.3 to 750 $\mu\text{g}/\text{kg}$ across different sites. Utilizing the available data, the annual range of dietary PFOS intake for male normal consumers ranged from 0.0021 to 5.4 $\mu\text{g}/\text{kg}/\text{yr}$, with median values falling between 0.02 and 0.16 $\mu\text{g}/\text{kg}/\text{yr}$. For male high consumers, the estimated total intake range was 0.04-93 $\mu\text{g}/\text{kg}/\text{yr}$, with median values of 0.27-1.6 $\mu\text{g}/\text{kg}/\text{yr}$. Women had slightly lower exposure estimates, and approximately 79% of the exposure observed in men. Despite the significant variation in PFOS concentrations in fish from different locations, the study concluded that even individuals who consume freshwater fish only a few times per year contribute significantly to the total annual PFOS intake.

Levels of PFAS in Africa

Unlike in developed countries, relatively few studies have been conducted to investigate PFAS contamination of environmental matrices in Africa (Zushi *et al.*, 2012). As a result of this, there is a poor understanding of the sources, distribution, and exposure risks of PFAS in Africa (Zushi *et al.*, 2012). Information is presently lacking regarding PFAS accumulation in sediments, soils, and other wildlife besides aquatic organisms in Africa. Information on human exposure and airborne levels of these PFAS are yet to be

investigated. As it has been described earlier, PFAS are widely used in many consumer products such as surface treatment in carpets, textiles, furniture, non-stick cooking utensils, fire-fighting foams, and insecticides, many of which are presently used in Africa (UNEP, 2009).

Toxicology of PFAS

The impact of per- and polyfluorinated alkyl substances (PFAS) on biological systems is closely linked to their interactions with proteins. Previous research has predominantly focused on serum albumin and liver fatty acid binding protein, and the binding affinities determined through various methods exhibit significant variability. The liver plays a crucial role in accumulating long-chain PFAS, and supporting experimental evidence of their toxicity includes the infiltration of fat in liver cells, activation of specific cytochrome P450 (CYP) pathways, cell death, the development of hepatocellular adenomas and carcinomas, and disturbance in the transport of fatty acids. These observed effects can occur through both peroxisome proliferator-activated receptor alpha (PPAR α)-dependent and PPAR α -independent mechanisms, and they have been documented in various species (Guillette et al., 2020; National Toxicology Program, 2020a; Xu et al., 2020a; Zhang et al., 2019).

The extended persistence of long-chain PFAS in the human body is mainly linked to the active reabsorption of these compounds in the renal tubules. Noteworthy is the tendency of legacy PFAS like PFOA and PFOS to accumulate in renal tissues. Numerous studies examining histopathology, molecular changes, oxidative stress, and epigenetics have provided evidence suggesting potential nephrotoxicity associated with these substances (Rashid et al., 2020; Sakuma et al., 2019; Stanifer et al., 2018; Wen et al., 2016). Additionally, the

substantial influence of renal reabsorption on the prolonged half-lives of long-chain PFAS is consistent with human protein binding data and experimental studies on PFAS excretion.

Adverse health effects associated with immunosuppression, such as childhood infections diagnosed by medical professionals, have been linked to prenatal exposures to PFOS and PFHxS (Goudarzi et al., 2017). A study conducted on a cohort of pregnant women found increased risks of throat infections and diarrhea in children up to the age of 10, and these risks were found to be correlated with PFAS levels measured in cord blood (Impinen et al., 2018, 2019). According to a recent review by Kvalem et al. (2020), exposure to PFAS during infancy and childhood was found to have an immunosuppressive effect, leading to an increased occurrence of atopic dermatitis and lower respiratory tract infections.

Cancer

The Leydig cells, situated in the testis, play a vital role in the production of testosterone (Liu et al., 2010). Animal studies conducted on Charles River cDNA rats, a strain with a low occurrence of tumors, revealed that PFOA caused dose-dependent increases in Leydig cell adenomas and affected Leydig cell steroidogenesis in vitro (Biegel et al., 1995; Liu et al., 2010). These tumors may be attributed to endocrine alterations, including decreased aromatase activity and sustained elevation of serum estradiol levels (Biegel et al., 2001). Consequently, based on these findings, the US Environmental Protection Agency has classified PFOA as a carcinogen in animals (US EPA, 2000).

PFAS Impact on Reproduction and Development

Studies examining the teratological effects of potassium and lithium salts of PFOS have been conducted in rats, rabbits, and mice (Lau et al., 2003; 2004). Remarkable results were found and findings were in agreement between the various laboratories which were part of the study (Lau *et al.* 2003; 2004). Observed developmental effects which include foetal weight reduction, cleft palate, oedema, delayed bones ossification, and cardiac abnormalities were observed (Lau *et al.* 2003; 2004). These effects were observed in the groups which were exposed to elevated PFOS levels (Lau *et al.*, 2004). Also, considerable reduction of body weight and reduced appetite were observed among the rats, rabbits and mice which were exposed to the highest PFOS levels (Lau *et al.*, 2004).

In rodent studies, high doses of EtFOSE (ethyl fluoroctanesulfonate) were found to cause reductions in maternal body weight and fetal weight (Lau et al., 2004). The effects were similar in all regards to those observed for its metabolite perfluorooctane sulphonate (Lau *et al.*, 2004). A dose 30 mg/kg per day of PFOA resulted in a significant reduction of maternal weight and a considerable mortality rate in pups (Lau *et al.*, 2004). However, at reduced PFOA levels, no considerable effects were observed in both maternal body and foetal weights (Lau *et al.*, 2004).

Endocrine Disruption

A study conducted on female rats demonstrated that the intraperitoneal injection of PFOS (perfluorooctane sulfonate) at doses of 1 and 10 mg/kg body weight for a duration of two weeks had notable effects. Exposure to PFOS was found to cause disturbances in estrous cyclicity, elevated levels of serum

corticosterone, and reduced levels of serum leptin and norepinephrine in the paraventricular nucleus of the hypothalamus (Austin et al., 2003). These findings indicate that PFOS has the ability to influence the neuroendocrine system in rats, leading to its classification as an endocrine disruptor.

A study conducted on adult male rats revealed that feeding them with ammonium perfluorooctanoate (PFOA) at a dose of 25 mg/kg through gavage led to specific hormonal changes. It was observed that serum testosterone levels and testicular interstitial fluid testosterone levels decreased, while serum estradiol levels increased. These changes were attributed to the induction of hepatic aromatase by PFOA, which converts testosterone to estradiol (Biegel et al., 1995).

In a different study, where ammonium perfluorooctanoate (PFOA) was administered through gavage for duration of two weeks, various hormonal changes were observed. These changes included decreased serum and testicular interstitial fluid testosterone levels, reduced weights of accessory sex organs, and increased serum estradiol levels (Cook et al., 1992). Similar hormonal changes, characterized by elevated estrogen levels, have been reported in other studies involving male rats exposed to PFOA (Biegel, 2001). However, a two-generation study in rats exposed to APFO (ammonium perfluorooctanoate) levels up to 30 mg/kg per day did not show any alterations in functional reproduction (Butenhoff, 2012). Additionally, a six-month oral study conducted on monkeys, with a daily dose of up to 20 mg/kg per day, did not yield observable changes in estrogen levels (Butenhoff, 2009).

Human Toxicity and Health Risk Assessment

The exact mechanisms by which humans are exposed to PFOS and PFOA are still not fully comprehended (Kennedy et al., 2004). Nevertheless, chronic toxicity studies in animals have provided insights into the potential harmful effects of PFOA and PFOS. These studies have revealed the occurrence of tumors in liver cells, Leydig cells (found in the testis), and pancreatic cells (Kennedy et al., 2004). It has been noted earlier that tumor growth can be a result of peroxisome proliferation. Consistent with these discoveries, a panel of experts advising the United States Environmental Protection Agency recommended the classification of PFOA as a carcinogen in rodents, which has potential implications for human health (USEPA, 2006).

Various studies have investigated the half-life and exposure pathways of PFOS and PFOA, shedding light on their potential health effects. The estimated half-life of PFOA in human serum is around 4 years, whereas studies have reported half-life values of 3.8 years for PFOA and 5.4 years for PFOS in retired workers from fluorochemical manufacturing plants. In contrast, rats exhibited much shorter half-lives of up to 5.6 days for PFOA and 7.5 days for PFOS (Burris et al., 2002; OECD, 2002; Olsen et al., 2003).

Renal elimination studies in individuals living in Kyoto suggested that there is no active excretion of PFOA and PFOS. Additionally, studies conducted in the United States have linked PFOA and PFOS to various cardiovascular diseases, thyroid dysfunction, alterations in liver gene expression, and increased mortality from diabetes (Harada et al., 2006; Costa et al., 2009; Fisher et al., 2013; Fitz-Simon et al., 2013; Geiger et al., 2013; Leonard et al., 2008; Olsen et al., 2007; Shankar et al., 2011; Steenland et al., 2010).

There is no doubt that humans are exposed to PFAS through various pathways, including prenatal exposure, breastfeeding, consumption of contaminated food and water, inhalation of contaminated dust, use of articles treated with perfluorinated surfactants, and occupational exposure (Kennedy et al., 2004). Studies have been conducted to assess the overall human exposure to these fluorinated compounds and to better understand the potential toxicity of PFOA and PFOS to humans.

PFAS exposure takes place through diverse pathways, encompassing in utero exposure, breast milk, water, consumption of contaminated food, inhalation of dust, and occupational exposure. Various studies have been conducted to estimate the daily intake levels of PFOS and PFOA from these different sources. Inhalation of outdoor dust particles was found to result in negligible exposure to PFOS, while higher levels of PFOA were detected in the air, leading to considerable daily intake. Chronic exposure to PFOA and PFOS through indoor dust absorption and drinking water has also been observed. Maternal blood and cord blood have shown a positive correlation for PFOS levels, indicating exposure during pregnancy. Breastfeeding mothers in Zhoushan, China, were found to have potential health risks associated with PFOS intake through breast milk (Sasaki et al., 2011; Harada et al., 2006; Shoeib et al., 2005; So et al., 2006; Washburn et al., 2005).

Consumer articles containing fluoropolymers or fluorotelomer-based products were associated with increased serum PFOA levels, but no immediate adverse health effects were reported. Seafood consumption, particularly fish, contributed to PFOS and PFOA exposure in certain regions. Dietary intake studies in the UK, Spain, and Canada provided estimates of daily intake levels

for PFOA and PFOS, with no immediate toxicological concerns raised (Gulkowska et al., 2006; U.K. Food Standard Agency, 2006; Ericson et al., 2012; Tittlemier et al., 2007).

In the UK's 2004 Total Diet Study, composite food samples were analyzed, revealing a daily intake of 0.07 $\mu\text{g}/\text{kg}$ body weight for PFOA and 0.1 $\mu\text{g}/\text{kg}$ body weight for PFOS. These findings did not raise immediate toxicological concerns, as assessed by the UK Food Standard Agency. In Tarragona County, Catalonia, Spain, PFOA and PFOS levels of 1.1 ng/kg per body weight per day were reported. During the period of 1992 to 2004, composite food samples collected as part of the Canadian Total Diet Study indicated increased levels of 250 ng per day for total perfluorocarboxylates and 4 ng per day for PFOS intake. These findings suggest that food is a significant source of exposure to PFOS and perfluorocarboxylates in Canada, surpassing air, water, dust, treated carpet, and apparel (U.K. Food Standard Agency, 2006; Ericson et al., 2012; Tittlemier et al., 2007). The variations observed among the studies could be attributed to different consumption patterns of the foods analyzed in each study.

PFAS Determination in Aqueous Samples

To evaluate the concentrations of PFAS, particularly PFOA and PFOS, in firefighting foam-contaminated water, an analytical method employing solid phase extraction (SPE) for pre-concentration and pre-cleaning, along with high-performance liquid chromatography (HPLC) coupled to negative electrospray ionization tandem mass spectrometry (ESI-MS/MS), was employed (Moody et al., 2001). The SPE step facilitated the concentration and purification of the target compounds, while HPLC coupled with negative ESI-MS/MS enabled

their quantification. The percent recoveries achieved for PFOA and PFOS were 93% and 68%, respectively, indicating the effectiveness of the method in extracting and measuring these compounds from water samples. The high limit of quantification values of 1.0 µg/L and 1.7 µg/L were observed for PFOA and PFOS in a 100-mL sample. These elevated values were attributed to the highly contaminated nature of the analyzed samples resulting from the use of firefighting foams (Moody *et al.*, 2001).

In another method used to determine PFOS levels in the part-per-million range, a direct injection of a sample and acetonitrile mixture in a 1:1 ratio was employed, followed by analysis using ESI-MS operating in the negative mode. This approach facilitated the accurate quantification of PFOS at higher concentrations (Moody *et al.*, 2001).

The method was only useful for determination of PFOS levels in less complex matrices (Moody *et al.*, 2003). Background contamination problem of perfluorinated surfactants analyses were first addressed during determination of PFAS levels in seawater in part per quadrillion. The method included solid phase extraction and quantification by HPLC-ESI-MS/MS (Hansen *et al.*, 2002; Taniyasu *et al.*, 2003; Yamashita *et al.*, 2004).

In order to analyze the concentrations of PFOS in river water samples, a different approach was utilized, which involved automated on-line turbulent flow chromatography in combination with high-performance-liquid-chromatography (HPLC) coupled to atmospheric pressure photoionization mass spectrometry (APPI-MS) (Takino *et al.*, 2003). This method enabled efficient and automated sample processing, separation, and detection of PFOS. The APPI technique did not exhibit any matrix effect as compared the negative ESI

(Takino *et al.*, 2003). The method resulted in reduction in sample preparation time but also achieved high LOQ of 18ng/L (Takino *et al.*, 2003). Also, large volume extraction of water samples and subsequent quantification by liquid chromatography (LC) coupled to negative ESI –MS-MS was done to determine the levels of PFOA and PFOS (Taniyasu *et al.*, 2003; Sinclair & Kannan, 2006). The LoQs determined for both PFOA and PFOS was 2.5 ng/L.

Remediation Technologies for PFAS

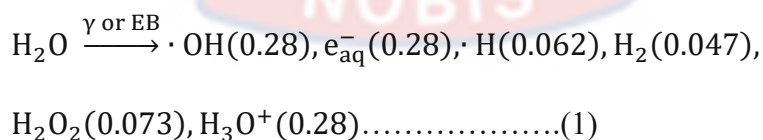
In recent times, substantial endeavors have been directed towards the development of efficient techniques for removing PFAS from water and wastewater. Conventional treatment methods like coagulation, flocculation, sedimentation, filtration, chlorination, ozonation, UV irradiation, and low-pressure membranes have demonstrated limited effectiveness in eliminating PFAS due to their remarkable stability (Mak *et al.*, 2008). To address this challenge, researchers have focused on Advanced Oxidation/Reduction Processes (AO/RPs) as promising alternatives. These processes involve the reaction of PFAS with either in-situ generated free radicals or hydrated electrons, aiming to degrade or transform PFAS into less harmful compounds (Anumol *et al.*, 2016; Merino *et al.*, 2016; Trojanowicz *et al.*, 2018; Wang *et al.*, 2017).

Advanced oxidation processes involve the use of hydroxyl radicals for environmental applications in aqueous solutions. Multiple techniques are employed to generate hydroxyl radicals, including photolytic methods such as vacuum photolysis of water, the Fenton reaction, photo-Fenton processes, ozonation, sonolysis, and water radiolysis through ionizing radiation (Trojanowicz *et al.*, 2018).

In contrast, reductive processes involve different approaches. UV-photolysis in the presence of sulphite (Gligorowski et al., 2015), reduction using nanoscale zero-valent iron, and electron beam irradiation (Ma et al., 2017) are among the methods used. Pyrolytic decomposition in deaerated solutions through sonolysis has been reported to be advantageous (Moriwaki et al., 2006). Out of these processes, the most efficient one has been found to be anodic oxidation employing a Magneli phase Ti_4O_7 anode, as demonstrated in studies conducted by Liang et al. (2018).

The search for efficient methods to generate radicals for the decomposition of PFAS has led to the exploration of water radiolysis, which involves irradiation with ionizing radiation. This area of research has shown promise and has been applied to the development of various techniques for decomposing organic pollutants in water and wastewater (Trojanowicz et al., 2018b).

The use of ionizing radiation to decompose pollutants in water relies on the reactions between the byproducts of water radiolysis and these compounds. Direct radiolysis of dissolved compounds in diluted solutions is minimal. As a result, the decomposition of pollutants in aqueous solutions through radiolysis can be considered an indirect process, in which highly reactive free radicals like OH and H, along with hydrated electrons e^-_{aq} , which are the primary products of water radiolysis, act as key reactants. Equation (1) in Getoff's work (1996) illustrates the formation of other species at lower concentrations.



The values enclosed in parentheses in the aforementioned equation represent the radiation chemical yields (G-values), expressed in $\mu\text{mol J}^{-1}$. These

G-values represent the quantity of molecules consumed or produced in a specific reaction per 100 electron volts (eV) of energy absorbed due to radiation.

G-values serve as indicators of the effectiveness of radiation-induced chemical processes.

One significant aspect of water radiolysis is the simultaneous formation of strongly oxidizing hydroxyl radicals (OH) and strongly reducing species such as hydrated electrons (e^-_{aq}) and hydrogen atoms (H). These reactive products can effectively react with pollutants of various structures, offering the potential for their degradation and removal from water systems (Getoff, 1996).

The main sources of ionizing radiation utilized for environmental applications consist of ^{60}Co sources, emitting gamma (γ) rays, and electronic accelerators producing electron beams (EB). One notable advantage of employing ionizing radiation from these sources to decompose environmental pollutants is their exceptional ability to generate hydroxyl radicals and hydrated electrons. These radiation sources are readily accessible commercially, owing to their wide application in various technological and medical fields. It is important to mention that γ -rays possess the advantage of deeper penetration into aqueous solutions in comparison to electron beams, making them commonly employed in laboratory radiation studies.

In initial investigations into the radiolysis of perfluorinated surfactants, scientists utilized the pulse radiolysis technique with a linear electron accelerator to ascertain the reaction rate constants between PFOA and PFOS and hydrated electrons and OH radicals (Szajdzińska-Piętek et al., 2000). The results indicated that unlike hydrocarbon surfactants, perfluorinated surfactants exhibit limited reactivity towards OH radicals, with radiolytic decomposition

primarily occurring through interactions with hydrated electrons. The conclusion was reinforced by investigations into the decomposition of PFOA using gamma irradiation (Zhang et al., 2014) and EB-irradiation (Ma et al., 2017). Furthermore, it was observed that the most effective degradation of PFOA took place in deaerated and highly alkaline solutions (Ma et al., 2017; Zhang et al., 2014; Trojanowicz et al., 2019).

In essence, the degradation of PFAS through radiation is a multifaceted process characterized by radical reactions, energy utilization, and ionic and redox equilibria. Its effectiveness is influenced by a range of chemical and physical factors, including the radiation type, accelerator power, radiation dose rate, initial pollutant concentration, solution pH, and the presence of scavengers or other reagents in the irradiated solution.

Polychlorinated Biphenyls (PCBs)

Introduction

Polychlorinated biphenyls (PCBs) are persistent organic pollutants known to potentially form 209 congeners based on the arrangement and quantity of chlorine atoms within the biphenyl rings (McFarland & Clarke, 1989). Each PCB congener is composed of two interconnected six-carbon rings linked by a single carbon bond. The position and number of chlorine atoms confer different chemical and biological properties to PCBs. Therefore, PCBs were divided into two distinct groups. One group is considered as “dioxin-like” (DL) because of their similarity in structure and toxicity to polychlorinated dibenzo-p-dioxins. This group contains 12 congeners and the most obvious property for this group is the absence of chlorine atoms in ortho-positions, which allows the PCB to adopt a coplanar configuration. Dioxin-like, coplanar PCBs have a high affinity

toward the aryl hydrocarbon receptor (AhR) with PCB 126 being considered the most potent AhR agonist among PCBs (van den Berg *et al.* 2006). Table 4 lists the 9 dioxin-like PCBs.

Table 4: Dioxin-Like PCB Congeners

I.U.P.A.C number	Congener
77	3', 3, 4, 4' - TeCB
81	3, 4, 4', 5 - TeCB
105	2, 3, 3', 4, 4' - PeCB
114	2, 3, 4, 4', 5 - PeCB
118	2, 3', 4, 4', 5 - PeCB
123	2', 3, 4, 4', 5 - PeCB
126	3, 3', 4, 4', 5 - PeCB
156	2, 3, 3', 4, 4', 5 - HxCB
157	2, 3, 3', 4, 4', 5' - HxCB

(Source: Rushneck *et al.* 2004)

Another group is “non-dioxin-like” (NDL), which are those congeners that have one or more chlorine atoms present in ortho-positions and reduce the planarity of molecule. According to Kim *et al.* (2021), NDL-PCBs, which do not exhibit affinity for the aryl hydrocarbon receptor (AhR), have been demonstrated to disrupt the activities of Jurkat T cells, cerebellar granule cells, and uterine cells. (NDL)-PCBs also exhibit a different spectrum of toxic modes of action, which nevertheless affect mostly the same tissues as DL-PCBs and which may lead to hepatotoxicity, neurotoxicity, immunotoxicity, endocrine disruption, or tumour promotion (Hamers *et al.* 2011; NTP, 2006a; Pessah *et al.* 2006; Robertson & Hansen, 2001). Some previous scientific reports indicated NDL-PCBs were far more abundant in both commercial and environmental mixtures, and may exert agonistic or antagonistic effects on the AhR-dependent processes, including CYP1A1 induction (Chen & Bunce, 2004; Parkinson *et al.*, 1981; Petrulis & Bunce, 2000; Safe, 1998). Some representative examples of NDL-PCBs may include the following but limited to PCB-19, PCB-47, PCB-

74, PCB-118, PCB-126, PCB-153, PCB-180 and so on. While the toxic mechanism of DL-PCBs primarily involves the aryl hydrocarbon receptor (AhR), as described by Hankinson (2005), the precise mechanisms responsible for the toxic effects of NDL-PCBs remain incompletely elucidated.

Moreover, PCBs have a propensity to distribute into lipid-rich tissues in organisms instead of entering the intracellular aqueous milieu, as stated by Jones and De Voogt (1999). This particular attribute contributes to the long-lasting presence of PCBs in biota, as their metabolic processes are slow and they can accumulate within food chains (Jones & De Voogt, 1999). While PCBs were once widely used in various industrial products, their production has been discontinued due to concerns about their long-term accumulation after continuous exposure (Carpenter, 2006). Traces of PCBs have been identified in the body tissues of individuals living in industrialized nations, mainly as a result of consuming fish from polluted water sources (Jensen, 1987). Additionally, animals exposed to PCB-contaminated feed and air have exhibited PCB presence (Annamalai & Namasivayam, 2015; Malisch & Kotz, 2014), and PCBs have been detected in human blood samples (Kraft et al., 2018). The presence of PCBs in these contexts has been associated with various disorders, including impairments in thyroid and cognitive functions, as well as motor performance (Berghuis et al., 2019; Li et al., 2018).

PCB Mixtures and Trade Names

PCBs were manufactured as a mixture of individual PCB congeners with only few exceptions. These mixtures were prepared by adding continuously more chlorine to batches of biphenyl until a certain target percentage of chlorine by weight was reached. Commercial mixtures with

higher percentages of chlorine contained higher proportions of the more heavily chlorinated congeners, but all congeners could be expected to be present at some level in all mixtures. While PCBs were manufactured and sold under many trade names, the most common was the Aroclor series (USEPA, 2000). There are many types of Aroclors and each has a distinguishing suffix number that indicates the degree of chlorination. The numbering standard for the different Aroclors is as follows:

The naming convention for polychlorinated biphenyls (PCBs) typically follows a pattern where the first two digits represent the number of carbon atoms in the phenyl rings, which is usually 12 for PCBs. The following two digits indicate the approximate percentage of chlorine by mass in the mixture. For instance, the name Aroclor 1254 indicates a mixture with approximately 54% chlorine content by weight. Table 5 provides examples of various Aroclor mixtures.

Table 5: Some Aroclor Mixtures

CASRN	IUPAC	TYPE
12674-11-2	Aroclor 1016	mixture
11104-28-2	Aroclor 1221	mixture
12672-29-6	Aroclor 1248	mixture
11097-69-1	Aroclor 1254	mixture
11096-82-5	Aroclor 1260	Mixture
11100-14-4	Aroclor 1268	mixture

(Source: USEPA, 2000)

Production and Use of PCBs

PCBs have gained significant utilization in industrial and commercial fields primarily owing to their non-flammability, chemical stability, elevated boiling point, and exceptional electrical insulating properties (Erickson et al.,

2010). These attributes have rendered PCBs highly sought-after for various applications. They have been utilized as dielectric fluids in capacitors and transformers, as plasticizers and sealants in plastics, paints, and rubber goods, and as coolants and hydraulic fluids in motors and hydraulic systems. Additionally, PCBs have been utilized in various other industrial applications (Safe, 1993).

The manufacturing of PCBs has taken place in multiple countries, including the United States, several European countries, China, and Russia (Kocan et al., 2001; Harrad et al., 2009). Their widespread production and use have contributed to their global distribution and environmental presence.

Commercial PCB products were produced under the names of Aroclor (United States), Chlophen (Germany), Kanechlor (Japan), Fenclor (Italy), and others. From 1930 to 1977, the United States held the position of the largest producer of PCBs, with a production exceeding 600,000 tons. The European region followed closely, producing approximately 450,000 tons of PCBs until 1984. On account of their severe toxic and persistent properties, industrial manufacturing of PCBs was banned worldwide. However, there were approximately 1.5 million tons of legacy PCBs produced during 1920–1980. In addition, PCBs are still inadvertently produced and can be found in a range of consumer products (Guo *et al.*, 2019; Herkert *et al.*, 2018; Hu *et al.*, 2010; Jahnke *et al.*, 2019; Rodenburg *et al.*, 2010;).

Physico-chemical Properties of PCBs

The location and number of chlorine atoms on the biphenyl influence water solubility, octanol-water partition coefficients, and fugacity among other properties (Table 1). The physiochemical properties of PCBs range for different

congeners from mono-PCBs to deca-PCBs, the more chlorinated PCBs are, the less volatile and soluble, and therefore have a greater affinity for particulate and organic matter, this can lead to differences between dissolved/vapour phase PCBs and those that are particle bound (Megson, 2019). Based on the chlorine substituents they possess, PCB congeners can be classified into semi-volatile and relatively non-volatile categories, with the highly chlorinated PCBs (HC-PCBs) typically exhibiting lower volatility. These differences in volatility play a crucial role in their environmental availability and exposure pathways. HC-PCBs possess an elevated capacity for bioaccumulation and biomagnification throughout the food chain, thereby establishing contaminated food, especially fish, as a notable source of exposure for human populations (Barron et al., 1994). Epidemiological studies have revealed an association between the intake of contaminated fish and increased levels of HC-PCBs in the bloodstream (Weintraub & Birnbaum, 2008; Domingo & Bocio, 2007).

While all PCBs exhibit some degree of volatility, the lower chlorinated PCBs (LC-PCBs) are more commonly reported. The release of airborne PCBs into the atmosphere is influenced by temperature and can originate from diverse environmental or industrial sources, including rivers, lakes, landfills, and contaminated building materials (Persoon et al., 2010). Exposure of human populations to low-chlorinated PCBs (LC-PCBs) is more likely to occur through inhalation of airborne particles rather than ingestion (Harrad et al., 2009; Robertson & Ludewig, 2013).

PCBs have low solubility and high lipophilicity. PCB concentrations in water are extremely low and high volumes of samples are often required. Passive sampling systems such as semipermeable membrane devices (SPMD)

or polyethylene passive samplers have been developed to address these issues and are now widely used to successfully monitor PCBs in both water and air (Megson, 2019).

The chemical characteristics of PCBs can be primarily defined by two factors: (a) the quantity of chlorine atoms and (b) the arrangement of the two phenyl rings in relation to each other (Figure 2). These chemical properties are mainly manifested through the electronegative impact of the chlorine atoms on the benzene rings. This influence leads to a partially polarized molecule with increased electron stability on the outer atoms and distributed electron density across the aromatic rings (Figure 2).

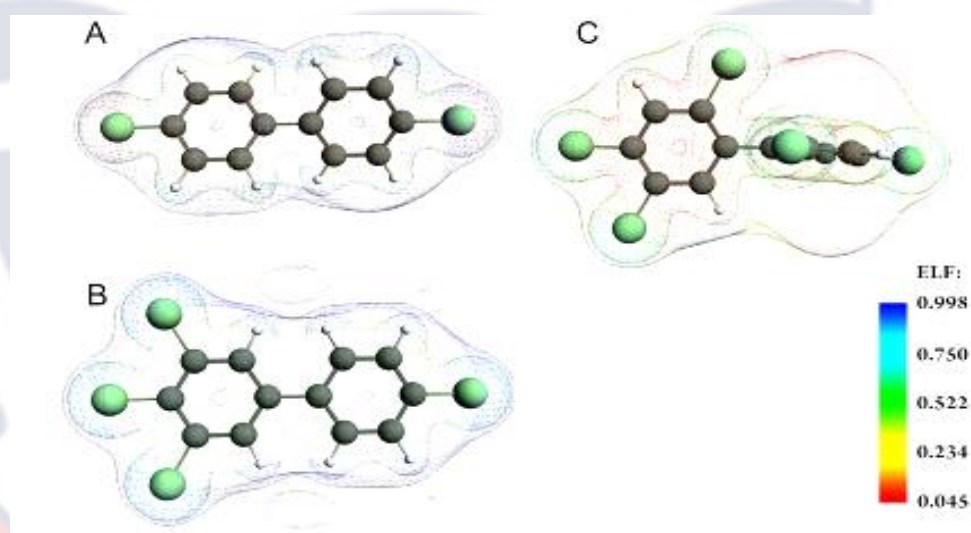


Figure 2: The electron density distribution (inner grid) and electrostatic potential (outer grid) of three different PCB congeners (A) 4,4'-dichloro-biphenyl (B) 3,4,4',5-tetrachloro-biphenyl and (C) 2,2',4,4',5,5'-hexachloro-biphenyl.

Studies on structure-activity relationships have demonstrated that the level of chlorination significantly contributes to the persistence of PCBs, leading to delayed degradation of both in vivo and ex vivo (Safe et al., 1985). Moreover, it has been observed that the presence of lateral chlorine atoms exerts the greatest toxicity impact (Figure 2). This suggests that fully planar congeners

with occupied para- and meta-positions, such as 3,3',4,4'-tetra-, 3,3',4,4',5-penta-, and 3,3',4,4',5,5'-hexachlorobiphenyl, exhibit the highest toxicity (Goldstein et al., 1978; Poland et al., 1977; Safe et al., 1985).

Human Exposure to PCBs

PCBs are widely present in the environment, and human exposure to these substances can transpire through multiple routes. The general pathways of human exposure include inhaling PCB-contaminated outdoor or indoor air, consuming PCB-contaminated drinking water and food, and direct contact with the skin. When PCB-containing wastes are dismantled, PCBs can be released into the atmosphere, and during combustion processes, dioxin-like PCBs may be formed (Tiernan et al., 1983; Ballschmiter & Zell, 1980). Inhalation plays a significant role as an exposure pathway, particularly for e-waste workers involved in open burning practices. These workers may face substantial PCB exposure through the inhalation of vapours, in addition to direct contact with the skin (Freels et al., 2007).

Exposure to PCB congeners directly through inhalation and contact with the skin can give rise to a broad spectrum of symptoms, including increased lipid levels in the bloodstream, chloracne, skin lesions, liver damage, and respiratory issues (Safe, 1993). PCB exposure can also disrupt various biological functions such as those of the immune and nervous systems (Carpenter, 2006), with fetuses being particularly susceptible to the adverse effects of PCB exposure (Jacobson et al., 1990).

Moreover, PCBs exhibit the ability to accumulate and magnify in higher trophic levels within the food chain. Consequently, the levels of PCBs in fish can be considerably higher than those detected in plankton, which occupies the

lowermost tier of the food chain. Numerous studies have reported a positive correlation between PCB concentrations in human samples and the consumption of fish and shellfish (Fitzgerald et al., 2011; Kostyniak et al., 1999; Stewart et al., 2008). Additionally, the monitoring of PCB levels in food has been implemented as a means to evaluate human exposure in various countries (Moon et al, 2010; Nakata et al., 2002; Schechter et al., 2010).

Occurrence of Polychlorinated Biphenyls (PCBs) in the Environment

Air

Although polychlorinated biphenyls (PCBs) have been banned for several decades in China, they were still detected at elevated levels due to their unintentional production from combustion and industrial thermal processes (UP-PCBs) (Mao *et al.* 2020).

To this end, Mao *et al.* (2020) investigated the composition and levels of UP-PCBs in ambient air. Air samples were collected between the period of 2012 and 2015 at a background site in eastern China. The results of the study indicated that predominant congeners observed in the analysis were PCB 47, 48 and 75 with an average concentration of 786 ± 63.7 pg/m³. This concentration was far higher than the concentration range (41-299 pg / m³) in Pakistan reported by Mahmood et al. (2014).

Water

Adeyinka et al. (2018) conducted a scientific investigation to assess the concentrations of eight different polychlorinated biphenyl (PCB) congeners in the Msunduzi River situated in KwaZulu-Natal, South Africa. The study involved the collection of soil, sediment, and water samples from ten distinct locations along the river during both the winter and spring seasons. The results

of the analysis revealed that the levels of PCBs in the sediment varied from 214.21 to 610.45 ng/g dry weight at the Du Toit sampling site during winter and from 30.86 to 444.43 ng/g dry weight at the wastewater treatment inlet during spring. Similarly, the levels of PCBs in the soil samples ranged from 76.53 to 397.75 ng/g dry weight at the Msunduzi Town sampling site during winter and from 20.84 to 443.49 ng/g dry weight at the Du Toit sampling site during spring. Notably, the authors observed higher levels of PCBs in the effluent of the wastewater treatment inlet compared to the other sampling sites. In the winter season, the PCB concentrations in the effluent ranged from 0.68 to 22.37 ng/mL, while in the spring season, the range was between 2.53 and 35.69 ng/mL.

In similar study conducted by Oliveira *et al.* (2005) in Lake Ontario basin, water samples collected from five tributaries between the period of 2004 and 2008. Findings showed that the total PCB levels in the water samples ranged between 0.31 and 42.75 ng / L. Congeners between Di and Hexa PCBs accounted between 70 and 99% of the total PCB. The tributary with highest PCB levels presented similar pattern and percentage levels to Aroclor 1242. Total average loads for the sampling events ranged between 1.85 g /d and 59.08 g/ d.

Biota

Adeogun et al. (2016) conducted a study examining the occurrence and distribution of polychlorinated biphenyl (PCB) congeners in the muscle tissue of the African sharp tooth catfish (*Clarias gariepinus*) found in the Ogun and Ona rivers in southwest Nigeria. The researchers discovered increased levels of high-molecular-weight PCB congeners in fish located downstream of discharge points in both rivers. Notably, a significant decline in fish body weight was

observed, which correlated with the high concentrations of PCB congeners found in the Ona River.

An analysis using a principal component (PC) biplot technique unveiled distinct patterns of PCB congener distribution in relation to the sampling sites.

In the Ogun River, high-molecular-weight PCB congeners accounted for 71.3% of the observed patterns, while the Ona River exhibited significant patterns for low-molecular-weight congeners, constituting 42.6% of the distribution. Overall, the results indicate that industrial discharges play a substantial role in the introduction of PCBs into these rivers. This raises concerns for nearby communities that rely on these rivers for fishing and other domestic purposes, as the presence of PCBs can pose potential health risks.

Dodoo et al. (2012) conducted a study in Ghana to examine the presence of polychlorinated biphenyls (PCBs) congener residues in two types of bivalves, specifically *Crassostrea tulipa* (oysters) and *Anadara senilis* (mussels). The study's findings indicated that the total PCB levels in the bivalves ranged from 5.55 to 6.37 $\mu\text{g}/\text{kg}$ wet weight in mussels and 2.95 to 11.41 $\mu\text{g}/\text{kg}$ wet weight in oysters. The composition of PCB homologues in the bivalves was primarily dominated by tri-, hepta-, and hexa-PCBs, in descending order. Based on risk assessments, it was suggested that the consumption of edible bivalves could potentially pose certain health risks to consumers. The presence of PCB residues in the bivalves suggested the need for monitoring and management strategies to minimize exposure and protect the health of individuals consuming these seafood products.

In a similar scientific investigation, Asante (2011) conducted an analysis of fish and cow milk samples collected from three different locations in Ghana:

Accra, Kumasi, and Tamale. The aim was to assess the levels and congener profiles of polychlorinated biphenyls (PCBs) and evaluate the associated risks to human health through fish consumption. Samples were gathered from both urban and rural areas within each location. The study's findings demonstrated the presence of PCBs in all the analyzed samples, indicating widespread contamination in the Ghanaian environment and human exposure to this contaminant. The concentrations of PCBs in fish displayed significant variation among the sampling locations. The total PCB concentrations ranged from 1.1 to 300 ng/g lipid weight, with an average concentration of 62 ng/g lipid weight across all sampling sites. Notably, Benya Lagoon was identified as the most heavily polluted water body (Asante et al., 2011).

The analysis of PCB homologue patterns revealed that hexa-PCBs exhibited the highest levels, followed by penta-PCBs, hepta-PCBs, and tetra-PCBs. The dominating congener pattern observed overall was PCB-153, followed by PCB-138, PCB-118, PCB-180, PCB-99, and PCB-52.

Comparing the summation of 62 PCB congeners reported in Ghana to other studies, it was found to exceed the levels reported in Slovenia (Cerkvenik et al., 2000), the UK (Stewart & Jones, 1996), and Siberia (Mamontova et al., 2007). However, the levels were lower than those reported in a study conducted in Poland (Pietrzak-Fiecko et al., 2005).

Soil and Sediments

Liu *et al.* (2019) conducted scientific investigation in Taizhou and Fengjiang, China to determine the levels of polychlorinated biphenyls (PCBs) released during e-waste dismantling process in the samples of soil and air collected from these locations. The results indicated that PCB still persisted in

the study areas. The PCB concentrations were clearly higher in the soil samples. The authors associated the persistence of PCBs in the study area (especially in the soil samples) to past and current emissions from e-waste dismantling processes since PCB production and use were banned. The long half-lives of PCBs have caused the target congener concentrations in soil not to decrease markedly over 10 years. The results also indicated the presence of PCBs in the air might have been caused by a "halo effect". Soil-air exchange of PCBs in heavily contaminated areas might have supplied PCBs to air because the temperatures were often high in the study areas. In another study initiated by Mahmood et al. (2014), the concentration of $\sum 33$ PCB in soil samples ($n = 28$) collected along the two tributaries of River Chenab, Pakistan ranged between 0.70-30.5 ng/ g per dry weight.

In a similar study, Wang et al. (2019) collected sediment samples from a depth of 40 cm in the Pearl River Delta of China undergoing the process of urbanization and reclamation to evaluate the levels of polychlorinated biphenyls (PCBs). The results showed that the total levels of PCBs in the river sediments ranged between 16.15 and 477.85 $\mu\text{g}/\text{kg}$.

Food Crops, Cereals and Vegetables

Mahmood et al. (2014) provided the first systematic data on PCB levels and their risk assessments by consumption of cereal food crops from Pakistan. Polychlorinated biphenyls (PCB) including dioxin-like PCBs (dl-PCBs) were analyzed in wheat and rice samples to assess the levels, spatial distribution pattern, and their risk assessments along the two tributaries of River Chenab, Pakistan. The concentrations of the $\sum 33$ PCB ranged between 0.15 and 2.22 ng / g per dry weight for wheat and 0.05-9.21 ng / g per dry weight for rice

respectively. The study also estimated the lower dioxin toxicity equivalency (TEQ) values from the previously reported data. Hazardous ratio (HR) for human health risk assessment allied to non-cancer was found lower than integrity.

In a study conducted by Luo *et al.* (2020), the distribution and composition of polychlorinated biphenyls (PCBs) within soil–plant systems around an e-waste recycling site were investigated. The average total PCB concentrations in rhizospheric soils (RSs) and non-rhizospheric soils (NRSs) were 2160 and 1270 pg g^{-1} dry weight (DW), respectively. PCBs were more enriched in RS than NRS for most vegetable species. PCB accumulation in plant tissues varied greatly among plant cultivars, ranging from 4020 to 14 500 pg g^{-1} dry weight in shoots and from 471 to 24400 pg g^{-1} dry weight in roots. The compositions of PCBs in soil and plants showed that hexa- and heptachlorinated PCBs were preferentially accumulated in soils, while tri- and tetra-PCBs were abundant in plant tissues. These results indicated that low-chlorinated PCBs might be prone to accumulation and transfer within plants, which was confirmed by the relationship between the root concentration factor and octanol–water coefficient. The first eluting enantiomers of PCB 84 and PCB 95 were preferentially transferred between the soil and plants, while the stereoselectivity of PCB 136 varied among plant species. A significant difference in enantiomeric fractionation of PCB 84 between the soil and roots indicated that enantiomeric enhancement of PCB 84 occurred during its translocation from soil to root, whereas no such difference was observed in these chiral PCBs during their translocation from the root to the shoot.

Human Biomonitoring

Kaifie *et al.* (2020) assessed the occupational PCB exposure in e-waste workers in relation to their specific recycling task (e.g., dismantling, burning) at Agbogbloshie, Ghana. Samples of blood plasma were taken from e-waste workers for the evaluation of PCB congeners. All plasma samples taken from the participants were evaluated for the PCB congeners PCB 28, 52, 101, 138, 153, 180 and sum of NDL-indicator congeners. Findings from the analyses revealed that significant difference existed between lower chlorinated PCB congeners (PCB 28, 52, and 101) for e-waste workers and the control group. The findings also pointed out that the workers who dismantle and those who burnt e-waste had the highest plasma levels of PCB 28 and 52. The authors concluded that the e-waste workers showed occupational related elevated PCB levels.

Abiotic Factors

Plastic resin pellets are industrial raw materials that are re-moulded finished products for industrial and domestic use, commonly used for packaging. Pellets can be unintentionally washed into the ocean where hydrophobic contaminants such as PCBs were also deposited (Agbo *et al.*, 2020). Plastic resin pellets from six beaches along the Accra-Tema coastline were collected and analysed. Results showed that PCB congeners such as PCB 28, 52, 101, 105, 138, 153, 156 and 180 were present in the samples. PCB 28 was detected at all six beaches, with a total concentration of 43.5 ng/g pellet (mean/beach 7.25 ± 2.47 ng/g pellet), while PCB 138 was only detected on one beach (Castle Beach) at a total concentration of 0.8 ng/g pellet. The concentration of PCBs ranged from 7.4 ng/g (Sunset Beach) to 47.5 ng/g (Castle

Beach) (mean 16.4 ± 15.4 ng/g per beach). PCB concentrations at Castle Beach have been studied previously, showing an increase from 39 ng/g to 47.5 ng/g, whereas levels decreased significantly from 28 ng/g to 14.2 ng/g in Sakumono Beach over the span of three years. The concentrations of four detected PCB congeners (28, 52, 101 and 156) were significantly higher than the World Health Organization (WHO) allowable daily intake of 6 ng/g food per day for PCBs. The authors advocated for a more efficient industrial and domestic waste disposal system for Ghana.

Toxicology of PCBs

The incidence rate of testicular germ cell tumours (TGCT) has continuously increased in Western countries over the last several decades (Cheng *et al.*, 2021). Some epidemiologic studies have reported that the endocrine disrupting polychlorinated biphenyls (PCBs) in serum may be associated with TGCT risk, but the evidence was inconsistent (Cheng *et al.*, 2021). To make the picture clearer, Cheng *et al.*, (2021) conducted a population-based case-control study of 308 TGCT cases and 323 controls to investigate whether serum levels of PCBs are associated with the increase of TGCT risk in the USA. Serum levels of 56 PCBs congeners were measured using gas chromatography and unconditional logistic regression model was used to evaluate the risk of TGCT associated with total PCBs exposure, groups of PCBs categorized by Wolff's functional groups, and individual PCB congeners. The results showed that there was no association between total serum levels of PCBs and risk of TGCT overall. However, strong positive association was observed between total serum levels of Wolff's Group 1 PCBs (potentially estrogenic) and risk of overall TGCT as well as seminoma and non-seminoma subtypes.

Wolff's Group 1 PCB congeners that showed an increased risk of TGCT included: 25, 44, 49, 52, 70, 101, 174, and 201/177. The authors were of the view that research should be replicated in different populations with larger sample size, considering the continuing increase of TGCT.

Identified Research Gaps and Measures Implemented to address them

The investigation into PFAS and PCB in the Pra River basin, as documented in the literature, reveals various gaps and limitations in the current understanding and data related to these pollutants. Some of the identified gaps include inadequate and comprehensive data regarding the presence, origins, and distribution of PFAS and PCB in surface water, sediment, and tap water, particularly concerning emerging and novel PFAS and PCB (Essumang et al., 2017; Niegowska et al., 2021). Moreover, there is limited information on bioaccumulation and biomagnification potential of PFAS and PCB in the aquatic organisms of the Pra River basin, along with the associated ecological and human health risks resulting from exposure to these contaminants (Cui et al., 2020; Niegowska et al., 2021). Additionally, uncertainty exists regarding the environmental fate and transport of PFAS and PCB in the Pra River basin, especially concerning the precursors and transformation products of PFAS, and the influence of environmental factors such as pH, temperature, and organic matter (Cui et al., 2020; Niegowska et al., 2021; Shao et al., 2016). Furthermore, there is limited information on the effectiveness and feasibility of various treatment technologies for the removal and destruction of PFAS and PCB from drinking water and wastewater, particularly in the context of water radiolysis and other advanced oxidation processes (Cui et al., 2020; Niegowska et al., 2021; Shao et al., 2016).

In addressing these knowledge gaps, this study aims to pursue the objectives set out earlier in this work. The proposed measures to tackle the identified gaps include generating data on the levels and spatial distribution of PFAS and PCB in the surface water and sediments of the Pra River basin. Additionally, assessing the ecological and human health risks associated with exposure to these contaminants using appropriate toxicity endpoints and exposure scenarios is important (Cui et al., 2020; Niegowska et al., 2021). Furthermore, the study aims to enhance the understanding of the environmental fate of PFAS and PCB in the Pra River basin. This involves identifying and determining the levels of these pollutants using advanced analytical techniques and modeling tools. Finally, the research intends to focus on determining the defluorination efficiency, identifying byproducts, and optimizing the water radiolysis process for the decomposition of PFAS (Cui et al., 2020; Niegowska et al., 2021; Shao et al., 2016).

Chapter Summary

This review has provided a comprehensive overview of organic micropollutants (PFAS and PCB) covering their sources, occurrence, environmental fate, health effects, method of detection, remediation technologies and associated research gaps regarding the Pra River basin. The review also emphasizes the need for continued research to understand the full of PFAS and PCB contamination and develop effective strategies for prevention and remediation. By consolidating the existing knowledge, this review aims to inform policymakers, scientists and stakeholders about the current state of PFAS and PCB research and guide future efforts in tackling the challenges associated with these persistent contaminants.

CHAPTER THREE

METHODOLOGY

Introduction

This chapter aims to provide an overview of the analytical methods used for the analysis of PFAS and PCBs in the Pra river basins, and as well as the optimized method for the decomposition of PFAS. It also covered the study area, sampling, analytical methods, quality assurance/quality control measures needed to ensure precise and reliable results, as well as data processing and analysis.

Study Area

The study was conducted in the Pra river basin. The basin is located in the southwestern part of Ghana and drains into the Gulf of Guinea. The river and its tributaries provide water for irrigation, domestic, and industrial use for communities within and beyond the basin. However, the basins face various environmental and social challenges that threaten its sustainability and productivity (WRC, 2022). The Pra river basins are a crucial water source for numerous communities surrounding Sekondi-Takoradi and the surrounding areas, providing drinking water to local residents. For the purpose of the study, samples of surface water and sediment were collected from the catchment areas of the Pra river (Table 6 and Figure 3).

Table 6: Sampling Locations with their Coordinates

Sampling Site Name	Sampling Site Number	Coordinates (N, W)
Atieku	P1	5.56667, -1.73240
Twifo Praso	P2	5.36599, -1.32599
Supong	P3	5.98580, -1.94344
Twifo Damang	P4	5.61379, -1.56545
Beposo	P5	5.12163, -1.61658
Sekyere Hemang	P6	5.183333, -1.56667
Twifo Hemang	P7	5.57118, -1.54650
Apetebi	P8	5.17440, -1.60710
Adiembra	P9	4.93673, -1.73319
Otodum	P10	5.16667, -1.65100
Daboase	P11	5.13850, -1.65910
Shama	P12	5.01948, -1.62690
Sekyere Nsuta	P13	5.31778, -1.97879
Atwereboanda	P14	5.33333, -1.88333
Supomu Dunkwa	P15	5.118269, -1.62188
Bosomase	P16	5.92160, -1.55930
Abetemasu	P17	5.38333, -1.63333
Dadieso	P18	5.85025, -2.01507
Kyekyewere	P19	5.91599, -1.67971
Sekyere Krobo	P20	5.24156, -1.60860

(Source: Fieldwork, 2021)

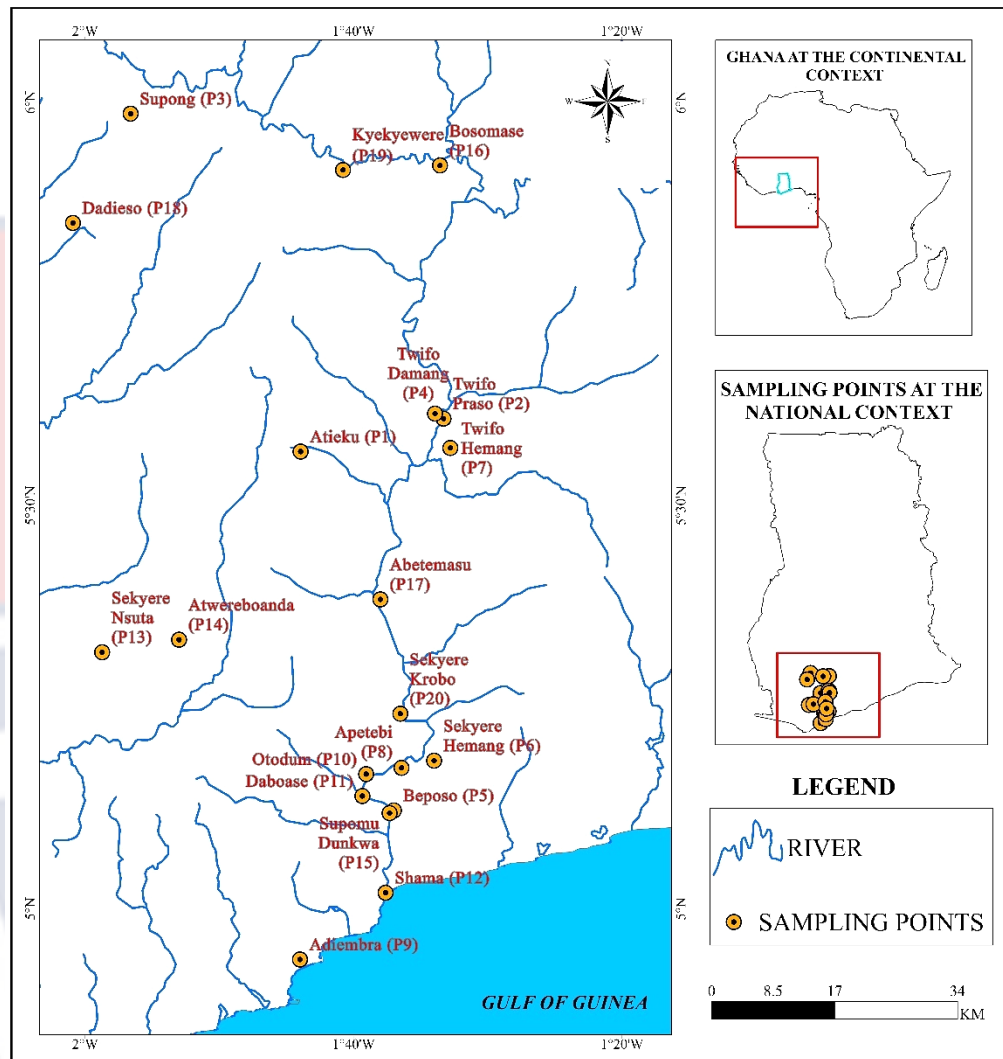


Figure 3: A map of Southern Ghana showing the sampling sites

Sampling

During the wet and dry seasons of August and September 2021, as well as November and December 2021, water and sediment samples were collected from the Pra River basin. To ensure comprehensive coverage, the sampling areas surrounding the lower Pra Basin were systematically divided into 30 locations along the river and its tributaries prior to the sampling process. Each location was assigned a location number (P1-P30) and sampled according to a predetermined, randomised plan. Twenty composite samples and their

duplicates were collected from each sampling point. Each composite sample consisted of four samples collected randomly in a 500 mL polypropylene bottle. Field blanks were also added to the batch and exposed to the same environmental conditions as the real samples.

Surface water samples were collected by aligning with the flow direction of the river. To maintain the samples' integrity, a rigorous procedure was followed. Before collection, the bottles underwent a thorough rinsing process, being rinsed three times using water from the specific sampling point. Then, each bottle was submerged to a depth of at least 10 cm below the water surface to acquire the sample.

Composite sediment samples (100 g) as well as their duplicates were collected using a corer and inserted into at least 10 cm below the surface of the sediment and then transferred into clean labelled containers for storage. After collection, the samples were carefully placed in an ice chest containing ice to maintain their integrity during transportation to the laboratory. Upon arrival, they were stored in a refrigerator at a temperature of 4°C to ensure proper preservation.

Analytical Techniques

Chemicals for PFAS Analysis

Fifteen PFAS were analysed as targeted compounds. Analytical standards were purchased from Wellington Laboratories (Ontario, Canada), Wako Pure Chemical Industries (Osaka, Japan), Kanto Chemical Industries (Chuo-ku, Japan), Tokyo Chemical Industries (Portland, OR, USA), Fluorochem (Derbyshire, UK) and Sigma Aldrich (Schnelldorf, Germany). The solvents used in samples preparation were purchased from Wako Pure Chemical

Industries (Osaka, Japan). Comprehensive information on chemicals and reagents used in the study are given in Appendix A.

Chemicals for Polychlorinated Biphenyls (PCBs) Analysis

Standard PCB mixture of “CEN PCB Congener Mix 1” (IUPAC No.’s 18, 28, 31, 44, 52, 101, 118, 138, 149, 153, 180, and 194) (Supelco, USA), which comprises 10 μ g/L of each component in heptane was employed for the six-point calibration technique. For the analysis, an internal standard solution was added to samples before extraction and it consisted of 50 ng/L 4, 4’ - dibromobiphenyl, Supelco (USA) in n-heptane. First-grade quality solvents namely n-heptane, methanol and acetone were also used for the analytical procedure, respectively. These solvents were procured from the Wako Pure Chemicals.

Chemicals for Fluoride Determination in Aqueous Samples after Gamma Irradiation

Unless otherwise specified, all chemicals used in the experiments were of analytical purity grade, ensuring their high quality and suitability for accurate analysis. Pentadecafluorooctanoic acid ammonium salts $\geq 98\%$, tert- butanol $\geq 99.7\%$, sodium hydroxide powder $\geq 97\%$ and potassium phosphate monobasic $\geq 99.0\%$ were obtained from Sigma Aldrich (Steinheim, Germany). Dipotassium hydrogen phosphate $\geq 99.5\%$ was purchased from VWR BDH Chemicals, while sodium formate $\geq 98\%$ was procured from the Thermoscientific (Germany). TISAB (Total Ionic Strength Adjustment Buffer) buffer for the potentiometric fluoride determination was prepared from glacial acetic acid 99–100% from J.T. Baker, disodium ethylenediaminetetraacetate dihydrate (Na₂EDTA. 2H₂O), sodium fluoride, potassium chloride and

potassium hydroxide pellets for analysis (max 0.002% Na) from Supelco. For the preparation of all solutions, deionized water with a resistivity of 18 MΩ cm, obtained from the Waters Milli-Q system (Waters, Bedford, MA, USA) was employed.

Solid Phase Extraction (SPE) of Perfluoroalkyl substances (PFAS)

Surface Water (Taniyasu *et al.* (2005))

Before the extraction process, the samples were thawed and allowed to reach room temperature. To enhance accuracy and consistency, the samples were fortified with a mixture of internal standards (I.S) at a concentration of 50 ng/L. Surface water samples and internal standard mixture of PFAS (Appendix A) were mixed thoroughly for 1 minute using voltex. The extraction procedure followed the method developed by Taniyasu *et al.* (2005). To begin with, weak anion exchange solid extraction was conducted using octadecyl C18 cartridges (6 mL, 200 mg, Bond Elut, Analytichem, Harbour City, CA, USA). Prior to usage, these cartridges underwent a preconditioning process. They were first treated with 5 mL of methanol containing 0.1% NH₄OH, followed by rinsing with 18 MΩ deionized water. Using polypropylene tubing, a volume of 500 mL of water samples was passed through the C18 column cartridges under vacuum at a flow rate of 5 mL per minute. This extraction process effectively captured the target compounds. Following the extraction, the cartridges were rinsed with 18 MΩ deionized water to remove any residual inorganic ions and impurities. Subsequently, the cartridges were dried by centrifuging at 2500 rpm for 15 minutes. Prior to elution, the cartridges were attached to envi-carb. Elution was carried out using 5 mL of 0.1% NH₄OH in methanol. The spiked extracts underwent nitrogen evaporation until the final volume reached 0.5 mL. To

ensure clarity, the spiked extracts were filtered using a 0.2 μm nylon membrane and then transferred into auto sampler vials for subsequent analysis.

Extraction of PFAS from Sediment

The methanol extraction method described by Lorenzo et al. (2015) was employed to extract sediment samples. Prior to the extraction, 5 g of sediment samples were spiked with 150 μl of a 50 ng/L solution. The sediment was then subjected to three extractions using 10 mL of methanol. Each extraction involved vortexing, sonication for 15 minutes, and centrifugation at 965 rpm for 15 minutes. The supernatant volume was reduced to 5 mL under a nitrogen stream and then adjusted to a final volume of 100 mL by adding 18 M Ω ultra-pure water.

The reconstituted supernatant was loaded onto the pre-conditioned cartridge at a flow rate of around 5 mL/min. To remove residual water in the sorbent, nitrogen gas was passed through the cartridge for approximately 20 minutes. The cartridges were fixed to envi-carb before elution. Elution was performed using 5 mL of 0.1% NH_4OH in methanol. The eluates were subjected to nitrogen evaporation until the final volume reached 1 mL. To ensure clarity, the spiked extracts were filtered using a 0.2 μm nylon membrane and then transferred into auto sampler vials for subsequent analysis (Lorenzo et al., 2015).

Equipment for PFAS Analysis

Liquid chromatograph (Agilent HP 1100, Santa Clara, CA, USA) coupled to a triple quadrupole mass spectrometer (6420 triple quad) was used to analyse the samples that contained PFAS. Varian vacuum filtration solid phase extraction manifold (Vac Elut SPS 24 manifold) and Bond Elut (Analytichem,

Harbour city, CA, USA) octadecyl (C18) cartridges were used to extract analytes from unfiltered water samples.

Liquid Chromatography – Mass Spectrometry analysis

Liquid Chromatography (LC) Conditions

The analysis of the samples was performed using an Agilent HP 1100 liquid chromatograph (Santa Clara, CA, USA) coupled to a triple quadrupole mass spectrometer (6420 triple quad). For each analysis, a 10 μ L aliquot of the extract was injected into a C18 column (Zorbax Eclipse plus C18) with dimensions of 2.1 mm x 150 mm and a particle size of 5 microns. The mobile phase utilized a binary system consisting of 10 mM ammonium acetate in water (Solvent A) and methanol (Solvent B) at a flow rate of 0.2 mL/min. The column temperature was maintained at 40°C throughout the analysis. Chromatographic separation was achieved using a gradient elution method with a total run time of 44.5 minutes. Specific details regarding the gradient elution can be found in Table 7.

Table 7: The Gradient Elution Profile of PFAS

Time/min	Solvent A (%)	Solvent B (%)
0	90	10
5	38	62
15	35	65
25	30	70
31	0	100
42	50	50
44.5	90	10

(Source: Laboratory Analysis, 2022)

The retention times for the various analyte are given in Table 8.

Table 8: Retention Times for the Various PFAS Analyte

Analyte	Retention time/min
PFBA	10.23
PFPeA	11.17
PFH _x A	13.98
PFHpA	14.68
PFOA	16.57
PFNA	18.81
PFDA	22.53
PFUnDA	29.14
PFDoDA	34.98
PFT _r DA	36.75
PFT _e DA	37.14
PFBS	13.29
PFH _x S	14.99
PFOS	16.57
PFDS	28.97

(Source: Laboratory Analysis, 2022)

Mass Spectrometer Configuration and Conditions

The mass spectrum data were acquired in a schedule multiple reaction mode with negative electro spray ionization. PFOS was monitored as $[M - H]^-$ at $m/z = 498.7$ and $m/z = 79.7$ for SO_3^- . PFOA was monitored as $[M-H]$ and $[M-COOH]^-$ at $m/z = 412.7$ and 368.7 respectively. The details of mass spectrometer configurations and conditions are provided in Table 9.

Table 9: Mass Spectrometer Configuration and Condition Used

Mass spectrometer	Condition
Ionization mode	Negative ionization
Scanning mode	Multiple reaction mode (MRM)
Capillary voltage	-3500V
Nozzle voltage	-500V
Nebulizer pressure	45psi
Dry gas temperature	300 ^o C
Dry gas flow rate	6 L/min
Sheath gas temperature	260 ^o C
Sheath gas flow rate	11 L/min

(Source: Laboratory Analysis, 2022)

The mass tune utilized the optimized parameters outlined in the study by Higgins et al. (2005). Argon gas was employed as the collision gas, and the collision energy was adjusted to optimize the analysis for each specific analyte.

Ionization and collision cell parameters were also optimized individually for each analyte, as detailed in Table 10.



Table 10: Mass Spectrometer Parameters of the Targeted Compounds

Native standard	precursor ion	product ion	cone (V)	collision (eV)	Labeled standard	precursor ion	product ion	cone (V)	collision (eV)
PFBA	112.9	168.7	35	9					
PFPeA	262.7	218.7	35	9					
PFH _x A	312.7	268.7	35	10	[¹³ C ₂]PFH _x A	314.7	269.6	35	9
PFHpA	362.7	318.7	35	10					
PFOA	412.7	368.7	35	10					
PFNA	462.7	418.7	35	10					
PFDA	512.7	468.7	35	11					
PFUnDA	562.7	518.7	35	11	[¹³ C ₂]PFDoDA	614.6	569.6	45	13
PFDoDA	612.7	568.7	35	13					
PFT _r DA	662.7	618.7	35	13					
PFT _e DA	712.7	668.7	35	13					
PFBS	298.7	79.8	35	25	[¹³ C ₄] PFOS	502.7	98.7	35	35
PFH _x S	398.7	79.8	35	35					
PFOS	498.7	79.7	35	35					
PFDS	598.7	79.5	35	45					

(Source: Laboratory Analysis, 2022)

Identification and Quantification of PFAS

Analytes were identified on the basis of their relative retention time, which is the ratio of the retention time of the analyte to that of the internal standard. In addition, the accurate mass of the deprotonated molecular ions ($[M-H]^-$) in the spectrum was taken into account when the chromatographic peak of interest had a signal-to-noise ratio of at least 3:1. Upon identification, area ratios were determined by integration of the area of an analyte under the obtained chromatograms in reference to the integrated area of the internal standard (Figure. 4). The analyte concentrations were calculated by fitting their area ratios in a six-point calibration curve, established by methanol spiked with a standard PFAS mixture obtaining concentrations in the range of 0–50 ng/ L (Figure 5). The curve covered a range equivalent to the concentration of the analytes after 500 mL water sample was concentrated to 0.5 mL extract (approximately 1,000-fold concentration). In cases where the concentration of sample extracts exceeded the calibration curve's range, appropriate dilutions were made using methanol before re-injecting them for analysis. Analyte concentrations in the measured extracts C_{extract} were calculated according to

$$C_{\text{extract}} = A/S \text{ (ug/L)}$$

where A is the peak area of the multiple reaction mode chromatogram and S is the slope of the calibration line obtained. The concentration in the water sample C_{sample} was calculated as

$$C_{\text{sample}} = \frac{C_{\text{extract}} \times D_f}{E_f \times R} \text{ (ng/L)}$$

where D_f is the dilution factor (number of times a particular extract is diluted in order to be within the calibration range), E_f is the enrichment factor (e.g., 1000 when 1000 mL sample is reduced to a final volume of 1mL extract) and R , the

recovery(%/100). For the twenty samples, 3 blank samples were analysed and the average concentrations obtained in the blanks was used to correct (subtracted from the analyte sample concentration) all concentration results.

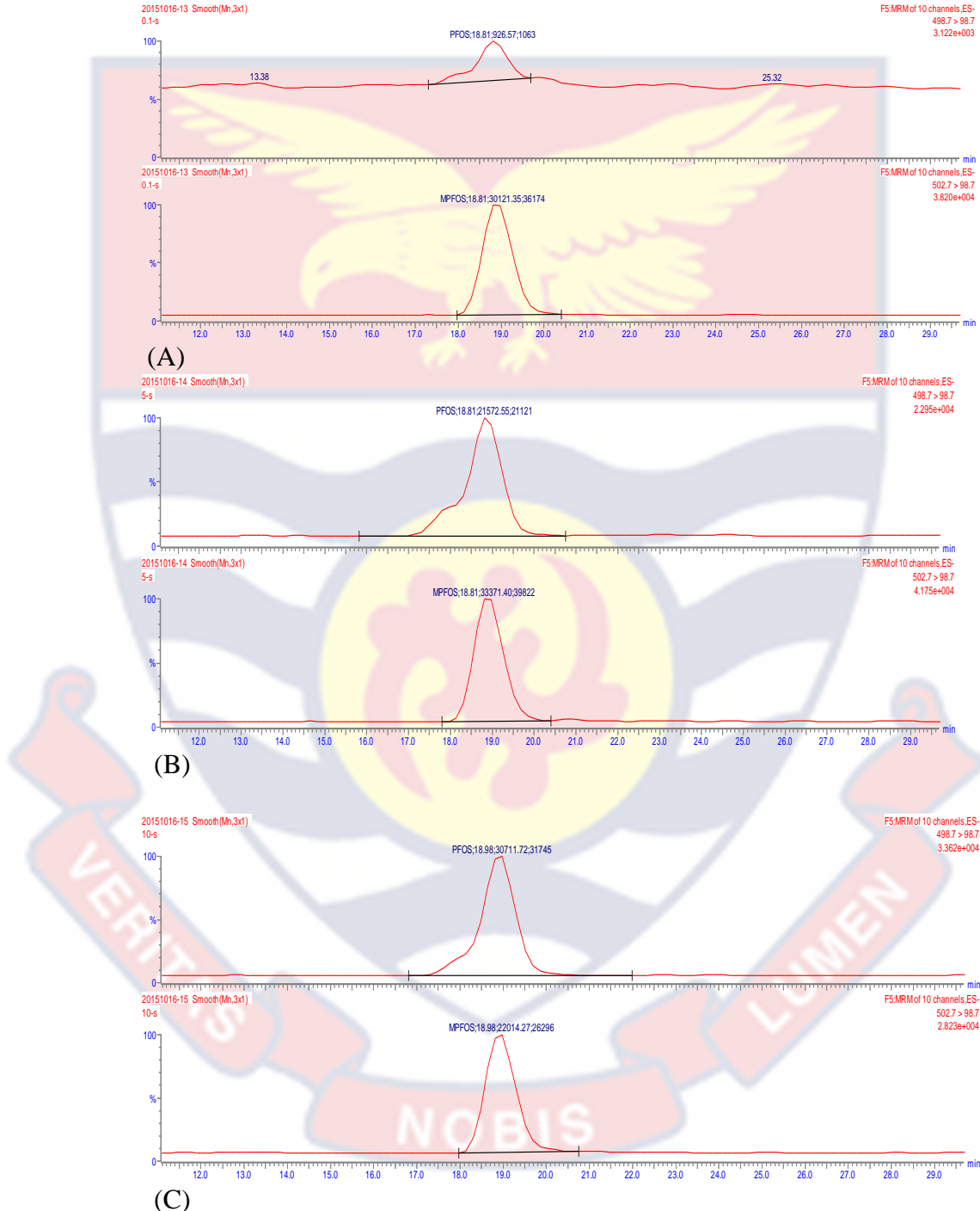


Figure 4: Some calibration chromatograms of 0.1,5,10 ppt PFOS (A, B, C) standards

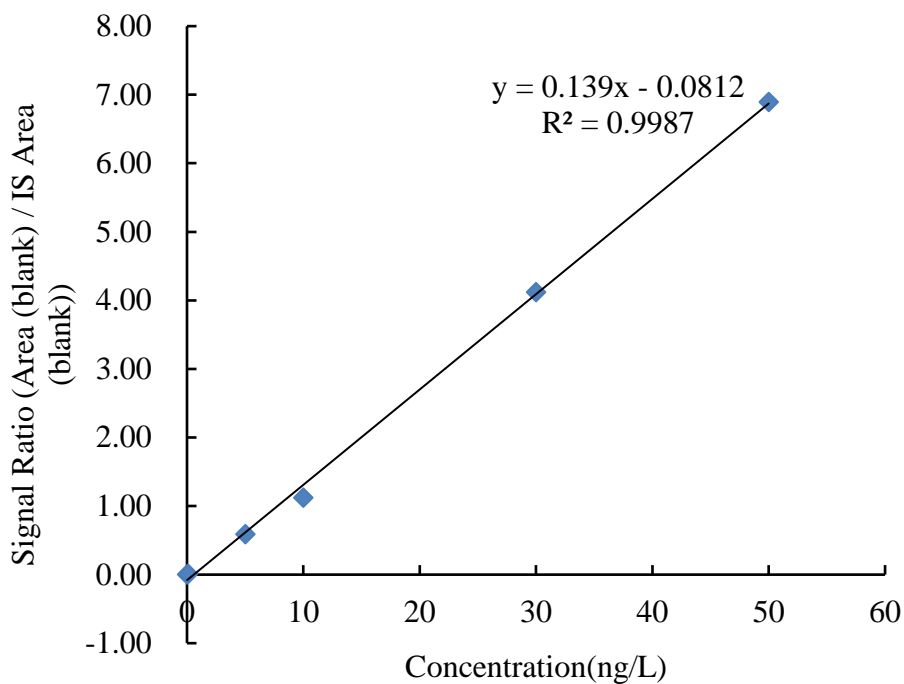


Figure 5: An example of a calibration curve of PFOS

Extraction of Polychlorinated Biphenyls (PCBs)

Both surface water and sediments from the Pra river basin were spiked with 4,4'-dibromobiphenyl as internal standard and extracted following the methods previously described by Taniyasu *et al.*, (2005) and Lorenzo *et al.* (2015) with n-hexane/acetone (1:1 v/v). All eluates from the Silicagel and Florisil cartridges (Sep-Pac1 Vac 6 cc, Waters) were concentrated in volume to 0.5 ml under nitrogen gas flow. Blank samples were analyzed according to the same procedures as those used for the samples, and no contamination was found.

Gas Chromatography–Mass Spectrometry Analysis of PCBs

The analysis of the samples was conducted using gas chromatography-mass spectrometry (GC-MS) with a Shimadzu QP-2010 Ultra instrument equipped with a flame ionization detector. A DB-5MS capillary column with a length of 30 m, an internal diameter of 0.25 μm , and a film thickness of 0.25 μm was employed. Helium gas was used as the carrier gas at a flow rate of 0.72

mL/min, resulting in a total flow of 31.8 mL/s and a linear velocity of 32.2 cm/s in splitless injection mode. The injection temperature was set at 150 °C, while the detector temperature was maintained at 320 °C.

The oven temperature was programmed to increase from 80 to 310 °C at a rate of 40 °C/min, followed by a further increase from 310 to 320 °C at a rate of 2 °C/min. This temperature gradient allowed for effective separation of the analytes. A 1- μ L injection volume was used. PCB homologues were determined by single ion monitoring (SIM). The following quantifying and qualifying ions were monitored simultaneously: m/z values were 256 and 258 for trichlorobiphenyls; 290 and 292 for tetrachlorobiphenyls; 326 and 328 for pentachlorobiphenyls; 360 and 362 for hexachlorobiphenyls; 394 and 396 for heptachlorobiphenyls; and 312 for 4,4' - dibromo biphenyl. Stringent quality control measures were implemented throughout the study.

To assess and maintain the accuracy and reliability of the analysis, laboratory blanks were included. For both water and sediment, the laboratory blanks underwent the same analytical procedures as the original samples. However, no significant peaks related to the analytes of interest were detected in these laboratory blanks. The laboratory blank used for the water samples in this study consisted of 18 M Ω water. As for the sediment laboratory blank, washed sand purchased from Sigma-Aldrich was utilized. These blanks were incorporated to account for any potential contamination or background interference during the analysis process.

Identification and Quantification of PCBs

The identification of PCB peaks was based on their retention times (RTs) and on intensity ratios of the monitored ions for quantification using gas

chromatography- mass spectrometry (GC-MS). The concentrations of PCBs were quantified according to the internal standard method. A solution of 4, 4'-dibromobiphenyl was used as an internal standard. The calibration technique employed was an internal standard multi-point (six point) calibration using several standard solutions. The PCB concentration in an analyzed sample was calculated as an average value for two replicate samples. For the twenty samples, 3 blank samples were analysed and the average concentrations obtained in the blanks was used to correct (subtracted from the analyte sample concentration) all concentration results. The retention times for the various PCB analytes are given below (Table 11).

Table 11: Retention Times for the various PCB analytes

Analyte	Retention time
PCB 18	7.97
PCB 28	8.16
PCB 31	8.27
PCB 44	8.39
PCB 52	10.23
PCB 101	9.89
PCB 118	10.86
PCB 138	11.12
PCB 149	10.63
PCB 153	10.76
PCB 194	12.14
PCB 180	11.94

(Source: Laboratory Analysis, 2022)

Radiolytic Decomposition of PFOA

Irradiation Instrumentation

In this study, aqueous solutions of PFOA (1mM, 0.5mM and 1 μ M) under two pH conditions (6 and 11) were γ -irradiated using the ^{60}Co source Gamma Chamber at the Institut de Chimie Physique-CNRS, Universite Paris Saclay, France. An exemplar dosimetry for PFOA has been presented in Table 12.

Table 12: An Exemplar Dosimetry of PFOA

Time	Dose/kGy	Dose rate/min	Position on platform	pH condition
9h 00 mins	20.0	2.23	6	11
8h 40 mins	20.0	2.31	5	6
7h 00mins	14.0	2.00	3	11
6h 28mins	14.0	2.17	4	6
5h 42mins	10.0	1.76	2	11
5h 18 mins	10.0	1.89	7	6
5h 40 mins	8.0	1.41	1	11
5h 02mins	8.0	1.59	8	6
4h 17 mins	6.0	1.41	9	11
4h 17 mins	6.0	1.41	25	6
4h 00 mins	5.0	1.25	23	11
3h 50 mins	5.0	1.31	24	6
3h 18 mins	4.0	1.21	10	11
3h 18 mins	4.0	1.22	27	6
2h 42mins	3.0	1.11	22	11
2h 50 mins	3.0	1.06	28	6
2h 00mins	2.0	0.95	29	11
2h 05 mins	2.0	1.02	11	6
1h 13mins	1.0	0.83	308	11
1h 13mins	1.0	0.86	30	6

(Source: Laboratory Analysis, 2022)

Fluoride determination in the irradiated aqueous solutions of PFOA

The fluoride ions in the irradiated aqueous solutions were determined by following the procedure described by U.S. Environmental Protection Agency (2017) as well as Michalska *et al.* (2017). The fluoride ion measurement was done by using an electrometer depicted in Figure 6.



Figure 6: Electrometer with Fluoride Ion Selective Electrode

In detail, the procedure was categorized into five sections;

Sample preparation

A known volume (2 mL) of irradiated aqueous solution of PFOA was transferred into a clean and dry sample vial and TISAB solution (2 mL) was added to adjust the pH to the range of 6 to 7.

Calibration and electrode conditioning

The Ion Selective Electrode probe was cleaned on the outside with deionized water thoroughly. The probe was filled with Orion Ionplus filling solution (Reference Electrode filling Solution) to the hole mark. Standard fluoride solutions with concentrations 0.5 ppm and 5 ppm were prepared and used for the calibration. The probe was dipped into the standard solution with

lower concentration first for 10 minutes to activate the sensor. The probe was then rinsed on the outside thoroughly and slightly wiped. The probe was also dipped into the standard fluoride solution with higher concentration to continue the calibration of the device. The probe was rinsed thoroughly again and made ready for measurement.

Analysis

The probe of the electrometer was immersed into the conditioned ISE into sample solutions and, potential difference between the electrode and a reference electrode measured.

Quality control

Blanks (deionized water with resistivity of 18Ω) were analysed to ensure that there was no contamination during analysis. Replicate analysis was performed to check the precision of the results.

Cleaning and storage

The probe of the electrometer was thoroughly cleaned and the sensor cap put into its place to maintain its sensitivity and accuracy.

Human Health Risk Computations

Carcinogenic risk

The carcinogenic risk associated with a potential receptor exposure to chemical constituents in water was estimated using the linear low-dose model (USEPA, 1989). This model assumes that there are multiple stages for cancer, and it is only applicable at low risk levels (i.e., estimated risks < 0.01). The assessment risk was based on ingestion and dermal contact for both water and sediments. Table 12 presents the parameters used with their definitions and exposure assumptions in the various equations stated.

Total Cancer Risk, $TCR_{low-risk} =$

$$\sum_{j=1}^p \sum_{i=1}^n (CDI_{ij} \times SF_{ij})$$

and Aggregate or Cumulative Total Cancer Risk, $ATCR_{low-risk} =$

$$\sum_{k=1}^s \left\{ \sum_{j=1}^p \sum_{i=1}^n (CDI_{ij} \times SF_{ij}) \right\}$$

In simple terms, cancer risk can be estimated following the relationship below:

$$\text{Cancer Risk} = SF_0 \times CDI_0$$

Carcinogenic effects for organic micropollutants (PFAS and PCBs) in water

$$\begin{aligned} \text{Risk}_{\text{water}} = & \left\{ SF_0 \times C_w \frac{(IR_{\text{adult}} \times FI \times ABS_{gi} \times EF \times ED_{\text{adult}})}{(BW_{\text{adult}} \times AT \times 365 \text{ day/year})} \right\} \\ & + \left\{ SF_0 \times C_w \frac{(SA_{\text{adult}} \times K_p \times CF \times FI \times ABS_{gi} \times EF \times ED_{\text{adult}} \times ET_{\text{adult}})}{(BW_{\text{adult}} \times AT \times 365 \text{ day/year})} \right\} \end{aligned}$$

$$\text{Cancer risk} = SF_0 \times CDI_0 \dots\dots\dots (2)$$

$$\text{Cancer risk} = (SF_0 \times C_w \times 0.0149) + (SF_0 \times C_w \times 0.0325 \times K_p)$$

Carcinogenic effects of organic micropollutants (PFAS and PCBs) in soils/sediment

$$\begin{aligned} \text{Risk}_{\text{sediment}} = & \left\{ SF_0 \times C_s \frac{(SIR_{\text{adult}} \times CF \times FI \times ABS_{gi} \times EF \times ED_{\text{adult}})}{(BW_{\text{adult}} \times AT \times 365 \text{ day/year})} \right\} \\ & + \left\{ SF_0 \times C_s \frac{(SA_{\text{adult}} \times AF \times CF \times FI \times ABS_{gi} \times ABS_s \times EF \times ED_{\text{adult}})}{(BW_{\text{adult}} \times AT \times 365 \text{ day/year})} \right\} \end{aligned}$$

$$\text{Risk}_{\text{sediment}} = \{\text{SF}_0 \times C_s \times [1.57 \times 10^{-6}] + \{\text{SF}_0 \times C_s \times [1.88 \times 10^{-5}] \times \text{ABS}_s\}$$

Table 13: Parameter Definition and Exposure Assumption

Parameter	Parameter Definition and Exposure Assumption
SF _o	Oral cancer potency slope (obtained from literature) ([mg/kg day] ⁻¹)
SF _i	Inhalation cancer potency slope (from the literature) ([mg/kg day] ⁻¹)
C _w	Chemical concentration in water (obtained from the sampling and) (mg/L)
C _s	Chemical concentration in soil (obtained from the sampling and) (mg/kg)
K _p	Chemical-specific dermal permeability coefficient from water (obtained from the literature) (cm /hr)
AF	Soil to skin adherence factor (1 mg/cm ²)
SA	Skin surface area available for water contact (adult = 23,000 cm ²); Skin surface area available for soil contact (adult = 5800 cm ²)
IR	Average water intake rate—where intake from inhalation of volatile constituents may be assumed as equivalent to the amount of ingested water (adult = 2 L/day; child = 1 L/day)
SIR	Average soil ingestion rate (adult = 100 mg/day;
IR _a	Inhalation rate (adult = 20 m ³ /day)
CF	Conversion factor for water (1 L/1000 cm ³); Conversion factor for soil (10 ⁻⁶ kg/mg)
FI	Fraction ingested from contaminated source (1)
ABS _{gi}	Bioavailability/gastrointestinal [GI] absorption factor (100%)
ABS _s	Chemical-specific skin absorption fraction of chemical from soil (%)
EF	Exposure frequency for water (350 days/year); Exposure frequency for soil (soil ingestion = 350 days/year; dermal contact—adult = 100 days/year)
ED	Exposure duration (adult = 24 years)
ET	Exposure time during showering/bathing (adult =0.25 h/day)
BW	body weight (adult = 70 kg)
AT	Averaging time (period over which exposure is averaged = 70 years or [70 x 365]

(Source: Asante-Duah, 2017)

Non-carcinogenic risks to human health

The potential non-cancer health effects resulting from a chemical exposure problem was estimated using hazard quotient (HQ) or the hazard index (HI) (USEPA 1989).

$$\text{Hazard Quotient, HQ} = \frac{E}{\text{RfD}}$$

where E is the chemical exposure level or intake (mg/kg-day); and RfD is the reference dose (mg/kg-day).

For single chemical contaminant, the hazard index can be calculated

using the relationship below:

$$\text{Hazard index} = \frac{1}{\text{RfD}} \times \text{CDI}$$

where non-cancer toxicity index or reference dose (RfD)

Concentration of contaminant in water C_w

Chronic daily intake (CDI)

For mixture of chemical contaminants, cumulative non-cancer risk was evaluated using a hazard index that is generated for each health or toxicological 'endpoint'.

The total hazard index and cumulative or aggregate non-cancer risk to human health could be evaluated based on the algorithm below:

Total hazard index =

$$\sum_{j=1}^p \sum_{i=1}^n \frac{E_{ij}}{\text{RfD}_{ij}} = \sum_{j=1}^p \sum_{i=1}^n (\text{HQ})_{ij}$$

For example, to compute Hazard Index for PFAS, the equations

$\text{HI}_{\text{PFAS}} =$

$$\sum_{j=1}^n \text{HQ}_{\text{PFAS}} = \text{HQ}_{\text{PFBA}} + \text{HQ}_{\text{PFPeA}} + \text{HQ}_{\text{PFHxA}} + \text{HQ}_{\text{PFOS}} + \text{HQ}_{\text{PFNA}} \\ + \text{HQ}_{\text{PFDA}} + \text{HQ}_{\text{PFHxS}} + \text{HQ}_{\text{PFOS}}$$

and

Aggregate or Cumulative Total Hazard Index

$$= \sum_{k=1}^s \left\{ \sum_{j=1}^p \sum_{i=1}^n \frac{E_{ij}}{RfD_{ij}} \right\}$$

$$= \sum_{k=1}^s \left\{ \sum_{j=1}^p \sum_{i=1}^n (HQ)_{ij} \right\}$$

where:

E_{ij} = exposure level (or intake) for the i th chemical and j th route (mg/kg day)

RfD_{ij} = acceptable intake level (or reference dose) for the i th chemical and

j th exposure route (mg/kg day).

HQ_{ij} = hazard quotient for the i th chemical and j th route

n = total number of chemicals showing non-carcinogenic effects

p = total number of pathways or exposure routes

s = total number for multiple sources of exposures to receptor

(e.g., dietary, drinking water, occupational, residential, recreational, etc.) were followed.

Non-carcinogenic Effects for Contaminants (PFAS and PCBs) in Water

$$\text{Hazard}_{\text{water}} = \left\{ \frac{1}{RfD_0} \times C_w \frac{(IR_{\text{adult}} \times FI \times ABS_{gi} \times EF \times ED_{\text{adult}})}{(BW_{\text{adult}} \times AT \times 365 \text{ day/year})} \right\}$$

$$+ \left\{ \frac{1}{RfD_0} \times C_w \times \frac{(SA_{\text{adult}} \times K_p \times CF \times FI \times ABS_{gi} \times EF \times ED_{\text{adult}} \times ET_{\text{adult}})}{(BW_{\text{adult}} \times AT \times 365 \text{ day/year})} \right\}$$

$$\text{Hazard}_{\text{water}} = \frac{1}{RfD_0} \times CDI_0 \dots\dots\dots(2)$$

$$\text{Hazard}_{\text{water}} = \left(\frac{1}{RfD_0} \times C_w \times 0.0149 \right) + \left(\frac{1}{RfD_0} \times C_w \times 0.0325 \times K_p \right)$$

Non-Carcinogenic Effects for Contaminants (PFAS and PCBs) in**Soils/Sediments**Hazard_{sediment}

$$\begin{aligned}
 &= \left\{ \frac{1}{\text{RfD}_0} \times C_s \times \frac{(\text{SIR}_{\text{adult}} \times \text{CF} \times \text{FI} \times \text{ABS}_{\text{gi}} \times \text{EF} \times \text{ED}_{\text{adult}})}{(\text{BW}_{\text{adult}} \times \text{AT} \times 365 \text{ day/year})} \right\} \\
 &+ \left\{ \frac{1}{\text{RfD}_0} \times C_s \times \frac{(\text{SA}_{\text{adult}} \times \text{AF} \times \text{CF} \times \text{FI} \times \text{ABS}_{\text{gi}} \times \text{ABS}_s \times \text{EF} \times \text{ED}_{\text{adult}})}{(\text{BW}_{\text{adult}} \times \text{AT} \times 365 \text{ day/year})} \right\} \\
 \text{Hazard}_{\text{sediment}} &= \left\{ \frac{1}{\text{RfD}_0} \times C_s \times [1.57 \times 10^{-6}] + \left\{ \frac{1}{\text{RfD}_0} \times C_s \times [1.88 \times \right. \right. \\
 &10^{-5}] \times \text{ABS}_s \left. \left. \right\} \right\}
 \end{aligned}$$

Ecological Risk Analysis**Risk Quotient of Single Organic Micropollutants**

The assessment of potential environmental risks associated with each individual micropollutant was conducted using the risk quotient (RQ) approach. The RQ was determined by calculating the ratio between the measured environmental concentration (MEC) and the predicted no effect concentration (NOEC). This calculation followed the guidelines outlined in the Technical Guidance Document on Risk Assessment published by the European Commission (Zhou et al., 2019). By applying the RQ methodology, the study aimed to evaluate the likelihood of adverse effects resulting from the presence of micropollutants in the environment. Risk quotients (RQs) were estimated as follows;

$$\text{RQ} = \frac{\text{MEC}}{\text{NOEC}}$$

$$\text{NOEC} = \frac{\text{EC}_{50} \text{ or } \text{LC}_{50}}{\text{AF}}$$

where MEC is the mean concentration derived from the detected concentrations from micropollutants measurement at an individual location; NOEC is calculated by the environmental toxicity data and assessment factor (AF).

Risk Quotient of Composite Organic Micropollutants

The risk quotients of mixtures were determined using the concentration addition (CA) model, as proposed by Backhaus and Faust (2012), for mixture interaction analysis. In this approach, the risk quotient of a mixture was calculated by summing the individual ratios of the measured environmental concentration (MEC) to the no observed effect concentration (NOEC). This calculation allowed for the assessment of potential combined effects and risks associated with mixtures of pollutants. By applying the CA model, the study aimed to gain insights into the cumulative impact of multiple pollutants and their potential effects on the environment. $RQ_{MEC/NOEC}$ was estimated as follows

$$RQ_{MEC/NOEC} = \sum_{i=1}^n \frac{MEC_i}{NOEC_i}$$

$$\sum_{i=1}^n \frac{MEC_i}{\min(E(L)C_{50,i,algae}, \min(E(L)C_{50,i,crustacea}, \min(E(L)C_{50,i,fish}))/AF}$$

Data Analysis

Statistical analyses were performed with Origin 2021 (OriginLab, Northampton, MA) and Microsoft Office Excel 2019 application. Statistic t-tests was used to test null hypotheses of no differences between wet and dry seasons for their respective mean proportions for both PFAS and PCBs for each congener identified in the different matrices. The significance level was set at p-value (α) ≤ 0.05 . Reported values are means \pm SD. Graphs were drawn using the Origin 2021 software.

A Principal Component Analysis was performed to identify patterns and reduce its dimensionality. The PCA helped identify which organic micropollutants (PFAS and PCBs) are most relevant in the dataset and which sources or pathways of contamination are most significant. Both 3- and 2-dimension analyses were applied to illustrate the variations among the first three principal components. The first principal component usually represents the overall contamination level, while the subsequent components may represent specific sources or pathways of contamination.

PCA was also used to identify the correlations between the compounds that helped in identifying co-occurring mixtures of both PFAS and PCBs that may have unique toxicological properties.

Chapter Summary

This chapter provides a comprehensive summary of the analysis of PFAS and PCB sampled from the Pra River basin. It describes the sampling techniques employed to collect representative environmental samples, the application of LC-MS and GC-MS for analysis, and the subsequent data analysis techniques. The chapter emphasizes the importance of accurate identification, quantification and data analysis to gain insights into the levels of PFAS and PCB contamination in the Pra river basin and inform effective mitigation strategies.

CHAPTER FOUR

RESULTS AND DISCUSSION

Introduction

Organic micropollutants released into the environment have been reported globally to have detrimental effect on human health and the environment. They have been found in both urban and rural areas, and at levels that are of concern for human and environmental health. The purpose of this chapter is to provide an overview of the results and discussions on organic micropollutants (PFAS and PCBs) and their impacts on human, water and sediment in the Pra Basin. This chapter discusses the quality assurance and control of method performance, spatial distribution, source contribution, health and ecological effects, and as well as the potential solutions for reducing their presence in these environments.

Perfluoroalkyl Substances (PFAS)

Quality Assurance and Control

Stringent measures were taken to minimize background contamination throughout the sample preparation and analysis procedures. To prevent instrumental and procedural contamination, the use of polytetrafluoroethylene (PTFE) materials was avoided. Additionally, all containers involved in the sample preparation and analysis processes underwent thorough washing with methanol prior to use.

The performance of the method was evaluated for linearity, limit of detection (LODs), limit of quantification (LOQs), relative recovery, precision, and blanks effects. Detailed information on the above parameters can be found in Tables 13 and 14 for PFAS.

Linearity assessment was conducted over a concentration range of 0.01-50 ng/L using six calibration points (three replicates) for both water and sediment samples. The purpose was to verify the linearity of the instrument response and ensure accurate quantification. Standard solutions were prepared by dissolving the standards in methanol at concentrations of 0.01, 0.1, 5, 10, 30, and 50 ng/L. The linearity of the calibration curves was assessed by calculating the regression coefficients (R^2), which were determined by plotting the ratio of the peak area to the concentration. The majority of the compounds exhibited regression coefficients greater than 0.9900, indicating a high level of linearity (refer to Tables 13 and 14 for specific values).

To account for potential contamination, three blank samples were included in the analysis. The average concentrations of each analyte detected in the blank samples were subtracted from the corresponding analyte concentrations observed in the test samples.

Table 14: Method Limits, Linearity, Variation and Recovery of the 8 PFAS in Water Samples

Analyte	LoD (ng/L)	LoQ (ng/L)	Linearity (r^2)	Recovery (%)	RPD _w (%)	RPD _d (%)
PFBA	0.037 - 0.045	0.12 - 0.15	0.9972	108.7	4.89	6.83
PFPeA	0.036 - 0.075	0.12 - 0.25	0.9983	93.6	3.16	3.90
PFHxA	0.06 - 0.078	0.2 - 0.26	0.9969	98.5	2.78	4.45
PFOA	0.06 - 0.075	0.2 - 0.25	0.9951	120.1	9.5	10.75
PFNA	0.064 - 0.076	0.21 - 0.25	0.9982	131.7	19.4	19.92
PFDA	0.045 - 0.048	0.15 - 1.16	0.9913	118.9	14.6	11.73
PFHxS	0.054 - 0.06	0.18 - 0.2	0.9824	83.6	2.83	3.76
PFOS	0.06 - 0.078	0.2 - 0.21	0.9925	109.5	19.6	4.94

(Source: Fieldwork,2022)

LoD = limit of detection; LOQ = limit of quantification; RPD_w = relative percent difference for duplicate samples for the wet season; RPD_d = relative percent difference for duplicate samples for the dry season.

Table 15: Method Limits, Linearity, Variation and Recovery of the 8 PFAS in Sediment Samples

Analyte	LoD (ng/g)	LoQ (ng/g)	Linearity (r^2)	Recovery (%)	RPD _w (%)	RPD _d (%)
PFBA	0.23 – 1.83	0.77 – 6.1	0.9981	81.7	7.4	7.9
PFPeA	0.03 – 1.5	0.1 – 5.0	0.9923	89.6	9.1	10.8
PFHxA	0.06 – 2.49	0.2 – 8.25	0.9962	90.7	4.89	6.75
PFOA	0.15 – 0.39	0.5 – 1.3	0.9975	95.6	10.3	14.92
PFNA	0.5 – 8.31	1.66 – 7.7	0.9951	102.6	15.7	21.5
PFDA	0.27 – 0.36	0.9 – 1.2	0.9924	102.9	19.6	19.5
PFHxS	0.11 – 0.15	0.35 – 0.5	0.9974	71.7	8.5	8.9
PFOS	0.06 – 0.24	0.2 – 0.80	0.9963	98.3	4.78	5.91

(Source: Fieldwork, 2022)

LoD = limit of detection; LOQ = limit of quantification; RPD_w = relative percent difference for duplicate samples for the wet season; RPD_d = relative percent difference for duplicate samples for the dry season.

The precision of the method was determined by evaluating the repeatability of the study. To accomplish this, duplicate measurements were performed for both water and sediment samples for every tenth sample. In general, the relative percent difference values (RPD) for both water (2.83-19.6%) and sediment (4.78-19.6%) were considered desirable as it indicates high degree of precision. This was consistent with common laboratory practice, in which a RPD (relative percent difference) threshold value of 20% is generally considered acceptable for environmental testing (Pihlström, 2011).

Since there was no certified reference material available, the accuracy of the measurements and the reproducibility within the laboratory were assessed using a spike recovery approach. This involved spiking surface water and sediment samples with a mixture of internal standards (50 ng/L) in deionized water, followed by extraction using the same procedure as used for the actual samples. This spike recovery experiment was performed in six replicates. The average recoveries for the various PFAS congeners ranged between 83.6% and 131.7% for water samples and 81.7-102.9% for sediment samples (Tables 13

and 14). According to the Pihlström, (2011), recoveries within the range of 70-120% are preferable. The recoveries obtained were generally satisfactory, indicating good precision for most of the analytes.

The limit of detection (LOD) and limit of quantification (LOQ) were determined. Limit of detection, defined as the concentration that yielded signal to noise ratio of ≥ 3 was determined for each analyte. LOQ, defined as the concentration that yielded signal to noise ratio of ≥ 10 , was also estimated in the same way for the individual analytes. The range of values for LOD and LOQ for each analyte were reported in Tables 12 and 13 for PFAS.

Occurrence and Detection Frequency of PFAS

The detection frequency of PFAS is an important parameter for the evaluation of the extent of their presence in the environment and potential impact on human health. The detection frequency of an OMP such as PFAS is influenced by several factors, including the type and use of products containing PFAS, the proximity of the sampling location to sources of PFAS release and as well as the analytical method used for testing.

In this study, 8 PFAS out of 15 were detected above the LOQ (limit of quantification) in both water and sediment. Although a suite of PFAS were analysed, 8 PFAS (including PFHpA, PFDoDA, PFTrDA, PFTeDA, PFUnDA, PFBS and PFDS) were not detected in any sample. These compounds were not included in Tables 13 and 14. Among the perfluoroalkyl substances (PFAS), perfluorooctanoic acid (PFOA) and perfluorooctane sulphonic acid (PFOS) were observed at very high levels in all the 20 sampling points in the Pra River Basin. Additionally, the other six congeners were observed in more than 52 % of the sampling points: PFBA, PFPeA, PFHxA, PFOA, PFNA, PFDA, PFHxS

and PFOS. It was clearly observed that the detection frequency of PFAS from the Pra River Basin were not the same for all the individual sampling locations (P1-P20) (Appendix B). Furthermore, the study identified 2 additional PFAS compounds (i.e., PFBA and PFNA) present in the Pra river basin as compared to the earlier research conducted in 2016 on the same river (Essumang *et al.* 2016).

The only long-chain PFAS observed was PFDA with very low concentration in both water (0.26 ng/L) and sediment (0.84 ng/g). PFDA was observed in the majority of water and sediment samples from Pra River. This observation is significant as it aligns with the known tendency of perfluorinated carboxylic acids (PFCAs) containing eight or more perfluorinated carbon atoms to exhibit bioaccumulation and biomagnification within food chains (Conder *et al.*, 2008). The presence of long-chain perfluorinated carboxylic acids (PFCAs) in the observed environment strongly suggests the existence of volatile precursors within that environment. (De Voogt, 2010).

The study also found that the levels of PFAS in the sediment were higher as compared to that of the surface water. A similar observation was also made in the United States Geological Survey (USGS) report (USGS, 2019). This report indicates that sediment is an important source of the PFAS exposure. This study compares well with other studies that PFAS are frequently detected in water sources. According to USEPA, PFAS have been detected in an approximately 40 % of public water systems in the United States (USEPA, 2020). A similar study conducted by Centers for Disease Control and Prevention (CDC) also indicated that the drinking water of 33 states in the United States contained PFAS (CDC, 2019). A study conducted by United States Geological

Survey (USGS) also concluded that PFAS were present in the sediment of nearly all of the rivers and streams tested in the United States (USGS, 2019).

Levels of PFAS in Water and Sediment Samples from the Pra River Basin as compared to Recommended W.H.O and US EPA limits

The results of total mean levels of PFAS in water and sediment from PRB are presented in the Table 16. The results of this study showed that the levels of 6 PFAS compounds in the water from the Pra River Basin do not exceed the recommended limits set by the World Health Organization (WHO) and USEPA except for PFOA (70.60 ng/L) and PFOS (83.71ng/L).

This study also indicated that the levels of PFAS especially for PFOA and PFOS in the sediment samples (0.17 to 94.02 ng/g) were above the interim guidance limits in sediment (USEPA, 2020). The interim guidance values were set at 10 ng/g for PFOA and 40 ng/g for PFOS. This recommendation was based on the toxicity of PFAS to aquatic life including fish and other organisms that live in and around waterways. This finding raises concern about the potential impacts on the health of local communities and ecosystems.

The sources of the elevated levels of PFAS in the Pra river basin are not yet known. It is possible that the potential sources of PFAS in Pra river basin may include but not limited to agricultural run-off, domestic wastes, improper waste disposal, and run-off from industrial and mining sites (Essumang *et al.*, 2016).

Table 16: Total Mean Levels of PFAS in Surface Water and Sediment in the Pra River Basin

Analyte	Mean level (ng/L) in water	Mean level (ng/g) in sediment	USEPA lifetime health advisory for drinking water (ng/L)
PFBA	0.67 ± 0.63	4.75 ± 4.87	70
PFPeA	0.46 ± 0.18	4.03 ± 3.85	70
PFHxA	0.30 ± 0.26	7.29 ± 6.26	37
PFOA	70.60 ± 25.69	94.02 ± 25.09	70
PFNA	0.68 ± 0.49	5.77 ± 4.50	14
PFDA	0.26 ± 0.31	0.84 ± 1.05	1000
PFHxS	0.38 ± 0.31	0.17 ± 0.25	70
PFOS	83.71 ± 21.89	90.27 ± 32.43	70

(Source: Fieldwork, 2022; USEPA, 2020)

Spatial Distribution of PFAS in the Pra River basin

Furthermore, it is noteworthy to mention that the levels of PFAS, particularly PFOA and PFOS, detected in the water and sediment samples from the Pra River Basin surpassed the recommended limits established by the United States Environmental Protection Agency (USEPA, 2020). Although the source of contamination remains unidentified, it is crucial to conduct further research to determine the origin of PFAS contamination in the Pra River basin. This region, including the Pra river basin, has been impacted by PFAS contamination, as documented in previous studies (Essumang et al., 2016). The river basin serves as a vital drinking water source for large human population and provides a habitat for diverse aquatic species. This study focused on investigating the spatial distribution of PFAS within the basin, aiming to assess the magnitude of PFAS contamination and its potential implications for the environment and human health.

The results of this study showed that the distribution of PFAS in the Pra river basin differed from each of the individual sampling location. The levels of PFAS in the surface water and sediments also varied. For example, the highest

levels of PFAS were detected at P18 (203.22 ng/L), P19(193.58 ng/L) and P12(186.77 ng/L), while the lowest levels were found in P3(62.77 ng/L), P1(71.19 ng/L) and P2(77.09 ng/L) for the water samples during the wet season (Figure 7 and Appendix C). In the dry season, high levels of PFAS were identified at P7(214.05 ng/L), P17(213.35 ng/L) and P6(201.2 ng/L) while the low levels were observed at P18(128.26 ng/L), P8(136.91ng/L) and P1(146.97 ng/L) (Figure 8 and Appendix D). Also, a paired samples t-test conducted to compare the levels of PFAS in the rainy and dry seasons indicated that there was statistically significant difference in the levels of PFAS for the rainy and dry seasons ($M = 136.69$, $SD = 40.76$) and ($M = 177.39$, $SD = 25.07$) $t(19) = -3.47$, $p = 0.0026$) as depicted in figure 9. The above findings were in contrast with a study conducted by Wang *et al.* (2022) on 13 Shandong rivers where levels of PFAS in the rainy season were higher than or almost equivalent to the levels in the dry season, but there was no statistically difference in the levels of PFAS between rainy and dry seasons. The same conclusion was also drawn by Chen *et al.*, 2017.

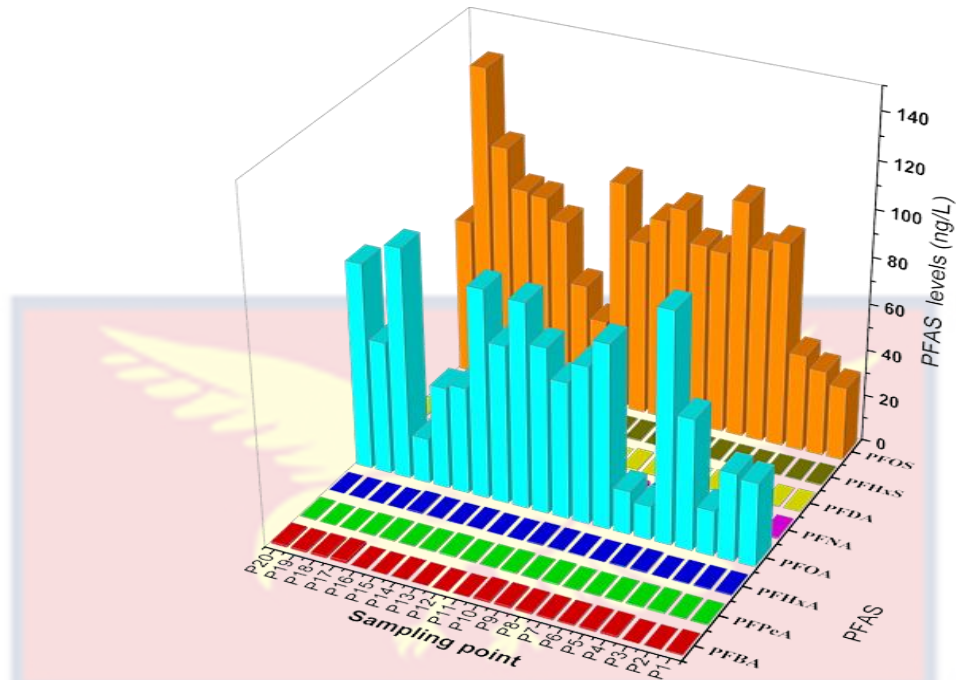


Figure 7: Distribution of PFAS in water samples collected from the Pra River Basin during rainy season (August-September, 2021).

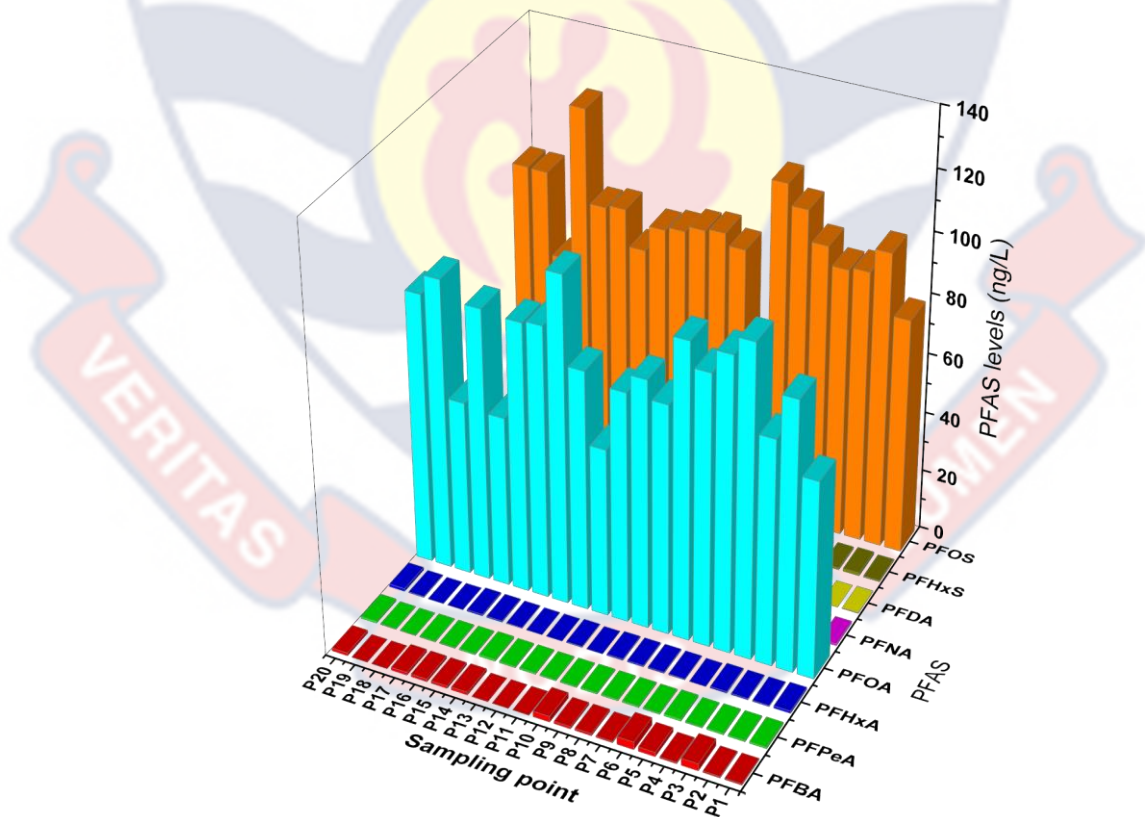


Figure 8: Distribution of PFAS in water samples collected from the Pra River Basin during dry season (November-December, 2021).

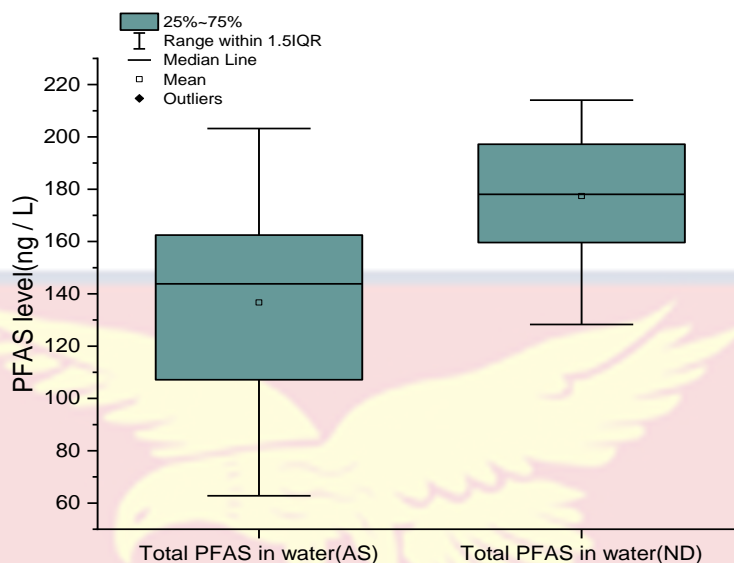


Figure 9: Boxplot of total PFAS levels in water samples collected from the Pra River Basin during rainy and dry seasons (August-December, 2021).

Similarly, the levels of PFAS in the sediment samples during the rainy and dry seasons varied. For example, the highest levels of PFAS were observed at P5(335.96 ng/g), P7(263.61 ng/g) and P6(240.0 ng/g) while the lowest levels were found at P15(159.15 ng/g), P18(171.61 ng/g) and P8(175.78 ng/g) during the rainy season (Figure 10 and Appendix E). However, the levels of PFAS in sediment were at elevated levels at P12(302.53 ng/g), P5(282.06 ng/g) and P20(248.66 ng/g) while the lowest levels were identified at P2(144.20 ng/g), P13(155.04 ng/g) and P19(144.20 ng/g) in the dry season (Figure 11 and Appendix F). A paired samples t-test was conducted to compare the levels of PFAS in sediment during the rainy and dry seasons ($M=208.33$, $SD = 38.12$) and ($M = 205.95$, $SD = 37.96$) $t(19) = 0.262$, $p = 0.796$) (Figure 12). This result indicates that there was no statistically significant difference in the levels of PFAS in the sediments during the rainy and dry seasons.

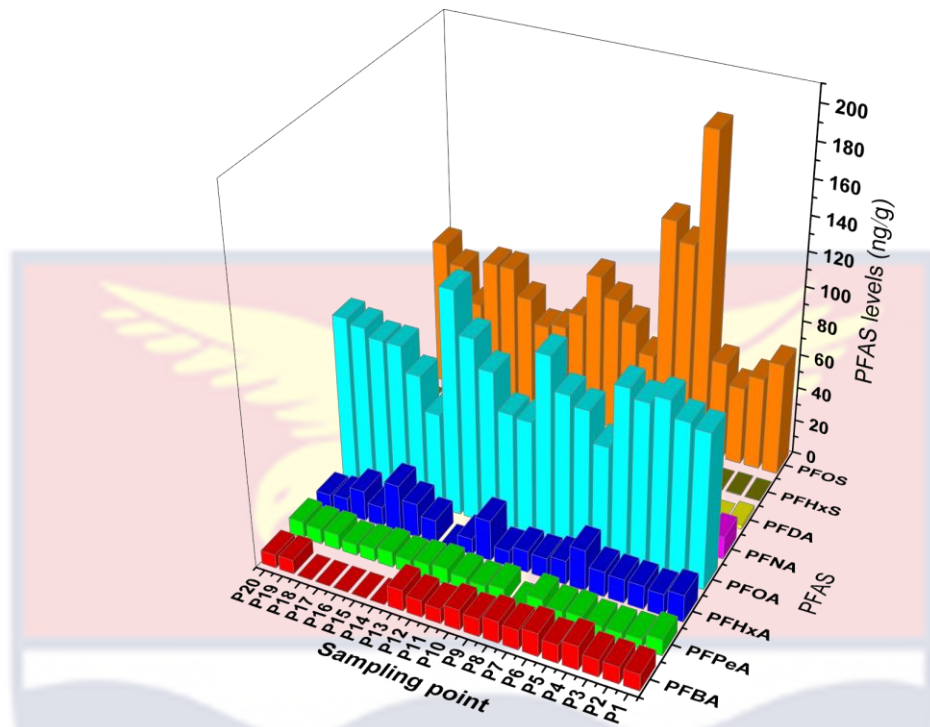


Figure 10: Distribution of PFAS in sediment samples collected from the Pra River Basin during rainy season (August-September, 2021).

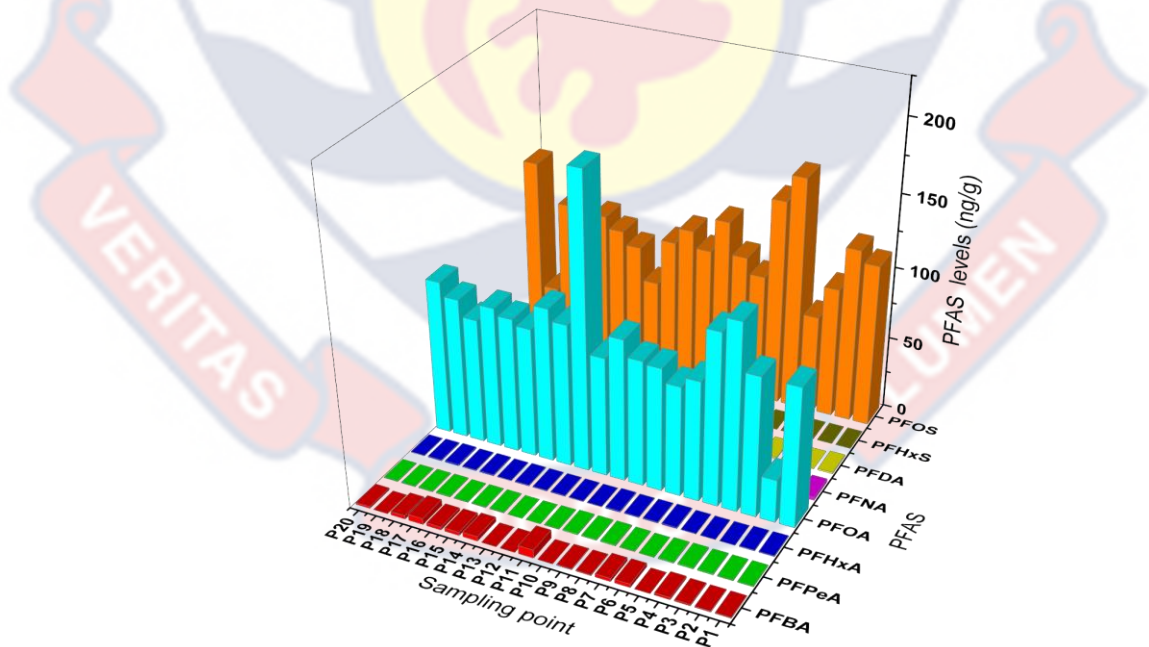


Figure 11: Distribution of PFAS in sediment samples collected from the Pra River Basin during dry season (November- December, 2021).

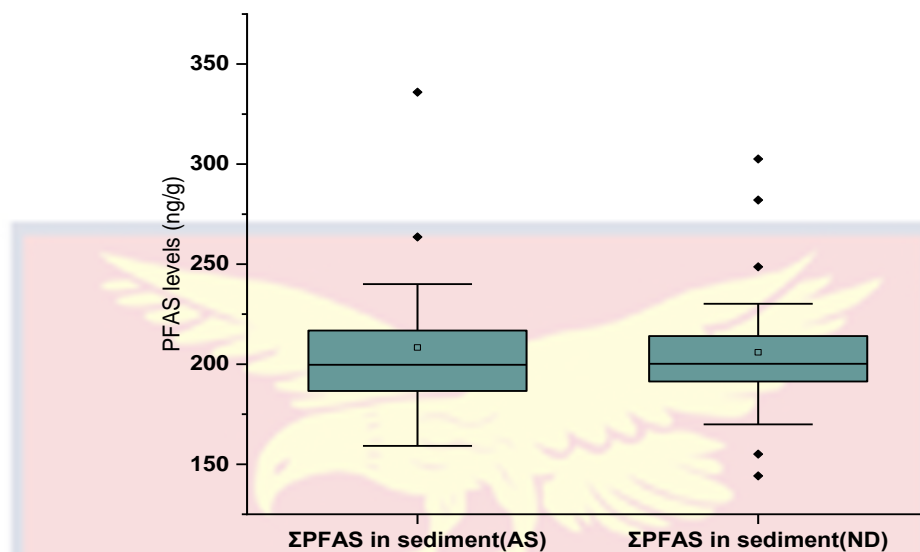


Figure 12: Boxplot of total PFAS in sediment samples collected from the Pra River Basin during rainy and dry seasons (August-December, 2021).

The implications of a significant difference in PFAS levels in the surface water samples between the rainy and dry seasons are important and can inform future research. For example, the lower levels of PFAS in the wet season could be due to the high flow rate of the river leading to the dilution and reducing the concentrations of these chemicals in the river basin. On the other hand, the elevated levels of PFAS in the dry season could be attributed to decreased dilution and dispersion causing them to accumulate in certain areas (Barkow et al., 2021).

However, the levels of PFAS in the sediment samples did not vary significantly between the wet and dry seasons. This suggests that factors such as rainfall, flow rate and runoff did not have immediate significant impact on the distribution and movement of the PFAS in the river basin during the sampling period. This finding is comparable to the results obtained by Green *et al.* (2017) where sediment samples collected from the Susquehanna River in the US

showed lack of significant difference in PFAS levels between the rainy and dry seasons.

The study also found high levels of PFAS in the sediment samples as compared to the water samples. The highest concentration of PFAS was detected at the downstream sites, which was attributed to the discharge of industrial effluent into the river. The upstream sites had the lowest concentration of PFAS, which was attributed to dilution and degradation of PFAS as the river flowed downstream.

The spatial distribution of PFAS in the Pra river recorded variations due to the sources of PFAS release, hydrological conditions and the type of PFAS. These findings have important implications for the management of PFAS contamination in the Pra river basin and the protection of the environment and human health.

Comparison of PFAS levels in the Pra River Basin with other Studies

Table 17 provides a comparison of PFAS levels in water samples collected from the Pra River basin with data from other countries. In the surface water of the Pra River basin, concentrations of PFOA ranged from 14.5 to 108.4 ng/L, while PFOS levels ranged from 31.8 to 112 ng/L. These values are comparable to, but slightly higher than, the levels reported in the Great Lakes region of the United States (PFOS: 21-70 ng/L; PFOA: 27-50 ng/L) as documented by Boulanger et al. (2004). Lower levels of PFOS (15–121 ng/L) and PFOA (15–70 ng/L) were reported in Lake Ontario, USA (Sinclair et al., 2006), suggesting slightly higher PFAS contamination levels in the surface water of the Pra River basin. Comparable concentration ranges of PFOS were also observed in Lake Shihwa, South Korea (2.24-651 ng/L) (Rostkowski et al., 2006). Concentrations

of PFOA and PFOS in water samples were similar to those observed in surface waters from the Tennessee River (USA), Yodo River (Japan), Yangtze River (China), and Tanaro River in Italy (Hansen et al., 2002; Loos et al., 2008; Saito et al., 2003; Saito et al., 2007). PFOS concentrations in the samples were within or slightly above the ranges measured for surface river water samples from Japan (0.4-157 ng/L), South Korea (2.24-651 ng/L), and water samples from Lake Ontario (Great Lakes) (15–121 ng/L).

In comparison to this study, higher concentration ranges of PFOA were observed in the Yodo River area (4.2-2600 ng/L) (Lein et al., 2008), Tennessee River (140-598 ng/L) (Hansen et al., 2002), and Tanaro River (<1300 ng/L) (Loos et al., 2008), which are heavily associated with industrial and urban activities. The levels of PFOS and PFOA in the samples from the Pra River were higher than those quantified in discharged wastewater samples into Lake Victoria from Kenya (PFOA: 1.3–28 ng/L; PFOS: 0.9–9.8 ng/L) (Chirikona et al., 2015). The current levels of PFOA (14.5–108.4 ng/L) and PFOS (31.8–112.4 ng/L) were comparatively lower than those reported in previous studies on PFAS in the same river basin (PFOA: 86-321 ng/L; PFOS: 95-277 ng/L) (Essumang et al., 2016).

Table 17: Comparison of PFAS Concentrations in Water Samples from Pra River Basin with those from other Countries and Previous Studies

Location	Sample type	Concentration (ng/L)		References
		PFOS	PFOA	
Pra River basin, Ghana	Surface water	31.8-112	14-108.4	This Study
Yodo river, Japan	Surface river water	0.4–123	4.2–2600	Lein <i>et al.</i> , 2008
Guangzhou	Surface river water	0.9–99		So <i>et al.</i> , 2007
Yangtze River, China	Surface river water	<0.01–14	2.0–260	So <i>et al.</i> , 2007
Lake Ontario (Great Lakes)	Freshwater	15–121	15–70	Boulangier <i>et al.</i> , 2004
Tama River, Japan	Surface freshwater	0.7 – 157	n.a	Saito <i>et al.</i> , 2003
Tennessee River, USA	surface freshwater	74.8- 144	140-598	Hansen <i>et al.</i> , 2002
Tanaro River, Italy	Surface river water	n.a	<1300	Loos <i>et al.</i> , 2008
River Po , Italy	Surface water	n.a	60 - 337	Loos <i>et al.</i> , 2008
Lake Victoria, Kenya	Wastewater	0.9-9.8	1.3-28	Chirikona <i>et al.</i> , 2015
Pra River (Ghana)	Surface river water	95 -277	86 - 321	Essumang <i>et al.</i> 2016
Kakum(Ghana)	Surface river water	77-163	1.78 -301	Essumang <i>et al.</i> 2016

Table 18 presents a summary of the detected levels of PFAS in sediment samples collected from the Pra River basin and compares them with levels from other countries. The concentrations of PFOA and PFOS in the sediment samples from the Pra River basin ranged from 55.9 to 129.7 ng/g and from 56.7 to 186.5 ng/g, respectively. These levels are comparable to, but slightly lower than those observed in the Mississippi River basin (USA; 3.3-438 ng/g) (Liu *et al.*, 2019). Lower levels of PFAS were reported in some US river basins, such as the

Columbia River basin (1.7-9.2 ng/g), Hudson River (10-15 ng/g), and Delaware River (5.5-17 ng/g) (Wang et al., 2017; Hale et al., 2016; Bradley et al., 2020). These findings suggest that the PFAS contamination levels in the sediment from the Pra River basin may be slightly higher.

Table 18: Comparison of PFAS Concentrations in Sediment Samples from Pra River Basin with those from other Countries

Location	Sample type	Concentration (ng/g)	References
		PFAS ng/g	
Pra River, Ghana	Sediment	55.9-186.5	Present study
Columbia River	Sediment	4.2–2600	Wang <i>et al.</i> ,2017
Hudson River	Sediment	10-15	Hale <i>et al.</i> 2016
Deleware River	Sediment	5.5–17	Bradley <i>et al.</i> ,2020
Mississippi river	Sediment	3.3- 438	Liu <i>et al.</i> , 2019

Multivariate Statistical Analysis of Surface Water and Sediment Data from the Pra River Basin

Source Identification (Surface Water)

Both hierarchical clustering and principal component analysis (PCA) identified three distinct components of PFASs in the surface water samples collected from the Pra river (Figures 13, 14 & 15). This was based on total mean of PFAS in surface water presented in Appendix G. The first component (PC1) explains 27 % of variability in the PCA and includes three different types of PFAS products namely PFPeA, PFHxA and PFOS. PC 1 correlates positively with both PFPeA and PFHxA, while it associates negatively with PFOS (Figure 10). Sampling point P19 (Kyekyewere) contains the highest summed PFASs (194.26 ng/L) across all sampling points and was dominated by a mixture of PFASs. PCA results suggest sampling location P19 is statistically similar to the

Supong sampling location (Site P3) (Figure 9), suggesting similarity in source contributions.

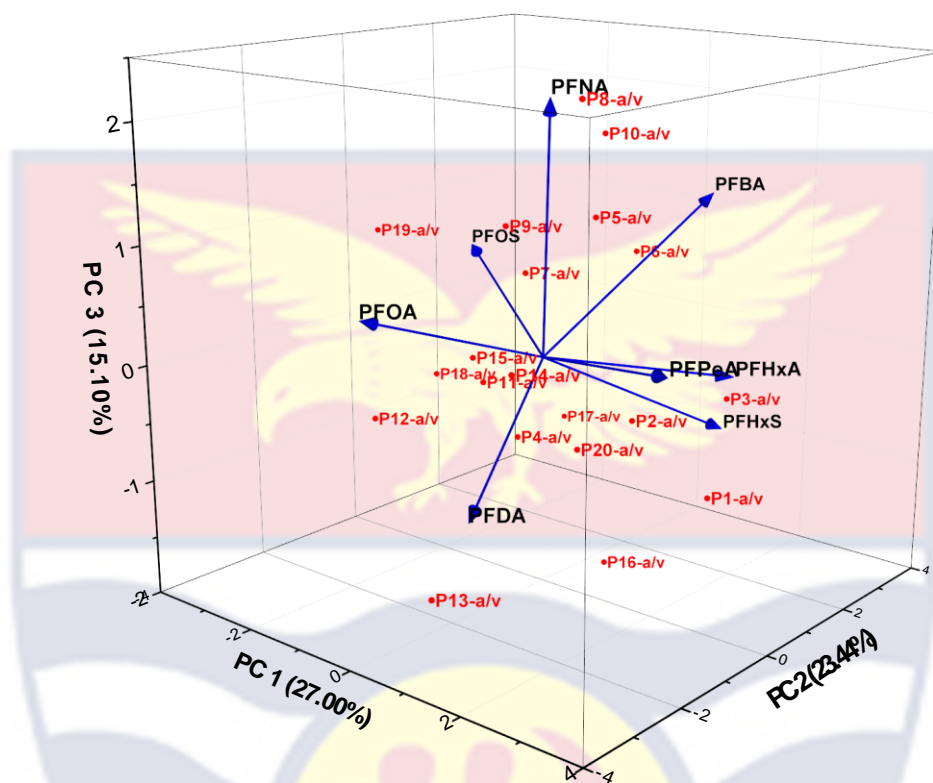


Figure 13: 3-dimensional plot of PCA showing loadings and score plots from three components in surface water across the sampling points

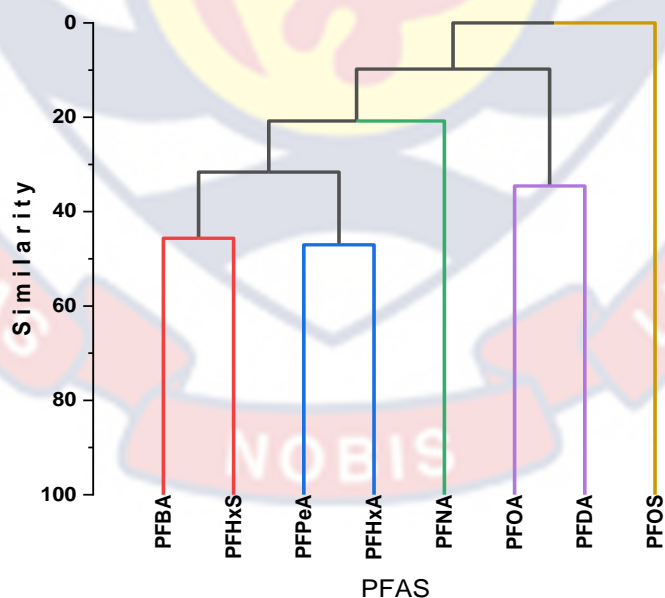


Figure 14: Dendrogram showing hierarchical clustering of PFAS in surface water from the Pra River according to similarity matrix

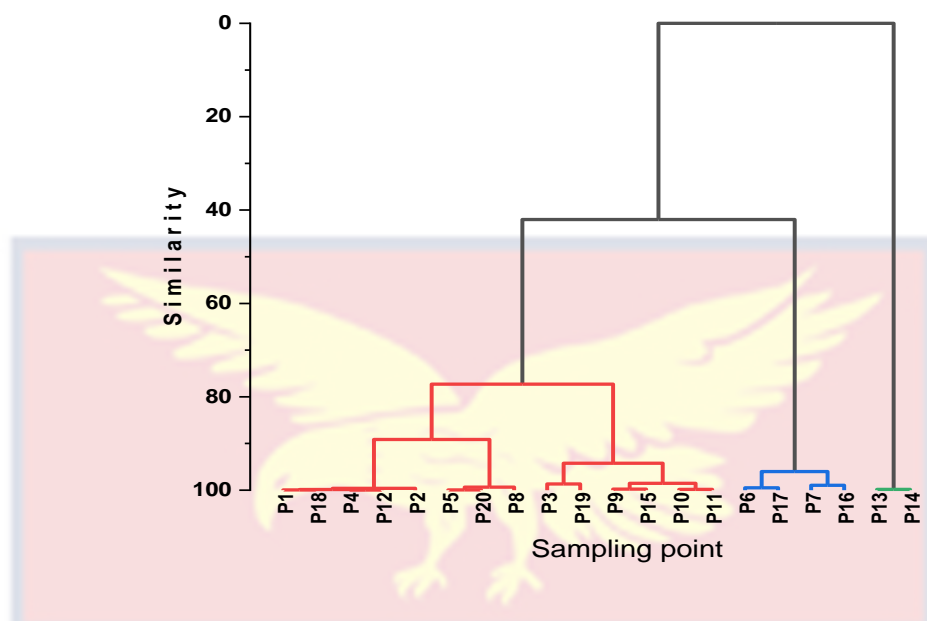


Figure 15: Dendrogram showing hierarchical clustering of sites contaminated with PFAS in surface water from the Pra River according to similarity matrix

The second component PC 2 explains 23.44 % of the variability in PFAS dataset and includes four PFAS compounds (PFBA, PFOA, PFDA and PFHxS (Figure 16). PC 2 correlates positively with PFBA and PFHxS while it correlates negatively with PFOA and PFDA. This suggests that the sources of these compounds in the river basin may originate from different anthropogenic sources which included but limited to industrial activities, domestic wastewater discharge and agricultural activities in the river basin (Essumang et al. 2016; Water Resources Commission, 2012). This profile was most pronounced at sampling location 13 (Sekyere Nsuta) and was also evident at Sampling location 14 (Atwereboanda). This is in line with cluster 3 in the Figure 9. PFHxS and PFBA were most evident at sampling location P6(Sekyere Hemang) and P17(Abetemasu) in the sampled water. It is not clear about the sources of these chemicals at these sampling locations but could be inferred that these chemical components are most likely from the domestic waste discharge, agricultural run-

off, degradation products of longer chain PFAS and the mining sector via water transported along the basin.

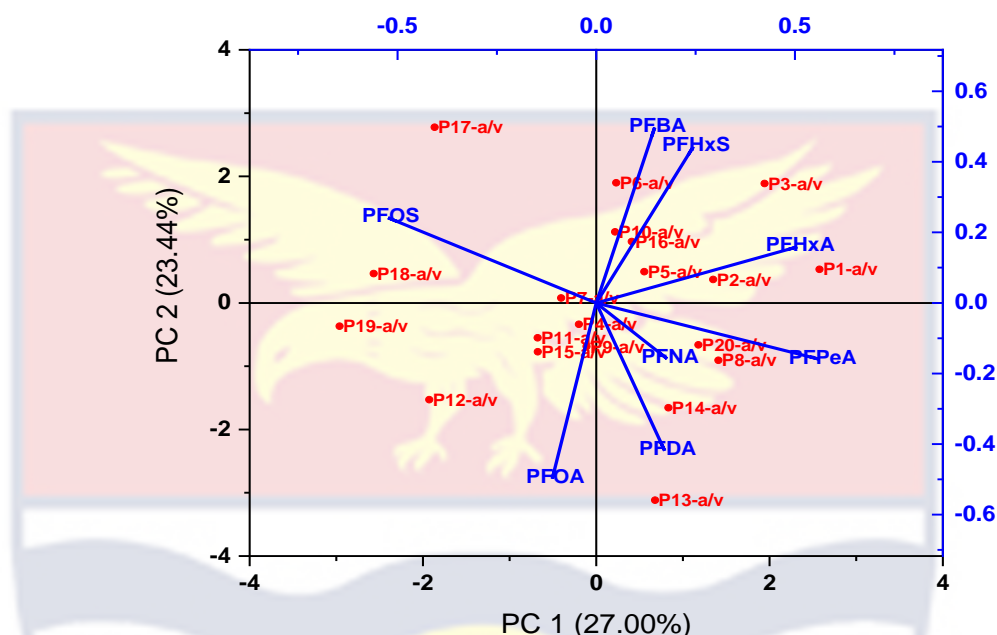


Figure 16: A PCA biplot showing loadings and score plots from PC1 and PC2 components across sampling points.

The third component (PC 3) explains 15.10 % of the variability in the PFAS dataset. PC 3 correlates positively with PFNA (Figure 17). This component was most pronounced at sampling locations P8(Apetebi) and P10(Otudum) along the Pra River Basin. The unexpected elevated presence of PFNA in these sampling locations was surprising since there is no production plant or its direct usage in these areas. However, PFNA are used as surfactant in the manufacturing of pesticides and also in consumer products such stain and water repellent coatings used on fabrics and carpets (Vierke *et al.*, 2018). The use and disposal of these products in these sampling locations may have contributed to the contamination of the river basin.

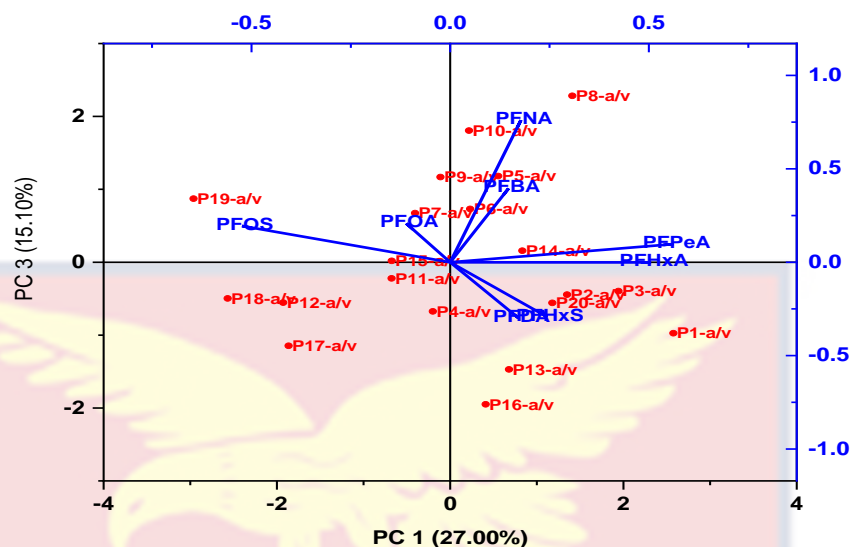


Figure 17: A PCA biplot showing loadings and score plots from PC1 and PC3 components across the sampling points.

To explore the similarities and differences in PFAS contamination in surface water among sampling sites, hierarchical clustering analysis (HCA) was conducted on the levels of PFAS (Figure 15). The analysis showed three clusters of sites, which differed in their PFAS composition and concentrations. Cluster 1 included sites with generally high PFAS levels. Cluster 2 included sites with moderate PFAS levels. Cluster 3 also showed sites with low PFAS levels. All the sites were dominated by PFOA and PFOS. The HCA suggests that the sources and transport pathways of PFAS in the Pra River Basin might be different for the three clusters of sites. HCA conducted on PFAS levels in the river basin showed 40-50 % similarity to each other (Figure 14).

Principal Component Analysis of PFAS in Sediment from the Pra River Basin

To identify the underlying patterns of PFAS levels in the sediments, PCA was conducted. This was based on the mean levels of PFAS in sediment presented in Appendix H. The analysis revealed that the first three principal

components (PCs) accounted 61.63% of the total variance in the PFAS data (Figure 12).

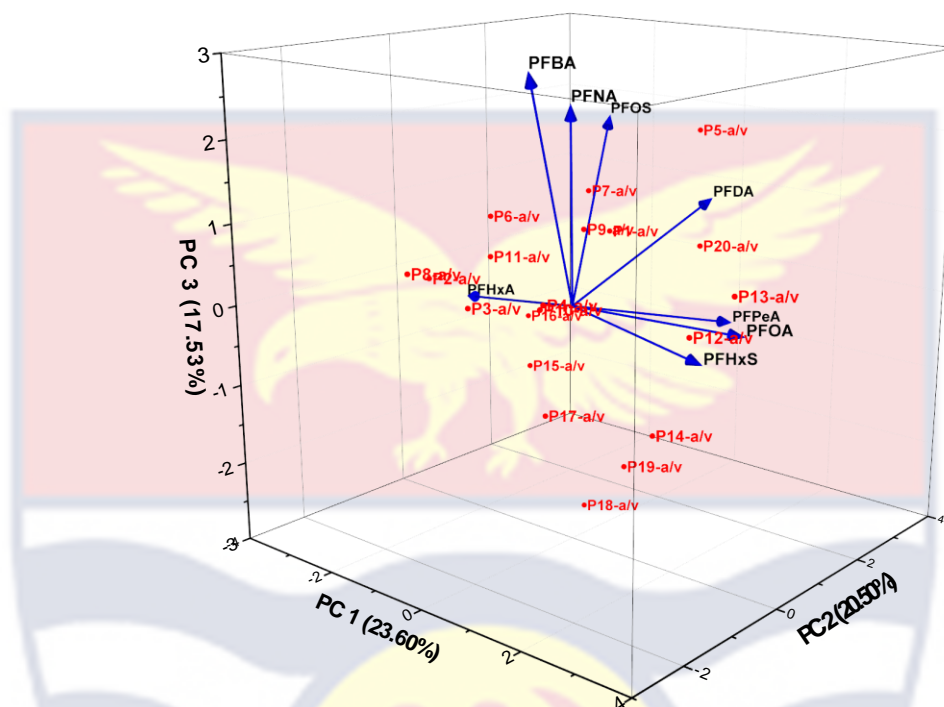
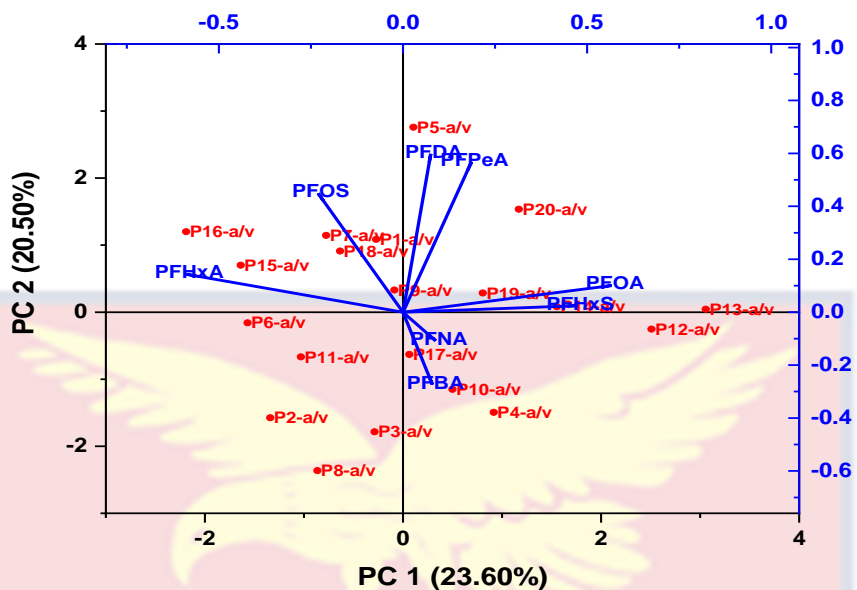


Figure 18: 3-dimensional plot of PCA showing loadings and score plots from three components in sediment across the sampling points

PC1 was positively correlated with PFOA and PFHxS, and negatively correlated with PFHxA suggesting different contribution sources. PC 1 accounted for 23.60 % of variability in the PFAS dataset. This finding was similar to the study conducted by Liu *et al.* (2020) where the levels of PFAS in the sediment from the Haihe river basin in China correlated positively with similar PFAS compounds in the industrial and urban areas, and negatively correlated with agricultural areas. PC2 on the other hand correlated with PFPeA, PFDA and PFOS positively and accounted for 20.50% of variance in the PFAS dataset (Figure 19).



Figure

19: A PCA biplot showing loadings and score plots from PC 1 and PC 2 components across the sampling points.

PC 3 was positively correlated with PFNA and PFBA (Figure 20). The PCA results suggested that PFAS contamination in the river basin may be influenced from varied sources including but not limited to the use and disposal of PFAS-containing products such as pesticides and fertilizers in the Pra river basin.

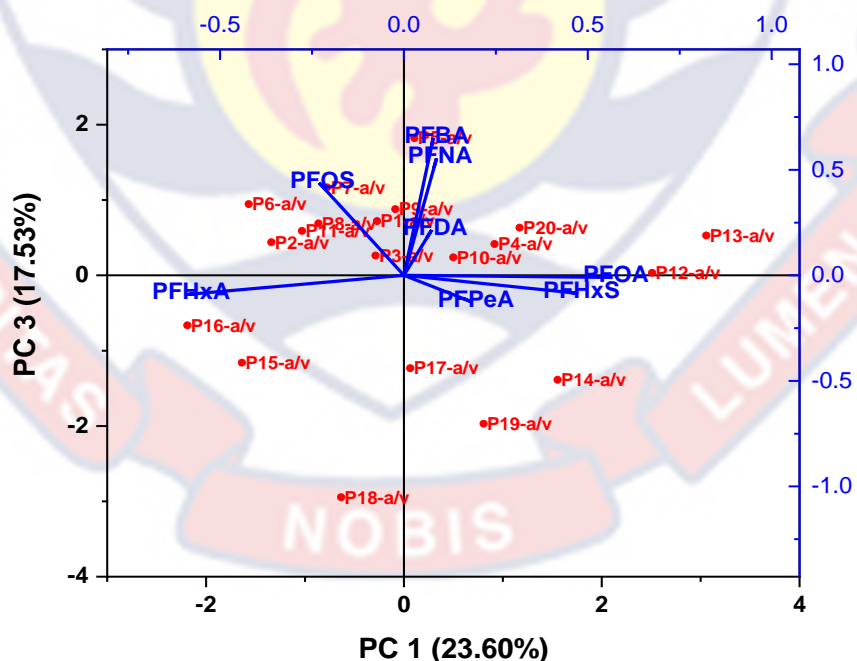


Figure 20: A PCA biplot showing loadings and score plots from PC1 and PC3 components across the sampling points

The HCA analysis grouped 8 PFAS into three clusters based on their co-occurrence pattern in the river basin (Figure 21). Cluster 1 included PFBA and PFNA, which are often less persistent in the environment but still pose health risk. Cluster 2 included PFOA and PFHxS. Cluster 3 included PFAS such as PFPeA, PFHxA and PFOS, and less commonly detected PFDA. Hierarchical clustering analysis (HCA) also grouped the various sampling points into 3 clusters based on their similarities and differences in the levels of PFAS in the PRB (Figure 22).

The results of the study provide insights into the distribution and co-occurrence patterns of different PFAS in the PRB in Ghana.

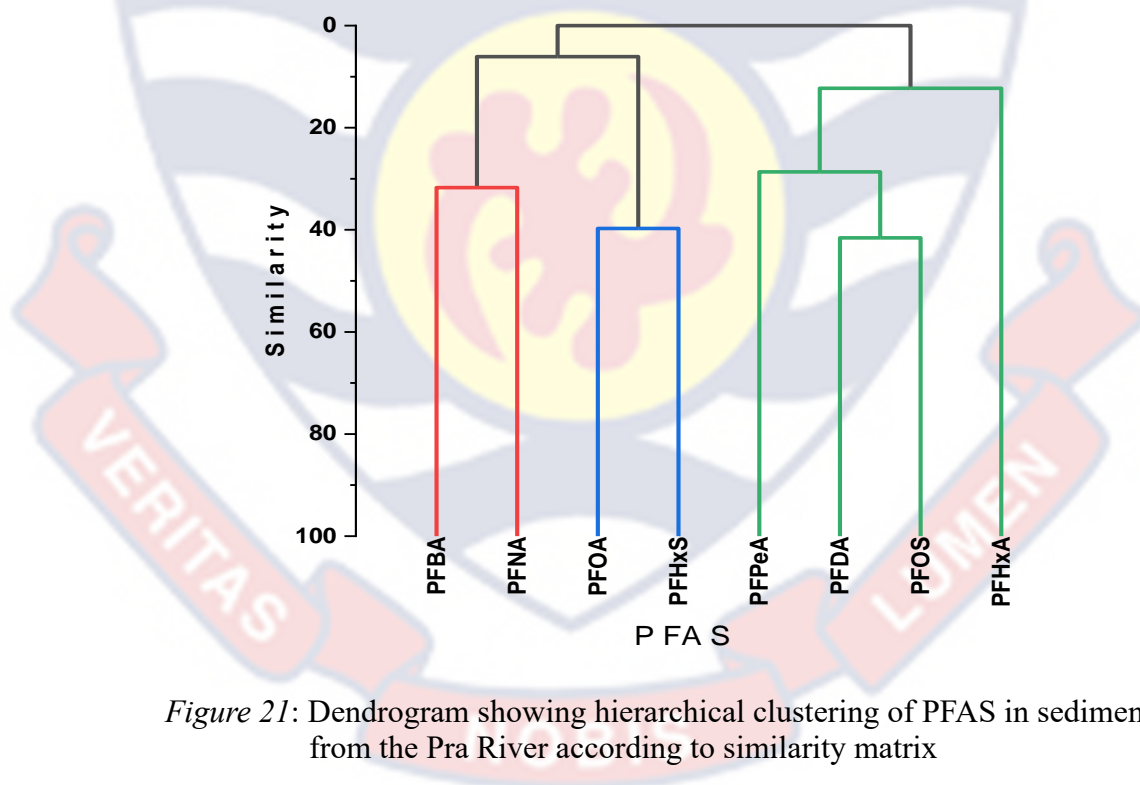


Figure 21: Dendrogram showing hierarchical clustering of PFAS in sediment from the Pra River according to similarity matrix

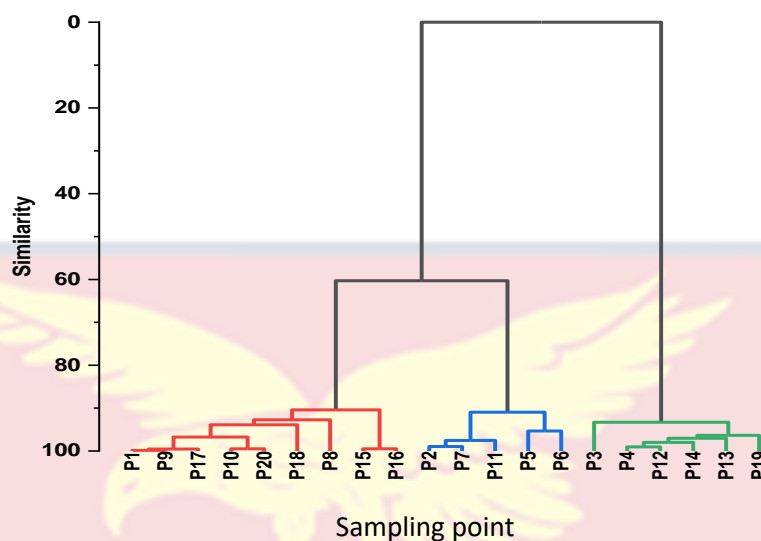


Figure 22: Dendrogram showing hierarchical clustering of sites contaminated with PFAS in sediment from the Pra River according to similarity matrix.

Carcinogenic and Non-carcinogenic Health Risk Assessment of PFAS in

Surface Water and Sediments from the Pra River Basin

Surface Water from the Pra River Basin

Table 19 provides the characteristics of the distribution of PFAS compounds, including PFBA, PFPeA, PFHxA, PFOA, PFNA, PFDA, PFHxS, and PFOS, in water samples from the Pra River Basin. The table includes information on the minimum, mean, median, and maximum levels of these compounds. Tables 19 and 20 present the minimum, mean, median, and maximum levels of chronic daily intake (CDI) for adults in the study area through ingestion and dermal contact pathways. The tables also provide information on the total CDI for both cancer and non-cancer risks. Table 22 displays the minimum, mean, and maximum levels of the hazard quotient (HQ) for adults in the study area through ingestion and dermal contact pathways. Additionally, the table presents the total HQ for these exposure routes. Table 24

focuses on the carcinogenic risk assessment for adults, providing relevant information related to the study area.

Table 19: Statistics of PFAS levels(ng/L) in Water Samples collected from the Pra River Basin during Wet and Dry Seasons

PFAS	Min ng/L	Max ng/L	Median ng/L	Mean ng/L	Wet Season ng/L	Dry Season ng/L	Df (%)
PFBA	ND	2.56	0.70	0.67 ± 0.63	0.52 ± 0.44	0.82 ± 0.76	65
PFPeA	ND	0.81	0.44	0.46 ± 0.18	0.42 ± 0.21	0.49 ± 0.14	95
PFHxA	ND	0.95	0.33	0.30 ± 0.26	0.27 ± 0.25	0.32 ± 0.27	65
PFOA	1.45	108.4	76.35	70.60 ± 25.69	57.72 ± 27.72	83.47 ± 15.40	100
PFNA	ND	1.56	0.80	0.68 ± 0.49	0.61 ± 0.53	0.75 ± 0.43	77.5
PFDA	0.018	0.89	N.D	0.26 ± 0.31	0.20 ± 0.30	0.31 ± 0.30	52.5
PFHxS	ND	0.98	0.35	0.38 ± 0.31	0.33 ± 0.25	0.42 ± 0.37	70
PFOS	31.8	134.7	87.75	83.71 ± 21.89	76.62 ± 26.16	90.81 ± 13.91	100

(Source: Fieldwork, 2022)

D_f = detection frequency

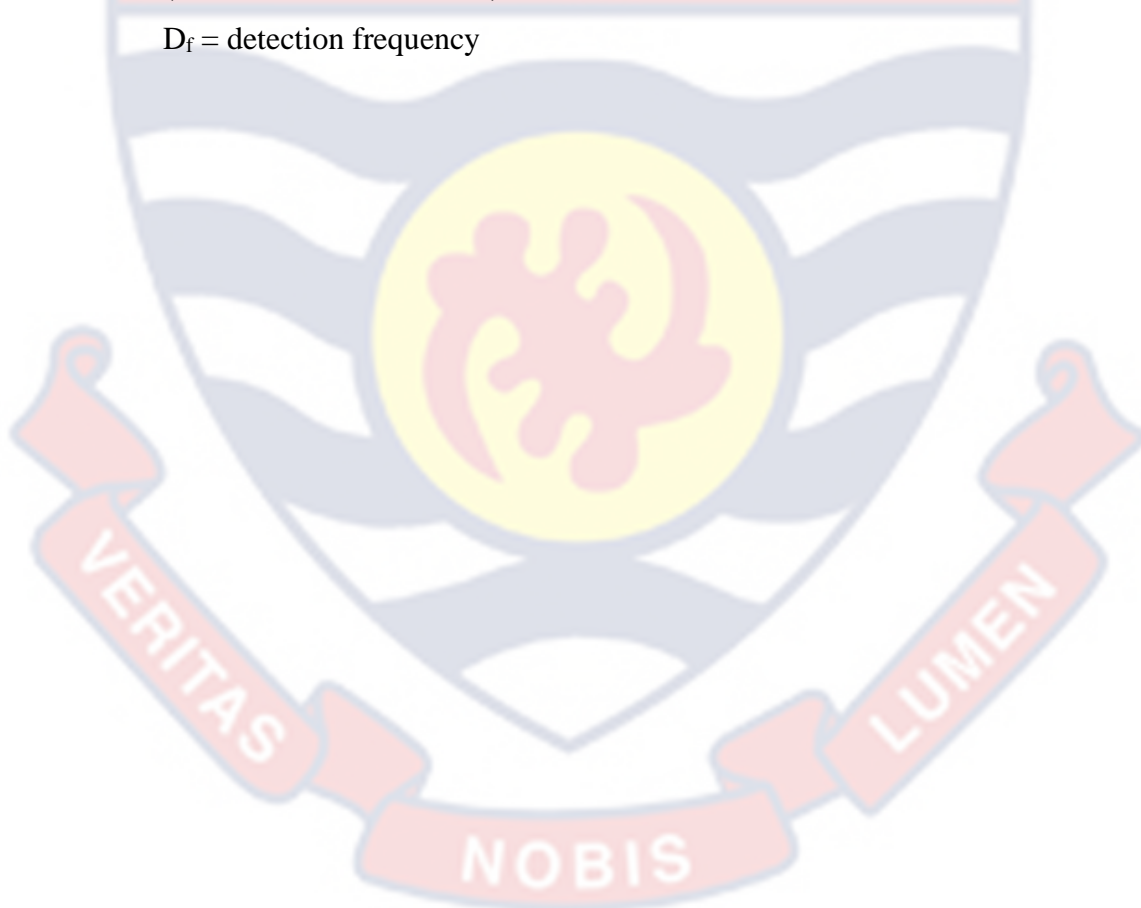


Table 20: Chronic Daily Intake (CDI) of PFAS for Cancer Risk through Oral Ingestion and Dermal Contact in Water

PFAS	CDI _{ing}			CDI _{der}			CDI _{total}		
	min	Max	mean	min	max	mean	Min	max	mean
PFOA	2.2E-08	1.6E-06	1.1E-06	5.4E-09	4.0E-07	2.6E-07	2.7E-08	2.0E-06	1.4E-06
PFOS	4.7E-07	2.0E-06	1.2E-06	2.4E-09	1.0E-08	6.4E-09	4.7E-07	2.0E-06	1.2E-06

(Source: Fieldwork, 2022)

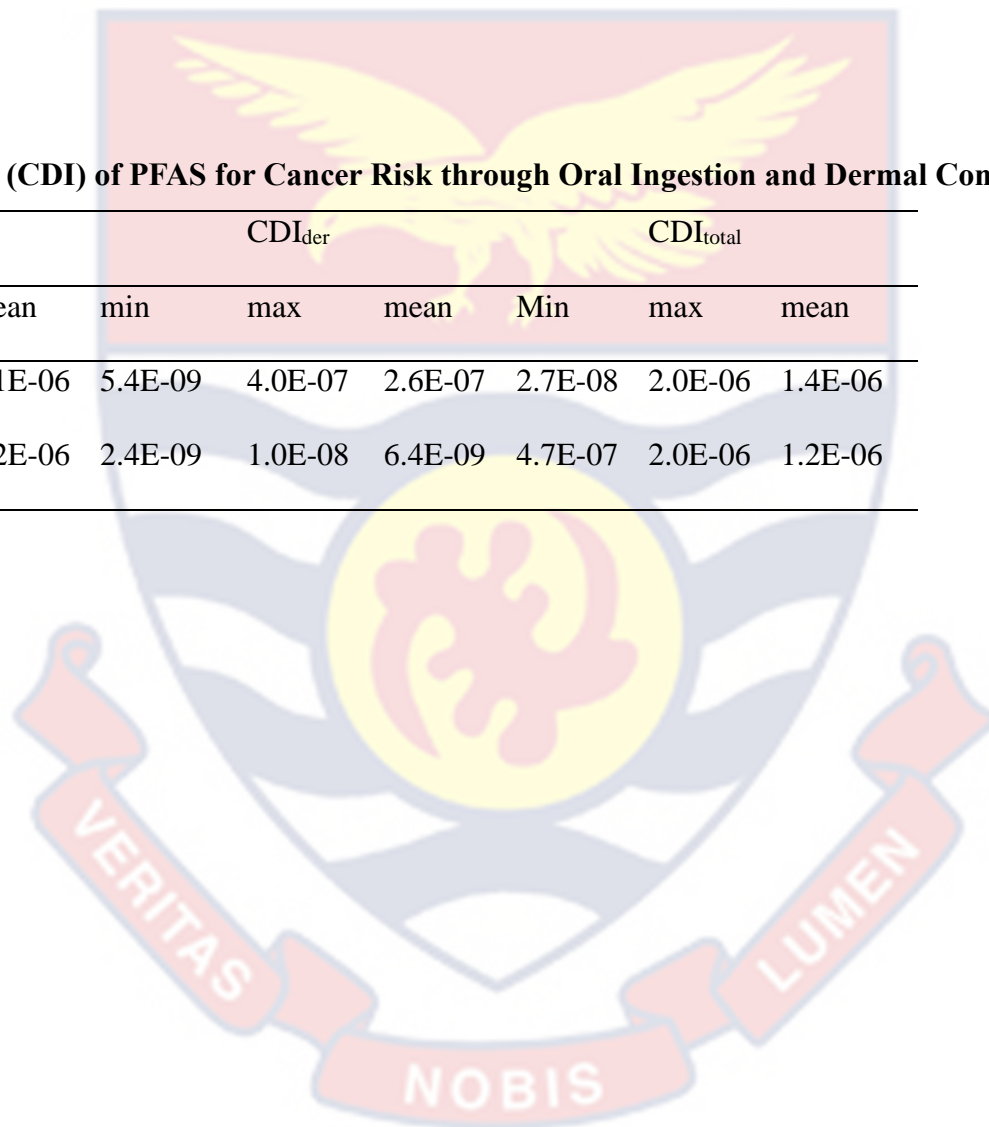


Table 21: Chronic Daily Intake (CDI) of PFAS for Non-Cancer Risk through Oral Ingestion and Dermal Contact in Surface Water

PFAS	CDI _{ing}			CDI _{der}			CDI _{total}		
	min	max	mean	min	max	mean	min	max	mean
PFBA	0	1.6E-07	4.3E-08	0	1.6E-13	4.1E-14	0	1.5E-07	4.3E-08
PFPeA	0	5.1E-08	3.0E-08	0	5.0E-13	2.9E-14	0	5.2E-08	3.0E-08
PFHxA	0	6.1E-08	1.9E-08	0	5.8E-14	1.8E-14	0	6.1E-08	1.9E-08
PFOA	9.0E-08	6.9E-06	4.5E-06	1.1E-08	8.0E-06	5.1E-07	1.0E-07	7.7E-06	5.2E-06
PFNA	0	1.0E-07	4.4E-08	0	1.0E-13	4.2E-14	0	1.0E-07	4.3E-08
PFDA	0	5.7E-08	1.7E-08	1.2E-15	5.4E-14	1.6E-14	1.2E-09	5.7E-08	1.7E-08
PFHxS	0	6.3E-08	2.4E-08	0	6.0E-13	2.3E-14	0	6.3E-08	2.4E-08
PFOS	2.3E-06	8.6E-06	5.4E-06	4.8E-09	2.0E-08	1.3E-08	2.0E-06	8.6E-06	5.9E-06

(Source: Fieldwork, 2022)

Table 22: Minimum, Maximum and Mean Values of Non-Carcinogenic Human Health Risks Posed by PFAS in Water of Study Area through Oral Ingestion and Dermal Contact

PFAS	HQ _{ing}			HQ _{der}			HQ _{total}		
	min	max	mean	min	Max	mean	min	max	mean
PFBA	0	5.6E-05	1.5E-05	0	5.4E-11	1.4E-11	0	5.6E-05	1.5E-05
PFPeA	0	1.4E-02	7.9E-03	0	1.3E-08	7.6E-09	0	1.4E-02	7.9E-03
PFHxA	0	1.6E-02	5.0E-03	0	1.5E-08	4.8E-09	0	1.6E-02	5.0E-03
PFOA	4.6E-03	3.5E-01	2.2E-01	5.3E-04	3.0E-02	2.6E-02	5.2E-03	3.9E-01	2.5E-01
PFNA	0	5.0E-03	2.2E-03	0	4.8E-09	2.1E-09	0	5.0E-03	2.1E-03
PFDA	7.7E-05	4.0E-03	1.1E-03	7.3E-11	3.6E-09	1.1E-09	7.7E-05	3.8E-03	1.1E-03
PFHxS	0	3.3E-03	1.2E-03	0	3.0E-09	1.2E-09	0	3.1E-03	1.2E-03
PFOS	1.0E-01	4.3E-01	2.7E-01	2.4E-04	1.0E-03	6.3E-04	1.0E-01	4.3E-01	2.7E-01
HI	1.1E-01	8.2E-01	5.1E-01	7.7E-04	4.1E-02	2.7E-02	1.1E-01	8.6E-01	5.4E-01

(Source: Fieldwork, 2022)

Table 23: Cancer Risk Assessment associated with the Use of Raw Water from the Pra River Basin

PFAS	CR _{ing}			CR _{der}			CRI _{total}		
	min	Max	mean	min	max	mean	min	max	mean
PFOA	1.5E-09	1.1E-07	7.4E-08	376E-12	2.8E-08	1.8E-08	1.9E-09	1.4E-07	9.2E-08
PFOS	2.2E-05	9.1E-05	5.7E-05	1.1E-07	4.7E-07	2.9E-07	2.2E-05	9.1E-05	5.7E-05
Σ	2.2E-05	9.1E-05	5.8E-05	1.1E-07	5.0E-07	3.1E-07	2.2E-05	9.1E-05	5.8E-08

(Source: Fieldwork, 2022)



The contamination of PFAS in water bodies, such as the Pra River Basin, poses potential risks to human health through various exposure routes. This study focused on assessing the non-carcinogenic and carcinogenic health risks associated with oral ingestion and dermal contact. Based on the data presented in Table 17, significant variations in mean values of PFAS were observed among the water samples. Among the PFAS compounds analyzed, PFOS exhibited the highest mean level of 83.71 ng/L, while PFDA showed the lowest mean level of 0.26 ng/L. This indicates a wide range of contamination levels for different PFAS compounds in the surface water of the Pra River Basin. The toxicity order of PFAS compounds, based on their mean levels in the surface water of the Pra River Basin, can be summarized as follows: PFOS > PFOA > PFPeA > PFHxA > PFNA > PFHxS > PFDA > PFBA.

Non-Carcinogenic Analysis of PFAS in Surface Water from Pra River Basin

The non-carcinogenic risks associated with PFAS exposure should not be overlooked particularly in communities that relied on surface water from the Pra river basin. In this study, the exposure and risk assessments were conducted following the methodology established by the USEPA. Human exposure to PFAS primarily occurs through various pathways, including, but not limited to, drinking water and surface water sources (Essumang et al., 2016). The level of toxicity posed by PFAS to human health is directly associated with the daily intake of these compounds. For the purposes of this study, the assessment focused on the intake through drinking water and dermal absorption. To evaluate the potential non-carcinogenic risks, the first step involved calculating the values for chronic daily intake (CDI). As given in Table 21, the mean levels

of total CDI (CDI_{total}) for non-cancer risk in mg/kg-day were $4.3E-08$ for PFBA, $3.0E-08$ for PFPeA, $1.9E-08$ for PFHxA, $5.2E-06$ for PFOA, $4.3E-08$ for PFNA, $1.7E-08$ for PFDA, $2.4E-08$ for PFHxS, and $5.9E-06$ for PFOS. Therefore, based on the mean values of the total chronic daily intake (CDI_{total}) for adults, the PFAS compounds were ranked in the following order: PFOS > PFOA > PFNA = PFBA > PFPeA > PFHxS > PFHxA > PFDA. As presented in Table 21, all the analyzed PFAS compounds exhibited total hazard quotients (HQs) below 1. The computation of the total HQs allows for the assessment of the non-carcinogenic health risks associated with these PFAS compounds. It can be concluded that, in terms of their contribution to non-carcinogenic health risks, the PFAS compounds were ranked as follows: PFOS > PFOA > PFPeA > PFHxA > PFNA > PFHxS > PFDA > PFBA. To assess the combined non-carcinogenic impacts of multiple PFAS compounds, the hazard quotient (HQ) for each compound was calculated and then summed to determine the Hazard Index (HI) following the methodology established by USEPA (2008). The mean values of HI, representing the potential non-carcinogenic impacts through ingestion and dermal adsorption, as well as the total HI, were determined to be $5.1E-01$, $2.7E-02$, and $5.4E-01$, respectively. These results indicate that there is negligible non-carcinogenic risk to the health of the residents, as the value of HI is below 1. The values of HI for the PFAS compounds in the study area are summarized in Table 20.

Carcinogenic Risk Analysis of PFAS in Surface Water from Pra River Basin

Studies conducted by Lau et al. (2007) and Olsen et al. (2007) have established a correlation between PFAS, specifically PFOA and PFOS, and an

elevated risk of various types of cancer in humans. The assessment of the carcinogenic potential of PFAS was carried out by evaluating the average chronic daily intake (CDI) values of PFOA and PFOS, as presented in Table 19. The assessment of carcinogenic risk relied on an average body mass weight (BMI) of 70 kg for adult individuals. The cancer slope factors (CSFs) employed for evaluating the carcinogenic potential of the two PFAS compounds were 0.07 mg/kg/day⁻¹ for PFOA and 45.5 mg/kg/day⁻¹ for PFOS. These CSF values were derived from a comprehensive scientific report compiled by the University of Florida (USEPA, 2017). In terms of PFAS, a human cancer risk below 1×10^{-6} is deemed insignificant. Conversely, a human cancer risk exceeding 1×10^{-4} is considered harmful. Among the various PFAS compounds studied, PFOS exhibits the highest probability of cancer risks, with a mean cancer risk of 5.7×10^{-5} . On the other hand, PFOA demonstrates the lowest likelihood of cancer risk, with a mean cancer risk of 9.2×10^{-8} . According to the findings of this study, the use of raw surface water from the Pra river basin indicates either no cancer risk or an extremely low cancer risk associated with PFAS exposure through cumulative ingestion and dermal contact routes. These results are evident from the data presented in Table 23.

Sediment

Table 24 presents a range of PFAS (including PFBA, PFPeA, PFHxA, PFOA, PFNA, PFDA, PFHxS, and PFOS) levels detected in sediment samples collected from the Pra River Basin. Table 24 provides data on the chronic daily intake of PFAS through ingestion and dermal contact routes for adults in the study area. Table 25 displays the values of the hazard quotient (HQ) for adults. Additionally, the table includes the total HQ value. Table 26 outlines the results

of the carcinogenic risk assessment for adults. It presents the relevant information related to the risk of cancer associated with PFAS exposure.



Table 24: Statistics of PFAS Levels(ng/g) in Sediment Samples collected from the Pra River Basin during Wet and Dry Seasons

PFAS	Min	Max	Median	Mean	Wet season	Dry season	Df
	ng/g	ng/g	ng/g	ng/g	ng/g	ng/g	(%)
PFBA	ND	13.78	2.40	4.75 ± 4.87	7.95 ± 4.97	1.56 ± 0.76	75
PFPeA	ND	9.8	1.0	4.03 ± 3.85	7.55 ± 2.07	0.51 ± 0.28	92.5
PFHxA	ND	27.4	0.92	7.29 ± 6.26	14.04 ± 6.14	0.55 ± 0.24	95
PFOA	29.78	201.6	92.89	94.02 ± 25.09	89.77 ± 16.94	98.27 ± 31.09	100
PFNA	ND	12.93	5.16	5.77 ± 4.50	9.20 ± 3.59	2.33 ± 1.95	80
PFDA	N.D	3.91	0.45	0.84 ± 1.05	1.11 ± 1.30	0.58 ± 0.33	57.5
PFHxS	ND	0.92	0.041	0.17 ± 0.25	0.32 ± 0.29	0.024 ± 0.12	60
PFOS	43.72	186.5	88.12	90.27 ± 32.43	78.40 ± 34.05	102.1 ± 26.52	100

(Source: Fieldwork, 2022)

Table 25: Chronic Daily Intake (CDI) of PFAS for Cancer Risk through Oral Ingestion and Dermal Contact in Sediment

PFAS	CDI _{ing}			CDI _{der}			CDI _{total}		
	min	max	mean	min	max	mean	min	max	mean
PFOA	4.5E-08	3.2E-07	1.5E-07	5.5E-06	3.8E-05	1.8E-05	5.5E-06	3.8E-05	1.4E-06
FOS	6.8E-08	2.9E-07	1.4E-07	8.1E-06	3.5E-05	1.7E-05	8.2E-06	3.5E-05	1.7E-05

(Source: Fieldwork, 2022)

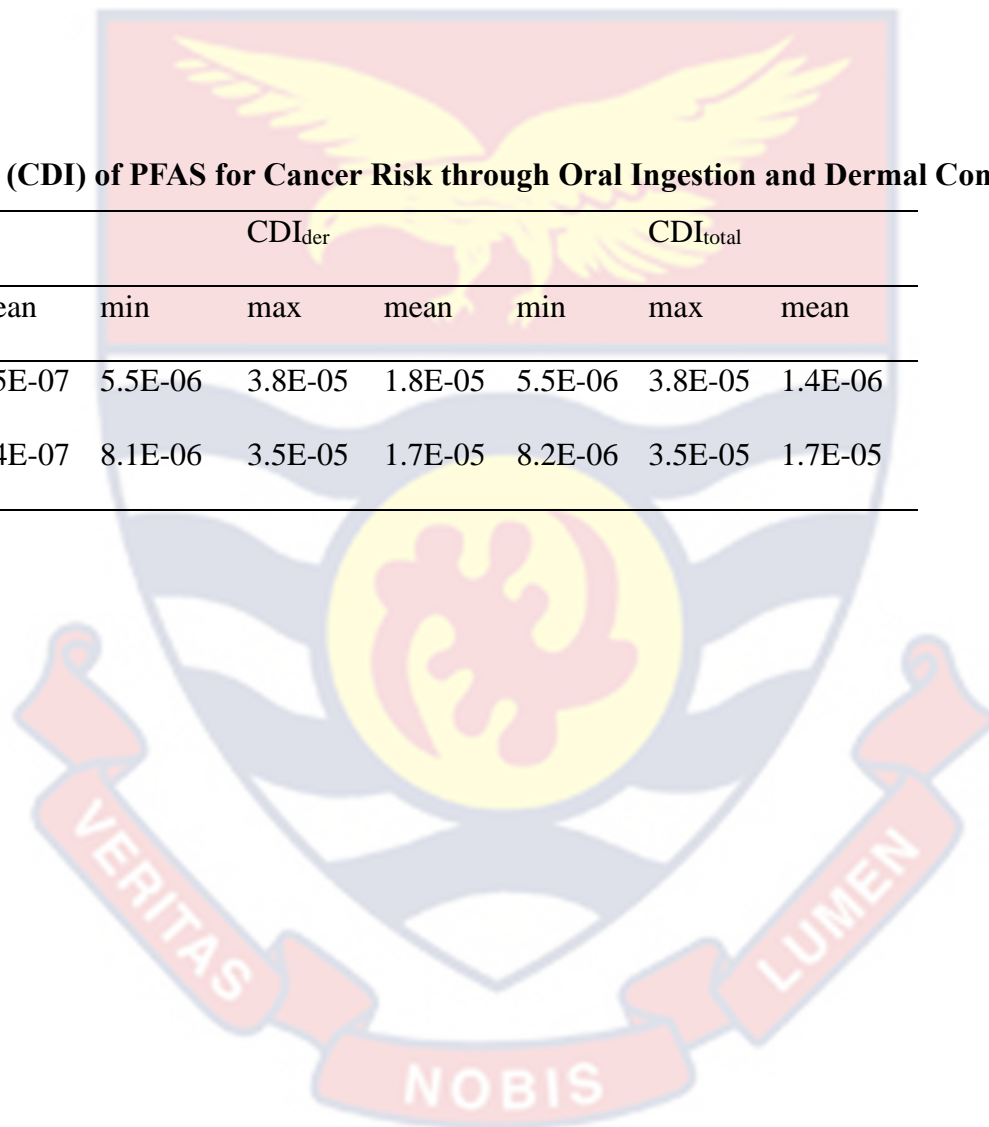


Table 26: Chronic Daily Intake (CDI) of PFAS for Non-Cancer Risk through Oral Ingestion and Dermal Contact in Sediment

PFAS	CDI _{ing}			CDI _{der}			CDI _{total}		
	min	max	mean	min	max	mean	min	max	mean
PFBA	0	1.8E-10	6.1E-11	0	1.8E-07	6.1E-09	0	1.8E-07	6.1E-09
PFPeA	0	1.3E-10	5.2E-11	0	1.3E-07	5.2E-09	0	1.3E-07	5.2E-09
PFHxA	0	3.5E-10	9.3E-11	0	3.5E-07	9.3E-09	0	3.5E-07	9.4E-09
PFOA	3.8E-10	2.6E-09	1.2E-09	3.8E-07	2.6E-06	1.2E-07	3.8E-07	2.6E-06	1.2E-07
PFNA	0	1.7E-10	7.4E-11	0	1.7E-07	7.4E-09	0	1.7E-07	7.5E-09
PFDA	0	5E-11	1.1E-11	0	5E-08	1.1E-09	0	5.0E-08	1.1E-09
PFHxS	0	1.2E-11	2.2E-12	0	1.2E-08	2.2E-10	0	1.2E-08	2.2E-10
PFOS	5.6E-10	2.4E-09	1.2E-09	5.6E-07	2.4E-06	1.2E-07	5.6E-07	2.4E-06	1.2E-07

(Source: Fieldwork, 2022)

Table 27: Minimum, Maximum and Mean Values of Non-Carcinogenic Human Health Risks Posed by PFAS in Sediment of Study Area via Different Pathways

PFAS	HQ _{ing}			HQ _{der}			HQ _{total}		
	min	max	mean	min	max	mean	min	max	mean
PFBA	0	6.1E-08	2.1E-08	0	6.1E-05	2.1E-06	0	6.1E-05	2.1E-06
PFPeA	0	3.3E-05	1.4E-05	0	3.3E-02	1.4E-03	0	3.3E-02	1.3E-03
PFHxA	0	9.2E-05	2.5E-05	0	9.2E-02	2.5E-03	0	9.2E-02	2.5E-03
PFOA	1.9E-05	1.3E-04	6.0E-05	1.9E-02	1.3E-01	6.0E-03	1.9E-02	1.3E-02	6.0E-03
PFNA	0	8.3E-06	3.7E-06	0	8.3E-03	3.7E-04	0	8.3E-03	3.7E-04
PFDA	0	3.3E-06	7.2E-07	0	3.3E-03	7.2E-05	0	3.3E-03	7.2E-05
PFHxS	0	5.9E-07	1.1E-07	0	5.9E-04	1.1E-05	0	5.9E-04	1.1E-05
PFOS	2.8E-05	1.2E-04	5.8E-05	2.8E-02	1.2E-01	5.8E-03	2.8E-02	1.2E-01	5.8E-03
HI	4.7E-05	3.9E-04	1.6E-04	407E-02	3.9E-01	1.6E-02	4.7E-02	3.9E-01	1.6E-02

(Source: Fieldwork, 2022)

Table 28: Cancer Risk Assessment Associated with the Exposure of Sediment from Pra River Basin

	CR _{inges}			CR _{der}			CRI _{total}		
	min	max	mean	min	max	mean	min	max	mean
PFAS	3.2E-09	2.2E-08	1.0E-08	3.8E-07	2.7E-06	1.2E-06	3.8E-07	2.7E-06	1.2E-06
PFOA	3.1E-06	1.3E-05	6.4E-06	3.7E-04	1.6E-03	7.7E-04	3.7E-04	1.6E-03	7.8E-04
Σ	3.1E-06	1.3E-05	6.4E-06	3.7E-04	1.6E-03	7.7E-04	3.7E-04	1.6E-03	7.8E-04

(Source: Fieldwork, 2022)

Non-Carcinogenic Analysis of PFAS in Sediment from Pra River Basin

As stated earlier, PFAS contamination in sediment of a river basin such as the Pra river basin can occur through a number of anthropogenic activities. PFAS can bind to sediment particles and once they settle, they can accumulate in sediment and other aquatic species. Human exposure to PFAS is normally through various pathways including but not limited to ingestion of contaminated fish or shellfish and direct contact with sediment. It is important not to overlook the non-carcinogenic risks (eg., birth defects, decreased in fertility and neurotoxicity) linked to PFAS exposure, especially in the areas that depend on surface water from the Pra river basin. This study employed the USEPA recommended procedure for conducting exposure and risk assessments. The potential harm of PFAS to human health is closely linked to their daily consumption or contact with a contaminated media. However, this study incorporated calculations based on assumed soil ingestion and dermal adsorption in its modeling. The non-carcinogenic assessment of sediment samples from the Pra river basin commenced by determining the chronic daily intake (CDI) values as an initial step. As given in Table 25, the mean levels of total CDI (CDI_{total}) in mg/kg-day were $6.1E-09$ for PFBA, $5.2E-09$ for PFPeA, $9.4E-09$ for PFHxA, $1.2E-07$ for PFOA, $7.5E-09$ for PFNA, $1.1E-09$ for PFDA, $1.2E-10$ for PFHxS, and $1.2E-07$ for PFOS. Therefore, the mean values of total chronic daily intake (CDI) of PFAS levels for adults were observed in the following order: $PFOS = PFOA > PFHxA > PFNA > PFBA > PFPeA > PFDA > PFHxS$. As indicated in Table 26, all the studied PFAS compounds exhibited total hazard quotients (HQs) below 1. Based on the computed total HQ values, it can be concluded that the relative contribution of the studied PFAS

compounds to the non-carcinogenic health risk followed the order of PFOA > PFOS > PFHxA > PFPeA > PFNA > PFDA > PFHxS > PFBA. Furthermore, in order to assess the cumulative non-carcinogenic impacts resulting from multiple PFAS compounds, the hazard quotient (HQ) calculated for each individual PFAS compound was summed and represented as a Hazard Index (HI). The mean values of HI, considering both ingestion and dermal adsorption, were determined to be $3.9\text{E-}04$ and $1.6\text{E-}02$, respectively. The total HI, which takes into account the combined effects of all PFAS compounds, was also calculated to be $1.6\text{E-}02$. The non-carcinogenic risk assessment indicated that the human population health around the Pra river basin was unlikely to be adversely affected as the HI value was found to be below 1, indicating negligible risk. The HI values for PFAS of the study area are summarized in Table 26.

Comparison of Non-Cancer Risk Index of PFAS in the Pra River Basin

The comparison of hazard indices (HI) values for surface water and sediment samples from the Pra river basin (Figure 23) showed that the HI values for the surface water were generally higher than those for the sediment samples.

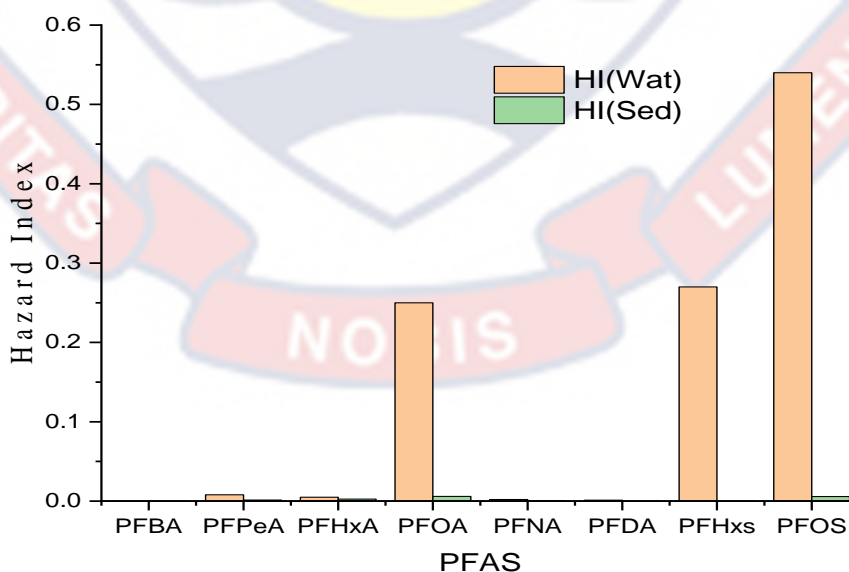


Figure 23: Non-cancer risk index of PFAS in the Pra River Basin

This could be attributed to higher mobility and easy transportation of PFAS in the surface water as compared to the sediment compartment (Liu *et al.*, 2022). The results of the study are consistent with previous studies that have evaluated the presence of PFAS in surface water and sediment in other parts of the world. However, the study was unique in that it provided important data on the comparison of hazard index of PFAS in different environmental matrices in the Pra river basin.

Carcinogenic Risk Analysis of PFAS in Sediment from Pra River Basin

The carcinogenic risk assessment of PFAS in sediment was also based on the mean CDI values using PFOA and PFOS given in Table 24. The carcinogenic risk assessment was based on average body mass weight (BMI) of 70 kg for adults. For PFAS, a human cancer risk of less than 1×10^{-6} is considered negligible and insignificant potential to cause harm. However, a human cancer risk exceeding 1×10^{-4} is considered harmful and should be addressed (USEPA, 2018). Among the studied PFAS, PFOS presents the highest likelihood of cancer risks, with a mean cancer risk of 7.8×10^{-4} . On the other hand, PFOA exhibits the lowest probability of cancer risk, with a mean cancer risk of 1.2×10^{-6} . The results of this study indicated that there was a potential cancer risk from PFOS to the health of the maximally exposed individuals around highly contaminated sites of Pra river basin through the cumulative ingestion and dermal contact routes (Table 27). However, the potential cancer risk of PFOA was estimated to be insignificant (Table 27).

Comparison of Cancer Risk and Exposure through Ingestion and Dermal Contact from Surface Water and Sediment

The study evaluated the cancer risk associated with PFAS exposure through ingestion route and it can be concluded that the potential risk linked to ingestion of surface water from the Pra river basin was relatively higher than the risk associated with ingestion of sediment from the same river as depicted in Figure 24. On the other hand, the potential cancer risk through dermal contact clearly indicates that the potential cancer risk associated with direct dermal contact with sediments from the Pra river basin increases with maximally exposed persons as compared with surface water from the same basin (Figure 24). The high risk associated with dermal contact is due to the high levels of PFOS in the sediments of river basin.

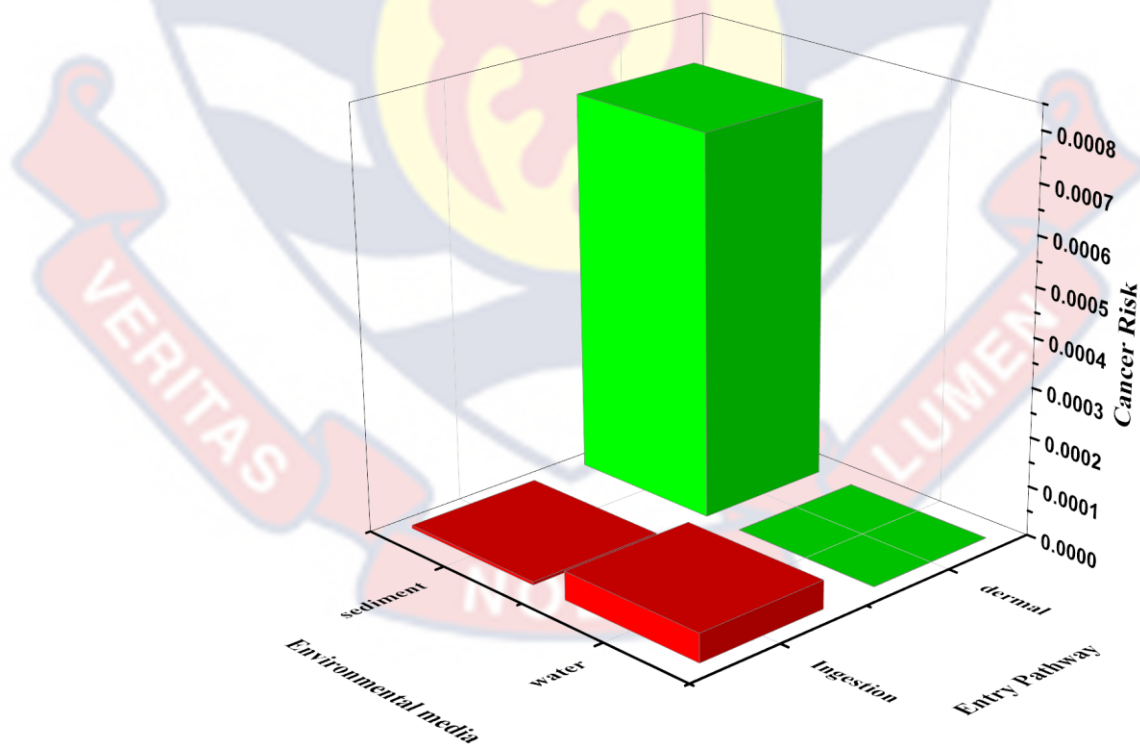


Figure 24: Vertical bar chart illustration of cancer risk summary results in surface water and sediments

Ecological Risk Assessment

The risk quotient (RQ) approach was adopted for ecological risk assessment of PFAS in the Pra river basin. The RQ is the ratio of the measured concentration of PFAS to a benchmark value such as No Observed Effect Concentration (NOEC), which is derived from available toxicity data (U.S. Environmental Protection Agency, 2002). The NOEC represents the highest concentration or dose of a substance at which no adverse effects are observed in the test organism, and is used to set safe exposure levels for organisms in the environment (Environment Canada, 2011). An RQ value greater than 1 indicates that PFAS may pose a potential risk to aquatic organisms. If the RQ is less than 1, it suggests that the predicted environmental concentration is below the benchmark value and there is likely no risk to the environment (U.S. Environmental Protection Agency, 2002). Aquatic organisms' native to the Pra river basin, including algae (phototrophic level), crustaceans (invertebrates), and fish (vertebrates), were specifically selected for investigation to evaluate the toxic effects of each PFAS compound.

Toxicity of PFAS in the Pra River Basin

The toxicity values of PFAS varied significantly, ranging from 0.005 $\mu\text{g/L}$ to 1600 $\mu\text{g/L}$, as depicted in Figure 25 and Table 28. Among the studied PFAS compounds, PFHxS exhibited the highest toxicity to algae, with a toxicity value of 0.1 $\mu\text{g/L}$, whereas PFPeA displayed the lowest toxicity, with a value of 32 $\mu\text{g/L}$. For crustaceans and fish, PFOA emerged as the most toxic compound, with NOEC (no observed effect concentration) values of 0.005 $\mu\text{g/L}$ for crustaceans and 0.03 $\mu\text{g/L}$ for fish. Conversely, PFPeA demonstrated the least toxicity, with NOEC values of 1600 $\mu\text{g/L}$ for crustaceans and 400 $\mu\text{g/L}$ for fish.

Among the three organisms tested (algae, crustaceans, and fish), crustaceans were found to be the most sensitive species to PFOA, PFOS, and PFNA. PFOA and PFNA exhibited higher toxicity to fish compared to algae and crustaceans. Additionally, only four substances (PFHxS, PFDA, PFNA, and PFOS) demonstrated higher toxicity levels towards algae. It has been shown that the toxicity of PFAS can vary among different species, with higher trophic levels such as fish having more pronounced effects (Benskin *et al.*, 2012; Giesy & Kannan, 2001; Wang *et al.*, 2018). Numerous studies have reported toxic effects of PFAS including developmental abnormalities, liver damage and reproductive effects (Kjeldsen *et al.*, 2013; Wang *et al.*, 2021). For instance, a study conducted by Lau *et al.* (2004) revealed that PFAS exposure in zebrafish led to developmental effects at levels as low as 3.3 μ g/L. In another study, Akbar *et al.* (2021) observed that PFAS led to reduced survival and growth of a common freshwater crustacean, *Daphnia magna*. The toxic effects were observed at levels ranging from 0.1 to 1 mg/L

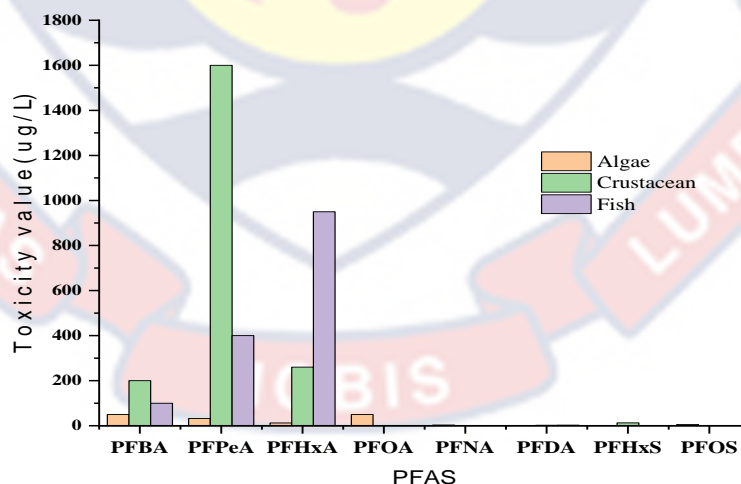


Figure 25: Toxicity data of PFAS on three trophic level organisms (algae, crustacea and fish) in freshwater ecosystems.

Table 29: NOEC Values of Single PFAS Compounds for Three Selected Aquatic Organisms in the Pra River Basin

PFAS	Algae ($\mu\text{g/L}$)	Crustacean ($\mu\text{g/L}$)	Fish($\mu\text{g/L}$)
PFBA	50	200	100
PFPeA	32	1600	400
PFHxA	12	260	950
PFOA	50	0.005	0.03
PFNA	3	0.69	0.5
PFDA	1	2	2.6
PFHxS	0.1	12.7	0.5
PFOS	5	0.2	0.25

(Source : Akbar et al. 2021, Kjeldsen *et al.*, 2013 ; Wang *et al.*, 2021)

Risk Assessment of Single PFAS Compounds

Based on the detected levels of PFAS, 160 toxicity values were obtained from the 20 sampling locations in the surface water from the Pra river basin. Based on the PFAS levels in the Pra river basin and toxicity values (NOEC), 160 individual RQ values (Appendix I), the mean RQ for the three trophic levels of aquatic organisms were listed in Table 30. The RQ values ranged from 2.66×10^{-5} to 17. Kyekyewere (P19), Abetemasu (P17), P6 (Sekyere Hemang) and Twifo hemang (P7) exhibited the highest RQ values respectively (Appendix H). From a general perspective, the values of PFOA and PFOS were found to be significant contributors to the overall risks associated with the studied PFAS compounds, as indicated in Table 30.

The mean RQ values for each single PFAS compound for the entire river basin were also shown in Table 19 and it ranged from 2.94×10^{-7} to 14.1. PFOS showed higher environmental risk with the RQ values between 4.19 and 0.0167 for fish and algae respectively. PFOA on other hand showed the highest environmental risk for crustacean (Daphina) with a mean RQ of 14.1. Aside

these, the risk quotient (RQ) for 7 of out of the detected PFAS compounds were less than 1 while the RQ for PFOA was greater than 1 indicating a potential risk to aquatic organisms. A similar investigation conducted by Chen *et al.* (2017) in Eastern China river basin (Liao) on potential risk of PFAS to aquatic organisms revealed that the highest RQ values for PFOA in surface water were up to 25.7. This RQ value is higher than the value obtained in the current study.

Table 30: Mean Risk Quotient of Single Organic PFAS Compounds

PFAS	Algae	Crustacean	Fish	Σ RQ
PFBA	1.34E-05	3.35E-06	6.70E-06	2.35E-05
PFPeA	1.47E-05	2.94E-07	1.18E-06	1.62E-05
PFHxA	2.50E-05	1.15E-06	3.16E-07	2.65E-05
PFOA	1.41E-03	1.41E+01	2.35E+00	1.65E+01
PFNA	2.27E-04	9.86E-04	1.36E-03	2.57E-03
PFDA	2.60E-04	1.30E-04	1.00E-04	4.90E-04
PFHxS	3.80E-03	2.99E-05	7.60E-04	4.59E-03
PFOS	1.67E-02	4.19E-01	3.35E-01	7.70E-01

(Source: Fieldwork, 2022)

Based on these findings, it is suggested that the focus of environmental risk management should primarily be directed towards the two major PFAS compounds, namely PFOA and PFOS, to prevent irreversible harm to the aquatic ecosystem. The results also indicate a low to medium level of environmental risk associated with PFOA in the Pra river basin.

Risk Assessment of PFAS Mixture

The mixture risk assessment considered all 20 sampling sites (P1-P20) for evaluation. The results, presented in Table 30, indicate that all $RQ_{MEC/NOEC}$ values exceeded 1. This finding provides further evidence that relying solely on single chemical toxicity for risk assessment is insufficient, highlighting the necessity of conducting mixture risk assessments. Among the 20 sampling sites, P19-Kykyewere exhibited the highest environmental risk, with an

RQMEC/NOEC value of 17.1. This was followed by P17-Abetemasu (15.3), P6-Sekyere Hemang (15.3), and P7-Twifo Hemang (14.1), indicating significant potential risks at these locations.

In the Pra river basin, among the eight detected PFAS compounds, PFOS and PFOA were found to pose the highest environmental risks in surface waters. Consequently, these two compounds warrant greater attention in terms of risk management efforts. It is important to note that although individual PFAS were present at low concentrations and did not exhibit significant toxic effects, the mixture of PFAS compounds could still pose considerable risks in environmental settings, as highlighted by Liu et al. (2020). In the current study, the risk assessment relied on acute toxicity data, despite the fact that PFAS compounds have a high potential for bioaccumulation, which may lead to subchronic or chronic toxicity in aquatic organisms. Furthermore, the comprehensive assessment of micropollutant risks in the study employed the concentration addition model (CA), which may not fully account for synergistic or antagonistic interactions that can occur in PFAS mixtures, as noted by Ferrari et al. (2019).

Table 31: Risk Quotient of Composite PFAS Compounds for an Aquatic System (Pra River Basin)

PFAS	RQ _{MEC/NOEC}
PFBA	1.34E-05
PFPeA	1.47E-05
PFHxA	2.50E-05
PFOA	1.41E+01
PFNA	1.36E-03
PFDA	2.60E-04
PFHxS	5.00E-07
PFOS	2.50E-07
Σ RQ _{MEC/NOEC}	1.41E+01

(Source: Fieldwork, 2022)

Decomposition of PFAS using Radiolytic Method: A Case Study of PFOA

Perfluorooctanoic acid (PFOA) is a persistent compound which is difficult to treat and degrade using the conventional chemical methods and other advanced oxidative processes (Mak *et al.*, 2008). One promising approach for degrading organic contaminant such as PFOA is through water radiolysis, which involves the use of ionizing radiation to generate reactive species such as but not limited to solvated electrons, hydroxyl radical, hydrogen radical and carbon dioxide radical ions that can break down PFOA.

The degradation of PFOA by irradiation at pH 6 and pH 11 are shown in Figure 26. The degradation efficiency of PFOA increased when the pH value was at 11.0. At pH 6.0, the decomposition efficiency was low. However, at pH 11.0 the degradation efficiency increased to almost 98 % after 8-hours irradiation at a dose of 20 kGy. Also, the defluorination efficiency of 1 μ M PFOA was also nearly 98 % at pH 11.0 (Figure 27). Furthermore, the released F⁻ concentration also decreased with the decreasing pH. At pH 6.0, the levels of F⁻ released was very low. This might be attributed to the loss of solvated electron via the process shown equation (1) which is much stronger reducing agent as compared to the hydrogen radical.



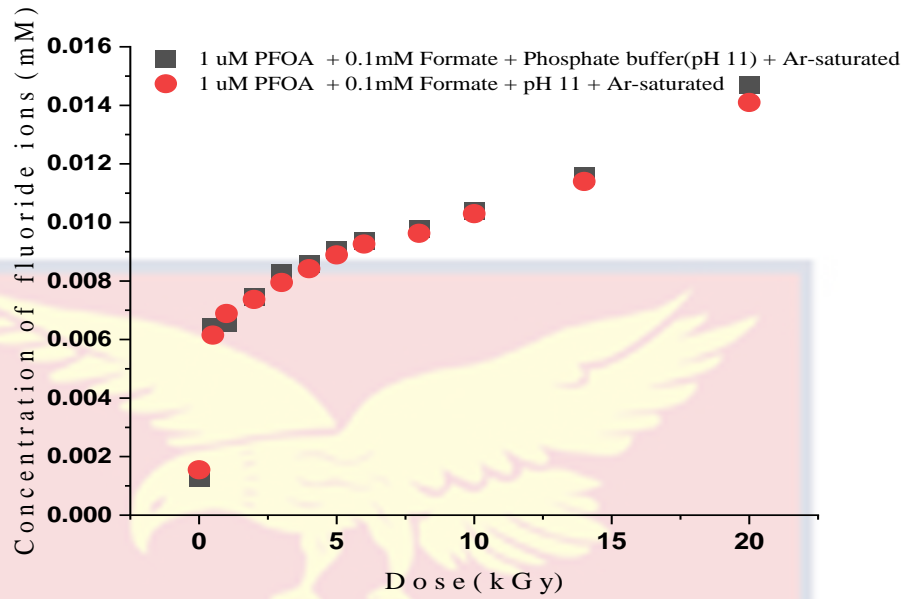


Figure 26: A graph showing the concentration of fluoride ions in 1 μM PFOA aqueous solution at pH 11 irradiated with gamma at defluorination efficiency of 98%.

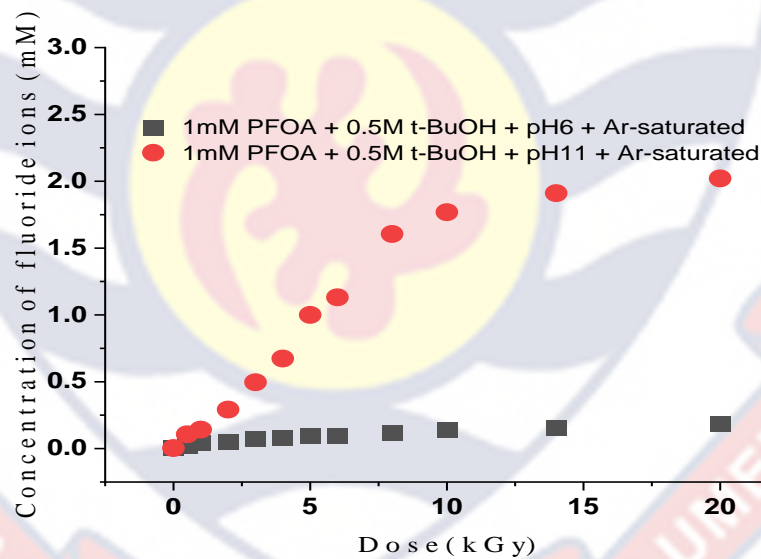


Figure 27: A graph comparing the levels of fluoride ions at pH 6 and pH 11.

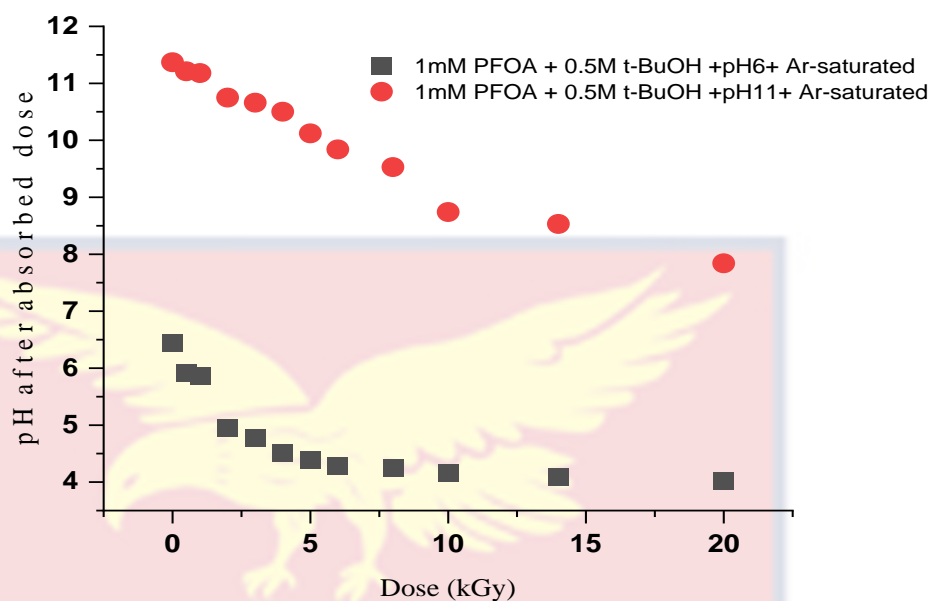
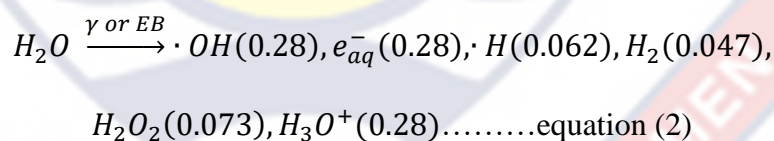


Figure 28: A graph comparing two pH values after absorbed γ -radiation

Role of Solvated Electron ($e_{(aq)}^-$), Carbon Dioxide Radical Ion ($CO_2^{\bullet-}$) and Phosphate Buffer in the Decomposition of PFOA

Initial experimental studies result indicates that PFOA can be degraded and defluorinated efficiently in alkaline media under argon-saturated conditions. The likely reactive species responsible for the degradation of PFOA through water radiolysis was based on the equation (2):



To investigate the contributions of reactive species produced by gamma-radiation on the degradation of PFOA, PFOA samples were exposed to varied conditions under N_2O - or Ar-saturated conditions respectively (Table 31).

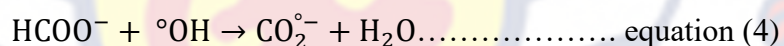
Table 32: Conditions Observed Before Gamma Irradiation of PFOA and Associated Reactive Species

pH	Gas used	Chemical reagents used	Reactive species
6 11	Argon	0.5 M t-butanol	$e_{(aq)}^-$
6 11	dinitrogen oxide(N ₂ O)	0.1 M Formate	$CO_2^{\circ-}$
6 11	Argon	0.1 M Formate	$e_{(aq)}^-$ and $CO_2^{\circ-}$

(Source: Fieldwork, 2022)

Reaction of PFOA with Carbon dioxide Radical ($CO_2^{\circ-}$) in N₂O-saturated Environment

PFOA seemed to be resistant to gamma irradiation under N₂O-saturated environment. The concentration of fluoride ions released was comparatively very low in both buffered and non-buffered solutions (Figures 29 & 30). The production of carbon dioxide radical ion ($CO_2^{\circ-}$) is postulated to follow through the chemical steps listed below (Vecitis *et al.*, 2009):



Solutions prepared for gamma-irradiation were saturated with N₂O and this led to the scavenging of the solvated electrons ($e_{(aq)}^-$) in equation (3).

The formate ion scavenges the ${}^{\circ}OH$ radical and oxidizes to carbon dioxide radical anion $CO_2^{\circ-}$ as the main reacting species with PFOA.

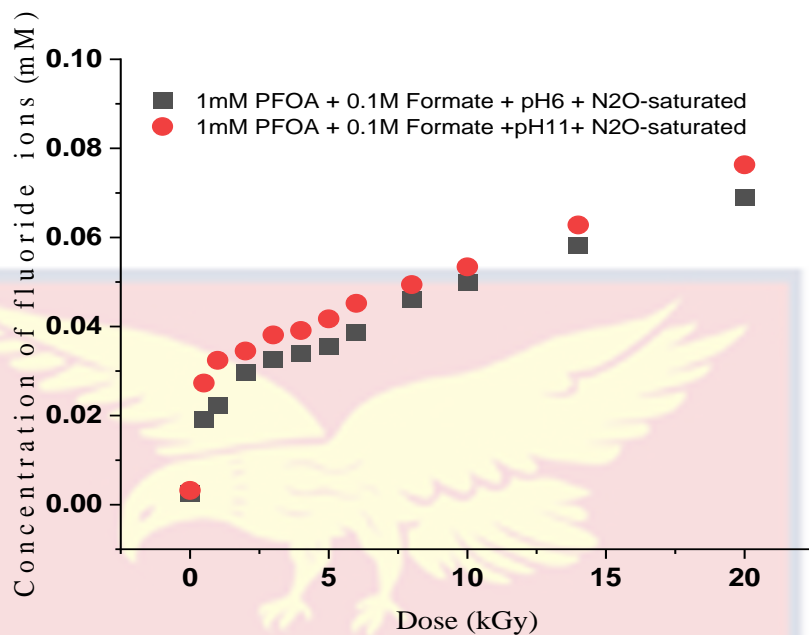


Figure 29: A graph comparing the levels of fluoride ions at pH 6 and pH 11 in an N₂O-saturated environment with main species being carbon dioxide radical anion.

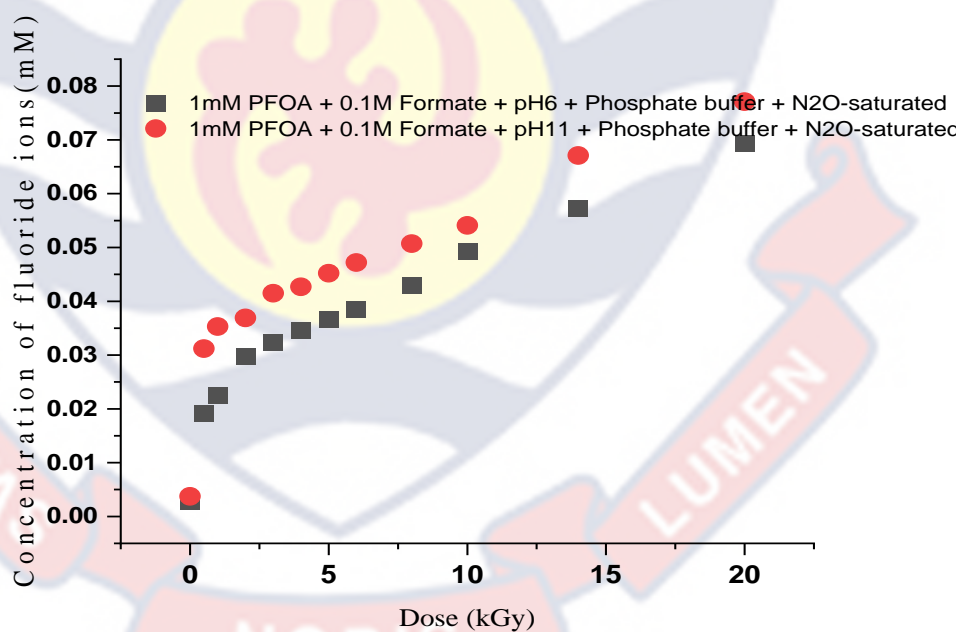


Figure 30: A graph comparing the levels of fluoride ions in buffered solutions at pH 6 and pH11 in a N₂O-saturated environment with main species being carbon dioxide radical anion.

Importantly, the pH of the reaction curve at pH 11 declined steadily while the reaction curve at pH 6 increased steadily as depicted in Figure 31.

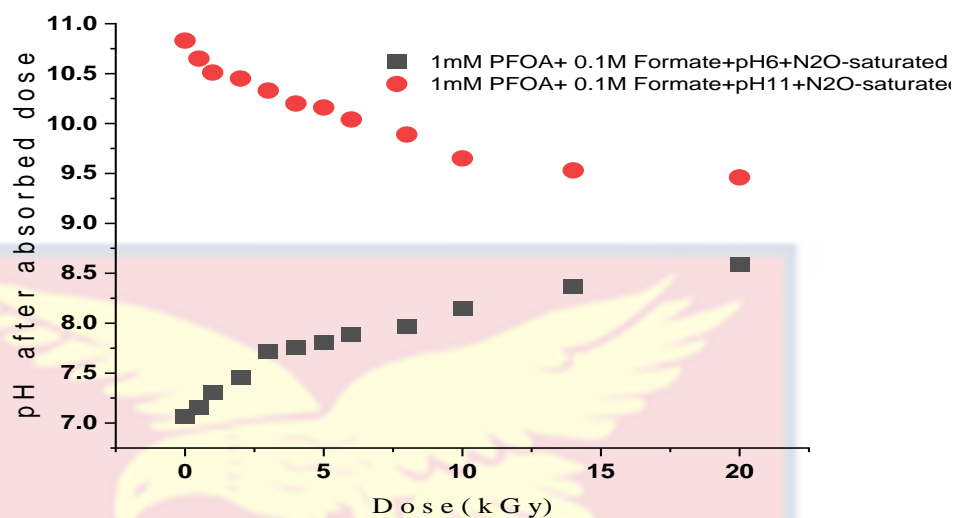


Figure 31: A graph showing pH of PFOA irradiated solution saturated with N_2O gas with main reacting species being carbon dioxide radical anion.

The radiolytic yield estimated from the graphs of both non-buffered solutions (yield at pH 6 = 0.00473 $\mu\text{mol}/\text{J}$; pH 11 = 0.00486 $\mu\text{mol}/\text{J}$) and buffered solutions (yield at pH 6 = 0.00478 $\mu\text{mol}/\text{J}$; pH 11 = 0.00498 $\mu\text{mol}/\text{J}$) were very low even though the yield of the buffered solutions were slightly higher as compared to non-buffered solutions.

Reaction of PFOA with solvated electron ($e_{(s)}^-$) in Argon saturated environment

The reaction of solvated electron with PFOA in argon saturated environment is summarized in chemical equation below (Rayne, S. & Forest, K., 2009):



Tert- butanol scavenges $^{\circ}\text{OH}$ radical which creates a situation where the main product of water radiolysis is the solvated electron ($e_{(aq)}^-$). $^{\circ}\text{H}$ atoms and t-butanol radicals also formed in small amounts in the reaction (Rayne *et al.*, 2009).

As shown in figures 32 and 33, the concentration of fluoride ions was at elevated levels at pH11 in both non-buffered and buffered irradiated solutions as compared the levels of fluoride ions at pH 6 in both situations.

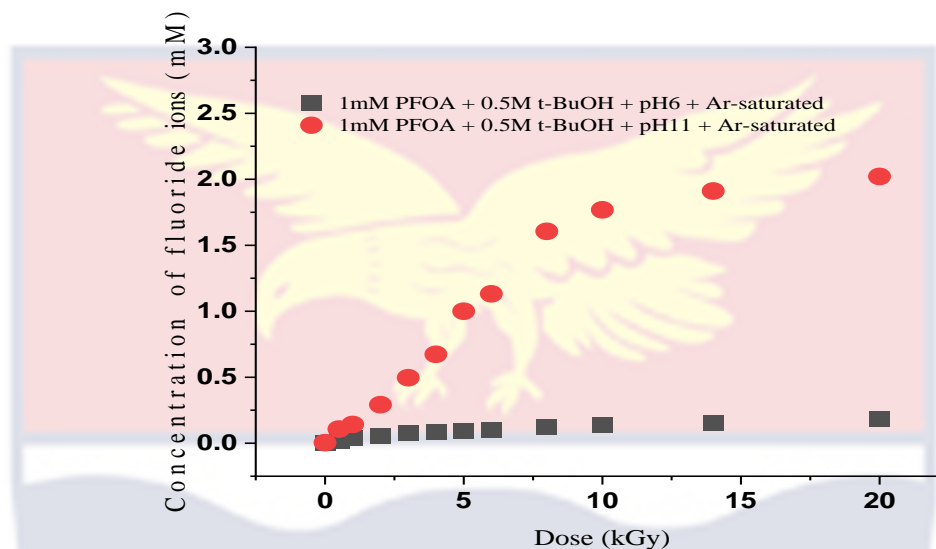


Figure 32: A graph comparing the levels of fluoride ions at pH 6 and pH11 in an argon-saturated environment with main species being solvated electron.

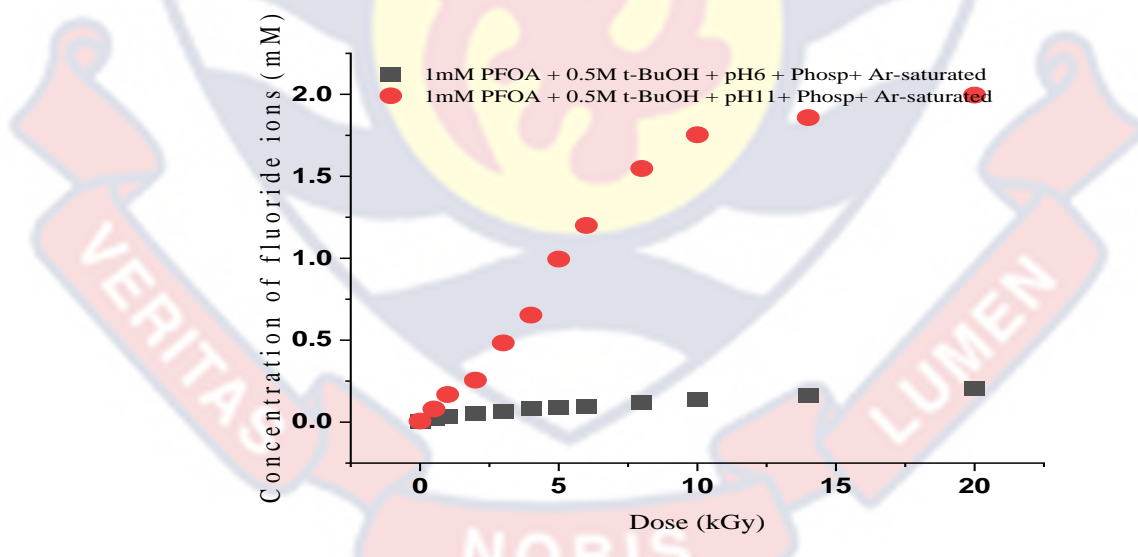


Figure 33: A graph comparing the levels of fluoride ions in buffered solution at pH 6 and pH11 in an argon-saturated environment with main species being solvated electron

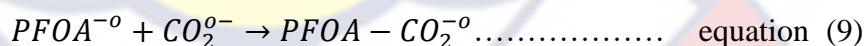
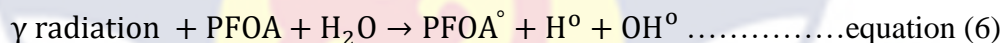
The corresponding pH values of the irradiated solution decreased as depicted in the figure 28. The possible reasons for the decline in pH values may

arise from a number of possible factors including but not limited to recombination and excess H after irradiation.

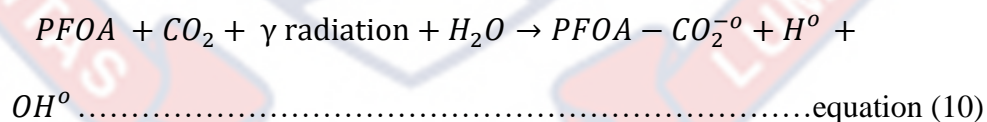
The radiolytic yield calculated from the graphs of both non-buffered solutions (yield at pH 6 = 0.0154 μ mol/J; pH 11= 0.192 μ mol/J) and buffered solutions (yield at pH 6 = 0.0152 μ mol/J; pH 11= 0.198 μ mol/J) were relatively higher as compared to the yields obtained from the reaction of PFOA and carbon dioxide radical ions in N₂O saturated environment.

Reaction of PFOA with solvated electron and carbon dioxide radical anion in argon-saturated environment

The chemical reaction between an argon-saturated PFOA aqueous solution, solvated electrons, and carbon dioxide radical ion using gamma radiation are represented in the equations below according to Deng *et al.*, 2021 and Huang *et al.*, 2007.



Overall reaction:



With regards to the sequence of the reactions above, gamma radiation is used to initiate the reaction leading to the formation of solvated electrons and PFOA^{-o}, while carbon dioxide radical anion reacts with PFOA^{-o} to form the PFOA – CO₂^{-o} adduct. The resulting adducts may undergo further

reactions depending on a number of experimental factors, such as reacting with other radical species or undergoing fragmentation.

As shown in Figures 34 and 35, the concentration of fluoride ions increased at pH 11 in both non-buffered and buffered irradiated solutions as compared to the concentration of fluoride ions at pH 6 in both solutions.

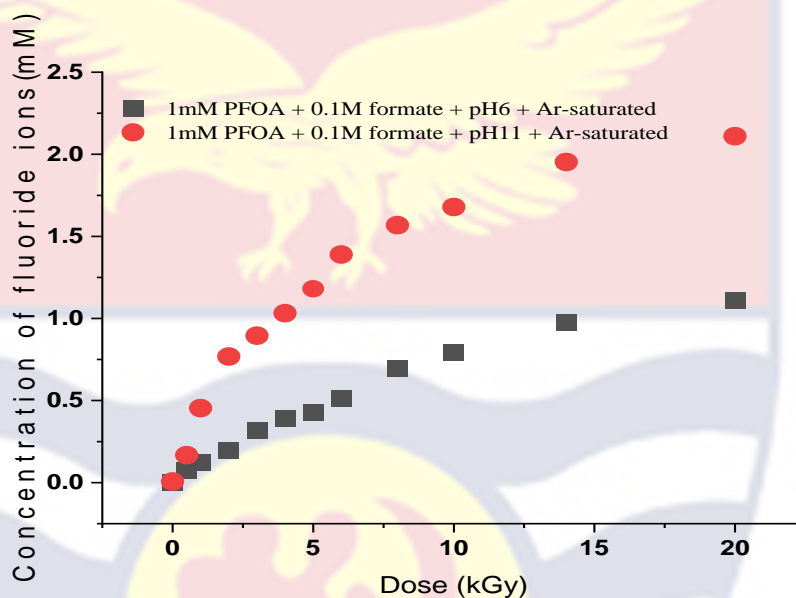


Figure 34: A graph comparing the levels of fluoride ions at pH 6 and pH 11 in an argon-saturated environment with main species being solvated electron and carbon dioxide radical anion.

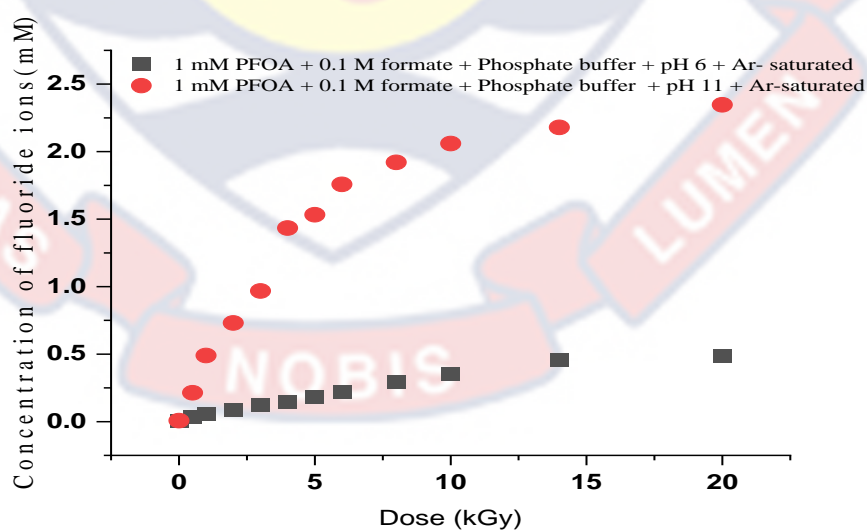


Figure 35: A graph comparing the levels of fluoride ions in buffered solution at pH 6 and pH11 in an argon-saturated environment with main species being solvated electron and carbon dioxide radical anion.

The pH of the irradiated solution also reduced as depicted in figure 36.

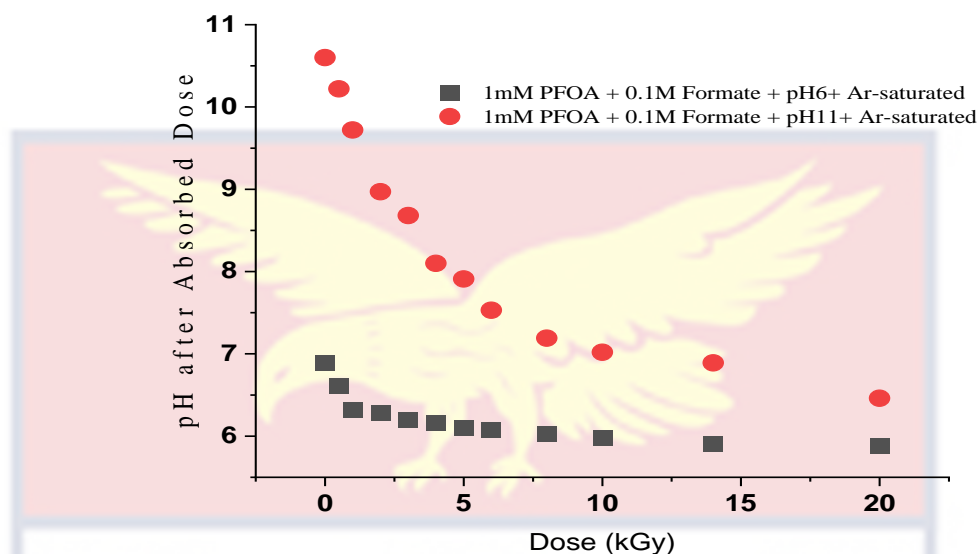


Figure 36: A graph comparing two pH values at 6 and 11 after absorbed radiation during PFOA reaction with solvated electrons and carbon dioxide radical anions

The radiolytic yield estimated from the graphs of both non-buffered solutions (yield at pH 6 = $0.0831\mu\text{mol}/\text{J}$; pH 11 = $0.218\mu\text{mol}/\text{J}$) and buffered solutions (yield at pH 6 = $0.034\mu\text{mol}/\text{J}$; pH 11 = $0.290\mu\text{mol}/\text{J}$) were relatively higher as compared to the yields obtained from the reaction of PFOA and solvated electrons in argon- saturated environment.

Identification of Optimum Conditions for Higher Yield

To identify the optimum conditions for elevated fluoride ion concentrations in both non-buffered and buffered conditions, the fluoride concentration at pH 11 as well as the yields were compared as seen in the figures 37, 38 and 39:

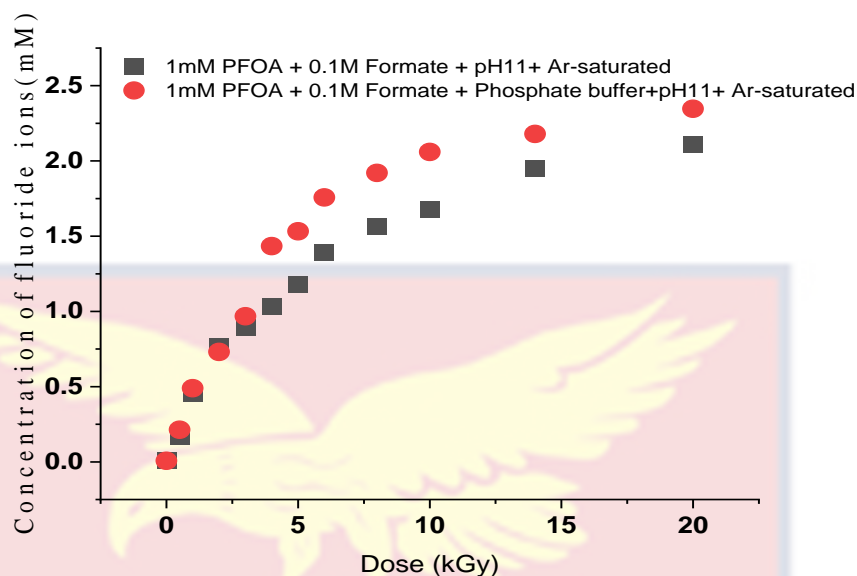


Figure 37: A graph comparing the levels of fluoride ions in buffered and non-buffered solutions at pH11 in an argon-saturated environment with main species being solvated electron and carbon dioxide radical anion.

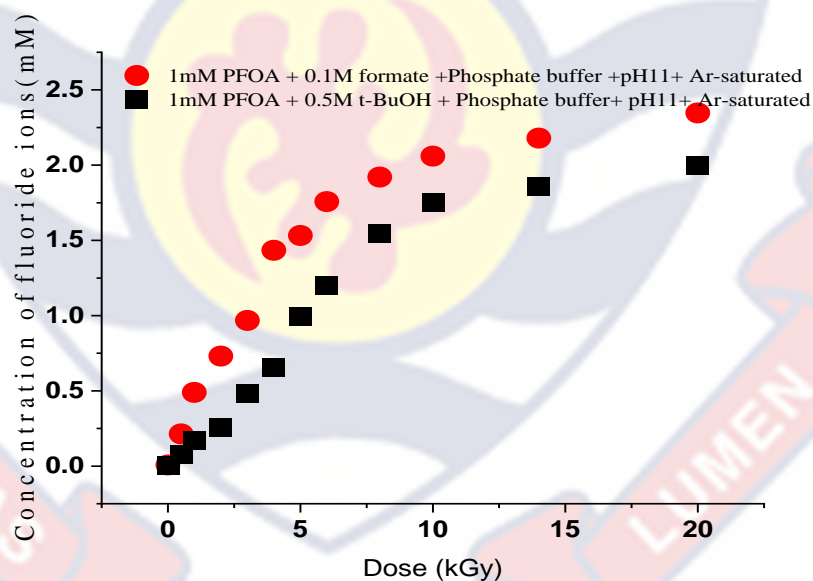


Figure 38: A graph comparing the levels of fluoride ions in two buffered solutions with main reacting species being (solvated electron and carbon dioxide radical anion) and (solvated electrons only) at pH11 in an argon-saturated environment.

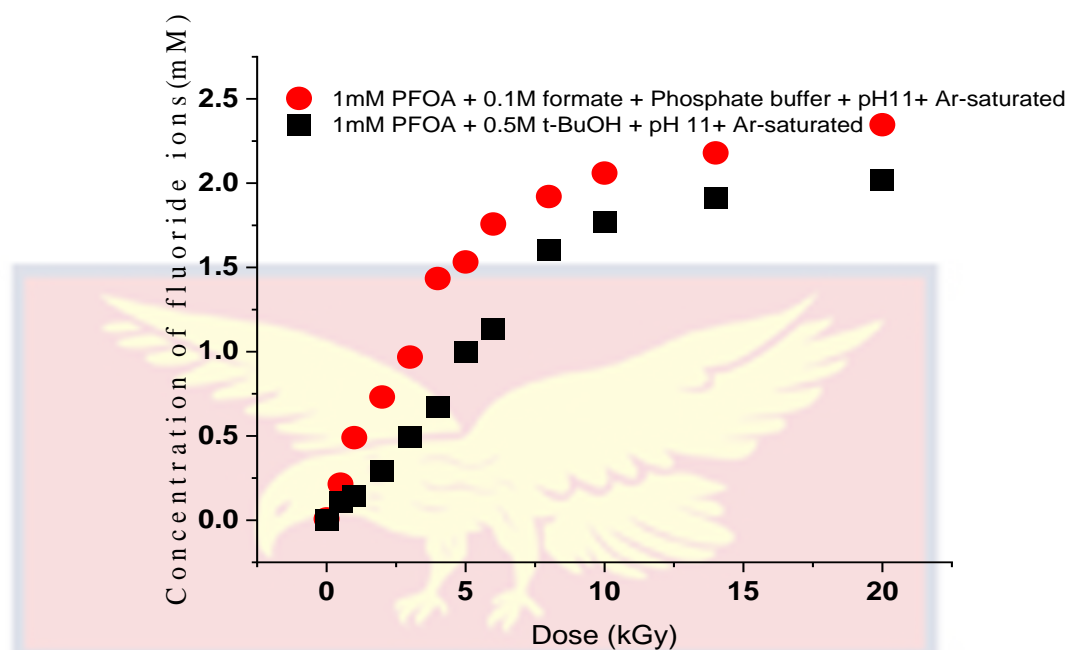


Figure 39: A graph comparing the levels of fluoride ions in buffered (solvated electron and carbon dioxide radical anion) and non-buffered (solvated electrons only) solutions at pH11 in an argon-saturated environment.

Based on figures 38 and 39, the reaction of 1mm PFOA (+ 0.1M formate + pH11+Argon-saturated (yield: $0.218\mu\text{mol/J}$) and reaction of 1mm PFOA (+ 0.1M formate + Phosphate buffer + pH11 + Argon-saturated (yield: $0.291\mu\text{mol/J}$) were identified as conditions that produced higher yields.

Further investigations were conducted with lower PFOA concentrations (0.5 mM and $1\mu\text{M}$) as depicted in the figures 40 and 41, and the percentage of defluorination and yield determined.

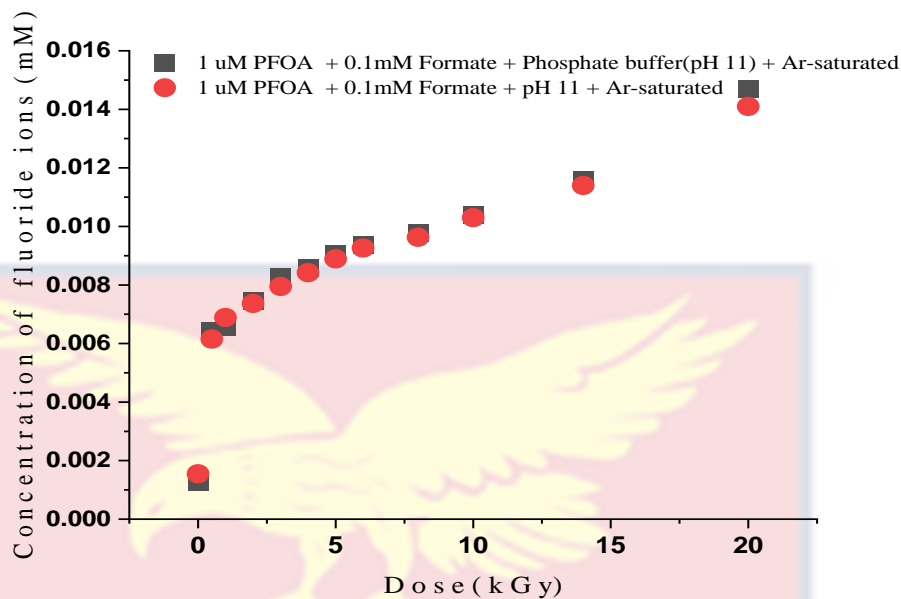


Figure 40: A graph comparing the levels of fluoride ions in both buffered and non-buffered solutions at pH11 in an argon-saturated environment with main reacting species being 1µM PFOA, solvated electrons and carbon dioxide radical anion.

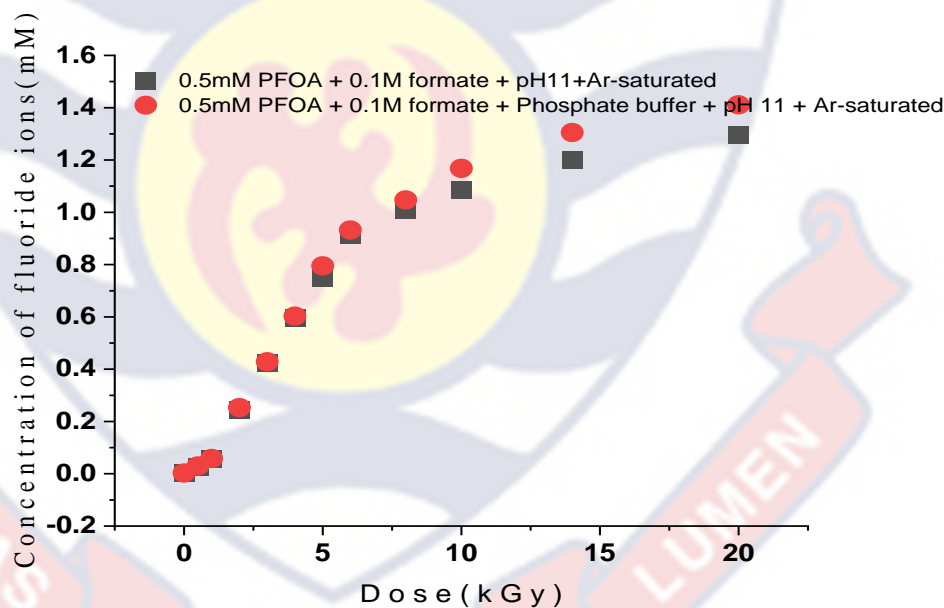


Figure 41: A graph comparing the levels of fluoride ions in both buffered and non-buffered solutions at pH11 in an argon-saturated environment with main reacting species being 0.5mM PFOA, solvated electrons and carbon dioxide radical anion.

The radiolytic yield and the percentage of defluorination of reactions involving PFOA, solvated electrons and carbon dioxide radical anions in argon-saturated environment are summarized in Table 33.

Table 33: Percentage of Defluorination and Yield of Fluoride Ions from Reactions Involving PFOA, Solvated Electrons and Carbon Dioxide Radical Anions

Level of PFOA	Percentage of defluorination (%) *	Yield($\mu\text{mol}/\text{J}$)
1mM PFOA at pH11	14.07	0.218
1mM PFOA buffered at pH11	15.65	0.290
0.5mM PFOA at pH11	17.26	0.123
0.5 mM PFOA buffered at pH11	18.81	0.130
1 μM PFOA at pH11	94.0	9.10E-04
1 μM PFOA buffered at pH11	98.0	9.59E-04

*Based on 20kGy absorbed dose

(Source: Fieldwork, 2022)

Polychlorinated Biphenyls (PCBs)

Quality Assurance and Quality Control

The results of analysis of precision and recovery of 12 indicator polychlorinated biphenyl (PCB) congeners, nos.18, 28, 31, 44, 52, 101, 118, 138, 149, 153, 194 and 180; as well as the limit of quantitation (LOQ) limit of detection (LOD) are shown (Tables 33 & 34). The limit of detection (LODs) determined for all congeners were in the range of 0.0047-0.057 ng/L and 0.036-7.02 ng/g for the water and sediments respectively. The range of the LOQ were respectively 0.017 -0.098 ng/L and 0.12 -27.00 ng/g for the water and sediments. The mean recoveries of spiked PCBs from water were 71.20- 105.7 %, with precision as relative percent difference (RPD) range of 2.41- 10.79%. The recoveries and precision for the sediments were respectively 72.81–94.61% and 2.41 -8.93%. Thus, the precision was relatively high and within the limit

$\pm 15\%$ recommended for PCB analysis. The calibration linearity was good and ranged from $r^2 = 0.992 - 0.998$, in line with the acceptance criteria of $r \leq 0.995$ (or $r^2 \leq 0.990$) for GC analysis of environmental samples.

Table 34: Method Limits, Variation and Recovery of 12 PCBs from Water

Analyte	LoD (ng/L)	LoQ (ng/L)	Linearity (r^2)	Recovery (%)	RPD _w (%)	RPD _d (%)
PCB18	0.012 - 0.021	0.039 - 0.069	0.997	71.20	3.21	3.19
PCB28	0.0047 - 0.014	0.16 - 0.046	0.998	86.47	2.41	2.83
PCB31	0.0086 - 0.018	0.029 - 0.059	0.996	75.74	2.60	2.70
PCB44	0.017 - 0.029	0.055 - 0.098	0.995	97.89	4.36	4.40
PCB52	0.0074 - 0.057	0.025 - 0.19	0.998	96.83	5.62	8.60
PCB101	0.011 - 0.015	0.038 - 0.049	0.990	94.10	2.71	3.72
PCB118	0.0058 - 0.023	0.019 - 0.078	0.992	98.70	3.32	2.83
PCB138	0.010 - 0.017	0.035 - 0.055	0.992	105.70	5.76	4.71
PCB149	0.013 - 0.020	0.042 - 0.065	0.990	99.38	8.23	6.72
PCB153	0.011 - 0.022	0.035 - 0.072	0.993	71.20	7.61	10.79
PCB194	0.0074 - 0.020	0.025 - 0.065	0.990	86.24	3.86	4.22
PCB180	0.0050 - 0.014	0.017 - 0.047	0.994	90.27	3.90	7.84

(Source: Fieldwork, 2022)

LoD = limit of detection; LOQ = limit of quantification; RPD_w = relative percent difference for duplicate samples for the wet season; RPD_d = relative percent difference for duplicate samples for the dry season.

Table 35: Method Limits, Linearity, Variation and Recovery of the 12 PCBs in Sediment Samples

Analyte	LoD (ng/g)	LoQ (ng/g)	Linearity (r^2)	Recovery (%)	RPD _w (%)	RPD _d (%)
PCB18	0.042 - 0.054	0.14 - 0.18	0.998	78.25	5.31	2.89
PCB28	0.22 - 0.27	0.72 - 0.91	0.992	82.42	4.90	4.81
PCB31	0.039 - 0.051	0.13 - 0.17	0.996	72.81	4.12	3.22
PCB44	0.045 - 3.60	0.15 - 12.00	0.997	74.22	3.60	3.63
PCB52	5.04 - 7.02	16.8 - 23.40	0.995	73.43	2.80	4.72
PCB101	0.24 - 4.08	0.81 - 13.60	0.990	89.10	3.32	3.60
PCB118	0.28 - 6.33	0.92 - 21.10	0.987	75.93	3.72	5.12
PCB138	0.29 - 3.03	0.98 - 10.10	0.996	80.61	2.61	2.80
PCB149	0.048 - 0.81	0.16 - 27.00	0.997	83.22	4.76	8.93
PCB153	5.22 - 7.86	17.4 - 26.20	0.998	94.61	7.83	2.41
PCB194	0.036 - 0.17	0.12 - 0.55	0.997	90.23	2.71	2.60
PCB180	5.43 - 9.42	18.0 - 31.40	0.992	91.44	6.39	8.71

(Source: Fieldwork, 2022)

LoD = limit of detection; LOQ = limit of quantification; RPD_w = relative percent difference for duplicate samples for the wet season; RPD_d = relative percent difference for duplicate samples for the dry season.

Total PCB Concentration (Σ PCB) in the Pra river basin

The data for the PCB measurements are presented in Appendix (J-M). Figure 42 displays the total PCB concentrations (Σ PCB) in the water collected from the sampling points during the dry season (November-December) and wet seasons (August-September). The highest concentration, Σ PCB, in the dry (ND) and wet (AS) season respectively were recorded at sites P18 (5.869 ng/L) and P15 (2.995 ng/L). The least concentrations were recorded at sites P3 (2.029 ng/L) and P9 (0.5285 ng/L) respectively in the dry and wet season.

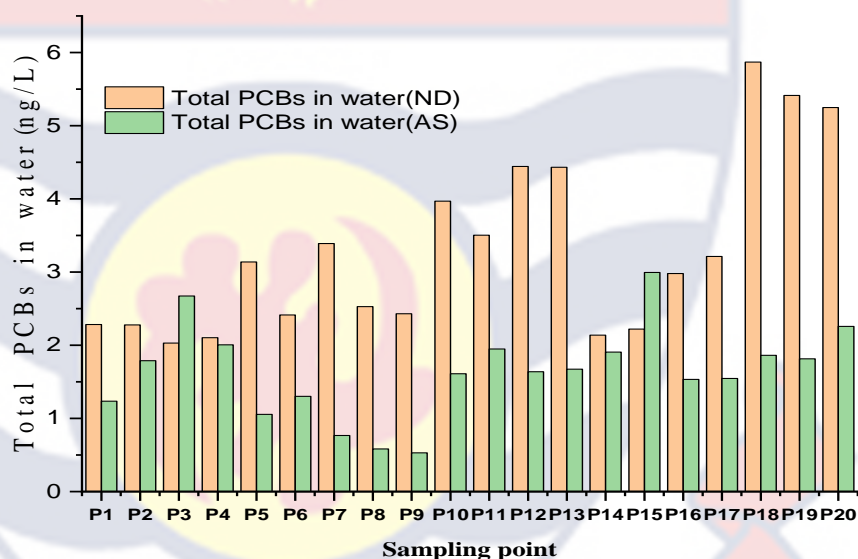


Figure 42: Total PCB Concentrations in water samples from the Pra River Basin

The range and mean total PCBs detected in the water for the wet seasons (AS) were 0.529-2.995 ng/L and 1.73 ± 0.71 ng/L, while the dry season (ND) recorded 2.029-5.869 ng/L and 3.47 ± 1.23 ng/L (Figure 43). The exact reason for the difference in Σ PCBs concentration between the two seasons is not clear. Interestingly, a contrasting trend was observed by Md. Habibullah-Al-Mamun et al. (2019), where they found higher concentrations of Σ PCBs during the winter (wet season) compared to the summer (dry season).

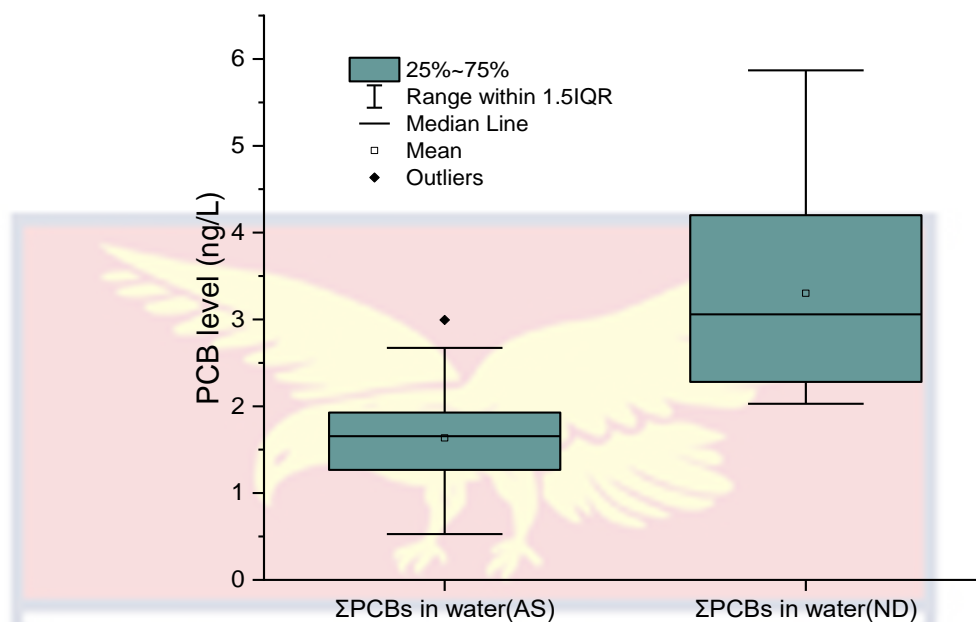


Figure 43: Box-plot of PCB distribution in water from the Pra River Basin

The sediment PCB concentrations were generally higher. The mean total PCB for the water and sediments over the period were respectively 2.60 ± 0.97 ng/L and 139.79 ± 29.24 ng/g. The distribution of the total PCBs of the sediments revealed that the concentrations of PCB in the dry season were higher than those of the wet season at all except for two sites P8 and P12 (Figure 44). During the dry season, the highest Σ PCBs was recorded at site P2 (242.16 ng/g) and the least at P12 (98.78 ng/g) while in the wet season, site P8 recorded the highest Σ PCBs of 158.11 ng/g and P19 the least (60.99 ng/g). The mean PCB concentration recorded for the sediment in the wet season (AS) was 112.59 ± 27.09 ng/g and ranged from 60.99 - 158.11 ng/g (Figure 45). The respective mean and range in the drying season (ND) were 167.019 ± 31.39 and 98.768-242.16 ng/g.

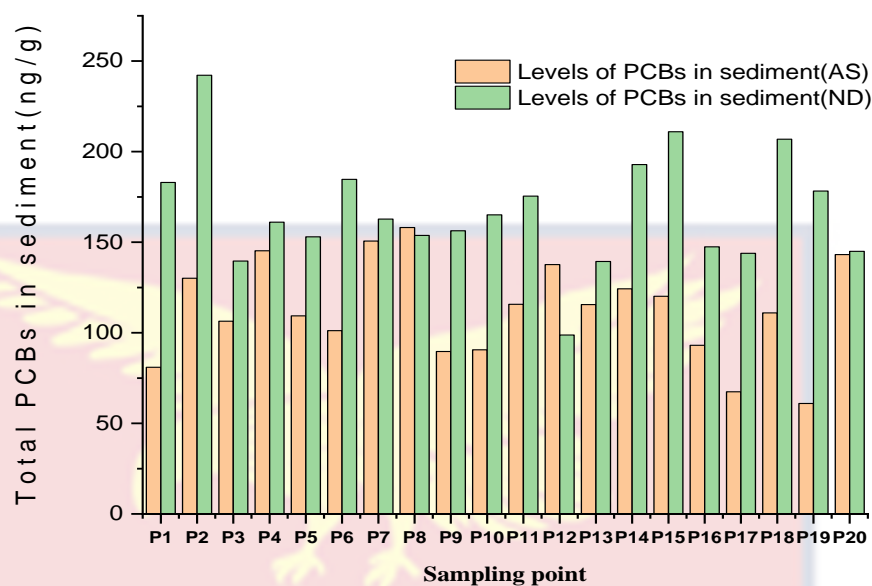


Figure 44: Total PCB Concentrations in sediments from the Pra River Basin

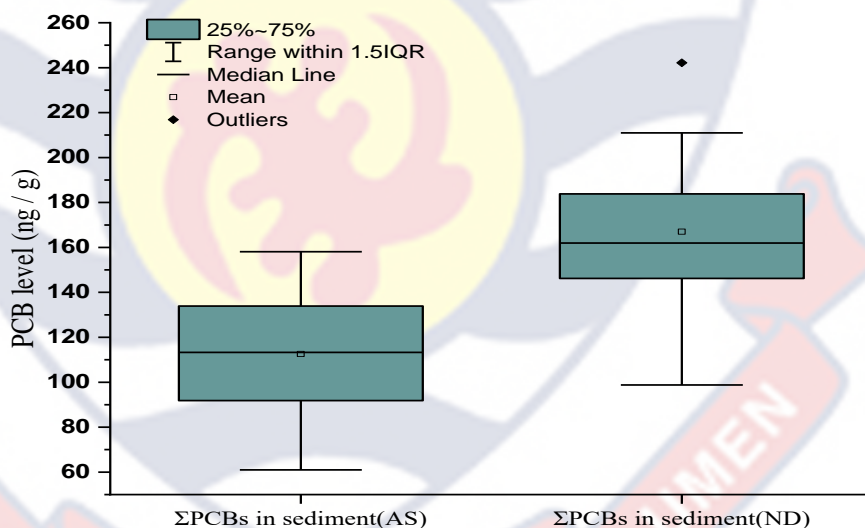


Figure 45: Box-plot of PCB distribution in Pra River Basin

There were spatial variations in the distribution of the Σ PCBs as shown by the coefficient of variation CV% (Appendix M); with water showing the greater variation of 38.33% and sediment 21.43%. In general, the Σ PCB distributions in the two media showed greater variations in the drying season,

41.27% for water and 24.07% for sediment, than the wet season with variations 35.40% and 18.793% respectively.

The higher PCB concentrations recorded for the sediments was not strange as the organic pollutant, including PCBs, are sorbed strongly onto the soil organic matter and clay, the soil serves as a sink for pollutants. The sorption and desorption of PCBs onto the soil, however depends on factors such as pH, organic matter, water solubility of PCB congeners, the degree of congener hydrophobicity and soil properties- surface area, and pore size distribution (Adeyinka *et al.*, 2018; Meili *et al.*, 2000).

Also, the higher PCB concentrations recorded in the drying season could be attributed to evaporation of the river water, while in the wet season dilution occurs due to the rains. The partitioning of these organic pollutants between the water, suspended particulate matter and the soil sediment leads to increasing sorption onto the sediment in the dry season as PCB concentration in the water increases, causing retention of the sediment PCBs. In the wet season, due to the PCB sorption –desorption kinetics, PCBs adsorbed onto the sediments act as secondary source of PCBs and are released into the water column (Chalhoub *et al.*, 2013). Desorption of PCBs from the sediment, however depends on PCB congener concentration in the sediment on the degree of the congener hydrophobicity.

The PCB concentrations in water from this study, 0.03- 6.20 ng/L, were compared with other studies worldwide. The levels were lower than PCB concentrations in water samples collected along the River Nile Egypt, and ranged from 14 to 20 $\mu\text{g/L}$ (Megahed *et al.*, 2015); in Cairo-14.503 ng/L and Nile Delta (18.771 $\mu\text{g/L}$) (Megahed *et al.*, 2015); in USA, raw water of Hudson

River 9.3–164.3 ng/L; Mississippi River, 22.2–163 ng/L; in water from the Bay of Bengal coast of Bangladesh, 17–199.4 ng/L in winter and summer respectively (Habibullah-Al-Mamuna, 2019); in seawater, 0.97–3.10 ng/L, (Jafarabadi et al., 2019); China, Pearl River Estuary, Beijing, and Minjiang River Estuary respectively, 0.02–14.8 ng/L, 31.58–344.9 ng/L, and 204–2473 ng/L, (Yang *et al.*, 2015).

Also, the levels were lower than the concentrations of PCBs in raw and finished drinking water at seven Public Water Systems (PWSs) along the Hudson River respectively ranged from < 9.3 to 164.3 ng/L and < 9.3 to 186.6 ng/L (Palmer et al., 2011), and the total concentrations of PCBs in bottled drinking water (0.035–0.039 µg/L) in Mexico City (Rutilio Ortiz Salinas)

The PCB concentration recorded for the sediments in this study, 67.43–242.16 ng/g, however, were higher than some of those detected in sediment samples in various studies worldwide: the Guanabara Bay in Brazil (range, 18–184 pg g⁻¹), Congo River Basin in the Democratic Republic of Congo (<50–1400 pg/g⁻¹), Istanbul Strait in Turkey (13–699 pg/g⁻¹), Dagu Drainage River in China (9687–22,148 pg/g⁻¹), and River Nile, Lake Qarun in Egypt (1480–137,200 pg/g⁻¹) (Sebugere, 2014); in surface sediments of Larak Island of Persian Gulf, 2.95–7.95 ng g⁻¹ dw (Jafarabadi *et al.*, 2019); in superficial sediments collected from The Ghar El Melh lagoon, Tunisia, PCBs ranged from not detected to 3.987 ng/g (Ameur et al., 2011); and in sediment from the Lake Chapala, Mexico, 9–27 ng g⁻¹ dw (Ontiveros-Cuadras et al., 2018); in Udu River sediments < 0.01–3.51 ng /g (Iniaghe & Kpomah, 2022). Sediment samples collected from San Diego Bay in Southern California have shown PCB

concentrations higher than those observed in this study, with reported values ranging from 23–1387 ng/g (Neira *et al.* 2018).

The relatively higher levels of sediment PCB in the current study has the potential for bioaccumulation in fish and other benthic species at much higher concentration that may pose health and ecological hazards. Jafarabadi and others observed that fish samples from the Larak coral Island, Persian Gulf, Iran had PCBs levels between 7.20 and 90.19 ng g⁻¹dw, about ten times more than levels observed for sediments (Jafarabadi *et al.*, 2019).

Regression and Correlation of Total PCBs in Water and Sediments

The expressed variation of total PCBs (\sum PCB) in water attributed to the sediment PCB was determined by evaluating the coefficient of determination, which is given by the square of the correlation coefficient multiplied by 100. The regression of \sum PCB in the river water on \sum PCB in the sediments revealed that $R^2 = 0.1482$. Thus, only about 14.82 % of the total PCBs in the water column was attributed to the river soil sediments, a secondary source. Other source in to the water may have been via interactions of multiple environmental matrices such as sediments, soils or surface water (Jing *et al.*, 2018; Mao *et al.*, 2021). The high PCB pollution of the sediments can potentially alter the PCB levels in the water.

Spatial Distribution of PCB Congeners

The distribution of PCB congeners in the water and sediment samples from the Pra river basin is presented (Appendix J-M). The congener profiles at the various sampling points are shown for the water (Figures 46 & 47) and that of the sediments (Figures 48 & 49). PCBs were detected at all sampling points; however, some congeners were not detected either in the dry or raining seasons.

At all the sampling sites, between 2- 6 of the 12 PCB congeners studied were not detected in both samples

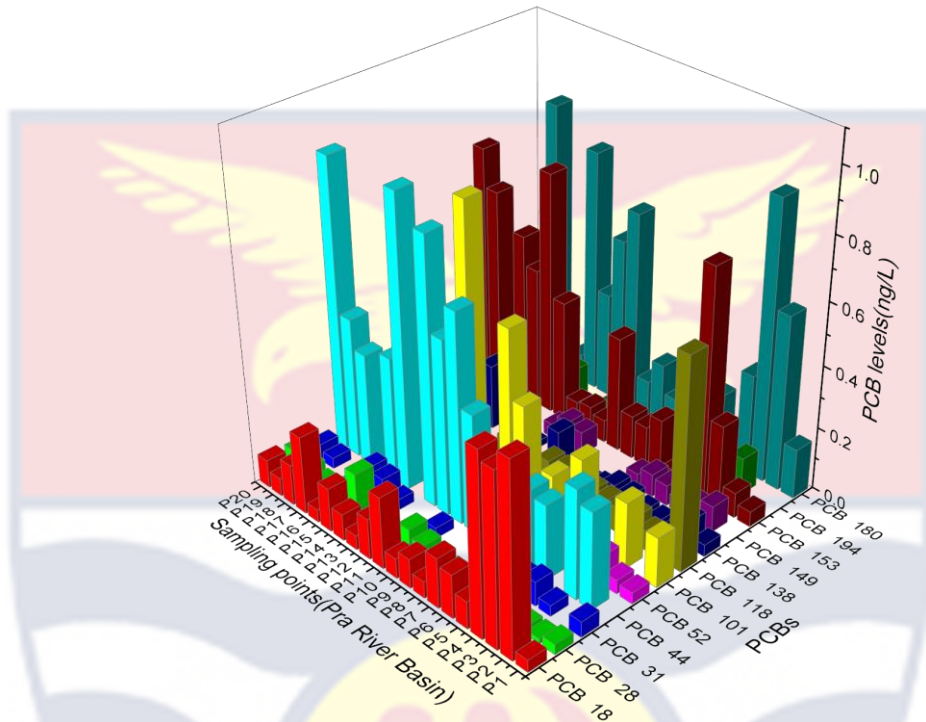


Figure 46: Spatial distribution of PCBs in water samples in the wet season

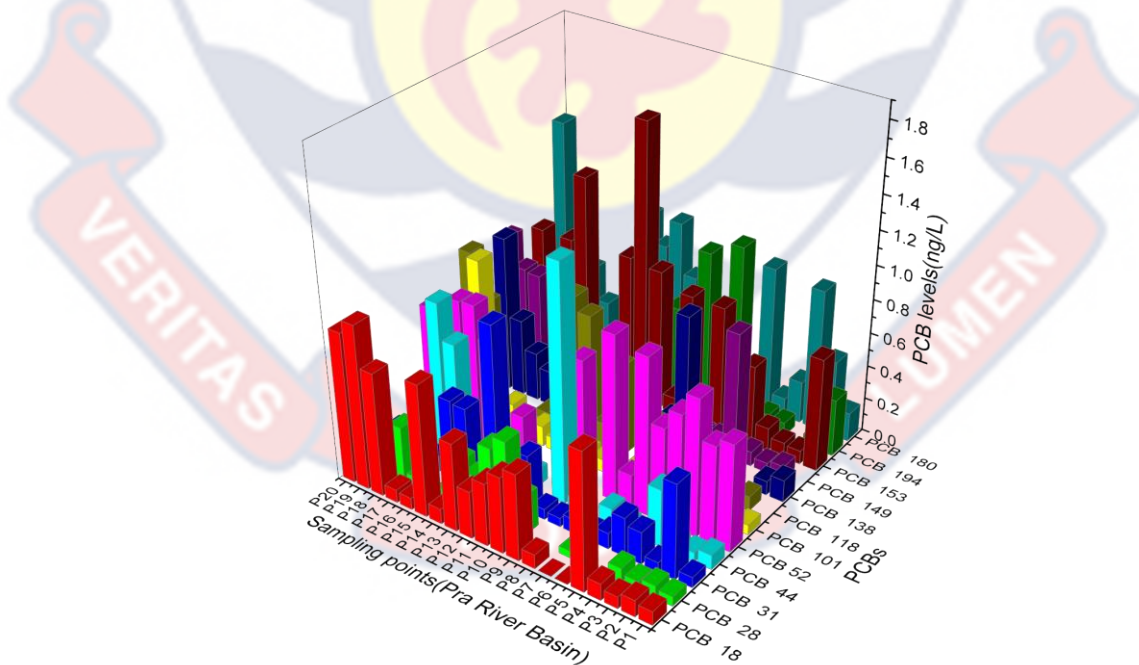


Figure 47: Spatial distribution of PCBs in water samples in the dry season

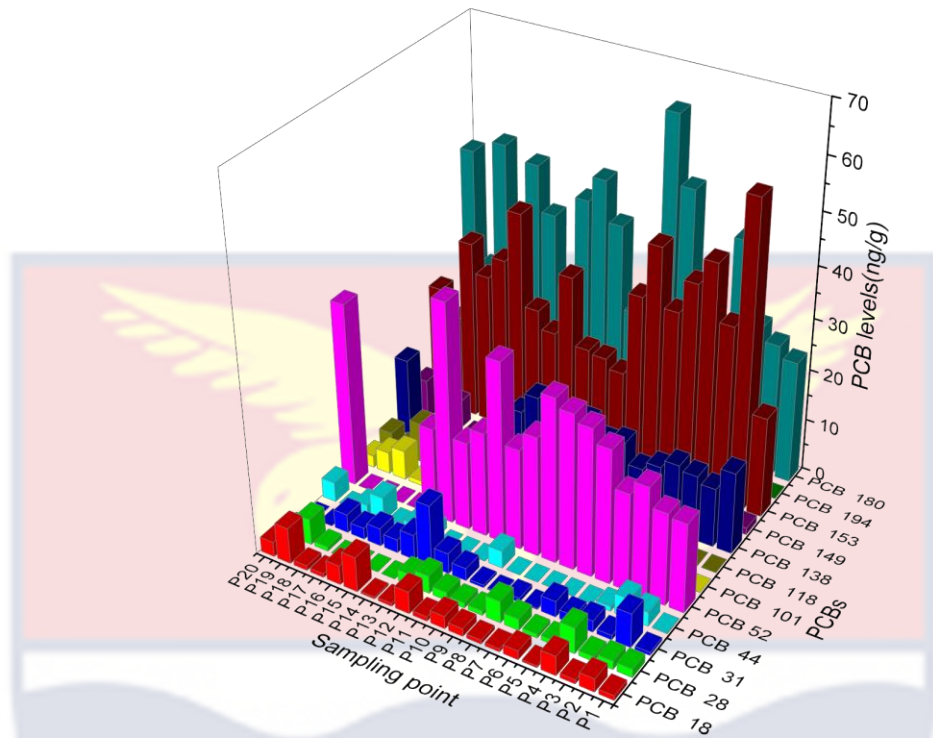


Figure 48: Spatial distribution of PCBs in sediments samples in the wet season

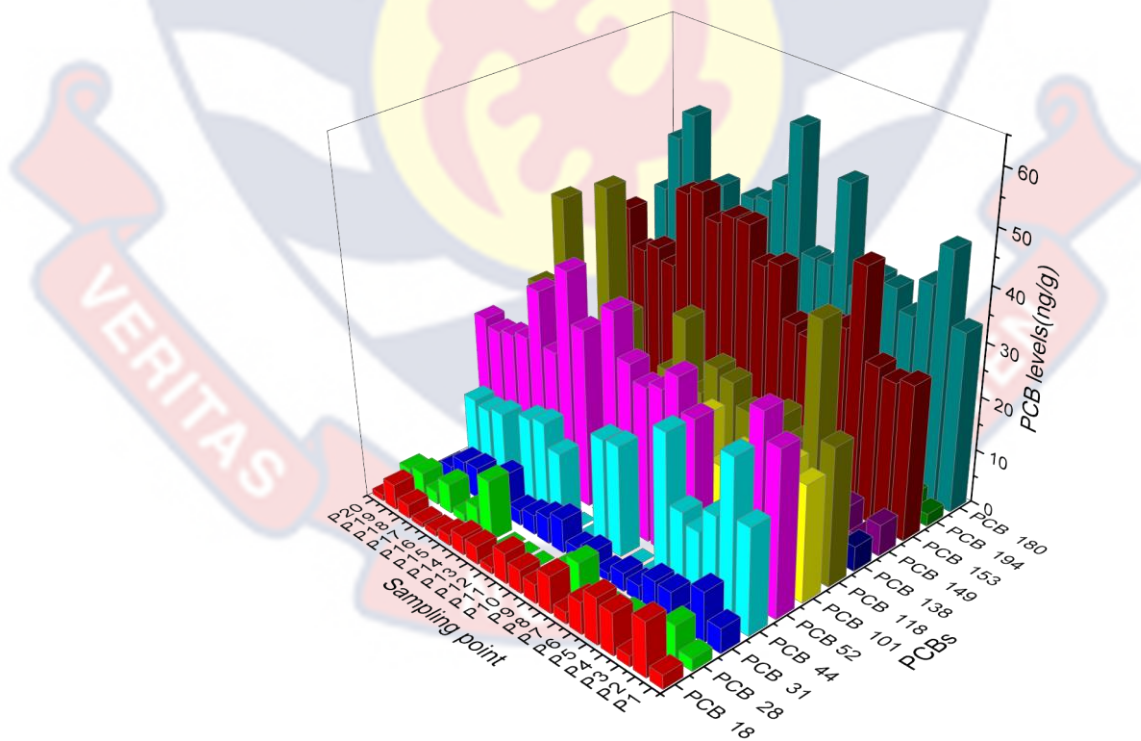


Figure 49: Spatial distribution of PCBs in sediments samples in the dry season

The detection frequency of various congeners detected in the samples



Figure 50: Proportions of PCB congeners detect in the Pra river Basin water and soil sediment

(Figure 50), ranged from 50-100%. The predominant congeners were PCB 18, 153 and 180. In all seasons these congeners recorded 100% detection for water and soil sediment samples, with no congener concentrations below the detection limit. PCB 31 recorded 100% detection for both samples in the drying season only. PCB 194 recorded the least percentage detections.

PCB Homologue Profile

The distribution of PCB homologs in both water and sediments indicated a prevalence of lightly to moderately chlorinated PCB homologs (3–8 Cl) (Figure 51). The most dominant homologs detected in water samples were the

hexachlorobiphenyl homologs (PCBs 138, 149 and 153) and constituted 25.51% and 30.37% respectively of the total PCBs in water and sediments. PCB153 was the most dominant congener in both water and sediment (the 6-CBs homologs) constituting 16.66 % and 24.07% respectively. Meanwhile, the hepta-chlorobiphenyl homologs (PCB 180) made up 16.27% and 26.90% of the total PCBs in water and sediments respectively. The least dominant homologs, octa homologs (PCBs 18) made up 4.17% and 1.17 % of the total PCBs in both water and sediments respectively.

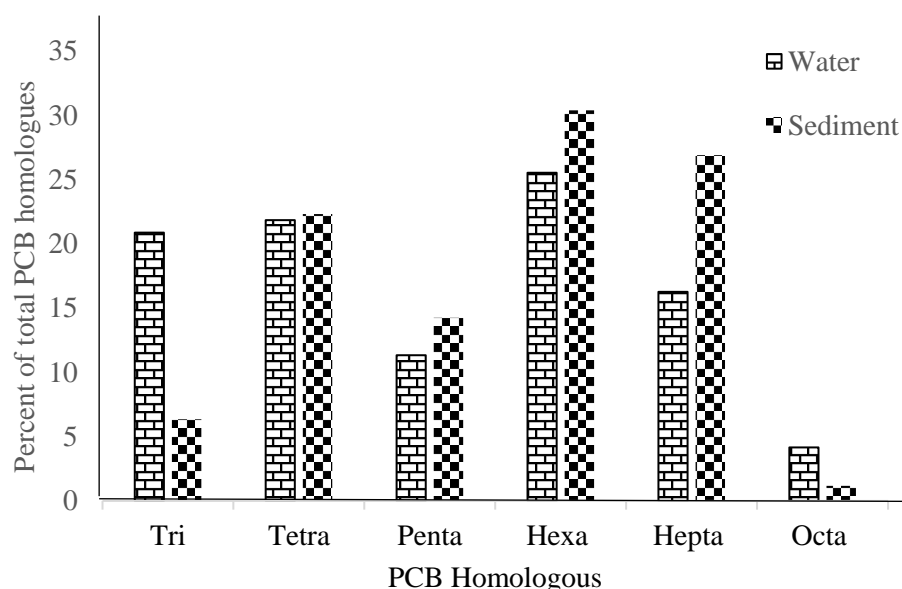


Figure 51: PCB Homologues in water and sediment samples from the Pra River Basin

Studies have shown that PCB profiles are typically dominated by lightly to moderately chlorinated homologs (2–6 Cl) (Habibullah-Al-Mamuna, 2019). To add more, in both summer and winter seasons, PCBs containing 4- and 5-chlorinated biphenyls have been reported to be dominant homologs (Gizem & Tasdemir, 2022). While previous reports have suggested a slight increase in

PCB concentration with higher chlorine numbers (Gizem & Tasdemir, 2022), this study found that the concentration of PCBs was not dependent on the number of chlorine atoms present.

PCB Congener Profile

The mean PCB congener concentration in the surface water were generally lower in the wet season than the drying season. Apart from PCB 44 and PCB 101 that recorded relatively higher concentrations in the wet seasons, all other congeners recorded lower concentrations in the wet seasons, August – September (Table 35). The mean congener concentrations in the wet season ranged from 0.03 ± 0.03 ng/L (PCB 31) - 0.35 ± 0.30 ng/L for PCBs 153. The concentrations in the dry season ranged from 0.10 ± 0.21 ng/L (PCB 101) - 0.52 ± 0.46 ng/L (PCB 153), and followed the order by PCB congeners 44, 153, 105, 180, 70, 101, 28, and 52. However, along the River Nile, Egypt, PCB 138 has been reported as the highest congener ($10.119 \mu\text{g/L}^{-1}$) and congener 118 was the lowest ($1.009 \mu\text{g/L}^{-1}$) (Megahed *et al.*, 2015). Also, the levels of PCB 28 (0.018-0.042 $\mu\text{g/L}$), PCB52 (0.006-0.015 $\mu\text{g/L}$) and PCB 101 (0.001-0.039 $\mu\text{g/L}$) reported in Mexico City (Salinas *et al.*, 2010) were found to be lower than those recorded in the Pra River basin in this study. The recorded concentrations of PCBs in the surface water were found to be below the USEPA's recommended value of 500 ng/L (USEPA, 2002).

The PCB congener profile of sediments in the wet season was between 1.31 ± 1.61 ng/g (PCB 44) and 35.14 ± 12.85 ng/g for PCB 180 (Table 36). The dry season profile ranged from 1.78 ± 2.28 ng/g (PCB 194) to 40.08 ± 6.94 ng/g for PCB 180. Generally, PCB concentrations of the congeners in sediment were higher than the corresponding congener concentration in the water (Megahed *et*

al., 2015). In Greater Cairo and the Nile Delta, PCB 138 was found to be the predominant contaminant with concentration values of 2.482 and 5.322 $\mu\text{g/L}^{-1}$, respectively. Due to their properties, PCB congeners are usually found in much higher concentrations in sediment and biota than in water. Thus, the sediment turns out to be a significant source as well, because of desorption, diffusion, and possible re-suspension of PCBs in the water column.

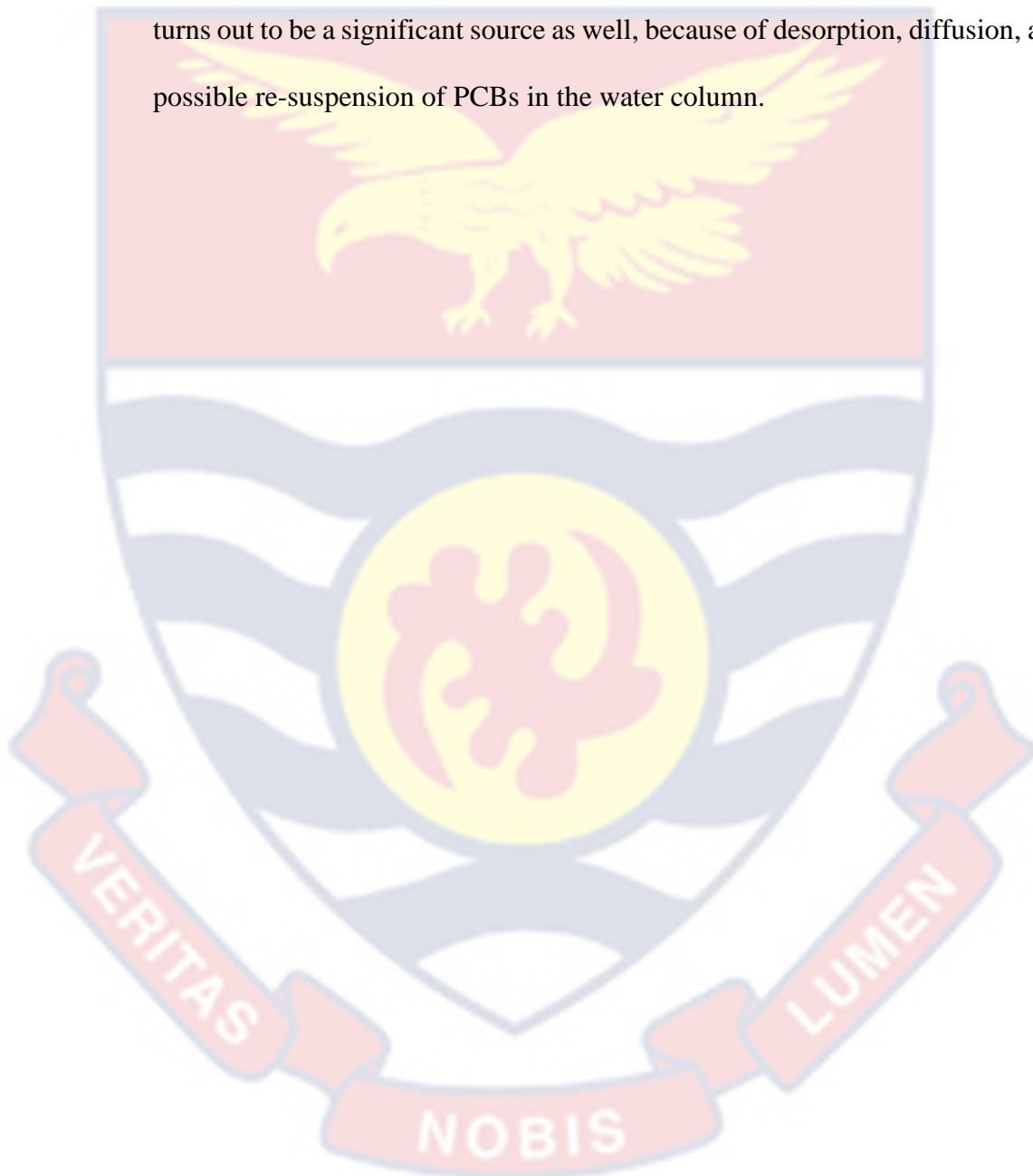


Table 36: Distribution Statistics of PCB Congener Profile of Water Samples from the Pra River Basin

		Concentration of PCB Congeners (ng/L) in Water Samples													Σ PCB
		PCB 18	PCB 28	PCB 31	PCB 44	PCB 52	PCB 101	PCB 118	PCB 138	PCB 149	PCB 153	PCB 194	PCB 180		
August- December	Mean	0.29	0.11	0.15	0.291	0.28	0.13	0.16	0.11	0.12	0.43	0.11	0.42	2.60	
	Std	0.29	0.15	0.23	0.35	0.34	0.22	0.25	0.21	0.25	0.39	0.23	0.33	1.33	
	CV	102.04	130.0	161.16	118.7	121.7	167.24	155.52	96.03	198.68	89.72	214.42	77.25	51.09	
	Median	0.13	0.06	0.06	0.11	0.08	0.06	0.08	0.03	0.05	0.32	0.03	0.33	2.30	
	Min	0.03	nd	nd	nd	nd	nd	nd	nd	nd	0.04	nd	0.01	0.77	
	Max	0.97	0.52	1.02	1.39	0.98	0.98	0.89	0.93	0.86	1.67	1.04	1.32	6.02	
	PCB%	10.94	4.34	5.58	11.19	10.65	5.06	6.26	4.07	4.77	16.66	4.17	16.27	100.00	
August- September	Mean	0.22	0.04	0.03	0.34	0.05	0.160	0.08	0.04	0.04	0.35	0.05	0.33	1.73	
	Std	0.23	0.03	0.03	0.32	0.04	0.23	0.14	0.05	0.03	0.30	0.08	0.29	0.71	
	CV	107.94	81.24	95.6	95.95	83.49	144.18	180.62	115.74	81.53	84.81	156.19	85.76	41.27	
	Median	0.130	0.028	0.035	0.330	0.043	0.063	0.06	0.03	0.045	0.225	0.03	0.20	1.66	
	Min	0.01	nd	nd	nd	nd	nd	nd	nd	nd	0.01	nd	0.01	0.03	
	Max	0.85	0.14	0.09	0.93	0.17	0.86	0.67	0.21	0.08	0.97	0.34	0.89	6.20	
	PCB%	12.57	2.39	1.938	19.354	2.891	9.243	4.60	2.51	2.233	20.123	2.892	19.26	100.00	
November- December	Mean	0.35	0.19	0.26	0.25	0.51	0.10	0.25	0.17	0.21	0.52	0.17	0.51	3.47	
	Std	0.33	0.18	0.29	0.37	0.35	0.21	0.31	0.28	0.33	0.46	0.31	0.35	1.23	
	CV	93.61	97.39	113.55	150.15	69.59	204.38	126.12	165.44	157.07	87.84	187.29	67.66	35.40	
	Median	0.19	0.08	0.10	0.09	0.64	0.07	0.09	0.05	0.03	0.48	0.03	0.47	3.09	
	Min	0.03	nd	0.05	nd	nd	nd	nd	nd	nd	0.07	nd	0.08	2.03	
	Max	0.97	0.97	1.02	1.39	0.98	0.98	0.89	0.93	0.86	1.67	1.04	1.32	6.02	
	PCB%	10.13	5.32	7.40	7.13	14.52	2.98	7.09	4.86	6.04	14.95	4.80	14.79	100.00	

(Source: Fieldwork, 2022)

Table 37: Distribution Statistics of PCB Congener Profile of Sediments from the Pra River Basin

		Concentration of PCB Congeners (ng/g) in Sediment Samples												
		PCB 18	PCB 28	PCB 31	PCB 44	PCB 52	PCB 101	PCB 118	PCB 138	PCB 149	PCB 153	PCB 194	PCB 180	ΣPCB
August- December	Mean	3.13	2.30	3.44	6.96	22.35	6.98	12.93	6.21	2.60	33.65	1.64	37.61	139.79
	Std	2.58	2.40	2.64	8.90	13.04	8.51	15.36	6.45	2.74	9.02	2.21	10.49	39.97
	CV	82.30	104.21	76.94	127.83	58.33	121.90	118.86	103.89	105.27	26.80	135.04	27.90	28.59
	Median	2.52	1.65	2.98	2.03	25.45	2.12	3.56	4.25	1.67	33.36	0.30	37.12	143.53
	Min	0.39	n.d	n.d	n.d	n.d	n.d	n.d	n.d	n.d	18.76	n.d	19.35	60.99
	Max	10.38	11.28	12.02	30.45	42.45	24.45	50.78	17.08	9.87	58.89	7.86	63.13	242.16
	PCB%	2.24	1.65	2.46	4.98	17.32	4.99	9.25	4.44	1.86	24.07	1.17	26.90	100.00
August- September	Mean	2.19	1.71	2.61	1.31	20.07	1.89	1.80	10.09	2.23	32.04	1.49	35.14	112.57
	Std	2.01	1.58	2.83	1.61	12.48	1.85	2.22	6.22	2.33	10.91	2.19	12.85	27.09
	CV	91.78	92.40	108.60	123.13	62.16	98.13	123.35	61.63	104.32	34.04	146.74	36.56	24.07
	Median	1.22	1.315	2.21	0.385	19.79	1.46	0.98	12.295	1.315	33.85	0.0039	33.17	113.275
	Min	0.39	n.d	n.d	n.d	n.d	n.d	n.d	n.d	n.d	18.76	n.d	19.35	60.99
	Max	6.97	5.04	12.02	4.67	42.45	5.78	7.82	17.08	7.98	58.89	6.87	63.13	158.11
	PCB%	1.95	1.52	2.32	1.16	17.83	1.68	1.60	8.96	1.98	28.47	1.32	31.22	100.00
November- December	Mean	4.08	2.89	4.26	12.61	24.63	12.07	24.05	2.34	2.97	35.25	1.78	40.08	167.02
	Std	2.78	2.93	2.21	9.63	13.50	9.51	14.79	3.90	3.11	6.52	2.28	6.94	31.39
	CV	68.21	101.20	51.80	76.34	54.82	78.83	61.49	167.01	104.80	18.49	127.88	17.31	18.79
	Median	3.455	2.32	3.735	13.73	28.205	15.135	24.78	0	2.87	32.825	0.785	37.725	161.925
	Min	0.89	n.d	0.22	n.d	n.d	n.d	n.d	n.d	n.d	27.75	n.d	32.1	98.78
	Max	10.38	11.28	9.46	30.45	41.89	24.45	50.78	15.89	9.87	45.56	7.86	56.56	242.16
	PCB%	2.44	1.73	2.55	7.55	14.75	7.23	14.40	1.40	1.78	21.11	1.07	23.99	100.00

(Source: Fieldwork, 2022)

The most prevalent congeners found were PCBs 18, 153 and 180 with overall average concentrations of 0.29 ng/L, 0.43 ng/L and 0.42 ng/L in the water, and 3.13 ng/g 33.65 ng/g and 37.61 ng/g in the sediments (Tables 20 & 21). Together, these congeners accounted for 10.94%, 16.66% and 16.27 % of the total PCB levels in the water; and 2.24%, 24.07% and 26.90 % of the total PCB levels in the sediments, respectively. Also, the relative amounts of PCBs 153 and 180 were higher in the sediment than the water. Thus, the order of contribution to the total burden in the water and sediment were respectively PCB18 < PCB180 < PCB 153 and PCB 18 < PCB153 < PCB 180. In the sediment, PCB 194 accounted for 1.17% of the total PCB burden, while PCB 18 and PCB 44 accounted for 2.24% and 4.98%, respectively. Among the water samples, the lowest percentages were recorded for PCB 138 at 4.07%, followed by PCB 194 at 4.17%. Iniaghe and Kpomah (2022) discovered that PCB 18 and PCB 44 were among predominant congeners found in the Udu River water, Nigeria, accounting for 8.90% and 15.6% respectively, of the total PCB burden in the sediments. PCBs 28 (0.018-0.042 µg/L) have been found amongst dominant congeners in Mexico City (Salinas *et al*, 2010).

Congener Profiled Similarity

To assess the nature of the similarity between the congener profiled in the two seasons, the PCB concentrations in the samples collected in the dry season was correlated with concentration in the wet seasons and the R^2 determined (Figure 52). The similarity between any two congener profiles is defined through the use of the coefficient of determination R^2 found by plotting the congener concentration results of one sample versus the other sample, and

calculating the square of the correlation coefficient (r) (Kay *et al.*, 2005; Tetko & Villa, 1997).

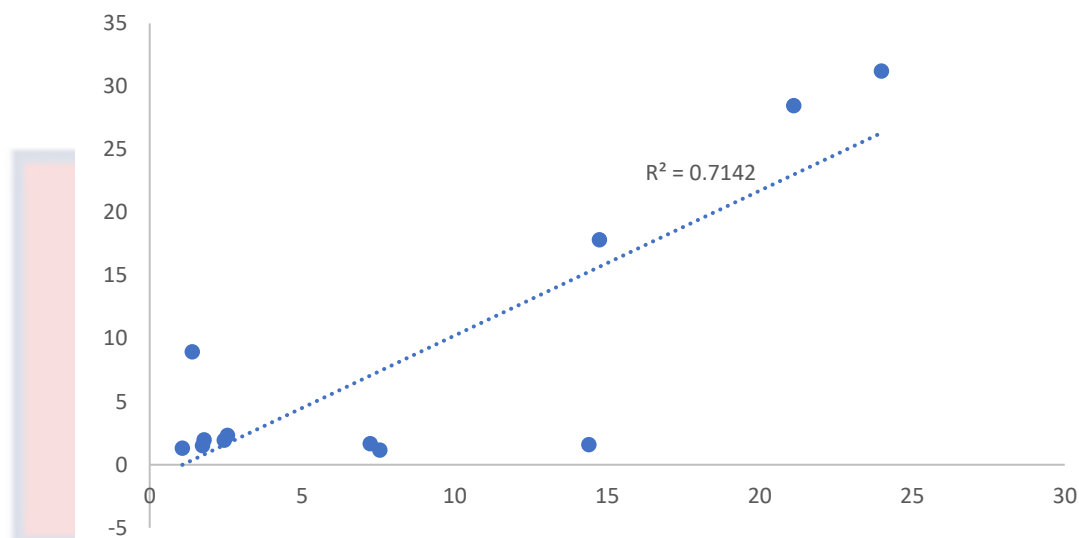


Figure 52: A graph showing correlation between concentration of PCBs in the dry and wet seasons

An R^2 value of 1.0 indicates a perfect match between the profiles, while an R^2 value of 0.0 indicates no relationship between profiles. The following criteria has been applied to qualified the degree of similarity between two sample congener profiles:

A fingerprinting match for R^2 is 0.9 or higher ($r \leq 0.949$)

Very similar fingerprints, R^2 is 0.8 to 0.89 ($0.894 \leq r \leq 0.943$)

Similar fingerprints R^2 is 0.7 to 0.79 ($0.837 \leq r \leq 0.888$)

Ambiguous relationship R^2 is 0.6 to 0.69 ($0.775 \leq r \leq 0.831$)

Distinctly different fingerprints R^2 less than 0.6 ($r < 0.775$)

The R^2 obtained for the water samples was 0.2. Thus, a weak relation, and only 20 % of the variation in the PCB data is explained by the relationship between the two seasonal PCB profiles. The water samples had distinctly different PCB congener fingerprints. The sediment data $R^2=0.714$ (Figure 45), suggests that the congener profile of PCBs was similar between the two seasons,

with similar fingerprints. Furthermore, there is a strong correlation between the sediment PCB congener profile of the wet and dry seasons, which accounts for 71.4% of the variation in the sediment PCB data.

Sampling Points PCB Congener Profile Comparison

Since R^2 value does not change for comparison of the PCB congener fingerprints between two sampling points, the congener concentrations were not normalized. The correlation coefficients are shown (Appendix N and P). Very few sediment sampling sites showed similarity: P6 and P3, $R^2 = 0.778$; P8 and P6, $R^2 = 0.755$; P2 and P3, $R^2 = 0.727$; P15 and P13, $R^2 = 0.634$.

Seasonal PCB Congener Profile Comparison

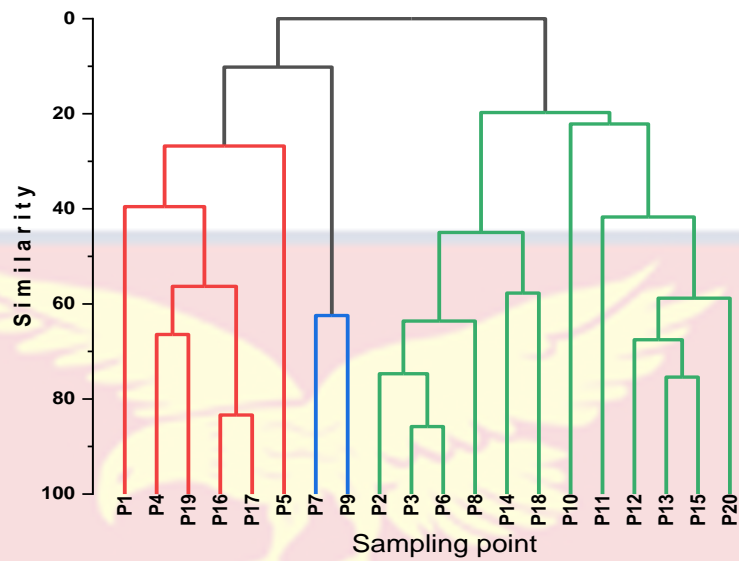
The correlation matrix for relationships between seasonal PCB profiles in water and sediments are presented (Appendices Q to R). Various degree of similarity for the water and sediment samples were observed in general profile comparison showing greater number of similarities amongst sediment samples than amongst the water samples. Also, the congener fingerprints or profiles similarity were fewer in the dry season than in the wet season. Only two sampling points; P3 and P6, congeners profiles of water showed fingerprints match in the dry season, with $R^2 = 0.945$ ($r = 0.972$). P1 and P16, P3 and P8, P3 and P14, P8 and P6 all showed ambiguous fingerprints, with the value of r ranging from 0.787 - 0.814 (Appendix S). The distinctly different fingerprints recorded $R^2 < 0.6$ ($r < 0.775$) represented 97.37%.

In the wet season, most water sample comparisons showed distinctly different fingerprints (Appendix T). Seven pairs of samples profiles comparison (representing 3.87 % of the total number of 181 sample comparison) with r from 0.90- 0.94 showed very similar fingerprints. Five (2.76 %) showed similar

fingerprints ($0.85 \leq r \leq 0.885$) 3.87% recorded ambiguous fingerprints. Significant numbers of comparable fingerprints were observed for the comparison of PCBs congener profile of the sediment. In the wet season 27 (14.92 %) of the 181-comparison showed fingerprinting match: 47 (25.97%) had very similar fingerprints; 31 (17.13%) had similar fingerprints, 15.46% had ambiguous fingerprints and 26.52 % distinctly different fingerprints (Appendix U). In the dry season higher proportion 38.67 % (48) showed distinctly different fingerprints and very few, 7 (3.86%), fingerprints match was observed (Appendix V). However, comparison of 34 correlations showed (18.78%) very similar fingerprints; 22 (12.15%) similar fingerprints, and 26.52 % ambiguous fingerprints.

Hierarchical Cluster Analysis of PCBs

The dendrogram shows the hierarchical clustering of the sampling sites. This shows the order of formation and the level of similarities amongst the sampling sites with respect to their PCB congener profiles. Clusters with the least Euclidean distance (shortest branch) are most similar, with the extent of similarity decreasing with increasing distance between clusters (increasing distance of branch). The clusters are dissimilar if the distance between is about half the whole Euclidian distance. The results of cluster analysis are shown for water (Figure 53) and sediment sampling sites (Figure 54). Clustering of the sampling site for water revealed that sites P3 and P6, had the highest level of similarity in terms of the PCB profile, followed by P16 and P17 > P12, P13 and P15 > P2, P3 and P6 > P4 and P19.



Figures 53: Dendrogram of water sampling sites PCB profiles

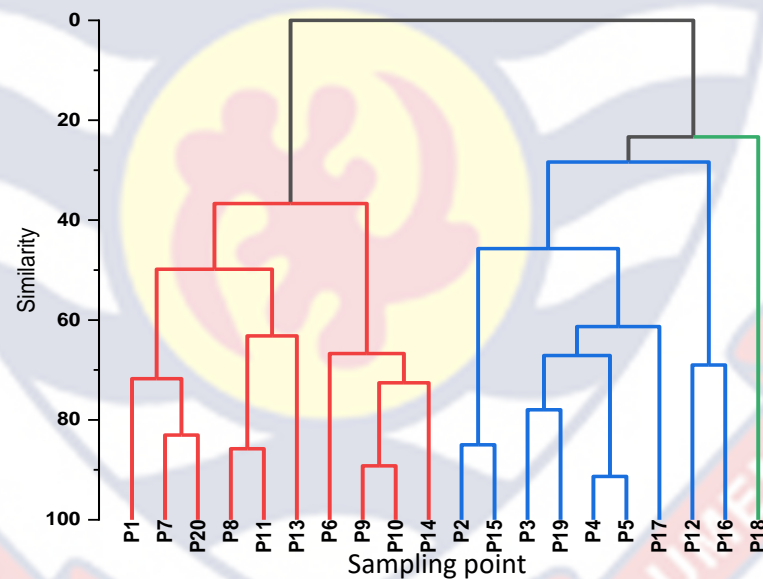


Figure 54: Dendrogram of sediment sampling sites PCB profiles

The sampling sites that were similar are arranged in order decreasing similarity between sites. Points P4 and P5 were the most similar relative to the congener profile followed by P9 and P10 > P8 and P11 > P2 and P15 > P7 and P20 (Figure 54).

Redundancy Analysis of PCBs

In order to examine the relationships (similarities and effects) among the PCB congeners, and sampling points; the PCB profiles (mean of PCB data) obtained over the period of study (August to December) was subjected to Redundancy analysis (RDA), a non-symmetric constrained multivariate Principal Component Analysis. The results are shown (Figures 55 and 59) respectively.

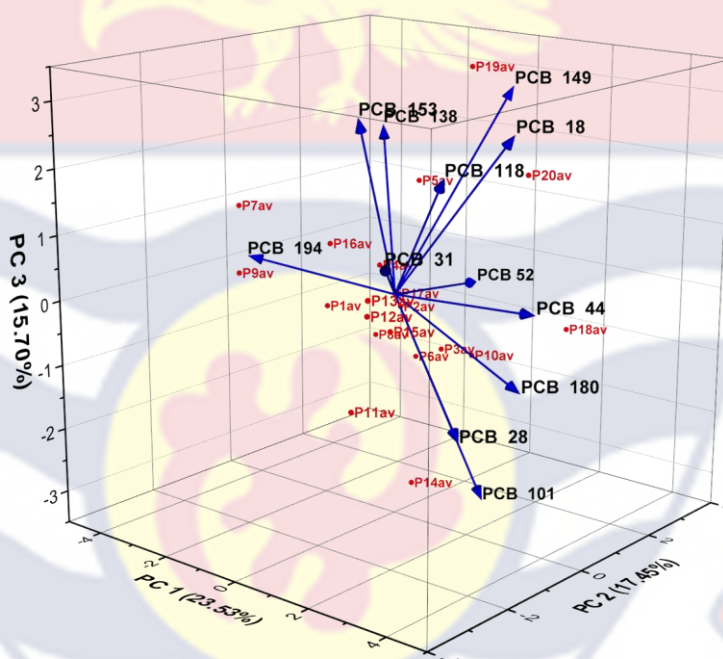


Figure 55: A 3D Principal Components of PCBs observed in water samples collected from PRB

The RDA output, a biplot, shows both scores of samples (sampling points P) and loadings of congeners (vectors). It includes scores plot (eigenvalues) on the horizontal and vertical axis, and also describes the major variance orthogonally to the principal components (Patel *et al.*, 2018). Each PC has one dimension, and the mid-point has value 0. The sign (positive or negative) indicates the direction that a given variable in that PC is going on a

single dimension vector. Variables (Congener) with small score value has small role in explaining the variation due to the PC, whereas those with larger values have substantial roles in explaining the variation due to that PC. Congeners with score value 0, does not account for any of the variation on the PC

If the score values of samples taken from a specific area are similar to those of samples from another area, then these two areas have similar PCB congener and homologue profiles (Saba & Boehm, 2011). The distances among sampling sites (red points) reflect their similarities. Sites (numbers) that are closer together have more similar congener profile or are in some way, but far apart across a PC are negatively related. Congeners (PCBs) that are closer together occupy more sites in common.

Loading plots (angles between congener vectors) also depicts how congeners correlate with one another. The approximated correlation between two variables (congeners) is equal to the cosine of the angle between the corresponding vectors. A small angle less than 90° (those pointing in the same direction) have positive correlation between variables; a large angle approaching 180° (with vectors or arrows pointing in opposite directions) suggests negative correlation, and Perpendicular vectors (angle 90°) indicate the lack of correlation between the congeners they represent. The more parallel to a principal component axis is a vector, the more it contributes only to that PC the longer the vector, the more variability of this variable is represented by the two displayed principal components. The correlations suggest that these congeners have common sources or mutual dependence and/or similar behavior during transport, or are subject to certain factors of control (Cheng et al, 2015)

The Principal Components of PCBs observed in 3D and 2D for water samples are shown (Figures 55 and 56) respectively. The results show that 56.68 % of the total variation in congener data is explained by first three components. Principal Component 1 (PC1), plotted on the horizontal axis, explain most (23.53%) of the variability. The second component (PC2) captured 17.45% and the third (PC3), 15.70%.

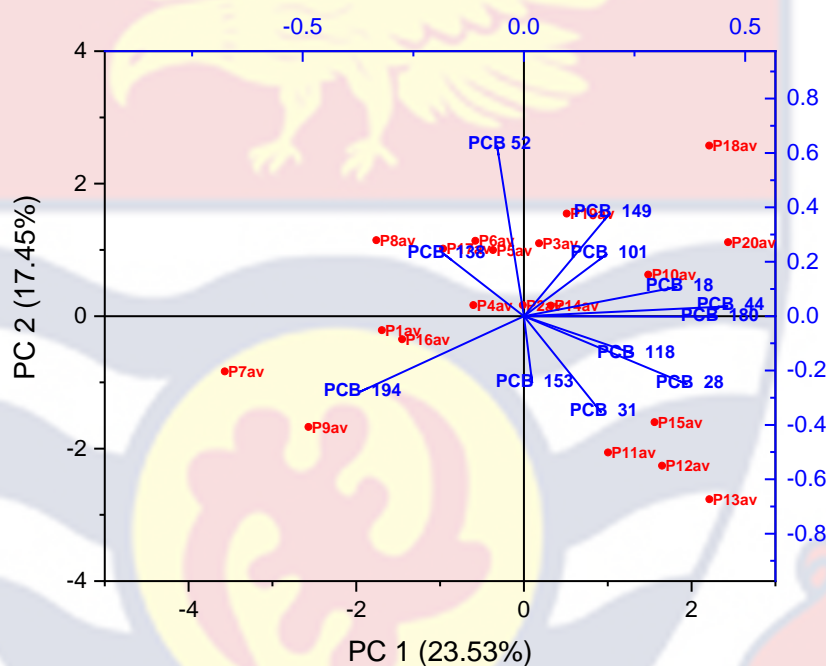


Figure 56: Principal Components of PCBs observed in water samples collected from PRB (2D)

Principal Component 1 is loaded with PCBs 18, 28, 44, 101, 138, 180 and 194 as these are closer (more parallel) to PC1 axis. However, PCB 44 with the largest score (longest vector) contributes greatest to the variability followed by PCB 194, 180 and 28. PCBs vectors of 138 and 194 pointing in opposite directions to the others have a *negative* relationship. Vectors pointing in the same direction (PCB 18, 44 and 180; PCB 28 and 31) correlate positively. The correlations suggest that these congeners have common sources or mutual

dependence and/or similar behavior during transport, or are subject to certain factors of control (Cheng *et al*, 2015).

The second component (PC2) is loaded with PCBs 31, 52, 101, 149 and 153 as these are closer (more parallel) to PC2 axis. However, PCB 52 with the largest score (longest vector) contributes greatest to the variability followed by PCB 31 PCBs vectors of 52 and 149 have a correlate negatively with vectors of PCBs 31 and 153. PCBs 52, and 149 as well as PCBs 28 and 31 correlated positively. Principal Component 3 is loaded explains 15.70% of the variations, and loaded with PCBs 44, 180 and 194.

The sampling sites (points P) that show similarity (with similar or close scores) included P3 and P6; P2, P16 and P17; P12, P13 and P15; P2, P3 and P6 > P4 and P19. These are the same as those observed with the cluster analysis (Figure 46). The PCA for the sediments reveals that 52.62% of the total variation in congener data is explained by first three components (Figure 59). Component 1 (PC1), with loadings PCBs, explain most (22.73%) of the variability. The second component (PC2) captured 16.70 of the variability.

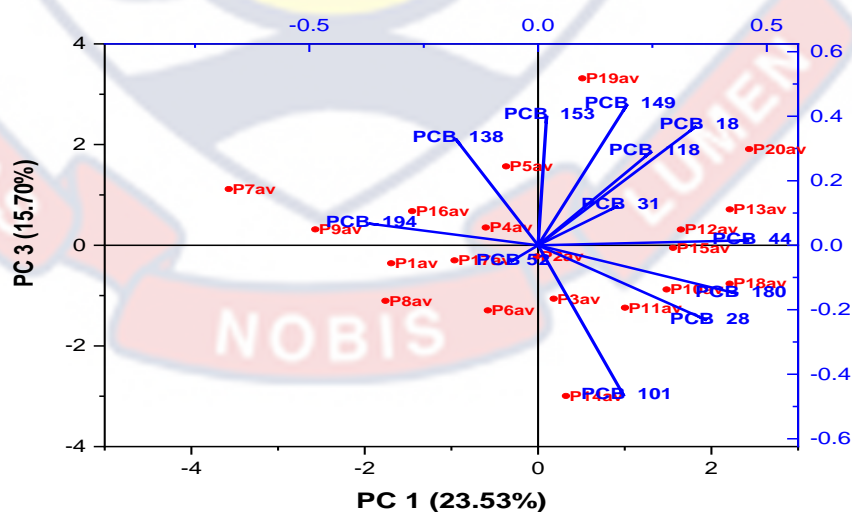


Figure 57: Principal Components of PCBs observed in water samples collected from PRB (2D)

The third component (PC3) explained 13.19% of the variation. PC3 is loaded with PCBs 18, 31, 44, 52, 118, 138, 153 and 194. PCBs 138 and 153 had the strongest effect on the component. PCBs 138 correlated negatively to all the other congeners in the component. Loadings that had positive relations were PCBs 44 and 118; PCBs 18 and 153.

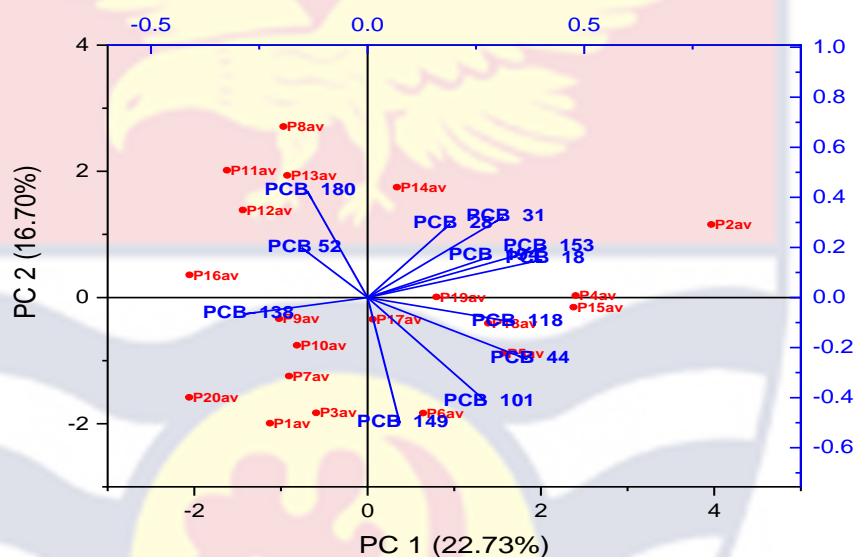


Figure 58: Principal Component Analysis of PCBs in sediments collected from PRB

The loadings in PC2 are PCBs 28, 31, 52, 101, 149 and 180 (Figure 58). However, PCB 149 and 180 with the largest score (longest vector) contributes greatest to the variability in the component. Vectors pointing in the same direction (PCB 52 and 180), and also (101 and 149) correlate positively. However, PCBs vectors of 52 and 180 are pointing in opposite directions to PCB 101, 149 and these have negative correlations. PCB 31 and PCB 44 correlated positively. The two had the strongest effect on the component, and correlated negatively to the other congeners 52, 138, 100 and 194 (Figure 60). The sampling sites (points P) that show similarity were P8, P11 and P13; P1, P7

and P20; P9, P14 and P10; P2 and 15; P4 and P5; P3 and P19; 12 and P16. This is confirmed by the dendrogram (Figure 54).

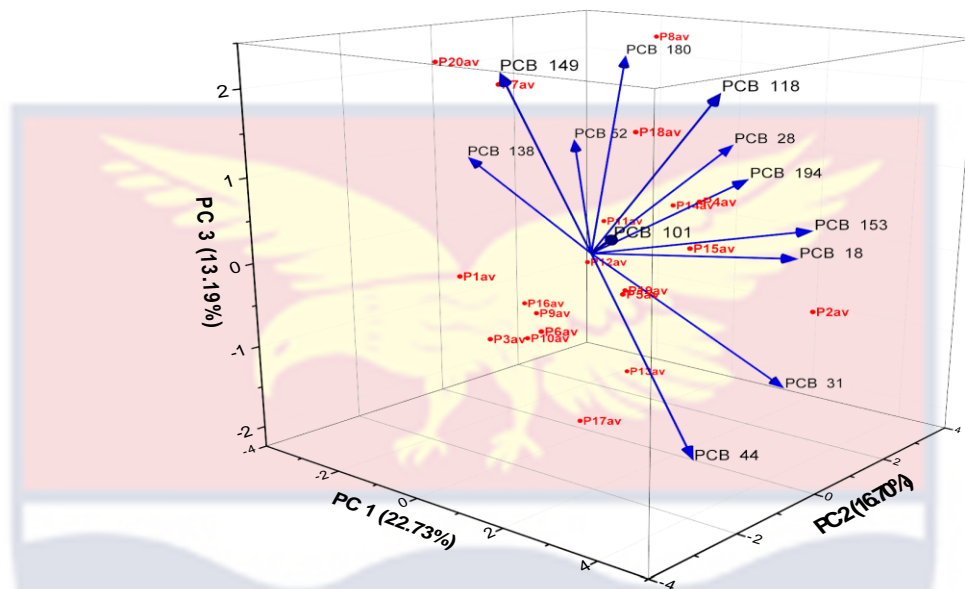


Figure 59: 3-D Principal Component Analysis of PCB in sediments collected from PRB

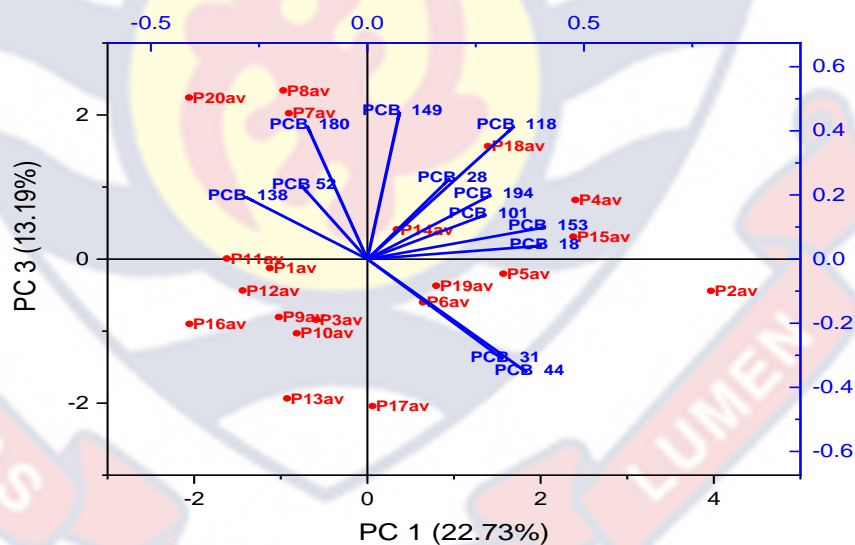


Figure 60: Principal Component Analysis of PCBs in sediments collected from PRB

Human Health Risk Assessment of PCBs

The PCB cancer risk from use of water from Pra River Basin is mainly due to PCB118, the only DL PCB detected in this study. The mean and ranges

of cancer risk values for human exposure to PCBs via ingestion (CR_{ing}) and dermal contact (CR_{der}) are respectively $4.8E-09$ (0 to $2.7E-08$) and $4.5E-10$ (0 to $2.0E-09$). The total cancer risk value is $5.3E-09$ (Table 37). Thus, a maximum of three chance in a hundred million and averagely five out of a billion of the population are at risk of exposure to cancer or related illness as a result of PCB118 exposure. The observed estimated probabilistic PCB cancer risk is much lower than the acceptable risk of one chance in a million ($1.0E-06$) of exposed persons to suffer the risk of cancer. This implies a very low PCB risk from the use of water from the Pra river basin.

Table 38: PCB Cancer Risk Values Associated with the use of Water from Pra River Basin

PCB	CR_{ing}			CR_{der}			CRI_{total}		
	min	max	mean	min	max	mean	min	max	mean
PCB118	0	$2.7E-08$	$4.8E-09$	0	$2.0E-09$	$4.5E-10$	0	$2.9E-08$	$5.3E-09$

(Source: Fieldwork, 2022)

The mean total cancer risk value due to exposure to sediment (Table 38), suggest that a maximum of one chance in a hundred million and averagely 3 out of a billion of the population are at risk of exposure to cancer or related illness, which is too low. However, the observed mean estimated probabilistic PCB cancer risk due to skin contact ($3.0E-06$) risk of three chance in a million is higher than the acceptable risk of one chance in a million ($1.0E-06$).

Table 39: Cancer Risk Associated with Exposure to Sediment PCBs from PRB

PCB	CR _{inges}			CR _{der}			CRI _{total}		
	min	max	mean	min	max	mean	min	Max	mean
PCB118	0	1.6E-10	4.0E-11	0	1.1E-08	3.0E-06	0	1.1E-08	3.0E-09

(Source: Fieldwork, 2022)

Hazard Quotient and Hazard Index of PCBs

A hazard quotient (HQ) is the ratio of the potential exposure from the specific source of interest to the respected reference level at which no adverse effects are expected (Goumenou & Tsatsaki, 2019). The mean HQs due to the individual PCBs in the Pra river water (Appendix W) ranged from 3.9E-04 – 1.9E-03. The hazard index (HI) which is the sum of the HQs (Docea *et al.*, 2019) had a mean of 1.1E-02, and ranged from 3.2E-04 to 5.8E-02. On the other hand, the average HQs resulting from the presence of individual PCBs in sediment (Appendix X) from the Pra river basin ranged from 6.4E-05 - 1.5E-03. The hazard index for sediment had a mean of 5.5E-03 and ranged from 1.5E-03 to 7.8E-02. The HQs and the HI were all lower than 1.

Chapter Summary

This chapter discussed the quality assurance and control of method performance. It has provided details of the concentrations, variations, relations, spatial distribution, source contribution, and the impact of the studied organic micropollutants (PFAS and PCBs) on water and sediment from the Pra River Basin. The chapter also discussed the potential non-cancer and cancer health risk, as well as the ecological effects due to the presence of these pollutants. Finally, the potential solution for reducing PFAS in these environments was proposed.

CHAPTER FIVE

SUMMARY, CONCLUSION AND RECOMMENDATIONS

Overview

This chapter presents a summary of the findings obtained from the analyses of organic micropollutants (PFAS and PCBs) in environmental samples collected from the Pra River Basin as well as the decomposition of PFOA using water radiolysis. The conclusion and recommendations based on the findings have also been stated.

Summary

Detectable levels of PFAS were found in all water and sediment samples, with concentrations measured in nanograms per liter and nanograms per gram, respectively. Out of the 15 PFASs analysed, 8 of the measured PFASs were detected at concentrations above their limit of quantification (LoQ) and the remaining 7 detected in none of the samples. Among the PFAS, PFOA and PFOS were found at very high levels at the twenty sampling points. The detection frequency of PFAS in the Pra River Basin also varied across the sampling locations. In addition, the study revealed the presence of two more PFAS compounds (PFBA and PFNA) in the Pra River Basin compared to previous research in 2016 (Essumang *et al.*, 2016). The only long - chain PFAS observed in both water and sediment was PFDA with very low levels of concentration.

The levels of PFAS in the surface water exhibited variation. The concentrations of PFOA ranged from 14.5 to 108.4 ng/L, with a mean concentration of 70 ng/L. Similarly, PFOS levels ranged from 31.8 to 112.4

ng/L, with a mean concentration of 83.71 ng/L. Lower levels of other PFAS compounds were also detected in the water samples. Concentration of PFBA ranged from non-detectable (n.d.) to 2.56 ng/L with (mean: 0.67 ng/L); n.d. to 0.81 ng/L (mean: 0.46 ng/L) for PFPeA; n.d. to 0.95 ng/L (mean: 0.30 ng/L) for PFHxA; n.d. to 1.56 ng/L (mean: 0.68 ng/L) for PFNA; n.d. to 0.89 ng/L (mean: 0.26 ng/L) for PFDA; and n.d. to 0.98 ng/L (mean: 0.38 ng/L) for PFHxS.

The levels of PFAS in sediment samples exhibited variability. PFOS concentrations ranged from 56.7 to 186.5 ng/g, with a mean concentration of 90.27 ng/g. Similarly, PFOA levels ranged from 55.9 to 129.7 ng/g, with a mean concentration of 94.02 ng/g. In addition, other PFAS compounds were also detected in the sediment samples. The low concentrations of PFBA ranged from non-detectable (n.d.) to 13.78 ng/g (mean: 4.75 ng/g); n.d. to 9.8 ng/g (mean: 4.03 ng/g) for PFPeA; n.d. to 23.6 ng/g (mean: 7.29 ng/g) for PFHxA; n.d. to 12.93 ng/g (mean: 5.77 ng/g) for PFNA; n.d. to 3.91 ng/g (mean: 0.84 ng/g) for PFDA; and n.d. to 0.98 ng/g (mean: 4.75 ng/g) for PFHxS.

Out of the eight PFAS compounds analysed in the water samples from the Pra River Basin, only PFOA (70.60 ng/L) and PFOS (83.71 ng/L) exceeded the recommended limits set by the World Health Organization (WHO) and USEPA, while the levels of the remaining six compounds were below the recommended limits. The study findings also revealed that the levels of PFAS in the sediment samples, particularly for PFOA and PFOS, ranged from 0.17 to 94.02 ng/g, exceeding the interim guidance limits set by the USEPA (2020) for sediment. The exact sources of the elevated levels of PFAS in the Pra River Basin are yet to be determined. However, potential sources of PFAS in the area may include, but are not limited to, agricultural run-off, domestic waste,

improper waste disposal, as well as run-off from industrial and mining sites, as suggested in an earlier study conducted (Essumang *et al.* 2016).

This levels of PFAS in the Pra river basin varied across different sampling locations, and the levels in surface water and sediments also differed. During both the rainy and dry seasons, certain locations in the Pra river basin showed the highest levels of PFAS (P18, P19, and P12 for rainy season; P7, P17, and P6 for dry season), while other locations had the lowest levels (P3, P1, and P2 for rainy season; P18, P8, and P1 for surface water in dry season). It was also observed that there was a statistically significant difference in the levels of PFAS in surface water samples between the rainy and dry seasons, as determined by a paired samples t-test.

The PFAS levels in sediment samples at various locations in the Pra river basin during the rainy and dry seasons were found to vary. Higher levels of PFAS were detected at Beposo (P5), Twifo Hemang (P7), and Sekyere Hemang (P6) during the rainy season, and at Shama(P12), Beposo (P5), and Sekyere Krobo(P20) during the dry season. Conversely, lower levels of PFAS were found at Supomu Dunkwa (P15), Dadieso (P18), and Apetebi (P8) during the rainy season and at Twifo Praso (P2), Sekyre Nsuta (P13), and Kyekyewere (P19) during the dry season. A paired samples t-test revealed that there was no statistically significant difference in the levels of PFAS in the sediment samples between the rainy and dry seasons. The significant difference in PFAS levels in surface water samples between the rainy and dry seasons has important implications for future research.

Hierarchical clustering and principal component analysis (PCA) were used to analyze PFAS data obtained. Three distinct components of PFASs were

identified by both methods. The first component (PC1) explained 27% of the variability in the PCA. PC1 correlated positively with PFPeA and PFHxA and negatively with PFOS. The second component PC2, which explains 23.44% of the variability in PFAS dataset, consists of four PFAS compounds (PFBA, PFOA, PFDA, and PFHxS). PC2 correlates positively with PFBA and PFHxS and negatively with PFOA and PFDA. The third component (PC3) explains 15.10% of the variability in the PFAS dataset and correlates positively with PFNA.

PCA results suggest that the sources of these compounds in the surface water from the river basin may originate from various anthropogenic activities. The results of HCA indicate that the sources and transport pathways of PFAS in the Pra River Basin may differ for the three clusters of sites.

PCA was also conducted to identify patterns of PFAS levels in sediments, based on the mean levels of PFAS in sediment. The analysis showed that the first three principal components (PCs) explained 61.63% of the total variance in the PFAS data. PC1 accounted for 23.60% of variability in the PFAS dataset and was positively correlated with PFOA and PFHxS, while it was negatively correlated with PFHxA, indicating different contribution sources. On the other hand, PC2 was positively correlated with PFPeA, PFDA, and PFOS and accounted for 20.50% of the variance in the PFAS dataset. PC3 was positively correlated with PFNA and PFBA. The results of PCA suggested that PFAS contamination in the river basin could be influenced by various sources, including the use and disposal of PFAS-containing products such as pesticides and fertilizers in the Pra river basin. The study provided valuable insights into

the distribution and co-occurrence patterns of various PFAS in the Pra River Basin (PRB) in Ghana.

The non-carcinogenic analysis revealed that all studied PFAS had total hazard quotients below 1, indicating that their contribution to non-carcinogenic health risk was low. The order of contribution to the risk was PFOS > PFOA > PFPeA > PFHxA > PFNA > PFHxS > PFDA > PFBA. The mean values of Hazard Index (HI) through ingestion and dermal adsorption, as well as the total HI, were determined to be below 1, suggesting a low non-carcinogenic risk to the health of the residents. Specifically, the mean HI values were calculated as 0.51 for ingestion, 0.027 for dermal adsorption, and 0.54 for the total HI.

The evaluation of the carcinogenic risk associated with PFOS indicated the highest probability of cancer risk, with a mean risk estimated at 5.7×10^{-5} , while PFOA had the lowest mean cancer risk estimated at 9.2×10^{-8} . However, the study concluded that the population using raw surface water from the Pra river basin faced little to no cancer risk from PFAS exposure through ingestion and dermal contact routes.

The non-carcinogenic and carcinogenic risk assessment of the river sediment from the Pra river basin was conducted. The study revealed the mean levels of chronic daily intake (CDI total) in mg/kg/day^{-1} for different PFAS compounds, indicating that PFOS and PFOA had the highest mean values among them. Specifically, the order of CDI total mean values for adults was found to be PFOS = PFOA > PFHxA > PFNA > PFBA > PFPeA > PFDA > PFHxS. However, all the studied PFAS had total hazard quotients (HQs) below 1, indicating that their contribution to non-carcinogenic health risks was low. The study determined the mean values of the hazard index (HI) through

ingestion and dermal adsorption, as well as the total HI, to be $3.9\text{E-}04$, $1.6\text{E-}02$, and $1.6\text{E-}02$, respectively. The non-carcinogenic risk assessment based on these values indicated that the human population's health around the Pra river basin was unlikely to be adversely affected, as the HI value was below 1, indicating negligible risk.

The carcinogenic risk of PFAS assessment in sediment was also based on the mean CDI values using PFOA and PFOS. The study found that PFOS had the highest potential cancer risk (mean cancer risk 7.8×10^{-4}), while PFOA had the lowest potential cancer risk (mean cancer risk 1.2×10^{-6}) among the studied PFAS. The study also concluded that there was a potential cancer risk from PFOS to the health of maximally exposed individuals around highly contaminated sites of the Pra river basin through cumulative ingestion and dermal contact routes. However, the potential cancer risk of PFOA was estimated to be insignificant.

The study also assessed the cancer risk of PFAS exposure through ingestion and dermal contact routes. The results showed that the potential cancer risk associated with ingestion of surface water from the Pra river basin was relatively higher than that associated with ingestion of sediment from the same river. However, the potential cancer risk through dermal contact was higher for direct contact with sediments compared to surface water, particularly for maximally exposed individuals, due to the high levels of PFOS present in the sediments of the river basin.

The study utilized the risk quotient (RQ) approach to conduct an ecological risk assessment of PFAS in the Pra river basin. Aquatic organisms, algae (phototrophic level), crustacea (invertebrates) and fish (vertebrates) were

selected for investigation regarding the toxic effects of each of the PFAS compound. The study revealed that PFAS had varying toxicity values ranging from 0.005 µg/L to 1600 µg/L for different species, with PFHxS being the most toxic for algae and PFOA being the most toxic for crustaceans and fish. Crustaceans were found to be the most sensitive species for PFOA, PFOS, and PFNA, while PFOA and PFNA were more toxic to fish than algae and crustaceans. The study emphasized that PFAS toxicity can differ among species, with higher trophic levels, such as fish, having more significant impacts.

The study also obtained 160 toxicity values based on the levels of PFAS detected in surface water from the Pra river basin at 20 sampling locations. Using these toxicity values, individual RQ values were calculated, and the mean RQ values for three trophic levels of aquatic organisms estimated. The RQ values ranged from 2.66×10^{-5} to 17, with Kyekyewere (P19), Abetemasu (P17), P6 (Sekyere Hemang), and Twifo hemang (P7) showing the highest RQ values. PFOA and PFOS were found to be the major contributors to the risks of the PFAS compounds studied. Based on the results obtained, it can be concluded that PFOA poses a low to medium environmental risk in the Pra river basin.

The study also involved mixture risk assessment of PFAS in the Pra river basin by considering all 20 sampling sites. The $RQ_{MEC/NOEC}$ values obtained were higher than 1, indicating potential risks to aquatic organisms. The results clearly demonstrate that relying solely on single chemical toxicity risk assessment is insufficient, and the inclusion of mixture risk assessment is necessary. Kyekyewere was found to have the highest environmental risk among the 20 sampling sites with an $RQ_{MEC/NOEC}$ value of 17.1, followed by Abetemasu, Sekyere Hemang, and Twifo Hemang. Of the eight PFAS

compounds detected in the Pra river basin, PFOS and PFOA showed the highest environmental risks in surface waters and therefore warrant greater attention.

Water radiolysis is considered as a promising approach for reducing the levels of organic contaminants like PFAS(PFOA). This method utilizes radiation to initiate chemical reaction in water, leading to the degradation of organic contaminants such as PFOA. The degradation of PFOA was observed to be more pronounced at pH 11 as compared to pH 6. At pH 11, the degradation efficiency was almost 98% after 8 hours of irradiation with gamma at 20 kGy. The defluorination efficiency of 1 μ M PFOA was also nearly 98% at pH 11 with solvated electrons and carbon dioxide radical anion as the main reactive species under argon-saturated atmosphere with a radiolytic yield of 9.59E-04. The released F⁻ concentration decreased with decreasing pH, with very low levels at pH 6, possibly due to the loss of solvated electrons which is seen as a stronger reducing agent as compared to hydrogen radical.

The study found that various congeners were detected in water and sediment samples, with detection frequencies ranging from 50-100%. The most commonly detected congeners were PCB 18, 153, and 180, which were present in all seasons with 100% detection. PCB 31 was highest only in the drying season, while PCB 194 had the lowest detection frequency among all congeners. No congener concentrations were below the detection limit.

The levels of PCBs in water samples from various sampling points in the dry season (November-December) and wet season (August-September) were determined. The study showed the total PCB concentrations (Σ PCB) for each sampling point in both seasons. During the dry season, the highest concentration of PCBs was observed at site P18, with a recorded value of 5.869

ng/L. In contrast, during the wet season, the highest concentration was observed at site P15, with a recorded value of 2.995 ng/L. The lowest concentrations were recorded at sites P3 (2.029 ng/L) and P9 (0.5285 ng/L) in the dry and wet seasons, respectively. The mean total PCB concentrations in water during the wet season (AS) were 1.73 ± 0.71 ng/L, with a range of 0.529-2.995 ng/L. In the dry season (ND), the mean total PCB concentration was higher at 3.47 ± 1.23 ng/L, with a range of 2.029-5.869 ng/L. The reason for the difference in total PCB concentrations between the two seasons is not known.

Generally, the concentrations of PCBs in sediment were higher than those in water samples. The mean total PCB concentration in water over the period was 2.60 ± 0.97 ng/L, while the mean total PCB concentration in sediment was much higher at 139.79 ± 29.24 ng/g. The distribution of total PCBs in sediment revealed that the concentrations during the dry season were higher compared to the wet season. However, it should be noted that two sites (P8 and P12) exhibited an exception to this trend, where the concentrations in the wet season were higher than those in the dry season. In the dry season, the highest total PCB concentration was recorded at site P2 (242.16 ng/g), while the lowest was recorded at P12 (98.78 ng/g). During the wet season, the highest total PCB concentration was recorded at site P8 (158.11 ng/g), while the lowest was recorded at P19 (60.99 ng/g). The mean PCB concentration for sediment during the wet season was 112.59 ± 27.09 ng/g, with a range of 60.99-158.11 ng/g. In the dry season, the mean PCB concentration was higher at 167.019 ± 31.39 ng/g, with a range of 98.768-242.16 ng/g.

There were spatial variations in the distribution of total PCBs in both water and sediment. The higher concentration of PCBs found in sediment

compared to water is not surprising because organic pollutants, including PCBs, tend to strongly absorb onto soil organic matter and clay, making soil a sink for pollutants. The higher PCB concentrations recorded in the dry season compared to the wet season may be attributed to the evaporation of river water, which can cause an increase in pollutant concentration. Conversely, in the wet season, PCB concentrations may be diluted due to increased rainfall.

The regression analysis showed that only about 14.82% of the total PCBs in the river water was attributed to the river soil sediments, indicating that the sediment was a secondary source of PCBs. Other sources of PCBs in the water could be from interactions between various environmental matrices, such as sediments, soils, or surface water. The high PCB pollution of the sediments could potentially affect the PCB levels in the water.

The distribution of PCB homologs in water and sediments showed a prevalence of lightly to moderately chlorinated homologs (3-8 Cl). The most dominant homologs detected were hexachlorobiphenyls (PCBs 138, 149, and 153). PCB153 was the most dominant congener in both water and sediment (the 6-CBs homologs) followed by heptachlorobiphenyls (PCBs 180) and the least dominant homologs was octachlorobiphenyls (PCBs 18).

The study assessed the similarity between the PCB congeners profiled in the dry and wet seasons. The PCB congener fingerprints in water samples were distinct fingerprints between the two seasons. In contrast, the sediment data showed an R^2 value of 0.714, suggesting a similar congener profile of PCBs between the two seasons. The strong correlation between the sediment PCB congener profiles of the wet and dry seasons accounted for 71.4% of the variation in the sediment PCB data.

Hierarchical clustering of sampling sites based on their PCB congener profiles was performed to determine the level of similarity among the sampling sites. The, sites P3 and P6 showed the highest level of similarity in terms of their PCB profiles in water, followed by P16 and P17, P12, P13 and P15, P2, P3 and P6, and finally, P4 and P19.

The results of PCA for PCBs indicated that the first three principal components explained 56.68% of the total variation in the congener data for water samples, whilst for sediments the first three principal components explained 52.62% of the total variation. Significant correlations were also observed amongst the congeners.

The estimated probabilistic PCB cancer risk from exposure to PCB118 in the Pra River Basin was very low, with a maximum risk of three in a hundred million and an average risk of five out of a billion. These values are much lower than the acceptable risk of one in a million for cancer exposure, indicating a very low PCB risk from using water from the Pra River Basin.

The mean total cancer risk value due to exposure to sediment was very low, suggesting that the risk of exposure to cancer or related illness was negligible. However, the mean estimated probabilistic PCB cancer risk due to skin contact is higher than the acceptable risk of one chance in a million, with a risk of three chances in a million.

The mean HQs for individual PCBs in the Pra river water and sediment were very low, all values were below 1, indicating that there was no significant risk from exposure to these PCBs in the Pra river basin.

Conclusions

The findings presented in this thesis corroborate the previously reported widespread occurrence of PFAS in surface water and sediment, and provide evidence of their presence in rivers across Ghana. The findings of the study indicate that PFAS compounds, including PFOA and PFOS, were present in detectable levels in both water and sediment samples collected from the Pra river basin. The concentration ranges of PFOS in surface river water and sediment were observed to be 31.8-112.4 ng/L and 56.7-186.5 ng/g, respectively. The concentration of PFOA ranged from 14.5–108.4 ng/L for surface river water and 55.9 –129.7 ng/g for sediment respectively. The only long - chain PFAS observed in both water (n.d -0.89 ng/L) and sediment (n.d- 3.91 ng/g) was PFDA with very low levels of concentration. These results highlight the widespread presence of PFAS compounds in the water and sediment of the Pra river basin. The study also found that PFOS and PFOA were present in higher levels than others. Overall, surface water had lower concentrations of PFAS compared to the sediment.

The levels of PFAS in both the surface water and sediment collected from the Pra River Basin exhibited variation across the 20 sampling locations in both the wet and dry seasons. The highest levels of PFAS were observed at P18, P19, and P12 for the rainy season and P7, P17, and P6 for dry season. For the sediment, elevated levels of PFAS were observed at at P5, P7, and P6 during the rainy season, and at P12, P5, and P20 during the dry season. The elevated levels of PFAS observed in these sampling locations may be attributed to increased human activities, such as mining and the disposal of PFAS-containing products. The observation of lower PFAS levels in surface water in the rainy

season could be due to the high flow rate of the river leading to dilution, while elevated levels in the dry season could be attributed to increased runoff from surrounding areas with PFAS-containing products and discharge of industrial and mining effluent into the river. However, the absence of a significant difference in PFAS levels in the sediment samples between the rainy and dry seasons suggests that environmental factors such as rainfall and flow rate of river did not have an immediate impact on the distribution of PFAS in the river basin during the sampling period.

Levels of PFOS (83.71 ng/L) and PFOA (70.60 ng/L) in the samples exceeded the interim lifetime health advisory level for PFOS (0.02 ng/L) and PFOA (0.004 ng/L) set by USEPA (USEPA, 2023). The levels of PFAS specifically PFOA and PFOS in the sediment samples which ranged from 0.17 to 94.02ng/g exceeded the interim guidance limits set by the USEPA (2020). The detected levels of PFAS, specifically PFOS and PFOA, in the Pra River Basin highlight the need for appropriate measures to address the excessive presence of these compounds. The elevated levels of PFAS in the basin may pose serious negative health effects to humans.

An analysis of PFAS in surface water and sediment using PCA and HCA revealed variability in the data set, suggesting multiple sources of PFAS contributions in the river basin. The sources of these compounds in the river basin may originate from various anthropogenic activities, including industrial activities, domestic wastewater discharge, mining and agricultural activities in the river basin, as reported in earlier studies.

Human health risk of exposure to PFAS through surface water and sediment from the Pra river basin indicated that non-carcinogenic hazard

quotients and indices for both surface water and sediment were below 1 suggesting that the human population's health around the Pra river basin was unlikely to be adversely affected, as the HI value was below 1, indicating negligible risk.

The human population using raw surface water from the Pra river basin faced little to no cancer risk from PFAS exposure through ingestion and dermal contact routes. However, there was a potential cancer risk from PFOS to the health of maximally exposed individuals around highly contaminated sites of the Pra river basin through cumulative ingestion and dermal contact routes.

The potential cancer risk associated with ingestion of surface water was relatively higher than that associated with ingestion of sediment from the same river. However, the potential cancer risk through dermal contact was higher for direct contact with sediments compared to surface water, particularly for maximally exposed individuals, due to the high levels of PFOS present in the sediments of the river basin.

An ecological risk assessment of PFAS in the Pra river basin indicated that PFHxS was the most toxic for algae and PFOA being the most toxic for crustaceans and fish. In all crustaceans were found to be the most sensitive species for PFOA, PFOS, and PFNA, while PFOA and PFNA were more toxic to fish than algae and crustaceans. The study emphasized that PFAS toxicity can differ among species, with higher trophic levels, such as fish, having more significant impacts. PFOA and PFOS were found to be the major contributors to the risks of the PFAS compounds studied. The $RQ_{MEC/NOEC}$ values obtained for PFAS mixture risk assessment were higher than 1, indicating potential risks to aquatic organisms. Kyekyewere was found to have the highest environmental

risk among the 20 sampling sites with an $RQ_{MEC/NOEC}$ value of 17.1, followed by Abetemasu, Sekyere Hemang, and Twifo Hemang. The study showed that single chemical toxicity risk assessment is not enough, and mixture risk assessment is necessary.

Water radiolysis was employed to decompose PFOA which belongs to the family of PFAS. The study showed the degradation of PFOA at pH 6 and 11, with higher degradation at pH 11. At pH 11, the degradation efficiency was almost 98% after 8 hours of irradiation with gamma at 20 kGy. The main reactive species involved solvated electrons and carbon dioxide radical anion under argon-saturated atmosphere producing a radiolytic yield of $9.59E-04$. The study indicates that PFAS can be degraded with ionizing radiation with little or no pollution.

The study provided evidence of PCB contamination in the Pra River Basin. The highest concentration of PCBs in the dry season was found at site P18 with a recorded value of 5.869 ng/L. Similarly, during the wet season, the highest concentration was observed at site P15, measuring 2.995 ng/L for the surface water samples. In the dry season, the highest total PCB concentration was recorded at site P2 (242.16 ng/g), while the wet season, the highest total PCB concentration was recorded at site P8 (158.11 ng/g) for sediment. The reason for the higher PCB concentrations at these locations in the Pra river basin is not yet known. The study found that the concentrations of PCBs in sediment samples were generally higher compared to the concentrations in water samples

Spatial variations in the distribution of total PCBs in both water and sediment, were observed. The higher concentration of PCBs found in sediment

compared to water. Also, higher PCB concentrations were recorded in the dry season.

The most dominant homologs detected were hexachlorobiphenyls (PCBs 138, 149, and 153) which constituted 25.51% and 30.37% of total PCBs in water and sediments, respectively. The analysis revealed that PCB153 was the predominant congener detected in both water and sediment samples. Principal component analysis and hierarchical cluster analysis revealed variability in the PCB data set. The sources of these compounds in the river basin may originate from various anthropogenic activities, including industrial activities, domestic wastewater discharge, mining and agricultural activities in the river basin, as reported in earlier studies.

PCB cancer risk from exposure to surface water and sediment from the Pra River Basin was mainly due to PCB118, which was the only DL PCB detected. The estimated probabilistic PCB cancer risk from exposure to PCB118 in the Pra River Basin was very low indicating negligible health effect from exposure to surface water and sediment from the Pra River Basin. The non-carcinogenic hazard quotients and indices of all the single PCBs were below 1, indicating that the risk from exposure to these PCBs in the Pra river basin was considered low.

Overall, PFAS and PCBs have been detected in water and sediment samples from the Pra River basin at low levels. PFOA (70.60 ng/L) and PFOS (83.71ng/L) exceeded the recommended limits. The levels of these pollutants do not pose significant cancer and non-cancer health risk. The environmental risk for PFOA was low or medium. The results of this study will serve as data base upon which other (including future) analysis of PFAS and PCBs in our

aquatic environment would be compared. Aqueous radiolysis was effective in decomposing the PFAS. The findings will also contribute significantly to the monitoring of these chemicals, protection of public health, the environment and the development of regulations and guidelines to manage risks associated with these chemicals by the various stakeholders concerned.

Recommendations

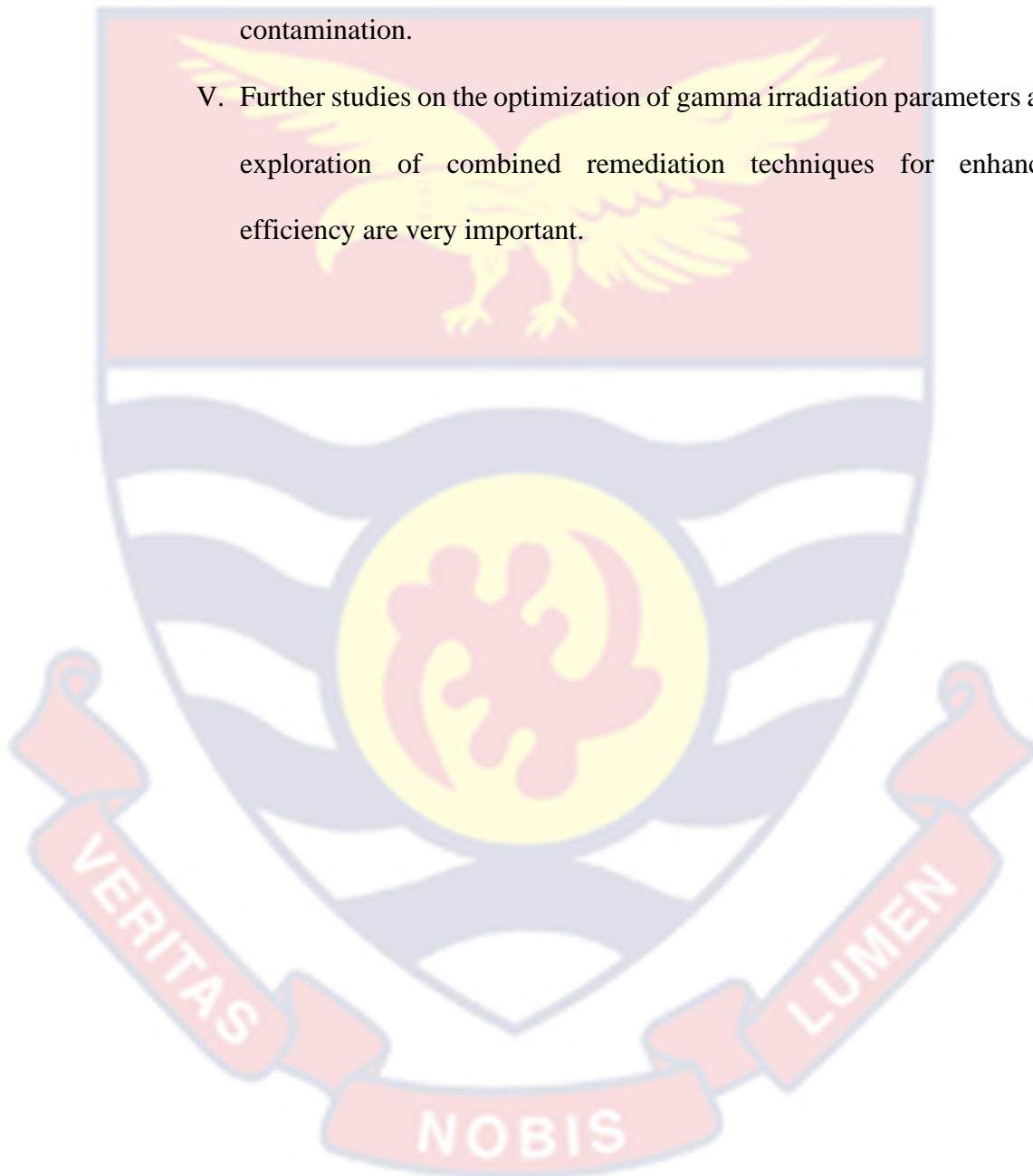
The presence of per- and polyfluoroalkyl substances (PFAS) and polychlorinated biphenyls (PCBs) in a river basin such as the Pra is a significant environmental and public health concern. To tackle this problem, a comprehensive set of measures must be taken to control the sources of these chemicals, monitor the levels of contamination, and reduce the exposure of humans and wildlife. On the basis of this, the following recommendations have been proposed:

- I. The regulatory agencies such as Ghana EPA and Pra river basin board must be empowered by the central government to strictly ensure compliance to regulations on effluent discharges from industries in order to control the discharge of these chemicals from industries.
- II. Establishment of monitoring programs to assess the level of PFAS and PCB contamination in the river basin is very essential. Regular monitoring of the water, sediment, and biota of the river basin can help determine the levels of contamination and identify hotspots that require immediate remediation.
- III. Public education on the risks associated with PFAS and PCBs and measures to reduce exposures to these chemicals is critical. This may include outreach programs to schools, community centers and other

public forum. Additionally, signs can be posted in areas where there is a risk of exposure to alert the public of the potential hazards.

IV. Other river basins in Ghana should be monitored for organic micropollutants (PFAS and PCBs) to ascertain the extent of contamination.

V. Further studies on the optimization of gamma irradiation parameters and exploration of combined remediation techniques for enhanced efficiency are very important.



REFERENCES

- 3M Company. (2000a). Voluntary Use and Exposure Information Profile for Perfluorooctanoic Acid and Salts. USEPA Administrative Record AR226-0595. Retrieved from: www.regulations.gov as document EPA-HQ-OPPT2002-0051-0009, Accessed on 5th October, 2022.
- 3M Company. (2000c). Re: Phase-Out Plan for POSF-based Products. USEPA Administrative Record AR226-0600. Retrieved from: www.regulations.gov, as document EPA-HQ-OPPT-2002-0051-0006, Accessed on 5th October, 2022
- Adeogun, A. O., Chukwuka, A. V., Okoli, C. P., & Arukwe, A. (2016). Concentration of polychlorinated biphenyl (PCB) congeners in the muscle of *Clarias gariepinus* and sediment from inland rivers of southwestern Nigeria and estimated potential human health consequences. *Journal of Toxicology & Environmental Health, Part A*, 79(21), 969–983.
- Adeyinka, G. C., & Moodley, B. (2018). Effect of aqueous concentration of humic acid on the sorption of polychlorinated biphenyls onto soil particle grain sizes. *Journal of Soils & Sediments*, 19, 1543–1553.
- Adombire, M, Adjewodah, P., & Abrahams, R (2013). Business as Usual (BAU) Scenario Information and Analysis Covering the Pra and Kakum River Basins; *Nature Conservation Research Centre*, 2, 17-23
- Adu Kumi, J. M., & Apraku, A. (2015). Threats to the conservation of wetlands in Ghana: the case of songor ramsar site. *Journal of Scientific Research Report*, 6, 13–25.

- Adu-Kumi, S., Kawano, M., Shiki, Y., Yeboah, P. O., Carboo, D., Pwamang, J. & Suzuki, N. (2010). Organochlorine pesticides (OCPs), dioxin-like polychlorinated biphenyls (dl-PCBs), polychlorinated dibenzo-p-dioxins and polychlorinated dibenzo furans (PCDD/Fs) in edible fish from Lake Volta, Lake Bosumtwi and Weija Lake in Ghana. *Chemosphere*, 81(6), 675–684.
- Adukpo, O.K., Faanu, A., Lawluvi, H. *et al.* (2015). Distribution and assessment of radionuclides in sediments, soil and water from the lower basin of river Pra in the Central and Western Regions of Ghana. *Journal of Radioanalytical & Nuclear Chemistry*, 303, 1679–1685.
- Agbo, K. E., Walgraeve, C., Eze, J. I., Ugwoke, P. E., Ukoha, P. O., & Van Langenhove, H. (2020). A review on ambient and indoor air pollution status in Africa. *Atmospheric Pollution Research*, 217.
- Akbar, S., Huang, J., Zhou, Q., Gu, L., Sun, Y., Zhang, L. & Yang, Z. (2021). Elevated temperature and toxic Microcystis reduce Daphnia fitness and modulate gut microbiota. *Environmental Pollution*, 271, e116409.
- Akrasi, S. A. & Ansa-Asare, O.D. (2008). Assessing Sediment and Nutrient Transport in the Pra Basin of Ghana. *West African Journal of Applied Ecology*, 13, 45-56.
- Altenburger, R., Scholze, M., Busch, W., Escher, B.I., Jakobs, G., Krauss, M., Krüger, J., Neale, P. A., Ait-Aissa, S., Almeida, A.C., Seiler, T.-B., Brion, F., Hilscherová, K., Hollert, H., Novák, J., Schlichting, R., Serra, H., Shao, Y., Tindall, A., Tolefsen, K.-E., Umbuzeiro, G., Williams,

- T.D., & Kortenkamp, A., (2018). Mixture effects in samples of multiple contaminants – An inter-laboratory study with manifold bioassays. *Environment International*, 114, 95–106.
- Ameur, W. B., Trabelsi, S., Bedoui, B. & Driss, M. R. (2011). Polychlorinated biphenyls in sediments from Ghar El Melh lagoon, Tunisia. *Bulletin of Environmental Contamination & Toxicology*, 86(5), 539-44.
- Annamalai, J., & Namasivayam, V. (2015). Endocrine disrupting chemicals in the atmosphere: Their effects on humans and wildlife. *Environment International*, 76, 78–97.
- Ansa-Asare, O. D. & Gordon, C. (2012). Water quality assessment of Densu, Birim and Ayensu rivers in the Okyeman area. *West African. Journal of Applied Ecology*, 20, 53–64.
- Anumol, T., Dagninio, S., Vandervort, D.R. & Snyder, S. A. (2016). Transformation of polyfluorinated compounds in natural waters by advanced oxidation processes, *Chemosphere*, 144, 1780–1787.
- Asante, K. A., Sudaryanto, A, Devanathan, G, Bello, M, Takahashi, S, Isobe T, & Tanabe, S. (2010). Polybrominated diphenyl ethers and polychlorinated biphenyls in cow milk samples from Ghana. Proceedings of Interdisciplinary Studies on Environmental Chemistry. Environmental Specimen Bank (ESB): Exploring Possibility of Setting-up ESBs in Developing Countries. Symposium held at Ehime University, Japan, from 3rd - 5th December, 2009. Vol. 4, 191–198.
- Asante, K.A., Adu-Kumi, S., Nakahiro, K., Takahashi, S., Isobe, T., Sudaryanto, A., Devanathan, G., Clarke, E., Ansa-Asare, O.D., Dapaah-Siakwan, S., & Tanabe, S., (2011). Human exposure to PCBs, PBDEs

and HBCDs in Ghana: temporal variation, sources of exposure and estimation of daily intakes by infants. *Environment International*, 37, 921–928.

Asante-Duah, K. (2017). Public Health Risk Assessment for Human Exposure to Chemicals. *Environmental Pollution*, vol 27(2), Netherlands: Springer Netherlands.

Augustsson, A. Lennqvist, T. Osbeck, C. M. G. Tibblin, P. Glynn, A. Nguyen, M. A. Westberg, E. & Vestergren, R. (2020). Consumption of freshwater fish: A variable but significant risk factor for PFOS exposure. *Environmental Research*, 192, e110284.

Austin, M. E., Kasturi, B. S., Barber, M., Kannan, K., MohanKumar, P. S. & MohanKumar, S. M. J. (2003). Neuroendocrine Effects of Perfluorooctane Sulfonate in Rats. *Environmental Health Perspectives*, 111, 1485–1489.

Azzouz A., Rascón A.J. & Ballesteros E. (2016) Simultaneous Determination of Parabens, Alkylphenols, Phenylphenols, Bisphenol A and Triclosan in Human Urine, Blood and Breast Milk by Continuous Solid-Phase Extraction and Gas Chromatography-Mass Spectrometry. *Journal of Pharmacology & Biomedical Analytics*, 119, 16–26.

Backhaus, T., & Faust, M. (2012). Predictive Environmental Risk Assessment of Chemical Mixtures: A Conceptual Framework. *Environmental Science & Technology*, 46(5), 2564–2573.

Ballschmiter, K., & Zell, M. (1980). Analysis of polychlorinated biphenyls (PCB) by glass capillary gas chromatography. *Fresenius' Zeitschrift For Analytische Chemie*, 302(1), 20–31.

Barkow, I. S., Oswald, S. E., Lensing, H.-J., & Munz, M. (2020). Seasonal dynamics modifies fate of oxygen, nitrate, and organic micropollutants during bank filtration — temperature-dependent reactive transport modeling of field data. *Environmental Science & Pollution Research*, 28, 9682-9700.

Barron, M. G., Yurk, J. J. & Crothers, D. B. (1994). Assessment of Potential Cancer Risk from Consumption of PCBs Bioaccumulated in Fish and Shellfish. *Environmental Health Perspectives*, 102, 562–567.

Barry V, Darrow LA, Klein M, Winqvist A. & Steenland K. (2014). Early life perfluorooctanoic acid (PFOA) exposure and overweight and obesity risk in adulthood in a community with elevated exposure. *Environmental Research*, 132,62–69.

Bassler, J., Ducatman, A., Elliott, M., Wen, S., Wahlang, B., Barnett, J.& Cave M.C. (2019). Environmental perfluoroalkyl acid exposures are associated with liver disease characterized by apoptosis and altered serum adipocytokines. *Environmental Pollution*, 247, 1055-1063.

Benskin, J. P., Muir, D. C. G., Scott, B. F., Spencer, C., De Silva, A. O., Kylin, H., & Yamashita, N. (2012). Perfluoroalkyl Acids in the Atlantic and Canadian Arctic Oceans. *Environmental Science & Technology*, 46(11), 5815–5823.

Bentum, J. K., Dodoo, D. K. & Kwakye, P. K. (2012). Accumulation of metals and polychlorinated biphenyls (PCBs) in soils around electric transformers in the Central Region of Ghana. *Advances in Applied Science Research*, 3(2), 634-643.

Berger, U., Glynn, A., Holmström, K. E., Berglund, M., Ankarberg, E. H., & Törnkvist, A. (2009). Fish consumption as a source of human exposure to perfluorinated alkyl substances in Sweden – Analysis of edible fish from Lake Vättern and the Baltic Sea. *Chemosphere*, 76(6), 799–804.

Berghuis, S. A., & Roze, E. (2019). Prenatal exposure to PCBs and neurological and sexual/pubertal development from birth to adolescence. *Current Problems in Pediatric and Adolescent Health Care*.

Bessah, E., Raji, A. O., Taiwo, O. J., Agodzo, S. K., Ololade, O. O., Strapasson, A., et al. (2021). Assessment of surface waters and pollution impacts in Southern Ghana. *Hydrological Research*, 52, 1423–1435.

Biegel, L. B., Hurtt, M. E., Frame, S. R., O'Connor, J. C., & Cook, J. C. (2001). Mechanisms of Extrahepatic Tumor Induction by Peroxisome Proliferators in Male CD Rats. *Toxicological Sciences*, 60(1), 44–55.

Biegel, L. B., Liu, R. C. M., Hurtt, M. E., & Cook, J. C. (1995). Effects of Ammonium Perfluorooctanoate on Leydig-Cell Function: In Vitro, in Vivo, and ex Vivo Studies. *Toxicology & Applied Pharmacology*, 134(1), 18–25.

Björklund, S., Weidemann, E., Yeung, L. W., & Jansson, S. (2021). Occurrence of per- and polyfluoroalkyl substances and unidentified organofluorine in leachate from waste-to-energy stockpile - A case study. *Chemosphere*, 278, 130380.

Bodin N, Ka RN, Loc'h FL, Raffray J, Budzinski H, Peluhet L, & Tito de Morais L (2011). Are exploited mangrove molluscs exposed to

persistent organic pollutant contamination in Senegal, West Africa?
Chemosphere, 84(3),318–327.

Boulangier, B., Vargo, J., Schnoor, J. L., & Hornbuckle, K. C. (2004). Detection of Perfluorooctane Surfactants in Great Lakes Water. *Environmental Science & Technology*, 38(15), 4064–4070.

Bradley, P. M., Padilla, I. Y., Romanok, K. M., Smalling, K. L., Focazio, M. J., Breitmeyer, S. E., & Wilson, V. S. (2021). Pilot-scale expanded assessment of inorganic and organic tapwater exposures and predicted effects in Puerto Rico, USA. *Science of The Total Environment*, 788, 147721.

Brian, J. V., Harris, C. A., Scholze, M., Backhaus, T., Booy, P., Lamoree, M. & Sumpter, J. P. (2005). Accurate Prediction of the Response of Freshwater Fish to a Mixture of Estrogenic Chemicals. *Environmental Health Perspectives*, 113(6), 721–728.

Bruce-Vanderpuije P., Megson D., Jones G.R., Jobst K., Reiner E., Clarke E., Adu-Kumi S., & Gardella J.A. (2021). Infant Dietary Exposure to Dioxin-like Polychlorinated Biphenyls (DIPCBs), Polybrominated and Mixed Halogenated Dibenzop-Dioxins and Furans (PBDD/Fs and PXDD/Fs) in Milk Samples of Lactating Mothers in Accra, Ghana. *Chemosphere*,263,128-156.

Buck, R. C., Franklin, J., Berger, U., Conder, J. M., Cousins, I. T., de Voogt, P. & van Leeuwen, S. P. (2011). Perfluoroalkyl and polyfluoroalkyl substances in the environment: Terminology, classification, and origins. *Integrated Environmental Assessment & Management*, 7(4), 513–541.

- Buck, R. C., Korzeniowski, S. H., Laganis, E. & Adamsky, F. (2021). Identification and Classification of Commercially Relevant Per- and Poly-fluoroalkyl Substances (PFAS). *Integrated Environmental Assessment & Management*, 17(5), 1045–1055.
- Burris, J. M., Lundberg, J.K., Olsen, G.W., Simpson, C., Mandel, J. H. (2002). Determination of Serum Half-lives of Several Fluorochemicals. Interim Report No. 2. St. Paul, MN:3M Company. U.S. EPA docket AR-226-1086. Washington, DC: U.S. Environmental Protection Agency.
- Butenhoff, J. L., Bjork, J. A., Chang, S.-C., Ehresman, D. J., Parker, G. A., Das, K., et al. (2012). Toxicological Evaluation of Ammonium Perfluorobutyrate in Rats: Twenty-Eight-Day and Ninety-Day Oral Gavage Studies. *Reproductive Toxicology*. 33, 513–530.
- Butenhoff, J. L., Chang, S.-C., Ehresman, D. J. & York, R. G. (2009a). Evaluation of Potential Reproductive and Developmental Toxicity of Potassium Perfluorohexanesulfonate in Sprague Dawley Rats. *Reproductive Toxicology*. 27, 331–341.
- Cardenas, A., Hauser, R., Gold, D. R., Kleinman, K. P., Hivert, M.-F., Fleisch, A. F. & Oken, E. (2018). Association of Perfluoroalkyl and Polyfluoroalkyl Substances with Adiposity. *Journal of America Medical Association Network Open*, 1(4), e181493.
- Carpenter, D. O. (2006). Polychlorinated Biphenyls (PCBs): Routes of Exposure and Effects on Human Health. *Reviews on Environmental Health*, 21(1), 1–24.
- Castello, G. (1999). Retention index systems: alternatives to the n-alkanes as calibration standards. *Journal of Chromatography A*, 842(1-2), 51–64.

Center for Disease Control (CDC) (2019). PFAS in Drinking Water. Retrieved from: <https://www.cdc.gov/pfas/national-and-regional-data/pfas/drinkingwater.html> , Accessed on 7th October, 2023

Cerkvenik V, Doganoc DZ, Jan J (2000) Evidence of some trace elements, organochlorine pesticides, and PCBs in Slovenian cow's milk. *Food Technology & Biotechnology*,38(2),155–160.

Chalhoub, M., Amalric, L., Touzé, S., Gallé, P., Reiller, P. E., Doucet, N., ... Bataillard, P. (2013). PCB partitioning during sediment remobilization—a 1D column experiment. *Journal of Soils and Sediments*, 13(7), 1284–1300.

Chen, G & Bunce, NJ (2004) Interactions between halogenated aromatic compounds in the Ah receptor signal transducing pathway. *Environmental Toxicology*, 19, 480-489.

Chen, H., Han, J., Zhang, C., Cheng, J., Sun, R., Wang, X., et al. (2017). Occurrence and seasonal variations of per- and polyfluoroalkyl substances (PFASs) including fluorinated alternatives in rivers, drains outlets and receiving Bohai Sea of China. *Environmental Pollution*, 231, 1223-1231.

Cheng C., Ma H., Deng Y., Feng J., Jie Y., Guo Z. (2021). Oxidative stress, cell cycle arrest, DNA damage and apoptosis in the mud crab (*Scylla paramamosain*) induced by cadmium exposure. *Chemosphere*. 263, 128277.

Cheng, H., Chen, J., Chen, S., Wu, D., Liu, D., & Ye, X. (2015). Characterization of aroma-active volatiles in three Chinese bayberry

(*Myrica rubra*) cultivars using GC–MS–olfactometry and an electronic nose combined with principal component analysis. *Food Research International*, 72, 8–15.

Chirikona, F., Filipovic, M., Ooko, S., & Orata, F. (2015). Perfluoroalkyl acids in selected wastewater treatment plants and their discharge load within the Lake Victoria basin in Kenya. *Environmental Monitoring & Assessment*, 187(5).

Choi, W.Y., Gemberling, M., Wang, J., Holdway, J.E., Shen, M.C., Karlstrom, R.O. & Poss, K.D. (2013). In vivo monitoring of cardiomyocyte proliferation to identify chemical modifiers of heart regeneration. *Development* (Cambridge, England). 140(3), 660-666.

Conder, J. M., Hoke, R. A., Wolf, W. de, Russell, M. H., & Buck, R. C. (2008). Are PFCAs Bioaccumulative? A Critical Review and Comparison with Regulatory Criteria and Persistent Lipophilic Compounds. *Environmental Science & Technology*, 42(4), 995–1003.

Cook, J. C, Mullin, L. S., Frame, S. R., and Biegel, L. B. (1993). Investigation of a mechanism for Leydig cell tumorigenesis by linuron in rats. *Toxicology & Applied Pharmacology*, 119, 195-204.

Costa, G., Sartori, S. & Consonni, D. (2009). Thirty years of medical surveillance in perfluooctanoic acid production workers. *Journal of Occupational & Environmental Medicine*, 51, 364–372.

Cui, X, Dong, J., Huang, Z et al. (2020). Polychlorinated biphenyls in the drinking water source of the Yangtze River: characteristics and risk assessment. *Environmental science Europe*, 32, (29).

D'eon J. C. & Mabury, S. A. (2007). Production of Perfluorinated Carboxylic Acids (PFCAs) from the Biotransformation of Polyfluoroalkyl Phosphate Surfactants (PAPS): Exploring Routes of Human Contamination. *Environmental Science & Technology*, 40(9), 2376-2458.

Das, K. P., Wood, C. R., Lin, M. T., Starkov, A.A, Lau, C., Wallace, K. B., Corton, J. C. & Abbott, B. D. (2017). Perfluoroalkyl acids-induced liver steatosis: Effects on genes controlling lipid homeostasis. *Toxicology*, 378, 37-52.

de Voogt, P., Saez, M. (2006). Analytical chemistry of perfluoroalkylated substances. *Trends in Analytical Chemistry*, 25(4), 326–342.

DeLuca, N. M.; Angrish, M.; Wilkins, A.; Thayer, K. & Cohen Hubal, E. A. (2021). Human exposure pathways to poly- and perfluoroalkyl substances (PFAS) from indoor media: A systematic review protocol. *Environment International*, 146, 106308.

Deng, Y., Liang, Z., Lu, X., Chen, D., Li, Z. & Wang, F. (2021). The degradation mechanisms of perfluorooctanoic acid (PFOA) and perfluorooctane sulfonic acid (PFOS) by different chemical methods: A critical review. *Chemosphere*, 283,1131168.

Derouiche, A., Driss, M. R., Morizur, J.-P., & Taphanel, M.-H. (2007). Simultaneous analysis of polychlorinated biphenyls and organochlorine pesticides in water by headspace solid-phase microextraction with gas chromatography–tandem mass spectrometry. *Journal of Chromatography*, 1138(1-2), 231–243.

- Dinglasan-Panlilio, M. J. A. & Mabury, S. A. (2006). Significant residual fluorinated alcohols present in various fluorinated materials. *Environmental Science & Technology*, 40(5), 1447–1453.
- Doceaa, A. O., Goumenou, M., Calina, D., Arsene, A. L., Dragoi, C. M., Gofta, E., Pisoschi, C. G., Zlatian, O., & Tsatsakis, A. (2019). Adverse and hormetic effects in rats exposed for 12 months to low dose mixture of 13 chemicals: *RLRS part III, Toxicological Letters*, 310, 70–91.
- Dodoo, D. K., Essumang, D. K., Jonathan, J. W. A., & Bentum, J. K. (2012). Polychlorinated biphenyls in coastal tropical ecosystems: Distribution, fate and risk assessment. *Environmental Research*, 118, 16–24.
- Domingo, J. L., & Bocio, A. (2007). Levels of PCDD/PCDFs and PCBs in edible marine species and human intake: a literature review. *Environment International*, 33, 397–405.
- Duncan, A.E., de Vries, N. & Nyarko, K. (2018). Assessment of Heavy Metal Pollution in the Sediments of the River Pra and Its Tributaries. *Water Air Soil Pollution*, 229, 272.
- Ellis, D. A. & Mabury, S. A (2003). Chemical ionization pathways of polyfluorinated chemicals – a connection to environmental atmospheric processes. *Journal of the American Society for Mass Spectrometry*, 14, 1177–1191.

Environment Canada. (2011). Guidance on ecological risk assessment of contaminated sites in Canada: Part 2 - Science and methods. ISBN: 978-1-100-18451-8.

Environment Canada. Environmental performance agreement (“agreement”) respecting perfluorinated carboxylic acids (PFCAs) and their precursors in perfluorochemical products sold in Canada. (2010). Retrieved from: http://ec.gc.ca/epe-epa/default.asp?lang=En&n=81AE_80CE-1 , Accessed on 11th October, 2023.

Erickson, M. D., & Kaley, R. G. (2010). Applications of polychlorinated biphenyls. *Environmental Science and Pollution Research*, 18(2), 135–151.

Ericson Jogsten, I., Nadal, M., van Bavel, B., Lindström, G., & Domingo, J. L. (2012). Per- and polyfluorinated compounds (PFCs) in house dust and indoor air in Catalonia, Spain: Implications for human exposure. *Environment International*, 39(1), 172–180.

Essumang, D. K., Eshun, A., Hogarh J. N., Bentum, J. K., Adjei J. K., Negishi J., Nakamichi S., Habibullah-Al-Mamun M. D. & Masunaga S. (2017). Perfluoroalkyl acids (PFAAs) in the Pra and Kakum River basins and associated tap water in Ghana. *Science of The Total Environment*, 579, 729–735.

European Parliament. (2006b). Directive 2006/122/EC of the European Parliament and of the Council of 12 December 2006. Official Journal of the EU, 27 December 2006, L372/32-L372/34

Falandysz, J., Taniyasu, S., Gulkowska, A., N. Yamashita, N. & Schulte-Oehlmann, U. (2006). Is fish a major source of fluorinated surfactants

and repellents in humans living on the Baltic coast? *Environmental Science & Technology*, 40, pp. 748-751.

Ferrari, F., Orlando, A., Ricci, Z., & Ronco, C. (2019). Persistent pollutants: Focus on perfluorinated compounds and kidney. *Current Opinion on Critical Care*, 25, 539-549.

Fisher, M., Arbuckle, T.E., Wade, M. & Haines, D.A. (2013). Do perfluoroalkyl substances affect metabolic function and plasma lipids? —analysis of the 2007–2009, Canadian Health Measures Survey (CHMS) Cycle 1. *Environmental Research*, 121, 95–103.

Fitzgerald E.F., Shrestha S., Palmer P.M., Wilson L.R., Belanger E.E., Gomez M.I., Cayo M.R., & Hwang S. (2011). Polychlorinated Biphenyls (PCBs) in Indoor Air and in Serum among Older Residents of Upper Hudson River Communities. *Chemosphere*, 85, 225–231.

Fitz-Simon, N., Fletcher, T., Luster, M.I., Steenland, K., Calafat, A.M., Kato, K., et al., (2013). Reductions in serum lipids with a 4-year decline in serum perfluorooctanoic acid and perfluorooctanesulfonic acid. *Epidemiology*, 24, 569–576.

Fluoropolymer Manufacturing Group. (2001). Guide to the safe handling of fluoropolymer dispersions. Washington (DC): Society of Plastics Industry.

Frame, G. M., Cochran, J. W., & Bøwadt, S. S. (1996). Complete PCB congener distributions for 17 aroclor mixtures determined by 3 HRGC systems optimized for comprehensive, quantitative, congener-specific analysis. *Journal of High-Resolution Chromatography*, 19(12), 657–668.

- Freels, S., Chary, L. K., Turyk, M., Piorkowski, J., Mallin, K., Dimos, J., & Persky, V. (2007). Congener profiles of occupational PCB exposure versus PCB exposure from fish consumption. *Chemosphere*, 69(3), 435–443.
- Gavrilescu, M., Demnerova, K., Aamand, J., Agathos, S., & Fava, F. (2015). Emerging pollutants in the environment: present and future challenges in biomonitoring, ecological risks and bioremediation. *New Biotechnology*, 32(1), 147-56.
- Geiger, S.D., Xiao, J., & Shankar, A., (2013). Positive association between perfluoroalkyl chemicals and hyperuricemia in children. *American Journal of Epidemiology*, 177, 1255–1262.
- Getoff, N. (1996). Radiation-induced degradation of water pollutants-state of the art, *Radiation & Physical Chemistry*, 47, 581–593.
- Ghana News Agency. (2009). Alluvial mining destroying River Pra. Retrieved from: <https://www.modernghana.com/news/734164/alluvial-mining-destroying-river-pra.html>, Accessed on 7th November, 2023.
- Giesy, J. P. & Kannan, K. (2001). Global distribution of perfluorooctane sulfonate in wildlife. *Environmental Science & Technology*, 35,1339–1342.
- Gizem, E. S. & Tasdemir, Y. (2022). Temporal Variations of PCBs and their estimated Air-Soil exchange fluxes measured in seven sites in Bursa-Turkey. *An International Journal of Soil & Sediment Contamination*,5, 78-89.

Gligorowski, S., Sterekowski, R., Barbati, S., & Vione, D. (2015). Environmental implications of hydroxyl radicals (OH), *Chemical Review*, 115, 13051–1309.

Goldstein, J. A., Hass, J. R., Linko, P., & Harvan D.J. (1978). 2,3,7,8-Tetrachlorodibenzofuran in a commercially available 99% pure polychlorinated biphenyl isomer identified as the inducer of hepatic cytochrome P-448 and aryl hydrocarbon hydroxylase in the rat. *Drug Metabolism & Disposal*, 6, 258–264.

Goudarzi, H., Araki, A., Itoh, S., Sasaki, S., Miyashita, C., Mitsui, T. & Kishi, R. (2017). The Association of Prenatal Exposure to Perfluorinated Chemicals with Glucocorticoid and Androgenic Hormones in Cord Blood Samples: The Hokkaido Study. *Environmental Health Perspectives*, 125(1), 111–118.

Goumenou, M., & Tsatsakis, A. (2019). Proposing new approaches for the risk characterisation of single chemicals and chemical mixtures: The source related Hazard Quotient (HQS) and Hazard Index (HIS) and the adversity specific Hazard Index (HIA). *Toxicology Reports*, 6, 632–636.

Green, L.E., Baynes, D.M., Kolpin, D. J., Harris, L.J., La Guardia, A. D., LaGrandeur, B.A., Philips & Sturges, W.L. (2017). Occurrence and distribution of per- and polyfluoroalkyl substances (PFASs) in the lower Susquehanna River, Pennsylvania, USA. *Science of the Total Environment*, 578, 1251-1262.

Guillette, T. C., McCord, J., Guillette, M., Polera, M. E., Rachels, K. T., Morgeson, C., et al. (2020). Elevated Levels of Per- and Polyfluoroalkyl Substances in Cape Fear River Striped Bass (*Morone saxatilis*) Are

Associated with Biomarkers of Altered Immune and Liver Function. *Environment International*, 136, 105358.

Gulkowska, A., Jiang, Q., So, M. K., Taniyasu, S., Lam, P. K. S. & Yamashita, N. (2006). Persistent perfluorinated acids in seafood collected from two cities of China. *Environmental Science & Technology*, 40, pp. 3736-3741.

Guo, W.J., Pan, B.H., Sakkiah, S., Yavas, G., Ge, W.G., Zou, W. Tong, W. D. & Hong, H.X. (2019). Persistent organic pollutants in food: contamination sources, health effects and detection methods. *International of Journal of Environment Reearch & Public Health*, 16, p. 29.

Guruge, K. S., Taniyasu, S., Yamashita, N., Wijeratna, S., Mohotti, K. M., Seneviratne, H. R. & Miyazaki, S. (2005). Perfluorinated organic compounds in human blood serum and seminal plasma: a study of urban and rural tea worker populations in Sri Lanka. *Journal of Environmental Monitoring*, 7, 371–377.

Habibullah-Al-Mamuna, Ahmed, K., Islamd, S., Tokumurae, M., & Masunaga, S. (2019). Occurrence, distribution and possible sources of polychlorinated biphenyls (PCBs) in the surface water from the Bay of Bengal coast of Bangladesh, *Ecotoxicology & Environmental Safety*, (167) 450 -458.

Hale, S. E., Arp, H. P. H., Slinde, G. A., Wade, E. J., Bjørseth, K., Breedveld, G. D., & Høisæter, A. (2017). Sorbent amendment as a remediation strategy to reduce PFAS mobility and leaching in a contaminated sandy

soil from a Norwegian firefighting training facility. *Chemosphere*, 171, 9–18.

Hall, & Greco. (2019). Perturbation of Nuclear Hormone Receptors by Endocrine Disrupting Chemicals: Mechanisms and Pathological Consequences of Exposure. *Cells*, 9(1), 13.

Hall, S. M. Patton, S. Petreas, M. Zhang, S. Phillips, A. L. Hoffman, K. & Stapleton, H. M. (2020). Per- and Polyfluoroalkyl Substances in Dust Collected from Residential Homes and Fire Stations in North America. *Environmental Science & Technology*, 54(22), 14558-14567.

Halldorsson, T. I., Rytter, D., Haug, L. S., Bech, B. H., Danielsen, I., Becher, G. & Olsen, S. F. (2012). Prenatal Exposure to Perfluorooctanoate and Risk of Overweight at 20 Years of Age: A Prospective Cohort Study. *Environmental Health Perspectives*, 120(5), 668–673.

Hamers, T, Kamstra, J. H, Cenijn, P.H, Pencikova, K., Palkova, L., Simeckova P, et al. (2011). In vitro toxicity profiling of ultra- pure non-dioxin-like polychlorinated biphenyl congeners and their relative toxic contribution to PCB mixtures in humans. *Toxicology & Science*, 121, 88–100.

Hankinson, O., 1995. The aryl hydrocarbon receptor complex. *Annual Review of Pharmacology & Toxicology*. 35, 307e340.

Hansen, K. J., Clemen, L. A., Ellefson, M. E., Johnson, H. O. (2001). Compound-Specific, Quantitative Characterisation of Organic Fluorochemicals in Biological Matrices. *Environmental Science & Technology*, 35, 766-770.

Hansen, K. J., Johnson, H. O., Eldridge, J. S., Butenhoff, J. L. & Dick, L. A. (2002). Quantitative Characterisation of Trace Levels of PFOS and

PFOA in Tennessee River. *Environmental Science & Technology*, 36, 1681-1685.

Hanson, K. B., Hoff, D. J., Lahren, T. J., Mount, D. R., Squillace, A. J. & Burkhard, L. P. (2019). Estimating n-octanol-water partition coefficients for neutral highly hydrophobic chemicals using measured n-butanol-water partition coefficients. *Chemosphere*, 218, 616-623.

Harada, K. H., Ishii, T. M., Takatsuka, K., Koizumi, A., & Ohmori, H. (2006). Effects of Perfluorooctane Sulfonate on Action Potentials and Currents in Cultured Rat Cerebellar Purkinje Cells. *Biochemical & Biophysical Research Communications* 351, 240–245.

Harrad, S., Ibarra, C., Robson, M., Melymuk, L., Zhang, X., Diamond, M., & Douwes, J. (2009). Polychlorinated biphenyls in domestic dust from Canada, New Zealand, United Kingdom and United States: Implications for human exposure. *Chemosphere*, 76(2), 232–238.

Herkert, N. J., Jahnke, J. C., & Hornbuckle, K. C. (2018). Emissions of Tetrachlorobiphenyls (PCBs 47, 51, and 68) from Polymer Resin on Kitchen Cabinets as a Non-Aroclor Source to Residential Air. *Environmental Science & Technology*, 52(9), 5154–5160.

Higgins, C. P., Field, J. A., Criddle, C. S., & Luthy, R. G. (2005). Quantitative Determination of Perfluorochemicals in Sediments and Domestic Sludge. *Environmental Science & Technology*, 39(11), 3946–3956.

Hoff, P. T., Scheirs, J., van de Vijver, K., Van Dongen, W., Esmans, E. L., Blust, R., & De Coen, W. (2004). Biochemical Effect Evaluation of Perfluorooctane Sulfonic Acid-Contaminated Wood Mice (*Apodemus sylvaticus*). *Environmental Health Perspectives*, 112(6), 681–686.

Hu, X., Adamcakova-Dodd, A., Lehmler, H.-J., Hu, D., Kania-Korwel, I., Hornbuckle, K. C., & Thorne, P. S. (2010). Time Course of Congener Uptake and Elimination in Rats after Short-Term Inhalation Exposure to an Airborne Polychlorinated Biphenyl (PCB) Mixture. *Environmental Science & Technology*, 44(17), 6893–6900.

Huang, L., Dong, W., Hou, & H., (2007). Investigation of the reactivity of hydrated electron toward perfluorinated carboxylates by laser flash photolysis. *Chemical Physics Letters*, 436, 124–128.

Huerta-Fontela, M., Galceran, M. T., & Ventura, F. (2011). Occurrence and removal of pharmaceuticals and hormones through drinking water treatment. *Water Research*, 45(3), 1432–1442.

Impinen A, Longnecker MP, Nygaard UC, London SJ, Ferguson KK, Haug LS, Granum B. (2019). Maternal levels of perfluoroalkyl substances (PFASs) during pregnancy and childhood allergy and asthma related outcomes and infections in the Norwegian Mother and Child (MoBa) cohort. *Environment International*, 124,462–472.

Impinen A, Nygaard UC, Lodrup Carlsen KC, Mowinckel P, Carlsen KH, Haug LS, Granum B. 2018. Prenatal exposure to perfluoroalkyl substances (PFASs) associated with respiratory tract infections but not allergy- and asthma-related health outcomes in childhood. *Environmental Research*, 160, 518–523.

Iniaghe, P. O., & Kpomah, E. D. (2022). Polychlorinated biphenyls (PCBs) in water and sediments from the Udu River, Niger Delta, Nigeria:

concentration, distribution and risk assessment. *Journal of Environmental Exposure Assessment*, 1, 20.

Jacobson, J.L., Jacobson, S.W. & Humprey, H.E.B. (1990). Effects of exposure to PCBs and related compound on growth and activity in children. *Neurotoxicology & Teratology* 12, 319-26.

Jafarabadia, A. R., Riyahi, A., Mitrab, B. S., Maisano, M., Cappelloc, T., & Jadotd, C. (2019). First polychlorinated biphenyls (PCBs) monitoring in seawater, surface sediments and marine fish communities of the Persian Gulf: Distribution, levels, congener profile and health risk assessment *Environmental Pollution*, 253, 78-88.

Jahnke, J. C. & Hornbuckle, K. C. (2019). PCB Emissions from Paint Colorants. *Environmental Science & Technology*.60(7), 512-530.

Jahnke, A & Berger, U. (2009) Trace analysis of per- and polyfluorinated alkyl substances in various matrices – How do current methods perform? *Journal of Chromatography*, 1216, 410–421.

Jensen, A. A. (1987). Polychlorobiphenyls (PCBs), polychlorodibenzo-p-dioxins (PCDDs) and polychlorodibenzofurans (PCDFs) in human milk, blood and adipose tissue. *Science of The Total Environment*, 64(3), 259–293.

Jiang, L., Luo, C., Zhang, D., Song, M., Sun, Y., & Zhang, G. (2018). Biphenyl-Metabolizing Microbial Community and a Functional Operon Revealed in E-Waste-Contaminated Soil. *Environmental Science & Technology*, 52(15), 8558–8567.

- Jones, K.C.; de Voogt, P.(1999). Persistent Organic Pollutants (POPs): State of the Science. *Environmental Pollution*, 100, 209–221.
- Kaifie, A., Schettgen, T., Bertram, J., Löhndorf, K., Waldschmidt, S., Felten, M. K., ... Küpper, T. (2020). Informal e-waste recycling and plasma levels of non-dioxin-like polychlorinated biphenyls (NDL-PCBs) – A cross-sectional study at Agbogbloshie, Ghana. *Science of The Total Environment*, 723, 138073.
- Kallenborn R, & Huhnerfuss H. (2001). *Chiral Environmental Pollutants - Trace Analysis and Ecotoxicology*. Berlin, Heidelberg: Springer Verlag.
- Kallenborn, R., Berger, U., & Järnberg, U. (2004). Perfluorinated alkylated substances (PFASs) in the Nordic environment (p. 552). Copenhagen DK: Nordic Council Publication.
- Kandie, F. J., Krauss, M., Beckers, L.-M., Massei, R., Fillinger, U., Becker, J., & Brack, W. (2020). Occurrence and risk assessment of organic micropollutants in freshwater systems within the Lake Victoria South Basin, Kenya. *Science of The Total Environment*, 714,136748.
- Kay, D. P., Blankenship, A. L., Coady, K. K., Neigh, A. M., Zwiernik, M. J., Millsap, S. D., Strause, K., Park, C., Bradley, P., Newsted, J. L., Jones, P. D., & Giesy J.P., (2005). Differential accumulation of polychlorinated biphenyl congeners in the aquatic food web at the Kalamazoo River superfund site, Michigan. *Environmental Science & Technology*, 39, 5964-5974.
- Kennedy, G. L., Butenhoff, J. L., Oslon, G. W., O'Connor, J. C., Seacat, A. M., Perkins, R. G., Biegel, L. B, Murphy, S. R. & Garrar, D. G. (2004). The

toxicology of perfluorooctanoate. *Critical Reviews in Toxicology*, 34(4), 351-384.

Kim, J.-T., Choi, Y.-J., Barghi, M., Kim, J.-H., Jung, J.-W. & Kim, K. (2021). Occurrence, distribution, and bioaccumulation of new and legacy persistent organic pollutants in an ecosystem on King George Island, maritime Antarctica. *Journal of Hazard Material*, 405, 124141.

Kissa, E. (1994). Fluorinated surfactants: Synthesis–Properties–Applications (Surfactant science series 50). New York (NY): Marcel Dekker. 469 p.

Kjeldsen, L. S., & Bonefeld-Jorgensen, E.C. (2013). Perfluorinated compounds affects the function of sex hormone receptors. *Environmental Science & Pollution Research*, 20, 8031-8044.

Kocan, A., Petrik, J., Jursa, S., Chovancova, J., & Drobna, B. (2001). Environmental contamination with polychlorinated biphenyls in the area of their former manufacture in Slovakia. *Chemosphere*, 43(4-7), 595–600.

Kodavanti, P.R., Senthil Kumar, K. & Loganathan, B.G., 2008. Organohalogen pollutants in the environment and their effects on wildlife and human health. *International Encyclopedia of Public Health*, 4, 686–693.

Kortei, N.N., Korley, K. Alice, K., Toah, A. P., B. Nana Yaw, & Manaphraim. M. (2020). Potential health risk assessment of toxic metals contamination in clay eaten as pica (geophagia) among pregnant women of Ho in the Volta Region of Ghana. *BMC Pregnancy & Childbirth*, 20 (1), pp. 1-7

- Kostyniak, P.J., Stinson, C., Greizerstein, H.B., et al. (1999). Relation of Lake Ontario fish consumption, lifetime lactation, and parity to breast milk polychlorobiphenyl and pesticide concentrations. *Environmental Research*, 80, S166-74.
- Kraft, M., Sievering, S., Grün, L., & Rauchfuss, K. (2018). Mono-, di-, and trichlorinated biphenyls (PCB 1-PCB 39) in the indoor air of office rooms and their relevance on human blood burden. *Indoor Air*, 28(3), 441–449.
- Kvalem, H. E., Nygaard, U.C., Lødrup, Carlsen, K.C., Carlsen, K.H., Haug L.S. & Granum B. (2020) Perfluoroalkyl substances, airways infections, allergy and asthma related health outcomes - implications of gender, exposure period and study design. *Environmental International*, 134,105259.
- Lapworth, D. J., Baran, N., Stuart, M. E., & Ward, R. S. (2012). Emerging organic contaminants in groundwater: A review of sources, fate and occurrence. *Environmental Pollution*, 163,287-303.
- Lau, C., Anitole, K., Hodes, C., Lai, D., Pfahles-Hutchens, A., Seed, J. (2004). Perfluoroalkly acids: a review of monitoring and toxicological findings. *Toxicology*, 34, 351-384.
- Lau, C., Thibodeaux, J. R., Hanson, R. G., Rogers, J. M., Grey, B. E., Stanton, M. E., et al. (2003). Exposure to Perfluorooctane Sulfonate during Pregnancy in Rat and Mouse. II: Postnatal Evaluation. *Toxicology & Science*, 74, 382–392.
- Lein, N. P. H., Fujii, S., Tanaka, S., Nozoe, M., & Tanaka, H. (2008). Contamination of perfluorooctane sulfonate (PFOS) and

perfluorooctanoate (PFOA) in surface water of the Yodo River basin (Japan). *Desalination*, 226(1-3), 338–347.

Leonard, R. C., Kreckmann, K. H., Sakr, C. J. & Symons, J. M. (2008). Retrospective cohort mortality study of workers in a polymer production plant including a reference population of regional workers. *Annals of Epidemiology*, 18, 15–22.

Li, F., Zhang, C., Qu, Y., Chen, J., Chen, L., Liu, Y., & Zhou, Q. (2010). Quantitative characterization of short- and long-chain perfluorinated acids in solid matrices in Shanghai, China. *Science of The Total Environment*, 408(3), 617–623.

Li, L., Arnot, J. A., & Wania, F. (2018). Revisiting the Contributions of Far- and Near-Field Routes to Aggregate Human Exposure to Polychlorinated Biphenyls (PCBs). *Environmental Science & Technology*, 52(12), 6974–6984.

Liang, S., Pierce Jr., R. D., Lin, H., Chiang, S.-Y. & Huang, Q.J. (2018). Electrochemical oxidation of PFOA and PFOS in concentrated waste streams, *Remediation*, 28, 127–134.

Liu G, Zhang B, Hu Y, Rood J, Liang L, Qi L, Bray GA, DeJonge L, Coull B, Grandjean P, Furtado JD, Sun Q. (2020). Associations of perfluoroalkyl substances with blood lipids and apolipoproteins in lipoprotein sub-species: The POUNDS-lost study. *Environmental Health*, 19, 5.

Liu, C., Wei, B. K., Bao, J. S., Wang, Y., Hu, J. C., Tang, Y. E., & Jin, J. (2019). Polychlorinated biphenyls in the soil–crop–atmosphere system in e-waste dismantling areas in Taizhou: Concentrations, congener profiles, uptake, and translocation. *Environmental Pollution*, 113622.

- Liu, J., Tan, Y., Song, E., & Song, Y. (2020). A Critical Review of Polychlorinated Biphenyls Metabolism, Metabolites and Their Correlation with Oxidative Stress. *Chemical Research in Toxicology*.
- Liu, X., Jin, Y., Liu, W., Wang, F. & Hao, S. (2011). Possible Mechanism of Perfluorooctane Sulfonate and Perfluorooctanoate on the Release of Calcium Ion from Calcium Stores in Primary Cultures of Rat Hippocampal Neurons. *Vitro Toxicology* 25, 1294–1301.
- Liu, Y., Li, X., Li, Q., Li, P., Wang, Y., Li, X., & Liang, X. (2010). Acute toxicity of perfluorooctane sulfonate (PFOS) to six freshwater algae. *Bulletin of Environmental Contamination and Toxicology*, 85(1), 59-63.
- Liu, Y.H., Wang, H.L., Jing, S.G., Gao, Y.Q., Peng, Y.R., Lou, S.R., Cheng, T.T., Tao, S.K., Li, L., Li, Y.J., Huang, 1315 D.D., Wang, Q., & An, J.Y. (2019). Characteristics and sources of volatile organic compounds (VOCs) in Shanghai during summer: Implications of regional transport. *Atmospheric Environment*, 215.
- Loos, R., Wollgast, J., Huber, T., & Hanke, G., (2008). Polar herbicides, pharmaceutical products, perfluorooctanesulfonate (PFOS), perfluorooctanoate (PFOA), and nonylphenol and its carboxylates and ethoxylates in surface and tap waters around Lake Maggiore in Northern Italy. *Analytical & Bioanalytical Chemistry*, 387, 1469–1478.
- Lorenzo, M., Campo, J., & Picó, Y., (2018). Analytical challenges to determine emerging persistent organic pollutants in aquatic ecosystems. *Trends in Analytical Chemistry*, 103, 137–155.

- Ludewig, G., & Robertson, L. W. (2013). Polychlorinated biphenyls (PCBs) as initiating agents in hepatocellular carcinoma. *Cancer Letters*, 334(1), 46–55.
- Luo, C., Hu, B., Wang, S., Wang, Y., Zhao, Z., Wang, Y., Li, J., & Zhang, G. (2020). Distribution and chiral signatures of polychlorinated biphenyls (PCBs) in soils and vegetables around an e-waste recycling site. *Journal of Agriculture & Food Chemistry*, 68 (39), pp. 10542-10549.
- Lyons, C. (2007). Stain Resistant, Nonstick, Waterproof, and Lethal: The Hidden Dangers of C8. Greenwood Publishing Group, Inc., USA, pp. 2–6.
- Ma, S.-H., Wu, M.-H., Tang, L., Sun, R., C. Zang, C., Xiang, J.-J., Yang, X.-X., Li, X. & Xu, G. (2017). EB degradation of perfluorooctanoic acid and perfluorooctane sulfonate in aqueous solution, *Nuclear Science & Technology*, 28, 137.
- Mahmood, A., Malik, R.N., Li, J., & Zhang, G., (2014a). Levels, distribution profile, and risk assessment of polychlorinated biphenyls (PCBs) in water and sediment from two tributaries of the River Chenab, Pakistan. *Environmental Science & Pollution Control Service*, 21, 7847e7855.
- Mak, Y. L., Taniyasu, S., Yeung, L.W.Y., Lu, G., Jin, L., Yang, Y., Lam, P.K.S., Kannan, K. & Yamashita, N. (2008). Perfluorinated compounds in tap water from China and several other countries, *Environmental Science & Technology*, 43, 4824–4829.

Malisch, R., & Kotz, A. (2014). Dioxins and PCBs in feed and food — Review from European perspective. *Science of The Total Environment*, 491-492, 2–10.

Mamontova, E. A., Tarasova, E. N., Mamontov, A. A., Kuzmin, M. I., McLachlan, M. S., & Khomutova, M. I. (2007). The influence of soil contamination on the concentrations of PCBs in milk of Siberia. *Chemosphere*, 67, S71–S78.

Mao, S., Liu, S., Zhou, Y., An, Q., Zhou, X., Mao, Z., & Liu, W. (2020). The occurrence and sources of polychlorinated biphenyls (PCBs) in agricultural soils across China with an emphasis on unintentionally produced PCBs. *Environmental Pollution*, 116171.

Martinsson M, Nielsen C, Bjork J, Rylander L, Malmqvist E, Lindh C, Rignell-Hydbom A. 2020. Intrauterine exposure to perfluorinated compounds and overweight at age 4: A case-control study. *Public Library of Science One*, 15: e0230137.

McFarland, V.A. & Clarke, J.U. (1989). Environmental occurrence, abundance, and potential toxicity of polychlorinated biphenyl congeners: considerations for a congener-specific analysis. *Environmental Health Perspectives* 81, 225–239.

Megahed, A. M., Dahshan, H., Abd-El-Kader, M. A., Abd-Elall, A. M. M., Elbana, M. H., Nabawy, E., & Mahmoud, H. A. (2015). Polychlorinated Biphenyls Water Pollution along the River Nile, Egypt. *The Scientific World Journal*, pp 1–7.

- Megson, D., Benoit, N., Sandau, C., Chaudhuri, S., Long, T., Coulthard, E., & Johnson, G. (2019). Evaluation of the effectiveness of different indicator PCBs to estimating total PCB concentrations in environmental investigations. *Chemosphere*, 124429.
- Meili, M., Jonsson, P., & Carman, R. (2000). PCB Levels in Laminated Coastal Sediments of the Baltic Sea along Gradients of Eutrophication Revealed by Stable Isotopes ($\delta^{15}\text{N}$, $\delta^{13}\text{C}$). *AMBIO: A Journal of the Human Environment*, 29(4), 282–287.
- Merino, N., Qu, Y., Deeb, R.A., Hawley, E.L., Hoffmann, M. R. & Mahendra, S. (2016). Degradation and removal methods for perfluoroalkyl substances in water, *Environmental Engineering & Science*, 33, 615–649.
- Michalska, A., Krolicka, A., & Sadowska, M. (2017). Ion-selective electrodes in environmental analysis. *Trends in Analytical Chemistry*, 88, 85-98.
- Min, J. Y., Lee, K. J., Park, J. B., Min, K. B. (2012). Perfluorooctanoic acid exposure is associated with elevated homocysteine and hypertension in US adults. *Occupational and Environmental Medicine*, 69, 658–662.
- Ministry of Works and Housing (MWH) (1998). Water Resources Management (WARM) Study-Information Building Block. Accra.
- Moody, C. A., Kwan, W. C., Martin, J. W., Muir, D. C. G., Mabury, S. A. (2001). Determination of perfluorinated surfactants in surface water samples by two independent analytical techniques: liquid chromatography/tandem mass spectrometry and ^{19}F NMR. *Analytical Chemistry*, 73, 2200–2206.

- Moody, C. A., Hebert, G. N., Strauss, S. H. & Field, J. A. (2003). Occurrence and persistence of perfluorooctanesulfonate and other perfluorinated surfactants in groundwater at a fire-training area at Wurtsmith Air Force Base, Michigan, USA Electronic supplementary information (ESI) available: Map of location of Wurtsmith Air Force Base, Oscoda, MI and surrounding states. *Journal of Environmental Monitoring*, 5(2), 341–345.
- Moon, H.-B., Kannan, K., Choi, H.-G., An, Y.-R., Choi, S.-G., Park, J.-Y., & Kim, Z.-G. (2010). Concentrations and accumulation features of PCDDs, PCDFs and dioxin-like PCBs in cetaceans from Korean coastal waters. *Chemosphere*, 79(7), 733–739.
- Moriwaki, M., Takagi, Y., Tanaka, M., Tsuruho, K., Okitsu, K. & Maeda, Y. (2006). Sonochemical decomposition of perfluorooctane sulfonate and perfluorooctanoic acid, *Environmental Science & Technology*, 39, 3388–3392.
- Nakata, H., Kawazoe, M., Arizono, K., Abe, S., Kitano, T., Shimada, H., et al., (2002). Organochlorine pesticides and polychlorinated biphenyl residues in foodstuffs and human tissues from China: status of contamination, historical trend, and human dietary exposure. *Archives of Environmental Contamination & Toxicology*, 43, 473–480.
- Nakayama, K., Iwata, H., Tao, L., Kannan, K., Imoto, M., Kim, E.-Y., ... Tanabe, S. (2008). Potential effects of perfluorinated compounds in common cormorants from lake biwa, japan: an implication from the

hepatic gene expression profiles by microarray. *Environmental Toxicology and Chemistry*, Vol. 27, No. 11, pp. 2378–2386, 2008.

National Toxicology Program NTP. (2006). Toxicology and Carcinogenesis Studies of 3,3',4,4',5-Pentachlorobiphenyl (PCB 126) (CAS No. 57465-28-8) in Female Harlan Sprague-Dawley Rats (Gavage Studies) *National Toxicology Program Technical Report Service*. 520, 4–246.

National Toxicology Program. (2020a). NTP Technical Report on the Toxicology and Carcinogenesis Studies of Perfluorooctanoic Acid (CAS No. 335-67-1) Administered in Feed to Sprague Dawley (Hsd: Sprague Dawley® SD®) Rats. Research Triangle Park, North Carolina, USA. No. Technical Report 598.

Neira, C., Vales, M., Mendoza, G., Hoh, E. & Levin, L. A. (2018). Polychlorinated biphenyls (PCBs) in recreational marina sediments of San Diego Bay, southern California. *Marine Pollution Bulletin*, 126, 204-214.

Niegowska, M.Z., Preto, P., Porcel Rodriguez, E., Marinov, D., Ceriani, & Lettieri, T. (2021). Per- and polyfluoroalkyl substance (PFAS) of possible concern in the aquatic environment, EUR 30710 EN, Publication Office of the European Union, Luxembourg.

Ntow, W. (2001). Organochlorine Pesticides in Water, Sediment, Crops, and Human Fluids in a Farming Community in Ghana. *Archives of Environmental & Contamination Toxicology*, 40, 557–563.

OECD (2021). Reconciling Terminology of the Universe of Per- and Polyfluoroalkyl Substances: Recommendations and Practical Guidance. Paris, France: OECD Series on Risk Management. No. 61.

Oliveira Ribeiro, C. A., Vollaire, Y., Sanchez-Chardi, A., & Roche, H. (2005). Bioaccumulation and the effects of organochlorine pesticides, PAH and heavy metals in the Eel (*Anguilla anguilla*) at the Camargue Nature Reserve, France. *Aquatic Toxicology*, 74, 53–69.

Olsen, G. W., Burris, J. M., Burlew, M. M., & Mandel, J. H. (2003). Epidemiologic assessment of worker serum perfluorooctanesulfonate (PFOS) and perfluorooctanoate (PFOA) concentrations and medical surveillance examinations. *Journal of Occupational & Environmental Medicine*, 45, 260–270.

Olsen, G. W., Zobel, L. R. (2007). Assessment of lipid, hepatic, and thyroid parameters with serum perfluorooctanoate (PFOA) concentrations in fluorochemical production workers. *International Archives of Occupational & Environmental Health*, 81, 231–246.

Organisation for Economic Co-operation and Development (OECD). (2002). Hazard assessment of perfluorooctane sulfonate (PFOS) and its salts. Report ENV/JM/ RD (2002)17/FINAL.

Organization for Economic Co-operation and Development(OECD). (2007). Report of an OECD Workshop on Perfluorocarboxylic Acids (PFCAs) and Precursors. ENV/JM/MONO (2007)11.

Palmer, M. P., Wilson, L. R., Casey, A. C., & Wagner, R. E. (2011). Occurrence of PCBs in raw and finished drinking water at seven public water

systems along the Hudson River. *Environmental Monitoring & Assessment*, 175(1-4), 487-99.

Parkinson, A., Robertson, L. W., Safe, L., & Safe, S. (1981). Polychlorinated biphenyls as inducers of hepatic microsomal enzymes: Effects of di-ortho substitution. *Chemico-Biological Interactions*, 35(1), 1–12.

Patel, J. F., Hartman, T.J., Sjodin, A., Northstone, K., & Taylor, E.V. (2018). Prenatal exposure to polychlorinated biphenyls and fetal growth in British girls. *Environment International*, 116, 116-121.

Patisaul, H. (2009). Long-term effects of environmental endocrine disruptors on reproductive physiology and behavior. *Frontiers in Behavioral Neuroscience*, 3.

Paul, A. G., Jones, K.C. & Sweetman, A. J. (2009). A first global production, emission and environmental inventory for perfluorooctane sulfonate. *Environmental Science & Technology*, 43 (2), 386-392.

Persoon C., Peters T.M., Kumar N., & Hornbuckle K.C. (2010). Spatial Distribution of Airborne Polychlorinated Biphenyls in Cleveland, OH and Chicago, IL. *Environmental Science & Technology*, 44, 2797–2802.

Pessah, I.N., Hansen, L.G., Albertson, T.E., Garner, C.E., Ta, T.A., Do, Z., Kim, K.H., & Wong, P.W., (2006). Structure– activity relationship for noncoplanar polychlorinated biphenyl congeners toward the ryanodine receptor-Ca²⁺ channel complex type 1 (RyR1). *Chemical Research & Toxicology*, 19 (1), 92–101.

Petruelis, J.R., & N.J. Bunce. (2000). Competitive behavior in the interactive toxicology of halogenated aromatic compounds. *Journal of Biochemistry & Molecular Toxicology*, 14(2), 73-81.

Pietrzak-Fiecko R, Smoczynska K. & Smoczynski, S.S (2005). Polychlorinated biphenyls in human milk, UHT cow's milk, and infant formulas. *Pollution Journal of Environmental Studies*, 14(2), 237–24.

Pignotti, E., Casas, G., Llorca, M., Tellbüscher, A., Almeida, D., Dinelli, E.& Barceló, D. (2017). Seasonal variations in the occurrence of perfluoroalkyl substances in water, sediment and fish samples from Ebro Delta (Catalonia, Spain). *Science of The Total Environment*, 607-608, 933–943.

Pihlström, T., (2011). Method validation and quality control procedures for pesticide residue analysis in food and feed. Document No. SANCO/12495/2011. <http://www.crlpesticides.eu/library/docs/fv/SANCO12495-2011.pdf>. Accessed on 15th September, 2021.

Prevedouros, K., Cousins, I. T., Buck, R. C. & Korzieniowski, S. H. (2006). Sources, fate and transport of perfluorocaboxyaltes. *Environmental Science & Technology*, 40(1), 32-44.

Qiu, C., Cochran, J., Smuts, J., Walsh, P., & Schug, K. A. (2017). Gas chromatography-vacuum ultraviolet detection for classification and speciation of polychlorinated biphenyls in industrial mixtures. *Journal of Chromatography A*, 1490, 191–200.

Rashid, F., Ramakrishnan, A., Fields, C. & Irudayaraj, J. (2020). Acute PFOA exposure promotes epigenomic alterations in mouse kidney tissues. *Toxicology Report*, 7,125-132.

Rayne, S., & Forest, K. (2009). Perfluoroalkyl sulfonic and carboxylic acids: a critical review of physicochemical properties, levels and patterns in

waters and wastewaters, and treatment methods, *Journal of Environmental Science & Health*, A 44, 1145–1199.

Robertson, L. W. & Hansen, L. G. (2001). "PCBs: Recent Advances in Environmental Toxicology and Health Effects". *Medicine and Health Sciences*. 8. Retrieved from: https://uknowledge.uky.edu/upk_medicine_and_health_sciences/8. Accessed on 25th June, 2023.

Rodenburg, L. A., Du, S., Fennell, D. E., & Cavallo, G. J. (2010). Evidence for Widespread Dechlorination of Polychlorinated Biphenyls in Groundwater, Landfills, and Wastewater Collection Systems. *Environmental Science & Technology*, 44(19), 7534–7540.

Rostkowski P, Yamashita N, So I M K, Taniyasu S, Lam P K S, Falandysz J, Lee K T, Kim S K, Kjim J S, Im S H, & Newsted J L. (2006). Perfluorinated compounds in streams of the Shihwa industrial zone and Lake Shihwa, South Korea. *Environmental Toxicology & Chemistry*, 25, 2374–2380.

Rushneck, D. R., Beliveau, A., Fowler, B., Hamilton, C., Hoover, D., Kaye, K., & Ryan, L. (2004). Concentrations of dioxin-like PCB congeners in unweathered Aroclors by HRGC/HRMS using EPA Method 1668A. *Chemosphere*, 54(1), 79–87.

Saba, T., & Boehm, P. D. (2011). Quantitative Polychlorinated Biphenyl (PCB) Congener and Homologue Profile Comparisons. *Environmental Forensics*, 12(2), 134–142.

- Safe, S. (1993). Toxicology, structure-function relationship, and human and environmental health impacts of polychlorinated biphenyls: progress and problems, *Environmental Health Perspectives*, 100 (1993) 259.
- Safe, S., Bandiera, S., Sawyer, T., Robertson, L., Safe, L., Parkinson, A., Thomas, P. E., Ryan, D. E., Reik, L. M., & Levin, W. (1985) PCBs: Structure-function relationships and mechanism of action. *Environmental Health Perspectives*, 60, 47-56.
- Safe, S., Safe, L. & Mullin, M. (1985). Polychlorinated biphenyls: congener-specific analysis of a commercial mixture and a human milk extract. *Journal of Agriculture & Food Chemistry*, 33, 24-9.
- Safe, SH (1998). Development validation and problems with the toxic equivalency factor approach for risk assessment of dioxins and related compounds. *Journal of Animal Science*, 76, 134-141.
- Saito, N., Harada, K., Inoue, K., Sasaki, Y., Yoshinaga, T., Koizumi, A. (2004). Perfluorooctanoate and perfluorooctane sulfonate concentrations in surface water in Japan. *Journal of Occupational Health*, 46, 49-59.
- Sakuma, A., Wasada, Ochi H, Yoshioka, M., Yamanaka, N., Ikezawa, M & Guruge, K. S. (2019). Changes in hepato-renal gene expression in microminipigs following a single exposure to a mixture of perfluoroalkyl acids. *Public Library of Science One*, 14(1):e0210110.
- Salinas, R. O., Bermudez, B. S., Tolentino, R. G., Gonzalez, G. D., & León, S. V. Y. (2010). Presence of Polychlorinated Biphenyls (PCBs) in Bottled Drinking Water in Mexico City. *Bulletin of Environmental Contamination and Toxicology*, 85(4), 372-376.

Sammut, G., Sinagra, E., Sapiano, M., Helmus, R., & de Voogt, P. (2019). Perfluoroalkyl substances in the Maltese environment – (II) sediments, soils and groundwater. *Science of The Total Environment*.682, pp. 180 – 189.

Sasaki, S., Braimoh, T.S., Yila, T.A., Yoshioka, E. & Kishi, R. (2011). Self-reported tobacco smoke exposure and plasma cotinine levels during pregnancy—a validation study in northern Japan. *Science of the Total Environment*, 412, pp. 114-118,

Schechter A., Colacino J., Haffner D., Patel K., Opel M., Pöpke O., & Birnbaum L. (2010). Perfluorinated Compounds, Polychlorinated Biphenyls, and Organochlorine Pesticide Contamination in Composite Food Samples from Dallas, Texas, USA. *Environmental Health Perspective*, 118,796.

Schwarzenbach, R., Gschwend, P., & Imboden, D. (eds). (2016). Environmental organic chemistry, 3rd edition. Wiley, New York. ISBN 978-1-118-76723-8.

Sebugere, P., Sillanpää, M., Kiremire, B. T., et al., (2014). “Polychlorinated biphenyls and hexachlorocyclohexanes in sediments and fish species from the Napoleon Gulf of Lake Victoria, Uganda,” *Science of the Total Environment*, 481(1), pp. 55–60.

Shankar, A, Xiao, J., & Ducatman, A. (2011). Perfluoroalkyl chemicals and elevated serum uric acid in US adults. *Clinical Epidemiology*, 3, 251–258.

Shao, Y., Han, S., Ouyang, J. et al. (2016). Organochlorine pesticides and polychlorinated biphenyls in surface water around Beijing. *Environmental Science & Pollution Research*, 23, 24824-24833.

Sharifan, H., Bagheri, M., Wang, D., Burken, J. G., Higgins, C. P., Liang, Y., Liu, J., Schaefer, C. E., & Blotvogel, J. (2021). Fate and transport of per- and polyfluoroalkyl substances (PFASs) in the vadose zone. *Science of the Total Environment*, 771, 145427.

Shi, R. Mao, R. Y. Zhang, M. Lü, Y. L. Song, S. & Zhao, J. X. (2021). Distribution, Sources, and Ecological Risks of Polyfluoroalkyl Substances in the Surface Water of the Wuliangshai Watershed. *Huan Jing Ke Xue*. 42(2), 663-672.

Shoeib, M., Harner, T., Wilford, B. H, Jones, K. C., & Zhu, J. (2005). Perfluorinated sulfonamides in indoor and outdoor air and indoor dust: occurrence, partitioning, and human exposure. *Environmental Science & Technology*, 39, 6599–6606.

Sinclair E & Kannan K. (2006) Mass loading and fate of perfluoroalkyl surfactants in wastewater treatment plants. *Environmental. Science & Technology*, 40,1408–1414.

Sinclair, E., Mayack, D. T., Roblee, K., Yamashita, N. & Kannan, K. (2006). Occurrence of perfluoroalkyl surfactants in water, fish and birds from New York State. *Archives of Environmental & Contamination Toxicology*, 50, 398–410.

Skutlarek, D., Exner, M., & Färber, H. (2006). Perfluorinated surfactants in surface and drinking waters. *Environmental Science & Pollution Research*, *13*, 299–307.

So, M. K., Miyake, Y., Yeung, W. Y., Ho, Y. M., Taniyasu, S., Rostkowski, P., Yamashita, N., Zhou, B.S., Shi, X.J., Wang, J.X., Giesy, J.P., Yu, H. & Lam, P.K.S. (2007). Perfluorinated Compounds in the Pearl River and Yangtze River of China. *Chemosphere*, *68*, 2085-2095.

So, M.K., Yamashita, N., Taniyasu, S., Jiang, Q., Giesy, J.P., Chen, K., & Lam, P.K.S. (2006). Health risks in infants associated with exposure to perfluorinated compounds in human breast milk from Zhoushan China. *Environmental Science & Technology*, *40*, 2924–2929.

Squadrone, S., Brizio, P., Nespoli, R., Stella, C., & Abete, M.C., 2015. Human dietary exposure and levels of polychlorinated dibenzo-p-dioxins (PCDDs), polychlorinated dibenzofurans (PCDFs), dioxin-like polychlorinated biphenyls (DL-PCBs) and non-dioxin-like polychlorinated biphenyls (NDL-PCBs) in free-range eggs close to a secondary aluminum smelter, northern Italy. *Environmental Pollution*, *206*, 429–436.

Stanifer, J. W., Stapleton, H. M., Souma, T., Wittmer, A., Zhao, X. & Boulware L.E. (2018). Perfluorinated Chemicals as Emerging Environmental Threats to Kidney Health: A Scoping Review. *Clin J Am Soc Nephrol*. *13*(10):1479-1492.

Steenland, K., Fletcher, T. & Savitz, D. A. (2010). Epidemiologic evidence on the health effects of perfluorooctanoic acid (PFOA). *Environmental Health Perspective, 118*, 1100–1108.

Stewart P.W., Lonky E., Reihman J., Pagano J., Gump B.B., & Darvill T. (2008). The Relationship between Prenatal PCB Exposure and Intelligence (IQ) in 9-Year-Old Children. *Environmental Health Perspectives. 116*, 1416–1422.

Stewart A, Jones KC (1996) A survey of PCB in U. K. cows' milk. *Chemosphere 32*(12), 2481–2492.

Szajdzińska-Piętek, E. & Gębicki, J. L. (2000). Pulse radiolytic investigation of perfluorinated surfactants in aqueous solutions, *Research Chemistry Intermediates 26*, 897–912,

Takino, M., Daishima, S., Nakahara, T., (2003). Determination of perfluorooctane sulfonate in river water by liquid chromatography/atmospheric pressure photoionization mass spectrometry by automated on-line extraction using turbulent flow chromatography. *Rapid Communication and Mass Spectrometry, 17* (5), 383–390.

Tan, K.-Y., Lu, G.-H., Yuan, X., Zheng, Y., Shao, P.-W., Cai, J.-Y. & Yang, Y.-L. (2018). Perfluoroalkyl Substances in Water from the Yangtze River and Its Tributaries at the Dividing Point Between the Middle and Lower Reaches. *Bulletin of Environmental Contamination and Toxicology. 101*(5), 598-603.

Taniyasu, S., Kannan, K., Horii, Y., Hanari, N., & Yamashita, N. (2003). A survey of perflourooctane sulfonate and related perfluorinated organic

compounds in water, fish, birds, and humans from Japan. *Environmental Science & Technology*, 37, 2634–2639.

Taniyasu, S., Kannan, K., So, M. K., Gulkowska, A., Sinclair, E., Okazawa, T., Yamashita, N. (2005). *Journal of Chromatography*, 1093(89).

Tetko, I. V., & Villa, A. E. P. (1997). Efficient Partition of Learning Data Sets for Neural Network Training. *Neural Networks* 10, 1361-1374.

Tiernan, T. O., Taylor, M. L., Garrett, J. H., VanNess, G. F., Solch, J. G., Deis, D. A. & Wagel, D. J. (1983). Chlorodibenzodioxins, chlorodibenzofurans and related compounds in the effluents from combustion processes. *Chemosphere*, 12, 595-606.

Tittlemier, S.A., Pepper, K., Seymour, C., Moisey, J., Bronson, R., Cao, X. L., *et al.* (2007). Dietary exposure of Canadians to perfluorinated carboxylates and perfluorooctane sulfonate via consumption of meat, fish, fast foods, and food items prepared in their packaging. *Journal of Agriculture & Food Chemistry*, 55, pp. 3203-3210.

Trojanowicz, M., Bartosiewicz, I., Bojanowska-Czajka, A., Kulisa, K. Szreder, T., Bobrowski, K., Garcia-Reyes, J.F., Naęcz-Jawecki, G., Męczyńska-Wielgosz, S., Nichipor, H. & Kisała, J. (2019). Application of ionizing radiation in decomposition of perfluorooctanoate (PFOA) in waters, *Journal of Chemical Engineering*, 357, 698–714.

Trojanowicz, M., Bobrowski, K., Szreder, T. & Bojanowska-Czajka, A.(2018b). Gamma-ray, X-ray and electron beam processes as an advanced oxidation process, in: S. Ameta, R. Ameta (Eds.), *Advanced Oxidation Processes for Wastewater Treatment*, Elsevier, pp. 257–331.

Trojanowicz, M., Bojanowska-Czajka, A., Bartosiewicz, I. & Kulisa, K. (2018a). Advanced Oxidation/Reduction Processes treatment for aqueous perfluorooctanoate (PFOA) and perfluorooctanesulfonate (PFOS) – A review of recent advances, *Journal of Chemical Engineering*, 336, 170–199.

U.S. Environmental Protection Agency 2020). Draft Interim Guidance for addressing PFAS in Soil, Sediment, and other Media. Retrieved from: <https://www.epa.gov/pfas/draft-interim-guidance-addressing-pfas-soil-sediment-and-other-media> -media. Accessed on 6th December, 2022.

U.S. Environmental Protection Agency. (2002). Framework for ecological risk assessment. EPA/630/R-02/002.

U.S. Environmental Protection Agency. (2018). Method 340.2: Determination of Total and Dissolved Fluoride in Ambient Water Samples by Ion-Selective Electrode. In *Methods for Chemical Analysis of Water and Wastes* (EPA/600/R-18/001). Office of Research and development.

U.S. EPA. (2000) Supplementary Guidance for Conducting Health Risk Assessment of Chemical Mixtures. EPA 630/R-00/002. Washington, DC: U.S. Environmental Protection Agency, Risk Assessment Forum.

UNEP (2009). Report of the Conference of the Parties of the Stockholm Convention on Persistent Organic Pollutants on the Work of its Fourth Meeting Presented at the United Nations Environment Programme: *Stockholm Convention on Persistent Organic Pollutants*. Geneva, 1–112.

UNEP/IPCS. (1999). Chemical risk assessment. World Health Organization (WHO). Retrieved from: https://apps.who.int/iris/bitstream/handle/10665/66398/WHO_PCS_99.2_eng.pdf;jsessionid=37A71C68BB2117009E068CC1F51B22D4?sequence=1. Accessed on 7th September, 2023.

United Kingdom Food standards agency, chemical safety division. (2006). Fluorinated chemicals: UK dietary intakes. Food survey information sheet 11/06, London.

United Nations Environment Programme (UNEP). (2009). The New POPs Under the Stockholm Convention. Retrieved from: <http://chm.pops.int/Convention/ThePOPs/TheNewPOPs/tabid/2511/Default.aspx>. Accessed on 10th July, 2022.

United States Environmental Protection Agency (2006). SAB review of EPA's draft risk assessment of the potential human health effects associated with exposure to perfluorooctanoic acid and its salts (EPA – SAB-06-006). Office of pollution prevention and Toxics RAD. Retrieved from: <http://www.epa.gov/opptintr/pfoa/pubs/pfoarisk.pdf>. Accessed on 25th March, 2023.

United States Environmental Protection Agency (USEPA). (2020). Per- and Polyfluoroalkyl Substances (PFAS). Retrieved from: <https://www.epa.gov/pfas>. Accessed on 8th August, 2023.

United States Environmental Protection Agency. (2021). Sediment Quality Criteria for PFAS. Retrieved from: <https://www.epa.gov/wgc/sediment-quality-criteria-pfas>.

United States Environmental Protection Agency. (2022). Fact Sheet: 2010/2015 PFOA Stewardship Program. Retrieved from: <https://www.epa.gov/assessing-and-managing-chemicals-under-tsca/fact-sheet-20102015-pfoa-stewardship-program>. Accessed on 9th September, 2022.

United States Geological Survey (USGS) (2019). PFAS in the Nation's Streams and Rivers. Retrieved from:

USEPA. (1989). (US Environmental Protection Agency). Risk Assessment Guidance for Superfund (RAGS), vol 1, Human Health Evaluation Manual (Part A). OWSER Directive 9285 7-01A. EPA-540/1-89-002. Office of Emergency and Remedial Response Washington, DC, USA.

Valsecchi, S., Babut, M., Mazzoni, M., Pascariello, S., Ferrario, C., De Felice, B., Polesello, S. (2020). Perfluoroalkyl Substances (PFAS) in Fish from European Lakes: Current Contamination Status, Sources, and Perspectives for Monitoring. *Environmental Toxicology and Chemistry*, 40(3),658-676.

Van den Berg, M., Birnbaum, L. S., Denison, M., De Vito, M., Farland, W., Feeley, M., et al. (2006). The 2005 World Health Organization re-evaluation of human and mammalian toxic equivalency factors for dioxins and dioxin-like compounds. *Toxicology & Science*, 93, 223–41.

Vecitis, C. D., Park, H., Cheng, J., Mader, B.T. & Hoffmann, M.R. (2009). Treatment technologies for aqueous perfluorooctanesulfonate (PFOS) and perfluorooctanoate (PFOA), *Frontiers of Environmental Science & Engineering China* 3, 129–151.

- Vierke, L., Staude, C., Biegel-Engler, A., & Wagner, M. (2018). Occurrence, fate and effects of perfluoroalkyl and polyfluoroalkyl substances (PFAS) in groundwater: A review. *Emerging Contaminants*, 4, 245-267.
- Wan, H. T., Zhao, Y. G., Wei, X., Hui, K.Y., Giesy, J. P. & Wong CK. (2012). PFOS-induced hepatic steatosis, the mechanistic actions on beta-oxidation and lipid transport. *Biochim Biophys Acta*. 1820(7), 1092-1101.
- Wang, J., Liu, X., Li, Y., Powell, T., Wang, X., Wang, G., & Zhang, P. (2019). Microplastics as contaminants in the soil environment: A mini-review. *Science of Total Environment*, 691, 848-857.
- Wang, L., Wang, Y., Liang, Y., Li, J., Liu, Y., Zhang, J., Zhang, A., Fu, J. & Jiang, G. (2013). Specific accumulation of lipid droplets in hepatocyte nuclei of PFOA-exposed BALB/c mice. *Sci Rep*. 3:2174.
- Wang, S., Wang, Q., Chen, F., Sun, J., Luo, K., Yao, F., Wang, X., Wang, D., Li, X. & Zeng, G. (2017). Photocatalytic degradation of perfluorooctanoic acid and perfluorooctane sulfonate in water; A critical review, *Journal of Chemical Engineering*, 328, 927–942.
- Wang, W., Bai, J., Zhang, G., Jia, J., Wang, X., Liu, X., & Cui, B. (2019). Occurrence, sources and ecotoxicological risks of polychlorinated biphenyls (PCBs) in sediment cores from urban, rural and reclamation-affected rivers of the Pearl River Delta, China. *Chemosphere*, 218, 359–367.
- Wang, X., Lin, Y., Wang, C., Zhang, M., Chen, J., Liu, Y., & Wang, Z. (2016). Toxicity of perfluoropentanoic acid on freshwater green algae

Raphidocelis subcapitata and Chlorella vulgaris. *Journal of Environmental Sciences*, 43, 86-92.

Wang, Z., DeWitt, J. C., Higgins, C. P., & Cousins, I. T. (2017). *A Never-Ending Story of Per- and Polyfluoroalkyl Substances (PFASs)?* *Environmental Science & Technology*, 51(5), 2508–251.

Washburn, S. T., Bingman, T. S., Braithwaite, S. K., Buck, R. C., Buxton, L. W., Clewell, H. J., ... Shipp, A. M. (2005). Exposure Assessment and Risk Characterization for Perfluorooctanoate in Selected Consumer Articles. *Environmental Science & Technology*, 39(11), 3904–3910.

Water Resources Commission (WRC) (2012). National Integrated Water Resources Management (IWRM) Plan. Water Resources Commission, Ministry of Water Resources Works and Housing, Accra.

Water Resources Commission (WRC) (2022). Pra River Basin - Integrated Water Resources Management Plan. Retrieved from: http://doc.wrc-gh.org/pdf/Pra_Basin_IWRM_Plan.pdf. Accessed on 11th July, 2023.

Weintraub, M., & Birnbaum, L. S. (2008). Catfish consumption as a contributor to elevated PCB levels in a non-Hispanic black subpopulation. *Environmental Research*, 107(3), 412–417.

Wen, L. L., Lin, C. Y., Chou, H. C., Chang, C. C., Lo, H. Y. & Juan, S. H. (2016). Perfluorooctanesulfonate Mediates Renal Tubular Cell Apoptosis through PPAR γ Inactivation. *PLoS One*. 11(5): e0155190.

Westerhoff, P., Yoon, Y., Snyder, S., & Wert, E. (2005). Fate of Endocrine-Disruptor, Pharmaceutical, and Personal Care Product Chemicals during

Simulated Drinking Water Treatment Processes. *Environmental Science & Technology*, 39(17), 6649–6663.

Wilkinson, J., Hooda, P. S., Barker, J., Barton, S., & Swinden, J. (2017). Occurrence, fate and transformation of emerging contaminants in water: An overarching review of the field. *Environmental Pollution*, 231, 954–970.

World Health Organization. (2021). PFAS in drinking-water. Retrieved from: <https://www.who.int/news-room/fact-sheets/detail/pfas-in-drinking-water>. Accessed on 15th November, 2022

Xu, M., Liu, G., Li, M., Huo, M., Zong, W. & Liu, R. (2020a). Probing the Cell Apoptosis Pathway Induced by Perfluorooctanoic Acid and Perfluorooctane Sulfonate at the Subcellular and Molecular Levels. *Journal of Agriculture & Food Chemistry*, 68(2), 633-641.

Yamashita, N., Kannan, K., Taniyasu, S., Horii, Y., Okazawa, T., Petrick, G. & Gamo, T. (2004). Analysis of Perfluorinated Acids at Parts-Per-Quadrillion Levels in Seawater Using Liquid Chromatography-Tandem Mass Spectrometry. *Environmental Science & Technology*, 38, 5522-5528.

Yang, Y., Xie, Q., Liu, X., & J. Wang, J. (2015). “Occurrence, distribution and risk assessment of polychlorinated biphenyls and polybrominated diphenyl ethers in nine water sources,” *Ecotoxicology & Environmental Safety*, 115, pp. 55–61.

Ye, X., Kato, K., Wong, L.-Y., Jia, T., Kalathil, A., Latremouille, J., & Calafat, A. M. (2018). Per- and polyfluoroalkyl substances in sera from children 3 to 11 years of age participating in the National Health and Nutrition

Examination Survey 2013–2014. *International Journal of Hygiene & Environmental Health*, 221(1), 9–16.

Yue R. (2008). Additional information on production and use of PFOS.

Retrieved from: http://chm.pops.int/Portals/0/Repository/addinfo/2008/UNEP-POPS-POPRC-SUB-F08-PFOS-ADIN-CHI_English.pdf.

Accessed on 9th April, 2022.

Zhang, H., He, J., Li, N., Gao, N., Du, Q., Chen, B., Chen, F., Shan, X., Ding, Y. & Zhu, W. et al. 2019. Lipid accumulation responses in the liver of *Rana nigromaculata* induced by perfluorooctanoic acid (PFOA). *Ecotoxicology & Environmental Safety*. 167, 29-35.

Zhang, Z., Chen, J., Lyu, X. Yin, H. & Sheng, G. (2014). Complete mineralization of perfluorooctanoic acid (PFOA) by γ -irradiation in aqueous solution, *Scientific Reports*, 4–7418.

Zhou, S., Di Paolo, C., Wu, X., Shao, Y., Seiler, T.-B., & Hollert, H. (2019). Optimization of screening-level risk assessment and priority selection of emerging pollutants – The case of pharmaceuticals in European surface waters. *Environment International*, 128, 1–10.

Zushi, Y., Hogarth, J. N., & Masunaga, S. (2011). Progress and perspective of perfluorinated compound risk assessment and management in various countries and institutes. *Clean Technologies and Environmental Policy*, 14(1), 9–20.

APPENDICES
APPENDIX A

PFAS analysed in this study with their abbreviations and names of suppliers of their standards

Classification	Abbreviation	Compound name	Supplier of standard and its purity	IS for quantitation		
(perfluoroalkyl carboxylic acids)	PFBA	Perfluorobutanoic acid	Tokyo Chemical	[¹³ C ₂]PFHxA		
	PFPeA	Perfluoropentanoic acid	Ind., 98%			
	PFHxA	Perfluorohexanoic acid	Tokyo Chemical Ind., 98%			
		PFHpA	Perfluoroheptanoic acid	Wako Pure Chemical Ind., 98%	–	
		[¹³ C ₂]PFHxA	Perfluoro-n-[1,2- ¹³ C ₂] hexanoic acid	Wellington Laboratories, 98%		
		PFOA	Perfluorooctanoic acid	Wako Pure Chemical Ind., 95%		
		PFNA	Perfluorononanoic acid	Wako Pure Chemical Ind., 98%		
		PFDA	Perfluorodecanoic acid	Wako Pure Chemical Ind., 98%		[¹³ C ₄] PFOA
		[¹³ C ₄] PFOA	Perfluoro-n-[1,2,3,4- ¹³ C ₄] octanoic acid	Wellington Laboratories, 98%		–
		PFUnDA	Perfluoroundecanoic acid	Wako Pure Chemical Ind., 96%		[¹³ C ₂] PFDoDA
		PFDoDA	Perfluorododecanoic acid	Wako Pure Chemical Ind., 97%		
		PFTTrDA	Perfluorotridecanoic acid	Aldrich, 97%		
		PFTeDA	Perfluorotetradecanoic acid	Fluorochem, 96%		
	[¹³ C ₂]PFDoDA	Perfluoro-n-[1,2- ¹³ C ₂] dodecanoic acid	Wellington Laboratories, 98%	–		
PFSAs (Perfluoroalkane sulphonic acids)	PFBS	Perfluorobutane sulphonic acid	Tokyo Chemical Ind., 98%	[¹³ C ₄]PFOS		
	PFHxS	Perfluorohexane sulphonic acid	Wellington Laboratories, 98%			
	PFOS	Perfluorooctane sulphonic acid	Kanto Chemical, 98%			
	PFDS	Perfluorodecane sulphonic acid	Wellington Laboratories, 98%			
Solvent	[¹³ C ₄]PFOS	Perfluoro[1,2,3,4- ¹³ C ₄]octane sulphonic acid	Wellington Laboratories, 98%	–		
		Ammonium hydroxide	Wako Pure Chemical Ind., 25%			
		Ammonium acetate	Wako Pure Chemical Ind., 97%			
		Methanol	Wako Pure Chemical, Ind.,			

(Source: Laboratory Analysis, 2021)

APPENDIX B

Detection Frequency of PFAS in the Pra River Basin Based on the 8 Detected PFAS

Sampling location	Water (%)		Sediment (%)	
	AS	ND	AS	ND
P1	100	100	100	100
P2	88.9	88.9	88.9	88.9
P3	62.5	88.9	75	62.5
P4	62.5	100	88.9	88.9
P5	75	75	100	62.5
P6	88.9	100	88.9	75
P7	75	100	88.9	75
P8	75	100	88.9	88.9
P9	88.9	88.9	88.9	88.9
P10	88.9	62.5	88.9	50
P11	75	62.5	88.9	75
P12	62.5	62.5	88.9	62.5
P13	75	62.5	88.9	62.5
P14	75	100	88.9	88.9
P15	62.5	75	62.5	88.9
P16	62.5	88.9	75	88.9
P17	62.5	62.5	75	62.5
P18	50	50	62.5	75
P19	62.5	75	88.9	75
P20	75	100	100	100

(Source: Fieldwork, 2022)

AS = August- September

ND= November-December

APPENDIX C

Levels of PFAS Determined in Water Samples Collected During August and September, 2021 from the Pra River Basin.

Sampling point	PFBA (ng/L)	PFPe A (ng/L)	PFHx A (ng/L)	PFOA (ng/L)	PFNA (ng/L)	PFDA (ng/L)	PFHxS (ng/L)	PFOS (ng/L)	ΣPFAS
P1	0.57	0.42	0.58	35.9	0.8	0.45	0.67	31.8	71.19
P2	N.D	0.44	0.57	37.6	0.91	0.34	0.34	36.89	77.09
P3	N.D	0.81	0.45	19.4	N.D	<LoD	0.36	41.75	62.77
P4	0.86	0.56	<LoD	56.1	N.D	<LoD	0.22	87.9	145.64
P5	0.77	0.52	0.65	98.6	N.D	<LoD	0.31	83.1	183.95
P6	0.63	0.34	0.54	14.5	0.96	<LoD	0.42	101.2	118.59
P7	0.72	0.34	<LoD	18.6	1.2	<LoD	0.39	78.2	99.45
P8	0.83	0.72	0.33	78.9	1.43	<LoD	<LoD	79.4	161.61
P9	0.91	0.29	0.42	67.4	0.94	0.76	<LoD	92.6	163.32
P10	0.88	0.65	0.56	58.6	1.24	N.D	0.65	86.2	148.78
P11	N.D	0.42	<LoD	71.2	0.98	0.33	0.68	75.2	148.81
P12	N.D	0.34	<LoD	87.9	N.D	N.D	0.33	98.2	186.77
P13	N.D	0.73	0.3	67.8	N.D	0.67	0.43	36.61	106.54
P14	0.19	0.46	<LoD	89.4	0.91	0.56	<LoD	50.45	141.97
P15	N.D	0.35	0.32	45.7	1.06	N.D	<LoD	76.5	123.93
P16	N.D	0.46	0.67	43.6	N.D	N.D	0.87	85.1	130.7
P17	1.34	0.28	<LoD	19.3	N.D	N.D	0.43	86.4	107.75
P18	0.94	N.D	<LoD	98.6	0.88	N.D	<LoD	102.8	203.22
P19	0.83	N.D	<LoD	56.9	0.93	N.D	0.22	134.7	193.58
P20	0.87	0.35	<LoD	88.4	N.D	0.89	0.33	67.3	158.14
Σ	10.34	8.48	5.39	1154.4	12.24	4.0	6.65	1532.3	

(Source: Fieldwork, 2022)

APPENDIX D

Levels of PFAS Determined in Water Samples Collected During November and December 2021 from the Pra River Basin

Sampling point	PFBA (ng/L)	PFPeA (ng/L)	PFHxA (ng/L)	PFOA (ng/L)	PFNA (ng/L)	PFDA (ng/L)	PFHxS (ng/L)	PFO S (ng/L)	ΣPFAS (ng/L)
P1	0.45	0.62	0.75	65.41	0.69	0.2	0.45	78.4	146.97
P2	0.5	0.5	0.35	89.3	0.95	N.D	0.98	98.4	190.98
P3	2.34	0.54	0.43	74.92	0.8	N.D	0.67	90.6	170.3
P4	0.45	0.41	0.52	103.4	0.78	0.78	0.62	89.6	196.56
P5	1.46	0.72	N.D	97.6	1.56	N.D	0.87	95.6	197.81
P6	2.56	0.43	0.32	90.1	0.78	0.87	0.54	105.6	201.2
P7	0.45	0.53	0.41	98.3	0.98	0.65	0.33	112.4	214.05
P8	0.76	0.52	0.43	76.3	1.56	0.23	0.41	56.7	136.91
P9	0.78	0.52	0.43	82.4	1.08	<LoD	0.23	87.6	173.04
P10	1.89	0.42	<LoD	76.4	0.76	N.D	N.D	91.4	170.87
P11	N.D	0.42	0.32	55.9	0.67	N.D	N.D	90.6	147.91
P12	N.D	0.53	<LoD	79.6	0.76	0.45	N.D	88.6	169.94
P13	N.D	0.52	<LoD	108.4	0.83	0.76	N.D	87.4	197.91
P14	0.98	0.71	0.23	90.4	0.92	0.34	0.87	78.9	173.35
P15	0.87	0.43	0.43	89.62	N.D	0.45	N.D	90.9	182.7
P16	0.94	0.34	0.52	56.7	0.17	0.75	N.D	89.9	149.32
P17	0.99	0.34	N.D	90.5	N.D	N.D	0.92	120.6	213.35
P18	N.D	0.19	N.D	57.9	N.D	N.D	0.87	69.3	128.26
P19	N.D	0.3	0.34	96.4	0.76	0.43	N.D	96.7	194.93
P20	0.98	0.76	0.95	89.9	0.98	0.32	0.65	96.9	191.44
Σ	16.4	9.75	6.43	1669.45	15.03	6.23	8.41	1816.1	

(Source: Fieldwork, 2022)

APPENDIX E
Levels of PFAS Determined in Sediment Samples Collected During
August and September, 2021 from the Pra River Basin

Sampling point	PFBA (ng/g)	PFPe A (ng/g)	PFHx A (ng/g)	PFOA (ng/g)	PFNA (ng/g)	PFDA (ng/g)	PFH xS (ng/g)	PFOS (ng/g)	ΣPFAS (ng/g)
P1	9.45	9.3	15.5	89.78	12.93	2.44	0.032	65.67	205.10
P2	9.78	5.8	12.4	92.32	11.41	N.D	0.043	54.43	186.18
P3	9.89	5.4	13.6	101.5	9.23	N.D	N.D	45.76	185.38
P4	13.78	5.6	13.7	96.79	9.78	N.D	0.41	57.73	197.79
P5	10.56	7.4	14.5	101.9	10.74	3.91	0.45	186.5	335.96
P6	13.34	6.7	23.6	65.89	8.32	N.D	0.55	121.6	240
P7	11.45	9.8	13.8	83.41	9.56	3.09	N.D	132.5	263.61
P8	12.46	1.1	11.7	88.9	8.97	1.67	N.D	50.98	175.78
P9	10.24	8.8	12.4	107.87	12.56	0.89	N.D	67.45	220.21
P10	11.76	6.8	8.9	67.6	12.57	N.D	0.56	78.9	187.09
P11	8.56	7.9	23.4	68.8	12.89	N.D	0.56	90.12	212.23
P12	9.78	9.8	9.3	89.9	12.65	N.D	0.43	64.3	196.16
P13	12.09	8.7	<LoD	105.67	9.45	2.78	0.92	54.32	193.93
P14	<LoD	7.6	13.4	129.7	8.78	1.4	0.74	51.82	213.44
P15	N.D	8.9	19.8	56.4	8.13	N.D	N.D	65.92	159.15
P16	N.D	7.6	27.4	75.89	9.45	1.29	N.D	81.76	203.39
P17	<LoD	6.4	11.3	90.34	9.38	N.D	0.41	81.92	199.75
P18	<LoD	8.9	17.5	90.31	<LoD	N.D	0.39	54.51	171.61
P19	8.09	8.7	9.8	94.9	<LoD	2.3	0.42	75.45	199.66
P20	7.71	9.7	8.7	97.6	7.23	2.39	0.41	86.45	220.19
Σ	158.94	150.9	280.7	1795.47	184.03	22.16	6.33	1568.09	

(Source: Fieldwork, 2022)



APPENDIX F
Levels of PFAS Determined in Sediment Samples Collected During
November and December, 2021 from the Pra River Basin

Sampling point	PFBA (ng/g)	PFPeA (ng/g)	PFHxA (ng/g)	PFOA (ng/g)	PFNA (ng/g)	PFDA (ng/g)	PFHxS (ng/g)	PFOS (ng/g)	ΣPFAS (ng/g)
P1	0.58	0.56	0.61	96.56	2.12	0.99	0.03	112.6	214.05
P2	0.67	0.57	0.54	29.78	2.9	<LoD	0.076	120.5	155.04
P3	0.98	0.78	N.D	96.89	5.54	<LoD	N.D	90.56	194.75
P4	1.56	0.89	0.11	129.3	1.98	0.94	N.D	67.9	202.68
P5	<LoQ	0.76	0.34	119.4	<LoD	0.96	N.D	160.6	282.06
P6	2.45	N.D	0.87	83.47	<LoD	0.91	0.056	142.4	230.16
P7	2.29	0.41	0.67	76.54	2.34	<LoD	N.D	87.69	169.94
P8	0.57	0.87	0.56	85.71	1.87	<LoD	0.045	98.34	188
P9	0.58	0.76	0.87	87.3	3.34	0.96	N.D	120.3	214.11
P10	N.D	0.87	0.33	98.56	N.D	N.D	N.D	97.3	197.06
P11	5.79	0.32	0.43	82.75	N.D	N.D	0.041	108.6	197.93
P12	N.D	N.D	0.59	201.6	2.67	N.D	0.072	97.6	302.53
P13	N.D	N.D	0.57	98.89	4.78	0.98	N.D	65.64	170.86
P14	3.21	0.45	0.61	106.7	3.08	N.D	0.043	88.54	202.63
P15	2.34	0.41	0.43	89.7	3.93	1.83	N.D	97.42	196.06
P16	2.12	0.37	0.78	93.45	4.09	1.72	N.D	105.4	207.93
P17	4.23	0.71	0.56	97.93	N.D	N.D	N.D	97.54	200.97
P18	2.45	0.56	0.97	86.54	N.D	1.32	N.D	107.5	199.36
P19	N.D	0.34	0.72	97.6	1.78	N.D	0.041	43.72	144.20
P20	1.32	0.52	0.43	106.7	6.23	0.98	0.083	132.4	248.66
Σ	31.14	10.15	10.99	1965.37	46.65	11.59	0.49	2042.6	

(Source: Fieldwork, 2022)

APPENDIX G
Mean Levels of PFAS in Water Samples at the Individual Sampling Points from August to December, 2021

Sampling point	PFBA (ng/L)	PFPeA (ng/L)	PFHxA (ng/L)	PFOA (ng/L)	PFNA (ng/L)	PFDA (ng/L)	PFHxS (ng/L)	PFOS (ng/L)
P1-a/v	0.51	0.52	0.665	50.655	0.745	0.325	0.56	55.1
P2-a/v	0.25	0.47	0.46	63.45	0.93	0.17	0.66	67.645
P3-a/v	1.17	0.675	0.44	47.16	0.4	0	0.515	66.175
P4-a/v	0.655	0.485	0.26	79.75	0.39	0.39	0.42	88.75
P5-a/v	1.115	0.62	0.325	98.1	0.78	0	0.59	89.35
P6-a/v	1.595	0.385	0.43	52.3	0.87	0.435	0.48	103.4
P7-a/v	0.585	0.435	0.205	58.45	1.09	0.325	0.36	95.3
P8-a/v	0.795	0.62	0.38	77.6	1.495	0.115	0.205	68.05
P9-a/v	0.845	0.405	0.425	74.9	1.01	0.38	0.115	90.1
P10-a/v	1.385	0.535	0.28	67.5	1	0	0.325	88.8
P11-a/v	0	0.42	0.16	63.55	0.825	0.165	0.34	82.9
P12-a/v	0	0.435	0	83.75	0.38	0.225	0.165	93.4
P13-a/v	0	0.625	0.15	88.1	0.415	0.715	0.215	62.005
P14-a/v	0.585	0.585	0.115	89.9	0.915	0.45	0.435	64.675
P15-a/v	0.435	0.39	0.375	67.66	0.53	0.225	0	83.7
P16-a/v	0.47	0.4	0.595	50.15	0.085	0.375	0.435	87.5
P17-a/v	1.165	0.31	0	54.9	0	0	0.675	103.5
P18-a/v	0.47	0.095	0	78.25	0.44	0	0.435	86.05
P19-a/v	0.415	0.15	0.17	76.65	0.845	0.215	0.11	115.7
P20-a/v	0.925	0.555	0.475	89.15	0.49	0.605	0.49	82.1

(Source: Fieldwork, 2022)

APPENDIX H

Mean Levels of PFAS in Sediment Samples at the Individual Sampling Points from August to December, 2021

Sampling point	PFBA (ng/g)	PFPeA (ng/g)	PFHxA (ng/g)	PFOA (ng/g)	PFNA (ng/g)	PFDA (ng/g)	PFHxS (ng/g)	PFOS (ng/g)
P1-a/v	5.02	4.93	8.06	93.17	7.53	1.72	0.03	89.14
P2-a/v	5.23	3.19	6.47	61.05	7.16	0.00	0.06	87.47
P3-a/v	5.44	3.09	6.80	99.20	7.39	0.00	0.00	68.16
P4-a/v	7.67	3.25	6.91	113.05	5.88	0.47	0.21	62.82
P5-a/v	5.28	4.08	7.42	110.65	5.37	2.44	0.23	173.55
P6-a/v	7.90	3.35	12.24	74.68	4.16	0.46	0.30	132.00
P7-a/v	6.87	5.11	7.24	79.98	5.95	1.55	0.00	110.10
P8-a/v	6.52	0.99	6.13	87.31	5.42	0.84	0.02	74.66
P9-a/v	5.41	4.78	6.64	97.59	7.95	0.93	0.00	93.88
P10-a/v	5.88	3.84	4.62	83.08	6.29	0.00	0.28	88.10
P11-a/v	7.18	4.11	11.92	75.78	6.45	0.00	0.30	99.36
P12-a/v	4.89	4.90	4.95	145.75	7.66	0.00	0.25	80.95
P13-a/v	6.05	4.35	0.29	102.28	7.12	1.88	0.46	59.98
P14-a/v	1.61	4.03	7.01	118.20	5.93	0.70	0.39	70.18
P15-a/v	1.17	4.66	10.12	73.05	6.03	0.92	0.00	81.67
P16-a/v	1.06	3.99	14.09	84.67	6.77	1.51	0.00	93.58
P17-a/v	2.12	3.56	5.93	94.14	4.69	0.00	0.21	89.73
P18-a/v	1.23	4.73	9.24	88.43	0.00	0.66	0.20	81.01
P19-a/v	4.05	4.52	5.26	96.25	0.89	1.15	0.23	59.59
P20-a/v	4.52	5.11	4.57	102.15	6.73	1.69	0.25	109.43

(Source: Fieldwork, 2022)

APPENDIX I
Risk quotient of PFAS for the individual sites

Sampling point	PFBA	PFPeA	PFHxA	PFOA	PFNA	PFDA	PFHxS	PFOS	ΣRQ
P1-a/v	3.00E-03	2.08E-04	1.23E-02	7.24E-02	2.33E-04	1.35E-04	1.44E-02	8.10E+00	8.21E+00
P2-a/v	1.47E-03	1.88E-04	8.52E-03	9.06E-02	2.91E-04	7.08E-05	1.69E-02	9.95E+00	1.01E+01
P3-a/v	6.88E-03	2.70E-04	8.15E-03	6.74E-02	1.25E-04	0.00E+00	1.32E-02	9.73E+00	9.83E+00
P4-a/v	3.85E-03	1.94E-04	4.81E-03	1.14E-01	1.22E-04	1.63E-04	1.08E-02	1.31E+01	1.32E+01
P5-a/v	6.56E-03	2.48E-04	6.02E-03	1.40E-01	2.44E-04	0.00E+00	1.51E-02	1.31E+01	1.33E+01
P6-a/v	9.38E-03	1.54E-04	7.96E-03	7.47E-02	2.72E-04	1.81E-04	1.23E-02	1.52E+01	1.53E+01
P7-a/v	3.44E-03	1.74E-04	3.80E-03	8.35E-02	3.41E-04	1.35E-04	9.23E-03	1.40E+01	1.41E+01
P8-a/v	4.68E-03	2.48E-04	7.04E-03	1.11E-01	4.67E-04	4.79E-05	5.26E-03	1.00E+01	1.01E+01
P9-a/v	4.97E-03	1.62E-04	7.87E-03	1.07E-01	3.16E-04	1.58E-04	2.95E-03	1.33E+01	1.34E+01
P10-a/v	8.15E-03	2.14E-04	5.19E-03	9.64E-02	3.13E-04	0.00E+00	8.33E-03	1.31E+01	1.32E+01
P11-a/v	0.00E+00	1.68E-04	2.96E-03	9.08E-02	2.58E-04	6.88E-05	8.72E-03	1.22E+01	1.23E+01
P12-a/v	0.00E+00	1.74E-04	0.00E+00	1.20E-01	1.19E-04	9.38E-05	4.23E-03	1.37E+01	1.39E+01
P13-a/v	0.00E+00	2.50E-04	2.78E-03	1.26E-01	1.30E-04	2.98E-04	5.51E-03	9.12E+00	9.25E+00
P14-a/v	3.44E-03	2.34E-04	2.13E-03	1.28E-01	2.86E-04	1.88E-04	1.12E-02	9.51E+00	9.66E+00
P15-a/v	2.56E-03	1.56E-04	6.94E-03	9.67E-02	1.66E-04	9.38E-05	0.00E+00	1.23E+01	1.24E+01
P16-a/v	2.76E-03	1.60E-04	1.10E-02	7.16E-02	2.66E-05	1.56E-04	1.12E-02	1.29E+01	1.30E+01
P17-a/v	6.85E-03	1.24E-04	0.00E+00	7.84E-02	0.00E+00	0.00E+00	1.73E-02	1.52E+01	1.53E+01
P18-a/v	2.76E-03	3.80E-05	0.00E+00	1.12E-01	1.38E-04	0.00E+00	1.12E-02	1.27E+01	1.28E+01
P19-a/v	2.44E-03	6.00E-05	3.15E-03	1.10E-01	2.64E-04	8.96E-05	2.82E-03	1.70E+01	1.71E+01
P20-a/v	5.44E-03	2.22E-04	8.80E-03	1.27E-01	1.53E-04	2.52E-04	1.26E-02	1.21E+01	1.22E+01
Mean									

(Source: Fieldwork, 2022)

APPENDIX J

Levels of PCBs Determined in Water Samples Collected During August and September, 2021 from the Pra River Basin(ng/L)

Sampling point	PCB 18	PCB 28	PCB 31	PCB 44	PCB 52	PCB 101	PCB 118	PCB 138	PCB 149	PCB 153	PCB 194	PCB 180	ΣPCBs
P1	0.039	0.033	0.05	ND	0.036	0.16	0.67	0.038	ND	0.049	ND	0.16	1.235
P2	0.61	0.017	N.D	0.31	0.044	ND	ND	0.083	0.084	0.081	ND	0.56	1.789
P3	0.55	0.018	0.035	0.35	0.089	0.21	0.064	0.02	0.056	0.27	0.12	0.89	2.672
P4	0.58	0.021	0.078	ND	0.075	ND	0.087	0.025	0.045	0.74	0.034	0.32	2.005
P5	0.088	0.065	0.061	0.24	0.079	ND	0.083	0.029	0.065	0.18	0.056	0.11	1.056
P6	0.14	0.065	0.077	0.26	0.025	0.26	0.08	0.047	0.073	0.04	0.034	0.2	1.301
P7	0.16	0.02	0.045	ND	0.047	ND	0.085	0.055	0.047	0.18	0.098	0.03	0.767
P8	0.054	0.028	N.D	ND	0.0098	0.15	0.023	0.023	ND	0.13	0.035	0.13	0.5828
P9	0.094	0.025	N.D	ND	0.0075	ND	0.095	0.011	ND	0.14	0.046	0.11	0.5285
P10	0.064	0.055	N.D	0.38	0.092	0.32	0.097	0.032	ND	0.37	ND	0.2	1.61
P11	0.23	0.078	0.034	0.67	ND	0.54	ND	0.12	0.075	0.073	0.0078	0.12	1.9478
P12	0.13	N.D	N.D	0.56	0.038	ND	0.023	ND	0.084	0.091	0.061	0.65	1.637
P13	0.046	N.D	N.D	0.85	ND	ND	0.087	0.023	0.045	0.082	ND	0.54	1.673
P14	0.085	0.027	0.034	ND	0.17	0.86	ND	ND	ND	0.39	ND	0.34	1.906
P15	0.14	0.14	0.078	0.93	ND	0.05	ND	ND	ND	0.78	0.097	0.78	2.995
P16	0.041	0.067	0.089	0.4	0.064	ND	0.041	0.21	0.053	0.45	0.032	0.087	1.534
P17	0.25	0.02	N.D	ND	0.083	0.45	0.067	0.081	0.043	0.54	ND	0.012	1.546
P18	0.13	0.023	N.D	0.36	0.032	0.12	ND	0.12	0.045	0.097	0.065	0.87	1.862
P19	0.058	0.045	0.035	0.45	0.067	ND	0.043	ND	0.057	0.64	ND	0.42	1.815
P20	0.09	0.078	0.054	0.93	0.041	0.075	0.045	0.047	ND	0.76	0.0078	0.13	2.2578
Σ	3.579	0.825	0.67	6.69	0.9993	3.195	1.59	0.964	0.772	6.083	0.6936	6.659	32.7199

(Source: fieldwork, 2022)

APPENDIX K

Levels of PCBs Determined in Water Samples Collected During November and December, 2021 from the Pra River Basin(ng/L)

Sampling Point	PCB 18	PCB 28	PCB 31	PCB 44	PCB 52	PCB 101	PCB 118	PCB 138	PCB 149	PCB 153	PCB 194	PCB 180	ΣPCBs
P1	0.081	0.056	0.061	0.086	0.63	0.059	ND	0.13	ND	0.67	0.34	0.17	2.283
P2	0.098	0.073	0.56	0.056	0.58	0.065	0.087	0.083	0.078	0.08	0.067	0.45	2.277
P3	0.07	0.05	0.056	0.057	0.81	ND	ND	ND	0.057	0.089	ND	0.84	2.029
P4	0.098	0.081	0.19	0.34	0.68	ND	0.095	0.059	0.086	0.14	0.084	0.25	2.103
P5	0.81	ND	0.23	ND	0.56	ND	0.091	ND	0.76	0.48	0.096	0.11	3.137
P6	0.037	ND	0.094	0.048	0.93	ND	0.25	ND	0.095	0.09	ND	0.87	2.414
P7	0.026	0.042	0.057	0.095	0.2	ND	0.088	0.87	0.087	0.76	1.04	0.15	3.415
P8	0.083	ND	0.083	ND	0.98	0.089	0.29	0.23	ND	0.13	0.082	0.56	2.527
P9	0.51	ND	0.052	0.059	ND	ND	ND	ND	ND	0.76	0.94	0.11	2.431
P10	0.45	0.23	0.062	1.39	0.76	0.075	0.55	0.064	ND	0.097	ND	0.29	3.968
P11	0.37	0.52	0.34	ND	ND	0.083	0.16	ND	ND	0.84	0.54	0.65	3.503
P12	0.28	0.44	0.095	0.097	ND	0.062	0.78	ND	ND	1.67	0.069	0.95	4.443
P13	0.52	0.23	1.02	0.083	ND	0.079	0.86	ND	ND	0.86	ND	0.78	4.432
P14	0.089	0.28	0.081	0.2	0.27	0.12	0.085	ND	ND	0.072	ND	0.94	2.137
P15	0.78	0.056	0.46	0.13	ND	0.076	0.079	ND	ND	0.08	ND	0.56	2.221
P16	0.069	ND	0.47	ND	0.64	0.18	ND	0.21	0.087	1.24	ND	0.083	2.979
P17	0.076	0.051	0.093	0.68	0.83	0.064	ND	0.29	ND	0.84	ND	0.29	3.214
P18	0.73	0.32	0.059	0.89	0.82	0.98	ND	0.46	0.66	0.47	ND	0.48	5.869
P19	0.97	0.054	0.098	0.067	0.69	0.054	0.62	0.93	0.67	0.84	ND	0.42	5.413
P20	0.89	0.064	0.14	0.075	0.71	0.085	0.89	0.0471	0.84	0.18	0.0078	1.32	5.2489
Σ	7.03	2.547	4.301	4.353	10.09	2.071	4.925	3.3731	3.42	10.388	3.2658	10.273	66.0439

(Source: Fieldwork, 2022)

APPENDIX L

Levels of PCBs Determined in Sediment Samples Collected during August and September, 2021 from the Pra River Basin(ng/g)

Sampling point	PCB 18	PCB 28	PCB 31	PCB 44	PCB 52	PCB 101	PCB 118	PCB 138	PCB 149	PCB 153	PCB 194	PCB 180	ΣPCBs
P1	0.93	1.65	0.61	0.23	17.2	0	<LoQ	15.78	1.34	19.45	ND	23.76	80.95
P2	2.58	1.67	6.56	2.76	17.8	1.89	ND	11.45	0.56	58.89	ND	25.97	130.13
P3	0.83	0.98	0.89	3.87	21.43	2.57	ND	12.67	ND	34.67	ND	28.45	106.36
P4	3.78	5.01	2.19	0.97	18.82	5.9	ND	13.53	2.45	45.34	3.56	43.71	145.26
P5	0.39	0.9	1.73	ND	25.9	0.98	ND	11.92	1.67	40.45	4.56	20.83	109.33
P6	1.75	0.78	3.08	ND	28.56	1.34	ND	10.23	0.67	34.1	1.34	19.35	101.2
P7	0.62	2.23	0.23	ND	30.02	4.31	ND	14.32	0.87	45.23	2.45	50.35	150.63
P8	0.79	4.23	0.83	ND	31.74	ND	ND	13.34	3.34	34.89	5.82	63.13	158.11
P9	1.51	0.89	0.27	ND	23.1	<LoQ	ND	16.01	4.09	18.98	3.34	21.45	89.64
P10	2.45	1.01	0.52	3.39	19.45	ND	0.97	14.1	3.33	20.78	0.97	23.67	90.64
P11	0.87	1.62	2.41	ND	34.89	ND	2.65	10.98	1.29	21.34	ND	39.71	115.76
P12	4.28	3.44	3.95	ND	20.13	0.97	4.98	17.08	0.98	34.4	ND	47.45	137.66
P13	0.59	2.23	12.02	ND	17.03	2.34	2.42	13.1	0.76	22.45	ND	42.65	115.59
P14	0.39	ND	4.87	2.17	42.45	1.58	0.99	11.87	2.54	25.89	6.87	24.67	124.29
P15	6.78	ND	2.61	1.87	17.32	0.9	2.34	ND	6.87	43.56	ND	37.89	120.14
P16	3.71	ND	3.47	0.54	ND	1.65	3.45	ND	ND	33.6	ND	46.65	93.07
P17	0.76	ND	2.23	4.67	ND	0.97	4.76	ND	ND	29.34	ND	24.7	67.43
P18	0.93	0.89	3.59	1.88	ND	5.78	7.82	ND	5.56	34.87	0.88	48.76	110.96
P19	6.97	5.04	ND	ND	ND	4.21	1.87	ND	0.34	18.76	ND	23.8	60.99
P20	2.89	1.64	0.14	3.86	35.6	2.35	3.67	15.32	7.98	23.87	<LoQ	45.84	143.1678
Σ	43.8	34.21	52.2	26.21	401.44	37.74	35.92	201.7	44.64	640.86	29.7978	702.79	2251.308

(Source: Fieldwork, 2022)

APPENDIX M

Levels of PCBs determined in sediment samples collected during November and December, 2021 from the Pra River Basin(ng/g)

Sampling point	PCB 18	PCB 28	PCB 31	PCB 44	PCB 52	PCB 101	PCB 118	PCB 138	PCB 149	PCB 153	PCB 194	PCB 180	ΣPCBs
P1	2.67	2.32	4.68	19.9	30.76	21.76	25.67	4.67	5.89	28.89	2.34	33.45	183
P2	10.38	6.45	9.46	30.45	35.56	23.89	45.78	n.d	1.67	27.75	4.34	46.43	242.16
P3	2.07	1.67	2.46	18.34	n.d	17.67	23.45	n.d	5.76	29.11	n.d	39.1	139.63
P4	7.98	n.d	5.59	13.67	n.d	17.85	26.54	2.67	4.73	45.34	4.57	32.1	161.04
P5	8.81	2.34	5.73	15.45	n.d	20.76	21.56	n.d	5.78	33.11	3.67	35.76	152.97
P6	6.07	1.45	2.99	28.12	27.78	16.67	23.85	n.d	8.87	32.54	n.d	36.35	184.69
P7	2.26	0.54	3.47	n.d	33.67	24.45	27.67	n.d	9.87	28.34	n.d	32.54	162.81
P8	7.03	6.56	1.63	n.d	29.9	n.d	28.72	n.d	n.d	29.56	n.d	50.34	153.74
P9	3.61	3.56	3.82	20.67	28.63	n.d	22.76	n.d	n.d	38.73	n.d	34.56	156.34
P10	4.46	n.d	2.67	20.23	31.34	n.d	34.54	n.d	n.d	37.34	n.d	34.55	165.13
P11	5.77	n.d	6.33	n.d	39.1	n.d	23.65	n.d	n.d	43.45	0.59	56.56	175.45
P12	1.23	n.d	4.93	n.d	n.d	n.d	n.d	n.d	2.98	43.34	1.08	45.22	98.78
P13	3.42	n.d	3.65	12.64	32.87	n.d	n.d	n.d	n.d	41.24	4.33	41.23	139.38
P14	3.49	11.28	2.81	16.78	41.89	n.d	29.67	1.09	n.d	45.56	n.d	40.32	192.89
P15	1.98	4.56	7.95	15.89	25.89	18.76	50.78	5.61	n.d	43.98	n.d	35.57	210.97
P16	0.99	1.45	2.47	n.d	35.65	20.98	n.d	15.89	n.d	29.54	n.d	40.45	147.42
P17	0.89	5.51	5.93	13.79	25.78	15.37	n.d	1.54	3.66	31.54	4.22	35.67	143.9
P18	2.61	2.32	5.52	12.87	24.76	14.5	45.34	6.78	3.78	29.76	7.86	50.76	206.86
P19	4.78	4.34	2.96	13.45	23.98	13.83	23.89	4.57	2.76	36.45	1.67	45.56	178.24
P20	1.09	3.54	0.22	n.d	25.11	14.9	27.22	3.92	3.56	29.45	0.98	34.99	144.98
Σ	81.59	57.89	85.27	252.25	492.67	241.39	481.09	46.74	59.31	705.02	35.65	801.51	3340.38

(Source: Fieldwork, 2022)

APPENDIX N
Correlation Matrix of Sampling Points from the PRB (Water Samples)

	P1	P2	P3	P4	P5	P6	P7	P8	P9	P10	P11	P12	P13	P14	P15	P16	P17	P18	P19	P20
P1																				
P2	0.9253																			
P3	0.8991	0.9337																		
P4	0.8155	0.8998	0.9666																	
P5	0.8646	0.9391	0.9652	0.9873																
P6	0.9563	0.9571	0.8857	0.8288	0.8962															
P7	0.9566	0.9010	0.8858	0.8561	0.8958	0.9232														
P8	0.8956	0.8367	0.8534	0.8092	0.8166	0.8404	0.9285													
P9	0.9457	0.9256	0.8623	0.8095	0.8599	0.9626	0.9093	0.9071												
P10	0.9399	0.9445	0.8671	0.8048	0.8502	0.9513	0.8891	0.8900	0.9842											
P11	0.9257	0.8666	0.8256	0.7794	0.8142	0.8947	0.9502	0.9792	0.9441	0.9240										
P12	0.8081	0.8193	0.9188	0.9368	0.9129	0.7884	0.8623	0.9039	0.8318	0.7946	0.8619									
P13	0.8945	0.8562	0.8736	0.8402	0.8636	0.8874	0.9096	0.9423	0.9245	0.8741	0.9501	0.9344								
P14	0.9142	0.8831	0.7579	0.7059	0.7800	0.9402	0.8978	0.8736	0.9714	0.9484	0.9376	0.7331	0.8788							
P15	0.8912	0.9780	0.9317	0.9197	0.9417	0.9118	0.9036	0.8469	0.8917	0.9246	0.8594	0.8357	0.8213	0.8434						
P16	0.8922	0.8416	0.9178	0.9013	0.9031	0.8418	0.9373	0.9243	0.8442	0.8017	0.9037	0.9547	0.9503	0.7798	0.8313					
P17	0.8647	0.9058	0.9520	0.9358	0.9530	0.8969	0.8854	0.8520	0.8628	0.8260	0.8418	0.9278	0.9310	0.7923	0.8766	0.9368				
P18	0.8366	0.8701	0.9278	0.8873	0.8665	0.7775	0.8542	0.8875	0.7920	0.8334	0.8361	0.8666	0.8093	0.7067	0.9161	0.8580	0.8445			
P19	0.8807	0.9227	0.9678	0.9419	0.9341	0.8611	0.9046	0.9137	0.8535	0.8641	0.8750	0.9213	0.8817	0.7753	0.9357	0.9297	0.9331	0.9547		
P20	0.9608	0.8616	0.8524	0.7879	0.8208	0.8939	0.9752	0.9621	0.9196	0.9100	0.9719	0.8368	0.9020	0.9041	0.8667	0.9087	0.8246	0.8603	0.8855	

(Source: Fieldwork, 2022)

APPENDIX O
Correlation Matrix of Sampling Points from the PRB (Sediment Samples)

	P1	P2	P3	P4	P5	P6	P7	P8	P9	P10	P11	P12	P13	P14	P15	P16	P17	P18	P19	P20
P1																				
P2	-0.01987																			
P3	0.2198	0.85301																		
P4	0.52622	0.59699	0.61037																	
P5	0.09268	0.3298	0.20526	0.65465																
P6	0.37673	0.72774	0.88228	0.47781	0.10231															
P7	0.33836	-0.31881	-0.19243	0.09696	-0.06642	-0.32609														
P8	0.63719	0.52588	0.69993	0.52307	0.09376	0.86916	-0.00796													
P9	0.33227	-0.05857	0.0401	0.40468	0.27475	-0.25712	0.68886	-0.11479												
P10	0.15311	0.22484	0.29216	0.33619	0.02888	0.35509	-0.33018	0.16265	-0.17813											
P11	-0.01543	0.1295	0.28081	0.28836	-0.10357	-0.06883	0.08725	-0.22413	0.52807	0.1966										
P12	0.46093	0.27786	0.51175	0.57488	0.10578	0.31209	0.11524	0.19169	0.38526	0.26239	0.65217									
P13	0.18635	0.49487	0.42348	0.40803	0.01464	0.30099	-0.22839	0.03892	0.08901	0.3598	0.48422	0.75043								
P14	0.18473	0.44828	0.72715	0.25832	-0.19087	0.65923	-0.29587	0.5192	-0.09586	0.14456	0.49039	0.48007	0.31372							
P15	-0.05583	0.65791	0.63531	0.56644	0.18698	0.3205	-0.14763	0.02439	0.27357	0.44643	0.73097	0.71177	0.79612	0.44943						
P16	0.51736	0.00439	0.04712	0.64947	0.32206	0.01366	0.38508	0.2044	0.32406	0.13089	0.26192	0.46074	0.23903	0.07227	0.23519					
P17	0.54112	0.08982	0.25733	0.70785	0.30183	0.23357	0.22602	0.3854	0.23375	0.45767	0.31622	0.44514	0.14048	0.29623	0.30234	0.86224				
P18	-0.18221	0.48972	0.66106	0.30901	0.14448	0.53956	-0.34226	0.30845	-0.22336	0.52099	0.30707	0.23917	0.12132	0.64977	0.52357	0.03064	0.40865			
P19	0.41149	0.28076	0.34103	0.72182	0.59549	0.20035	0.26227	0.30065	0.25656	0.1647	0.06145	0.56632	0.29386	0.04583	0.36822	0.59029	0.60438	0.27665		
P20	0.27924	0.5885	0.69608	0.64402	0.50585	0.6062	-0.28881	0.35458	0.04647	0.50943	0.20082	0.68392	0.63057	0.35814	0.66091	0.16049	0.3142	0.5261	0.6463	

(Source: Fieldwork, 2022)

APPENDIX P
Correlation matrix of PCBs in water samples from PRB

	PCB 18	PCB 28	PCB 31	PCB 44	PCB 52	PCB 101	PCB 118	PCB 138	PCB 149	PCB 153	PCB 194	PCB 180
PCB 18												
PCB 28	0.125											
PCB 31	0.151	0.081										
PCB 44	0.440	0.491	0.150									
PCB 52	-0.095	-0.457	-0.410	-0.003								
PCB 101	-0.121	0.524	-0.260	0.307	0.184							
PCB 118	0.106	0.154	0.136	0.305	-0.100	-0.305						
PCB 138	-0.010	-0.187	-0.211	-0.071	0.209	0.038	-0.090					
PCB 149	0.656	-0.070	-0.112	0.167	0.301	0.015	0.165	0.328				
PCB 153	0.044	0.160	0.100	0.079	-0.334	-0.223	0.237	0.315	0.091			
PCB 194	-0.192	-0.074	-0.224	-0.412	-0.489	-0.236	-0.225	0.246	-0.214	0.052		
PCB 180	0.330	0.398	0.129	0.341	-0.096	0.234	0.250	-0.317	0.115	-0.166	-0.450	

(Source: Fieldwork, 2022)

APPENDIX Q
Correlation Matrix of PCBs in Sediment Samples from PRB

	PCB 18	PCB 28	PCB 31	PCB 44	PCB 52	PCB 101	PCB 118	PCB 138	PCB 149	PCB 153	PCB 194	PCB 180
PCB 18												
PCB 28	0.310											
PCB 31	0.224	-0.048										
PCB 44	0.259	0.081	0.280									
PCB 52	-0.140	0.225	-0.047	-0.079								
PCB 101	0.159	-0.107	0.021	0.190	-0.377							
PCB 118	0.342	0.228	0.022	0.342	0.203	0.229						
PCB 138	-0.143	-0.183	-0.265	-0.246	0.237	-0.122	-0.198					
PCB 149	-0.126	-0.161	-0.374	0.036	-0.078	0.513	0.393	0.119				
PCB 153	0.510	0.106	0.548	0.093	-0.135	0.251	0.269	-0.133	0.027			
PCB 194	0.153	0.372	0.263	0.131	-0.109	0.054	0.170	-0.107	0.111	0.276		
PCB 180	-0.047	0.098	0.081	-0.731	0.080	-0.196	0.041	0.050	-0.133	0.137	0.082	

(Source: Fieldwork, 2022)

APPENDIX R

Correlation Matrix for Concentration of PCB Congeners in Water Samples in the Dry Season

	P1	P2	P3	P4	P5	P6	P7	P8	P9	P10	P11	P12	P13	P14	P15	P16	P17	P18	P19	P20	
P1	1																				
P2	0.28	1.00																			
P3	0.44	.738**	1.00																		
P4	0.16	0.33	0.42	1.00																	
P5	0.27	0.14	0.16	0.57	1.00																
P6	0.41	.744**	.972**	0.44	0.16	1.00															
P7	0.50	-0.27	-0.18	-0.28	-0.19	-0.22	1.00														
P8	0.43	.596*	.799**	0.24	0.00	.814**	-0.08	1.00													
P9	0.44	-0.33	-0.23	-0.37	0.12	-0.31	.614*	-0.20	1.00												
P10	0.02	0.06	0.23	0.21	-0.08	0.26	-0.37	0.19	-0.28	1.00											
P11	0.37	0.02	0.10	-0.41	0.00	0.02	0.34	0.01	0.748**	-0.37	1.00										
P12	0.39	-0.07	0.14	-0.26	0.04	0.16	0.16	0.07	0.38	-0.10	.748**	1.00									
P13	-0.01	0.33	0.07	-0.31	0.05	0.13	-0.21	-0.06	0.07	-0.12	0.56	0.67*	1.00								
P14	0.04	0.48	.787**	0.05	-0.20	.723**	-0.28	0.54	-0.18	0.19	0.33	0.32	0.26	1.00							
P15	-0.24	0.32	0.22	-0.21	0.30	0.15	-0.42	-0.09	0.05	0.05	0.32	0.14	0.56	0.40	1.00						
P16	0.790**	0.29	0.18	0.09	0.33	0.17	0.27	0.16	0.22	-0.16	0.35	0.53	0.34	-0.12	-0.11	1.00					
P17	0.55	.596*	0.32	0.20	0.09	0.30	0.01	0.20	-0.11	0.31	0.07	0.18	0.31	0.07	0.06	.723**	1.00				
P18	0.08	-0.07	0.24	0.34	0.27	0.14	-0.38	0.06	-0.34	0.40	-0.42	-0.22	-0.47	0.12	0.03	0.07	0.12	1.00			
P19	0.21	-0.13	0.10	0.27	0.52	0.13	0.04	0.01	-0.14	0.32	-0.22	0.21	0.02	-0.12	0.13	0.27	0.18	0.34	1.00		
P20	-0.08	0.33	.604*	0.39	0.47	.665*	-0.44	0.35	-0.25	0.10	0.04	0.23	0.31	0.55	0.47	-0.17	-0.22	0.06	0.35	1	

(Source: Fieldwork, 2022)

APPENDIX S
Correlation Matrix for Concentration of PCB Congeners in Water Samples in the Wet Season

	P1	P2	P3	P4	P5	P6	P7	P8	P9	P10	P11	P12	P13	P14	P15	P16	P17	P18	P19
P1	1																		
P2	-0.14	1																	
P3	-0.03	0.90**	1																
P4	-0.12	0.43	0.48	1															
P5	-0.12	0.38	0.37	0.33	1														
P6	0.05	0.48	0.57	-0.19	0.25	1													
P7	0.04	0.18	0.12	0.885**	0.18	-0.47	1												
P8	0.10	0.24	0.55	0.49	-0.04	0.39	0.18	1											
P9	0.37	0.42	0.54	0.83**	0.31	-0.12	0.73**	0.53	1										
P10	0.03	0.17	0.40	0.21	0.61*	0.63*	-0.0	0.59*	0.24	1									
P11	-0.15	0.29	0.31	-0.19	0.37	0.90**	-0.40	0.23	-0.28	0.71*	1								
P12	-0.08	0.72**	0.80**	0.11	0.65*	0.62*	-0.24	0.20	0.22	0.48	0.45	1							
P13	-0.04	0.54	0.59*	-0.07	0.76**	0.66*	-0.34	0.03	0.06	0.58	0.60*	0.93**	1						
P14	-0.03	0.44	0.50	0.44	-0.15	0.47	0.27	0.72**	0.29	0.38	0.41	0.01	-0.12	1					
P15	-0.17	0.50	0.65*	0.38	0.86**	0.46	0.05	0.37	0.41	0.75**	0.45	0.82**	0.82**	0.06	1				
P16	-0.25	0.09	0.10	0.31	0.80**	0.07	0.23	0.08	0.24	0.64*	0.28	0.35	0.51	-0.16	0.75**	1			
P17	0.01	-0.03	0.11	0.53	0.02	0.14	0.47	0.73**	0.39	.58*	0.24	-0.25	-0.26	0.73**	0.15	0.22	1		
P18	-0.0	0.44	0.68*	0.62*	0.59*	0.23	0.30	0.66*	0.67*	.66*	0.12	0.61*	0.48	0.24	0.85**	.63*	0.41	1	
P19	-0.1	0.37	0.54	0.51	0.85**	0.26	0.24	0.41	0.53	0.75**	0.27	0.65*	0.64*	0.07	0.94**	0.81**	0.32	0.92**	1
P20	-0.19	0.20	0.24	0.28	0.91**	0.35	0.12	0.10	0.20	0.81**	0.55	0.50	0.67*	-0.01	0.85**	0.92**	0.30	0.61*	0.84**

** . Correlation is significant at the 0.01 level (2-tailed)

* . Correlation is significant at the 0.05 level (2-tailed)

APPENDIX T

Correlation Matrix for Concentration of PCB Congeners in Sediment Samples in the Wet Season

(Source:Fieldwork, 2022)

	P1	P2	P3	P4	P5	P6	P7	P8	P9	P10	P11	P12	P13	P14	P15	P16	P17	P18	P19	P20
P1	1																			
P2	.788**	1																		
P3	.946**	.925**	1																	
P4	.910**	.911**	.966**	1																
P5	.878**	.944**	.959**	.902**	1															
P6	.886**	.902**	.952**	.873**	.986**	1														
P7	.949**	.866**	.978**	.981**	.914**	.909**	1													
P8	.925**	.721**	.899**	.925**	.797**	.803**	.964**	1												
P9	.972**	.736**	.910**	.840**	.888**	.909**	.908**	.883**	1											
P10	.989**	.804**	.960**	.909**	.900**	.912**	.955**	.927**	.977**	1										
P11	.926**	.664*	.880**	.837**	.805**	.854**	.923**	.950**	.931**	.939**	1									
P12	.949**	.810**	.935**	.962**	.832**	.826**	.972**	.967**	.874**	.938**	.907**	1								
P13	.897**	.705*	.857**	.892**	.730**	.742**	.917**	.951**	.817**	.875**	.900**	.962**	1							
P14	.850**	.685*	.847**	.735**	.872**	.925**	.836**	.802**	.926**	.884**	.916**	.748**	.718**	1						
P15	.807**	.906**	.917**	.952**	.873**	.850**	.932**	.873**	.752**	.840**	.794**	.901**	.825**	.704*	1					
P16	.723**	.760**	.792**	.903**	.665*	.622*	.855**	.856**	.595*	.719**	.693*	.895**	.868**	0.470	.908**	1				
P17	.678*	.867**	.819**	.894**	.738**	.675*	.827**	.759**	0.555	.692*	.605*	.834**	.763**	0.459	.922**	.951**	1			
P18	.687*	.729**	.761**	.878**	.633*	.583*	.830**	.832**	0.559	.685*	.664*	.866**	.841**	0.434	.890**	.989**	.945**	1		
P19	.654*	.725**	.736**	.869**	.612*	0.569	.801**	.788**	0.517	.645*	.614*	.836**	.774**	0.380	.872**	.962**	.907**	.943**	1	
P20	.934**	.652*	.879**	.845**	.783**	.824**	.924**	.957**	.931**	.951**	.986**	.915**	.896**	.876**	.803**	.716**	.623*	.697*	.638*	1

**. Correlation is significant at the 0.01 level (2-tailed).

*. Correlation is significant at the 0.05 level (2-tailed).

APPENDIX U

Correlation Matrix for Concentration of PCB Congeners in Sediment Samples in the Dry Season

	P1	P2	P3	P4	P5	P6	P7	P8	P9	P10	P11	P12	P13	P14	P15	P16	P17	P18	P19	P20
P1	1																			
P2	.925**	1																		
P3	.766**	.767**	1																	
P4	.688*	.641*	.913**	1																
P5	.712**	.700*	.975**	.957**	1															
P6	.957**	.904**	.817**	.729**	.764**	1														
P7	.900**	.799**	.637*	.616*	.622*	.791**	1													
P8	.797**	.800**	.684*	.632*	.644*	.770**	.817**	1												
P9	.872**	.829**	.719**	.719**	.678*	.915**	.727**	.864**	1											
P10	.885**	.885**	.709**	.708**	.659*	.904**	.766**	.873**	.975**	1										
P11	.817**	.751**	.660*	.656*	.642*	.794**	.828**	.969**	.899**	.877**	1									
P12	0.559	0.437	.763**	.802**	.796**	.620*	0.528	.722**	.711**	.606*	.791**	1								
P13	.756**	.607*	.582*	.591*	.577*	.792**	.663*	.799**	.886**	.787**	.902**	.815**	1							
P14	.857**	.805**	.626*	.635*	.582*	.859**	.778**	.902**	.975**	.959**	.921**	.656*	.869**	1						
P15	.876**	.882**	.784**	.811**	.754**	.825**	.825**	.798**	.843**	.906**	.773**	0.551	0.588*	.840**	1					
P16	.745**	0.529	0.480	0.445	0.470	.645*	.764**	.715**	.647*	0.572	.801**	.659*	.824**	.685*	0.520	1				
P17	.804**	.623*	.650*	.598*	.642*	.808**	.711**	.719**	.798**	.682*	.820**	.789**	.939**	.777**	0.565	.882**	1			
P18	.867**	.906**	.821**	.738**	.757**	.816**	.828**	.903**	.816**	.878**	.848**	.618*	.634*	.810**	.913**	.592*	.609*	1		
P19	.918**	.856**	.858**	.809**	.827**	.910**	.846**	.924**	.920**	.899**	.934**	.809**	.857**	.902**	.867**	.784**	.853**	.913**	1	
P20	.896**	.824**	.740**	.727**	.714**	.809**	.950**	.922**	.824**	.851**	.911**	.673*	.734**	.866**	.896**	.775**	.735**	.922**	.938**	1

** . Correlation is significant at the 0.01 level (2-tailed).

APPENDIX V

Hazard Quotient and Index for non-carcinogenic human health risks posed by PCBs in water of study area via different pathways

PFAS	HQ _{ing}			HQ _{der}			HQ _{total}		
	min	max	mean	min	max	mean	min	max	mean
PCB18	0	3.1E-03	8.6E-04	0	1.3E-03	3.8E-04	0	4.4E-03	1.2E-03
PCB28	0	1.7E-03	2.7E-04	0	7.2E-04	1.2E-04	0	2.4E-03	3.9E-04
PCB31	0	3.3E-03	3.8E-04	0	1.4E-03	1.7E-04	0	4.7E-03	5.5E-04
PCB44	0	4.4E-03	9.0E-04	0	1.9E-03	3.9E-04	0	6.4E-03	1.3E-03
PCB52	0	3.1E-03	9.0E-04	0	1.4E-03	3.9E-04	0	4.5E-03	1.3E-03
PCB101	5.8E-05	3.1E-03	4.2E-04	2.5E-05	1.4E-03	1.8E-04	8.3E-05	4.5E-03	6.0E-04
PCB118	0	2.8E-03	5.1E-04	0	1.2E-03	2.2E-04	0	4.1E-03	7.3E-04
PCB138	0	3.0E-03	3.5E-04	0	1.3E-03	1.5E-04	0	4.3E-03	5.0E-04
PCB149	0	2.7E-03	3.5E-04	0	1.2E-03	1.5E-04	0	3.9E-03	5.0E-04
PCB153	1.3E-04	5.3E-03	1.3E-03	5.7E-05	2.3E-03	5.7E-04	1.8E-04	7.7E-03	1.9E-03
PCB194	0	3.3E-04	3.2E-04	0	1.4E-03	1.4E-04	0	4.8E-03	4.6E-04
PCB180	3.8E-05	4.2E-03	1.3E-03	1.7E-05	1.8E-03	5.8E-04	5.5E-05	6.1E-03	1.9E-03
HI	2.2E-04	4.0E-02	7.9E-03	9.7E-05	1.7E-02	3.4E-03	3.2E-04	5.8E-02	1.1E-02

(Source: Fieldwork, 2022)

APPENDIX W

Hazard Quotient and Index for non-carcinogenic human health risks posed by PCBs in sediment of study area via different pathways

Congener	HQ _{ing}			HQ _{der}			HQ _{total}		
	min	max	mean	min	max	mean	min	max	mean
PCB18	2.5E-07	6.6E-06	2.0E-06	1.5E-05	2.4E-03	1.2E-04	1.52E-05	2.4E-03	1.2E-04
PCB28	0	7.2E-06	1.5E-06	0	2.6E-03	8.8E-05	0	2.6E-03	9.0E-05
PCB31	0	7.7E-06	2.2E-06	0	2.8E-03	1.3E-04	0	2.8E-03	1.3E-04
PCB44	0	2.0E-05	4.5E-06	0	7.0E-03	2.7E-04	0	7.0E-03	2.7E-04
PCB52	0	2.7E-05	1.4E-05	0	9.8E-03	8.6E-04	0	9.8E-03	8.7E-04
PCB101	0	1.6E-05	4.7E-06	0	5.6E-03	2.8E-04	0	5.6E-03	2.9E-04
PCB118	0	3.3E-05	8.3E-06	0	1.2E-02	5.0E-04	0	1.1E-02	5.0E-04
PCB138	0	1.1E-05	3.8E-06	0	3.9E-03	2.3E-04	0	3.9E-03	2.3E-04
PCB149	0	6.3E-06	1.7E-06	0	2.3E-03	1.0E-04	0	2.3E-03	1.0E-04
PCB153	1.2E-05	3.8E-05	2.2E-05	7.2E-04	1.4E-02	1.3E-03	7.3E-04	1.4E-02	1.3E-03
PCB194	0	5.0E-06	1.1E-06	0	1.8E-03	6.3E-05	0	1.8E-03	6.4E-05
PCB180	1.2E-05	4.0E-05	2.4E-05	7.4E-04	1.5E-02	1.4E-03	7.6E-04	1.5E-02	1.5E-03
HI	2.5E-05	2.2E-04	1.0E-04	1.5E-03	7.8E-02	5.4E-04	1.5E-03	7.8E-02	5.5E-03

(Source: Fieldwork, 2022)

Mean HI = 5.5E-03 range 1.5E-03 - 7.8E-02 mean HQ range = 6.4E-05 - 1.5E-03